Stress adaptation and ageing is controlled by senescence-inducing age-related changes in *Arabidopsis thaliana*

A thesis presented in partial fulfilment of the requirements for the degree of

Doctor of Philosophy

in

Plant Biology

at Massey University, Palmerston North,
New Zealand.

Aakansha Kanojia

2018

Abstract

Senescence is the final stage of leaf development and leads to the death of a leaf. In leaves, chloroplasts are the major source of nitrogen (75%-80%), which is found mainly in proteins. The disassembly of chloroplasts during the senescence process releases a considerable amount of nitrogen, which is then remobilized to other growing parts of the plant. Thus, nutrients from dying parts of the plants are crucial for the initial development of seeds and new plant organs. Therefore, while leaf senescence is a destructive process, efficient senescence also increases viability of the whole plant and its survival to the next season or generation. However, senescence can also be induced prematurely by abiotic stress. Early senescence caused by environmental stress can be undesirable as it may affect the growth and yield of a plant. Plants grown under abiotic stress conditions such as high salinity, drought, cold or heat, display a variety of molecular, biochemical and physiological changes. Plants under environmental stress conditions activate several signalling pathways which, in coordination with hormones such as ethylene and abscisic acid, allow for an adaptive response to stress, resulting in adjustments of plant growth and development, in an attempt to maximise survival chances. Early senescence of old leaves is one of the important strategies adapted by plants for the survival of young growing tissues. The remobilisation of nutrients from old leaves to young tissues allows survival of the whole plant under stressed conditions. However, the outcome of the stress, i.e. survival or death, depends on the strength and duration of the stress in combination with the stress response.

A plant's response to stressed conditions also depends on the age of the plant. It has been reported by multiple studies that the tolerance to stress decreases with age, however, the underlying molecular mechanisms are not well understood. In chapter 1, it is reviewed and proposed that plants of different age show distinct responses to environmental stress because of senescence-inducing age-related changes (ARCs). Research work in chapter 3 sought to understand the synchrony between ageing and reduction of plant stress tolerance, using *Arabidopsis thaliana* as a model plant. Transcriptomic studies were carried out to examine the occurrence of senescence-inducing ARCs in *Arabidopsis* first rosette early expanding leaves (EEL), mid expanding leaves (MEL) and fully expanded leaves (FEL). The transcriptomic dataset showed that, as the leaf grows, genes associated to DNA repair mechanisms are downregulated and genes linked to stress hormone biosynthesis, oxidative stress, senescence and other stress responses, are upregulated. This research confirmed that *Arabidopsis* young, mature and adult plants, when treated with drought, salt, and dark stresses, had greater stress sensitivity with increased age, consistent with the role of senescence-inducing ARCs in stress resistance. This study suggests that young plants are more tolerant to stress because

of negligible senescence-inducing ARCs in young leaves, whereas the gradual accumulation of ARCs in mature leaves, and rapid accumulation in old leaves, results in decreased resistance to stress.

Next, to characterise mutants that modulate senescence-induced ARCs, I used stress-sensitive ***o****nset of* ***l****eaf* ***d****eath* (*old*) mutants of *Arabidopsis thaliana*. The mutants were characterised based on stress responses observed in *old13* and *old14* mutant plants compared to the wild type (WT) (Chapter 4). The *old13* mutant was selected as an appropriate mutant to study the regulatory pathway of senescence-inducing ARCs as I found that the *old13* mutant plants are susceptible to stress in an age-dependent manner (Chapter 5). The transcriptomes of *old13* leaves compared with the WT samples illustrate that stress susceptibility in the *old13* mutant is because of early acquisition of senescence-inducing ARCs. Compared to the WT leaves, *old13* showed significant downregulation of genes involved in antioxidant activity, stress tolerance, and cell-wall morphology, while genes involved in oxidative stress, senescence and stress responses were upregulated. Furthermore, transcriptional and metabolomic data illustrated that an unbalanced sugar level in *old13* leaves is one of the important senescence-inducing ARCs involved in ageing and stress responses. Chapter 6 includes an attempt to identify the mutated gene in *old13* using high throughput next generation sequencing. Further study on *old13* gene recognition will offer an exciting opportunity to gain an in-depth knowledge of the coupling between ageing and stress responses in plants. Together, this study suggests that the occurrence of senescence-inducing ARCs is an intrinsic process integrated into the stress response and ensures certain death in plants.

Acknowledgements

First and foremost, I would like to express my deepest gratitude to my supervisor, Dr Paul Dijkwel, for his excellent guidance, encouragement and immense knowledge that he has provided throughout my PhD, whilst giving me the space to work in my own way. I am very grateful for all your help, invaluable advice on both research as well as on my career. Also, I would like to thank Paul for the opportunity to work in the laboratory of the Institute of Biochemistry and Biology, Potsdam University, Germany. I consider myself lucky to have such a supportive and friendly supervisor. I would like to thank my co-supervisors Prof Kathryn Stowell and Prof Derek White for proofreading my thesis chapters, their enlightening suggestions and knowledge they offered me to aid in my research project. I would also like to thank Prof Michael McManus, who, although is no longer with us, helped and supported me during the first year of my PhD. I would also like to thank Erlinde Dijkwel for her friendliness and support during my stay in Palmerston North as well as in Potsdam.

Thank you, Prof Bernd Mueller-Roeber and Dr Tsanko Gechev for your support and scientific discussions during my research at Potsdam University. I am thankful to Dr Maria Benina, from Max Plank Institute of Germany who helped me by performing metabolic profiling, and Saurabh Gupta from Potsdam University who helped in RNA sequencing data analysis. Thank you to the Institute of Fundamental Science for 6 months of research funding and financial support to attend an international conference. I am thankful for the funding provided by Massey University Doctoral Completion Bursary for the successful completion of my thesis writing.

During my research, I have been blessed with a friendly and cheerful group in my lab. Thank you Matthew Denton-Giles, for giving me detailed explanations to my every question, I have learnt a lot from the guidance you provided. I am much obliged to all my lab members Muhammad Srishti, Shane, Julia, Jibran, Rachael, Hannah, Xi Xu, Elva, Nikolai, Rama, Nikola, Meriem, Pallavi and Saurabh from Massey University and Potsdam University who helped me directly or indirectly in every step of my learning process. I would like to make special mention of Susanna and Tina who was always very helpful and provided unlimited assistance in the lab. A special thanks too goes to Yasmin Dijkwel and Srishti Joshi, for being great friends to me and are always willing to help. I also want to show my sincere gratitude to Late Patricia Lopdell, my landlady, who opened both her home and heart to me and stood by me through the good times and bad.

Above all, I would like to thank my father Rakesh Kanojia, mother Anita Kanojia and brother Arpit Raj Kanojia for their unconditional support, I would not be where I am today without their love and

encouragement. My special and heartfelt thanks to my father for the education he provided and for teaching me to set goals and to strive for more. Lastly, to my husband, Ishan Pardeshi, I really appreciate your patience when I was busy completing my research, you understood and gave me time to complete my work without complaining, just so I could focus on finishing my thesis.

Table of Contents

List of Figures

List of Tables

Abbreviations

AAF	*ARABIDOPSIS A-FIFTEEN*
AAO3	*ABSCISIC ALDEHYDE OXIDASE 3*
AA	Ascorbic acid
ABA	Abscisic acid
ABP1	Auxin-Binding Protein 1
ACC	1-aminocyclopropane-1-carboylic acid
ACS	1-aminocyclopropane-1-carboylic acid synthase
ACO	1-aminocyclopropane-1-carboylic acid oxidase
ACT 2	*ACTIN 2*
AOS	Allene Oxide Synthase
AOC	Allene Oxide Cyclase
ARCs	Age-related changes
ATP	Adenosine Triphosphate
APX	Ascorbate peroxidase
BAM	Binary Alignment Map
ºC	Degrees celcius
CAT	Catalases
cDNA	Complementary DNA
Chr.	Chromosome
CTAB	Cetrimonium bromide
COI1	*CORONATINE INSENSITIVE 1*

Col-0	Columbia
CW	Cell-wall
DAG	Days after germination
DAB	3,3-diaminobenzidine
DDB2	*DAMAGED DNA-BINDING PROTEIN 2*
DHA	Dehydroascorbic acid
DHAR	Dehydroascorbate reductase
DMF	N, N'-dimethylformamide
DNA	Deoxyribose nucleic acid
DNase	Deoxyribonuclease
EDS1	*ENHANCED DISEASE SUSCEPTIBILITY 1*
EDTA	Ethylene diamine tetra acetic acid
EEL	Early expanding leaves
EIN	Ethylene Insensitive
EMS	Ethyl methanesulfonate
ETCs	Electron transport complexes
ERFs	Ethylene response factors
FC	Field capacity
FEL	Fully expanded leaves
FSD3	*Fe SUPEROXIDE DISMUTASE*
FW	Fresh weight
GA	Gibberellic acid
GAST1	*GA-STIMULATED TRANSCRIPT 1*

gDNA	Genomic DNA
GGC-MS	Gas Chromatography-Mass Spectrometry
Gi	Gigantea
GO	Gene Ontology
GSH	Glutathione
GR	Glutathione reductase
H_2O_2	Hydrogen peroxide
•OH	Hydroxyl radical
ICS	*ISOCHORISMATE SYNTHASE*
IGV	Integrative genomics viewer
IKI	Lugol's Iodine
JA	Jasmonic acid
Kb	Kilobase Pair
L*er*-0	Landsberg *erecta*
LD	Long-day
LOX	Lipoxygenase
MAPKs	Mitogen-activated protein kinases
MDHAR	Monodehydroascorbate reductase
MDA	Monodehydroascorbate
MEL	Mid expanding leaves
MGS	Massey Genome Service
Mb	Megabase Pair
µg	Micro-gram

µL	Micro-litre
mM	Milli-molar
mg	Milli-gram
mL	Milli-litre
mm	Milli-metre
min	Minute(s)
mRNA	Messenger ribonucleic acid
MPI	Max Planck Institute
NAD	Nicotinamide adenine dinucleotide
NADP	Nicotinamide adenine dinucleotide phosphate
NADPH	Nicotinamide adenine dinucleotide phosphate (reduced form)
NCED3	*NINE-CIS-EPOXYCAROTENOID DIOXYGENASE 3*
NIKS	Needle in a K-stack
ng	Nano-gram
NGS	Next generation sequencing
OD	Optical density
old	*onset of leaf death*
O_2	Oxygen
$^1O_2$	Singlet oxygen
$O_2^{\bullet-}$	Superoxide
OGBF	Otago Genomics and Bioinformatics Facility
ORE	*ORESARA*
PAD4	Phytoalexin Deficient 4

PCD	Programmed cell death
PCR	Polymerase chain reaction
PEN2	*PENETRATION2*
PE	Paired end
phs	*pre-harvest sprouting*
pmol	Picomoles
PS I	Photosystem I
PS II	photosystem II
PYL	*PYRABACTIN RESISTANCE 1-LIKE*
qRT-PCR	quantitative Real-Time polymerase chain reaction
RBOHD	*RESPIRATORY BURST OXIDASE HOMOLOG D*
ROS	Reactive Oxygen Species
RNA	Ribonucleic acid
rRNA	Ribosomal ribonucleic acid
RNase	Ribonuclease
RPS18	RIBOSOMAL PROTEIN S18
RuBisCO	Ribulose-1,5-bisphosphate carboxylase oxygenase
RWC	Relative water content
SA	Salicylic acid
SAM	S-adenosyl-L-methionine
SAG	Senescence-associated gene
SD	Short-day
SDS	Sodium dodecyl sulfate

sec	Seconds
SFC	Soil field capacity
SNPs	Single nucleotide polymorphisms
SOD	Superoxide dismutase
TET	Tetraspanin
TFs	Transcription factors
TPM	Transcripts per million
TUB 2	*TUBULIN BETA-2*
UPL 7	*UBIQUITIN-PROTEIN LIGASE 7*
UV	Ultraviolet
WT	Wild type
ZEP	*ZEAXANTHIN EPOXIDASE*

Chapter 1 Abiotic stress responses are governed by reactive oxygen species and age

1.1 Introduction

The earth's environment is constantly changing and this has accelerated in the past century as a result of the industrial era (Abram et al., 2016). Current global warming is believed to increase the frequency of extreme weather events (Cai et al., 2014b) and globally impacts ecosystems and crop production (Chapin et al., 2000; Lesk et al., 2016). Since plants cannot move away to escape from stressful environmental conditions, they have evolved sophisticated mechanisms to adapt to stress. Plants respond differently to multiple environmental stress such as drought, cold, salinity and ozone, but, early ageing and onset of senescence are common stress-induced responses (Munné-Bosch and Alegre, 2004). Early ageing due to stress is also accompanied with over-production of reactive oxygen species (ROS). ROS are a group of free radicals derived from oxygen and are continuously generated as by-products of basic metabolic processes such as photosynthesis and respiration (Arora et al., 2002; Gill and Tuteja, 2010). ROS in moderate levels are actively involved in plant growth and development, such as trichome development, leaf shape, root hair elongation, reproductive growth and senescence (Gapper and Dolan, 2006). However, excessive generation of ROS occurs when plants are exposed to biotic or abiotic stress (Bhattacharjee, 2012). High ROS levels may add to the already present burden of growing in unfavourable conditions, but they also function as stress signalling molecules (Suzuki et al., 2012) and therefore ultimately allow plants to adapt and survive the imposed stress. ROS are also regulated by and regulate the stress-related phyto hormones abscisic acid and ethylene (Steffens, 2014; Zhang et al., 2016). Abscisic acid, together with ROS, can provide stress resistance by adjusting the stomatal aperture (Sah et al., 2016). Ethylene plays a role in the induction of leaf senescence and as such helps decrease leaf surface area and evaporation, while valuable nutrients present in the senescing leaves can be remobilised (Müller and Munné-Bosch, 2015). Thus ROS, together with the hormones ethylene and abscisic acid play essential roles in the plant stress response and below I summarise a selection of research in this area and present ideas on how plants may optimise survival.

1.2 Reactive oxygen species

ROS radicals contain unpaired electrons that attack stable molecules to find another electron (Tripathy and Oelmüller, 2012). When the attacked molecule loses its electron, it becomes a free radical itself. Once the process has started, the chain reaction can continue for thousands of events resulting in the production of different ROS radicals (Hekimi et al., 2011). Typical characteristics of ROS are that they

are short lived, unstable and react with other molecules to achieve stability (Halliwell, 2006). ROS radicals include singlet oxygen ($^1O_2$), superoxide ($O_2^{\bullet-}$), hydrogen peroxide (H_2O_2) and hydroxyl radical (•OH) (Miller et al., 2010; You and Chan, 2015). Plants continuously produce ROS as normal by-products of metabolism that are generated in all cellular compartments, but a wide range of stressful conditions such as UV radiation, salinity, chilling, heat, drought etc. can lead to the overproduction of ROS (Tripathy and Oelmüller, 2012). Different types of ROS and their production sites are described below.

The chloroplast is one of the major sites that acts as a source for ROS generation during photosynthesis (Foyer and Noctor, 2009). Photosynthesis involves major electron transport complexes (ETCs) namely, photosystem I (PS I), photosystem II (PS II) and the cytochrome b6f complex (Nelson, 2011). Under regular conditions, the electron flows from excited PS centres to Nicotinamide adenine dinucleotide (NADP), which is further reduced to Nicotinamide adenine dinucleotide reduced form (NADPH) and then enters the Calvin cycle to reduce the final electron acceptor CO_2. Stress conditions such as salinity lead to the excessive uptake of Na^+ and Cl^- ions which results in limited CO_2 fixation due to overcrowding of ETCs (Elstner and Osswald, 1994; Hasegawa et al., 2000; Abogadallah, 2010). The impaired photosynthetic electron transport chain induces the formation of $^1O_2$ at PSII and $O_2^{\bullet-}$ radicals at PSI and PSII as waste products (Elstner and Osswald, 1994). The $^1O_2$ radicals are very toxic as they can react with biological molecules and directly oxidise unsaturated fatty acids, proteins and DNA (Halliwell, 2006). The $O_2^{\bullet-}$ radicals are short-lived and moderately reactive radicals (Apel and Hirt, 2004). When plants are treated with herbicides like oxadiazon, oxyfluorfen, bentazon etc. $^1O_2$ and $O_2^{\bullet-}$ radicals are most likely overproduced in the chloroplast, which may damage the whole photosynthetic machinery (Halliwell, 1991; Krieger-Liszkay, 2005; Balasaraswathi et al., 2017).

Similar to chloroplasts, mitochondria also have ETCs through which ATP is formed from ADP and Pi. The well-known sites of ROS generation in mitochondria ETC are complexes I and III (Sharma et al., 2012). A number of enzymes existing in the mitochondrial matrix are known to generate ROS (Taylor et al., 2002; Taylor, 2005). The enzyme 1-galactono-γ-lactone dehydrogenase produces $O_2^{\bullet-}$ indirectly by feeding electrons to the ETC while, enzymes like aconitase produce $O_2^{\bullet-}$ directly (Rasmusson et al., 2008). Although mitochondrial ROS generation takes place under regular respiratory conditions, ROS levels increase in response to changes in the environment (Kaushik and Roychoudhury, 2014). Paraquat, cold and drought stress lead to the production of $O_2^{\bullet-}$ radicals in mitochondria which causes severe damage to proteins (Murphy, 2009). UV-B stress induces a H_2O_2 burst which further produces •OH radicals by reacting with Fe^{2+} and Cu^+ within the mitochondria (Huang et al., 2016; Niu and Liao, 2016). Amongst all radicals, •OH are one of the most reactive in the family of ROS and can possibly react with all biomolecules including lipids, proteins and DNA (Apel and Hirt, 2004; Dikalov, 2011).

Peroxisomes can also efficiently produce ROS under stressed conditions including drought, salinity, ozone or cadmium (Del Río and López-Huertas, 2016) and are a major site of H_2O_2 generation (Del Río et al., 2006). H_2O_2 radicals are very stable but moderately reactive, as compared to other ROS species and these radicals can also travel easily across cell membranes (Rani et al., 2015). Depending on the concentration, H_2O_2 functions as a messenger by signalling a stress response in plants, or is involved in initiation of programmed cell death (PCD) (Møller et al., 2007). Flavin oxidase is a basic enzymatic component of peroxisomes that produces H_2O_2 radicals (Van der Zand and Tabak, 2013). In peroxisomes, $O_2^{\bullet-}$ radicals are produced at two sites: one site is positioned in the matrix, where xanthine oxidase is involved in generation of $O_2^{\bullet-}$, the second site is located in the membrane where $O_2^{\bullet-}$ generation is NAD(P)H-dependent (Del Rio et al., 2002).

NADPH-oxidase is a membrane bound enzyme complex that plays an important role in ROS generation under stressed conditions (Laloi et al., 2004). NADPH-oxidase catalyses the transfer of electrons from cytoplasmic NADPH to oxygen, to form $O_2^{\bullet-}$ radicals. Thus NADPH facilitates the formation of $O_2^{\bullet-}$ in the plasma membrane which is dismutated to H_2O_2 (Kwak et al., 2003; You and Chan, 2015). Due to overproduction of ROS in the plasma membrane NADPH-dependent oxidase is found to be involved in damaging proteins (Apel and Hirt, 2004; Qu et al., 2017).

A plant cell wall is a dynamic and an essential component of several biological processes. During developmental processes and interactions with the environment, the cell wall provides mechanical strength to withstand stress or stressful conditions (Tenhaken, 2015). Cell walls are considered as active sites for ROS generation. Under stressed conditions such as drought or salinity, cell wall-localised lipoxygenases are actively involved in the generation of ROS radicals like H_2O_2, $O_2^{\bullet-}$, •OH and $^1O_2$ (Hou et al., 2015). Cell wall-localised peroxidases are also involved in synthesis of ROS radicals (Gupta et al., 2016). During stressed conditions like drought or potassium deficiency, cell-wall localised peroxidase promotes ROS generation, which makes plants sensitive to stress if overproduced (Kim et al., 2010; Maia et al., 2013). Interestingly, a number of cell wall proteins are also known to be involved in the oxidative burst namely, hydroxyproline-rich glycoproteins, chitin-binding proline-rich glycoprotein and proline-rich proteins (O'Brien et al., 2012).

In summary, excess ROS production in response to abiotic stress can occur at multiple sites within and outside plant cells. Moreover, the long-lived ROS H_2O_2 can cross membranes and for these reasons - despite being potentially damaging, ROS are effective stress signalling molecules as well.

1.2.1 ROS scavenging antioxidants

ROS have dual effects on plant metabolism: on the one hand they act as damaging by-products of general metabolism and on the other hand they act as signalling molecules. This requires that plants have sophisticated measures to keep ROS under tight control (Sharma et al., 2012). In plants, ROS homeostasis is controlled by enzymatic and non-enzymatic antioxidant systems. Non-enzymatic antioxidants include the chief cellular redox buffers glutathione (GSH), ascorbic acid (AA), carotenoids and tocopherols. Enzymatic antioxidants include superoxide dismutase (SOD), catalases (CAT), ascorbate peroxidase (APX), monodehydroascorbate reductase (MDHAR), dehydroascorbate reductase (DHAR) and glutathione reductase (GR) (Mitton et al., 2017). They all contribute to ROS homeostasis (Kaushik and Roychoudhury, 2014).

The non-enzymatic antioxidant GSH is an essential antioxidant located in almost all cellular organelles like ER, cytosol, mitochondria, vacuole, chloroplasts, apoplast as well as in peroxisomes (Islam et al., 2017; Jiménez et al., 1998). GSH is the potential scavenger of H_2O_2 and the most toxic ROS like •OH radicals (Briviba et al., 1997; Gill et al., 2012; Yousuf et al., 2012). AA is another important non-enzymatic antioxidant which is abundantly present in most plant cell types, organelles and apoplast (Conklin and Barth, 2004; Podgórska et al., 2017). AA can directly detoxify $O_2^{\bullet-}$, •OH, $^1O_2$ and H_2O_2 to H_2O by the ascorbate peroxidase reaction (Noctor and Foyer, 1998; Zechmann, 2014). The oxidation of AA further leads to the formation of enzymatic antioxidants like monodehydroascorbate (MDA) and dehydroascorbic acid (DHA) (Park et al., 2016). DHA is then further reduced to AA by DHAR using GSH as a reducing substrate (Yang et al., 2009). Thus, DHAR plays an important role in maintaining AA in its reduced form (Hernández et al., 2001). Amongst enzymatic antioxidants, SOD catalyses the dismutation of $O_2^{\bullet-}$ to H_2O_2 and constitutes the first line of defence in nearly all cells exposed to oxygen (Gupta et al., 1993; Perl et al., 1993; Scandalios, 2005; Szőllősi, 2014; Moustaka et al., 2015). The enzyme catalase (CAT) was the first enzymatic antioxidant discovered and characterised (Kirkman and Gaetani, 1984). CAT catalyses the breakdown of chemical H_2O_2 to H_2O and O_2 (Sharma and Ahmad, 2014) and has one of the highest turnover rates of all enzymes: in one minute, one catalase enzyme can convert approximately 6 million molecules of H_2O_2 to O_2 and H_2O (Gill and Tuteja, 2010).

Plant cells are evidently equipped with outstanding enzymatic and non-enzymatic antioxidant defence mechanisms to keep ROS under tight control. A number of studies have shown that high levels of ROS scavengers induce resistance to different environmental stress conditions in plants. For example, it was found that the oxidative stress produced during drought stress could be minimized by increasing the production of ROS scavenging enzymes such as SOD and APX as well as non-enzyme GSH, ultimately resulting in resistance to water deficit conditions in *Arabidopsis* (Nakabayashi et al., 2014; Ramanjulu

and Bartels, 2002). In *Arabidopsis*, the overexpression of cytosolic APX provided tolerance to salt stress as compared to the control wild type plants (Lu et al., 2007). Also, under high temperature stress plants induce expression of stress-related proteins, which increases the antioxidant activity of SOD and CAT (Fahad et al., 2017a). These antioxidants scavenge the ROS, and thereby reduce the oxidative damage otherwise caused by the ROS. The importance of SOD in response to cold stress was confirmed in SOD-overexpressing alfalfa lines, which showed increased tolerance to chilling stress (Lee and Lee, 2000; Mckersie et al., 1993).

Consistent with expectations, a number of studies have also shown that cell damage increases with reduced antioxidant activity and over production of ROS. For example, a decline in the activity of ROS scavenging enzymes CAT and SOD promoted ROS levels and resulted in senescence-associated lipid peroxidation (Bhattacharjee, 2005). Moreover, an antioxidant APX-deficient mutant of *Arabidopsis* displayed increased sensitivity to salt stress because of elevated H_2O_2, indicating that APX is a salt stress-induced ROS scavenger (Chen et al., 2015; Huang et al., 2005). Another recent study in rice showed that gene silencing of *OsAPX4* caused ROS-mediated early senescence (Ribeiro et al., 2017).

Thus, plants have efficient ROS scavenging systems and scavenging effectiveness plays a role in the outcome of the stress-induced ROS production, i.e. damage and/or adaptive changes in plant growth and development leading to death or survival (Liebthal and Dietz, 2017; Podgórska et al., 2017; Suzuki et al., 2012).

1.2.2 ROS and Ethylene

Ethylene is well-known for its commercial use in the stimulation of ripening of crops, fruits and vegetables (Pech et al., 2012). Indeed, it is a key hormone in regulating leaf senescence, flower senescence, abscission and fruit ripening (Jibran et al., 2013; Zacarias and Reid, 1990). The relatively simple ethylene biosynthesis pathway was elucidated by Yang and Hoffman in 1984 and starts with the formation of the amino acid 1-aminocyclopropane-1-carboxylic acid (ACC) from S-adenosyl-L-methionine (SAM), catalysed by ACC synthase (ACS). ACC oxidase (ACO) subsequently catalyses the conversion of ACC to ethylene gas. The multigene family that encodes the enzymes ACS and ACO are expressed differentially in response to a range of external and internal cues (Müller and Munné-Bosch, 2015). Consistently, the production of ethylene varies during plant growth and increased ethylene biosynthesis is observed during stress-induced senescence, age-induced senescence or as a result of damage (Koyama, 2014).

Ethylene and H_2O_2 are both important cell signalling molecules, also known to work in concert to modulate stomatal aperture, cell elongation and a variety of stress responses (Desikan et al., 2006;

Mittler et al., 2004; Wi et al., 2010). Studies have shown that ethylene along with H_2O_2 act as a positive regulator of PCD during stress, through the activation of ACS and ACO (Dennis et al., 2000; Wang et al., 2002). In cotton, exogenous ethylene enhanced the production of H_2O_2 within 6 hours, whereas exogenous H_2O_2 stimulated the biosynthesis of ethylene but only after 1 day of application (Qin et al., 2008). In plants, aerenchyma tissue forms air channels, which provide gaseous exchange between the shoots and the roots (Dennis et al., 2000). It has been found in *Arabidopsis*, that hypocotyls and roots can induce formation of lysigenous aerenchyma in response to hypoxia and this process involves H_2O_2 and ethylene signalling (Muhlenbock et al., 2007; Feifei et al., 2017). A connection between ROS and ethylene is also confirmed by various studies on mutants that are defective in ethylene signalling or biosynthesis. For example, the ethylene overproduction mutants *eto1* and *eto2* displayed sensitivity to oxidative stress and promoted cell death, while the ethylene insensitive mutants *ein3* and *etr1* exhibited resistance to oxidative stress (Jung et al., 2009; Overmyer et al., 2000; Tuominen et al., 2004). All these studies support an intricate relationship between ethylene and ROS in the regulation of various plant responses.

Despite being a positive regulator of senescence in plants, the action of ethylene also induces tolerance to several abiotic stresses. Ethylene plays an important role in mediating the response to low potassium conditions by increasing ROS accumulation and changing root morphology in *Arabidopsis* (Jung et al., 2009). Additionally, ethylene, accompanied by ROS accumulation, induced root hair elongation in *Arabidopsis* seedlings adapting to low ammonium levels (Zhu et al., 2016). In *Arabidopsis*, members of Ethylene-responsive element-binding factors (ERFs) were identified that are involved in normal plant growth and development, but also function in response to stress by modulating the ROS regulatory pathway (Ecker, 1995; Nakano, 2006). For instance, the increase in expression of *ERF1* in plants displayed resistance to drought, low temperature and salinity suggesting its positive role in abiotic stress tolerance (Cela et al., 2011; Cheng et al., 2013; Xu et al., 2007). Moreover, enhanced expression of the ERF protein JERF3 in tobacco plants also induced resistance to drought, freezing and salinity coinciding with reduced ROS accumulation (Wu et al., 2008). Also, in tobacco plants the function of ERF transcription factor TERF1 was investigated confirming its role in ROS scavenging and providing tolerance to oxidative stress (Zhang et al., 2016a). Recently, EMS-induced ethylene-insensitive tobacco mutants were isolated and found to exhibit drought tolerance as well when grown on mannitol-containing medium. The mutants showed a higher survival rate along with increased antioxidant activity suggesting a role for ethylene in water deficit conditions (Wang et al., 2016b). In *Arabidopsis*, overexpression of *ERF74* displayed enhanced resistance to water deficit, heat, high light and aluminium stress coinciding with a ROS burst in the early stages of the imposed stress, while, transgenic lines with reduced *erf74* expression showed increased stress sensitivity along with a negligible ROS burst (Yao et al., 2017). This study furthermore provided evidence that ERF74 is involved in controlling stress tolerance by managing ROS homeostasis in a *RbohD*-dependent way. It was also found that ethylene

delays ABA-induced stomatal closure, suggesting a role for ethylene in increasing the rate of transpiration. However, it could also be that the function of ethylene-dependent inhibition of stomatal closure under drought stress is to avoid an overburden of O_2 molecules as waste by-product of photosynthesis and this could explain the two-fold role of ethylene during osmotic stress tolerance (Tanaka et al., 2005).

All these studies together suggest that despite the positive regulators of senescence and potential toxicity, ethylene and ROS have a dual role either in cell survival or cell death under abiotic stress conditions. The intricate role of ethylene in ripening and senescence furthermore suggests that the dual effect of ethylene and ROS signalling on plant responses probably not only depends on the type and severity of the stress, but also on the age of the stressed plant tissue.

1.2.3 ROS and ABA hormone regulation

The plant hormone abscisic acid (ABA) is involved in the regulation of various plant developmental processes including cell division, elongation, seed development, seed dormancy, vegetative growth and floral induction (Finkelstein 2013; Raghavendra et al., 2010). In addition to ethylene, ABA levels also increase in response to various abiotic stresses and therefore, both hormones are suggested to have roles during abiotic stress responses (Lee and Luan, 2012; Leng et al., 2014).

Abiotic stresses like cold, temperature, salinity and drought increase both ABA and ROS in plant tissues (Mehrotra et al., 2014). It was also shown that drought and salinity promote the biosynthesis of ABA, coinciding with massive change in expression of stress responsive genes (Boursiac et al., 2013; Shinozaki and Yamaguchi-Shinozaki 2007). It was also found that exogenous application of ABA delays drought-induced wilting and provides resistance to water deficit conditions (Mehrotra et al., 2014). An increase in ABA levels by abiotic stress leads to stomatal closure through the increase of NADPH oxidase activity and a resulting increase in H_2O_2 production. This causes reduced transpiration and results in drought-stress tolerance (Assmann, 2003; Desikan et al., 2004; Li et al., 2011; Liu et al., 2010; Melotto et al., 2006; Neill et al., 2002; Sinclair et al., 1984; Xu et al., 2016; Ye et al., 2011). Li et al., (2017a) showed that overexpression of the *OsASR5* gene, caused a rise in ABA and H_2O_2-induced stomatal closure as well as prevented inactivation of drought stress-related proteins and provided enhanced drought tolerance to transgenic rice plants. In *Arabidopsis* the combined effect of heat and salt stress on ABA signalling mutant *abi1* resulted in increased susceptibility to the stress as compared to the wild type plants (Suzuki et al., 2016). Later it was found that the increased sensitivity to salt stress of the *abi1* mutant plants resulted from the defective stomatal closure and elevated H_2O_2 in leaves (Zandalinas et al., 2016). Additionally, the silencing of the ABA-activated kinase *SAPK2* in *Arabidopsis*, resulted in highly drought susceptible plants, presumably caused by the higher

transpiration rate as a consequence of the increased ROS level, decreased antioxidant machinery and fully open stomata (Lou et al., 2017). While these studies show how stress-induced increases in ABA and H_2O_2 levels cause stomatal closure and drought resistance in stomatal cells, other studies highlight the antagonistic effect of ABA in decreasing the ROS levels and increasing stress tolerance. For instance, the *ABP9* gene, which encodes a *bZIP* transcription factor, plays an important role in regulating ABA responses (Wang, 2002). Transgenic *Arabidopsis* and cotton plants overexpressing *ABP9* had reduced stomatal aperture, ROS levels and cell death and greater tolerance to drought, salinity, cold and oxidative stress as compared to wild type plants (Wang et al., 2017; Zhang et al., 2011). Likewise, in cadmium-stressed purple flowering stalk it was found that exogenous application of ABA lowered the H_2O_2 and $O_2^{\bullet-}$, induced SOD, APX and GR antioxidant activity and provided resistance to cadmium stress (Shen et al., 2017). Moreover, *pre-harvest sprouting* (*phs*) rice mutants with impaired carotenoid and ABA biosynthesis were isolated and these mutants displayed higher ROS abundance and pre-harvest sprouting, suggesting that ABA plays an important role in inhibition of pre-harvest sprouting in crops through limiting ROS accumulation (Fang et al., 2008). Treatment of drought-stressed apple species with melatonin furthermore enhanced stress tolerance by increasing the antioxidant activity and decreasing the ABA and H_2O_2 levels and this resulted in the stomata to be more closed during the imposed stress (Li et al., 2015). These studies indicate that in addition to reducing the transpiration rate through ABA and ROS-induced stomatal closure, plants comprise other adaptive mechanisms like ABA-induced reduction of ROS coupled with elevated antioxidant levels. Nevertheless, the effect of ABA on ROS levels likely depends on stress levels and cell type, especially in the case of the highly specialised stomatal cells.

1.2.4 ROS signalling: Interplay between MAPKs, ethylene and ABA

In *Arabidopsis*, 60 MAPKKKs, 10 MAPKKs and 20 MAPKs have been classified (MAPK Group, 2002). A number of MAPK cascades were found to be activated in response to abiotic stress (De Zelicourt et al., 2016) and *Arabidopsis* MPK3 and MPK6 where shown to play key roles in ROS signalling under environmental stress conditions (Jalmi and Sinha, 2015). The expression of the genes encoding these proteins is induced by ozone treatment and plants that lack MPK3 or MPK6 are hypersensitive to ozone (Miles et al., 2005) and stress-induced *MPK3* and *MPK6* expression leads to ROS accumulation and ethylene biosynthesis, which induces early leaf senescence (Li et al., 2012). Biosynthesis of the stress-hormone ethylene is also regulated by MPK3 and MPK6: synthesis of the hormone requires ACS and both ACS2 and ACS6, which belong to type 1 ASC isoforms, are substrates of MPK3 and MPK6 (Liu and Zhang, 2004; Wang et al., 2002). As a consequence of unfavourable environmental conditions, MPK3 and MPK6 phosphorylate ACS2 and ACS6, which leads to an

increase in ACS activity and concomitant ethylene biosynthesis (Han et al., 2010). Thus, abiotic stress conditions link *MPK3* and *MPK6* functions with ethylene signalling and ROS overproduction.

Various studies have increased the understanding of ABA signalling in the activation of MAPKs to mediate stress responses through stomatal closure and balancing ROS and antioxidant activity (de Zelicourt et al., 2016). Several genes encoding MAPKs were reported in *Arabidopsis* to be activated via ABA signalling such as *MPK1, MPK2, MPK9, MPK7, MPK12, MPK14* (Danquah et al., 2015; Jammes et al., 2009; Ortiz-Masia et al., 2007). MAPK cascades involving MKK4, MKK5, MPK3, MPK6 were also found to be involved in both stomatal development and aperture and this was mediated in an ABA-dependent manner (Gudesblat et al., 2007). *MKKK18* is an ABA-activated kinase involved in stomatal development, plant growth regulation and senescence (Mitula et al., 2015; Matsuoka et al., 2015) and the recent knockout and overexpression of *MAPKKK18* in *Arabidopsis* confirmed a role for this gene in suppression of drought-stress resistance mediated by the ABA signalling pathway (Li et al., 2015). Moreover, in cotton plants the overexpression of *GhMKK3* displayed enhanced tolerance to drought stress via ABA-induced stomatal closure (Wang et al., 2016a). Similarly, in *Arabidopsis*, overexpression of *ZmMKK1* showed enhanced antioxidant activity and high expression of ABA-responsive genes resulting in increased tolerance to water deficit and salt stress (Cai et al., 2014a). In addition, overexpression of the Raf-like MAPKKK gene, *GhRaf19* in cotton plants, displayed higher ROS abundance and reduced resistance to drought and salinity in transgenic plants, suggesting a function for this gene in osmotic stress responses by modulating cellular ROS levels (Jia et al., 2016). All these studies have uncovered a crucial role for MAPKs and ABA signalling in regulating abiotic stress responses.

The hormones ethylene and ABA, ROS messengers and MAPK cascades all play central roles in plant development and abiotic stress responses. ROS and MAPKs are activated in response to hormone actions, but also feedback, or regulate hormone responses. Therefore, all these stress signallers are intricately connected and likely play diverse roles during different types of stress, in different tissues or a tissue of a different age. Nevertheless, ROS overproduction seems to be key to many stress responses, although the effect of these can differ. For example, as a result of many abiotic stresses, ROS-mediated closing of stomata takes place through various signalling pathways and this limits the gaseous exchange in the cell (Hetherington and Woodward, 2003). During drought stress this may be lifesaving but it also increases the production of ROS within the leaf (Singh et al., 2017). This may further induce a stress response which may cause leaf death, a potentially harmful response. Indeed, a variety of transgenic studies, as mentioned above, show that limiting ROS levels can cause increased stress resistance. Moreover, activation of MPK3/MPK6 during stress induces ROS production and ethylene biosynthesis that ultimately results in early ageing or cell death in plants (Li et al., 2012; Ye et al., 2015). However, stress-induced expression of MPK3 and MPK6 also contributes to the survival of plants by controlling

ROS overproduction (Pitzschke and Hirt, 2008). It may depend on the amount of ROS over production whether the MAPK signalling pathway induces ethylene biosynthesis leading to cell death or promotes ABA-mediated stress tolerance via stomatal closure or an enhanced antioxidant mechanism. Thus, while the past decades have seen rapid progress in the understanding of ROS signalling, the many gaps in our knowledge may make it difficult to predict what happens under field conditions to plants that efficiently limit ROS production (Liu and He, 2017).

1.3 Adaptive mechanism in plants to cope with Abiotic stress

Plants are sessile in nature and cannot move away from adverse environmental conditions. Therefore, plants need to respond in other ways to protect themselves from environmental stress. In nature, different stresses such as cold, drought or heat may demand diverse responses, leading to distinct adaptations in plants (Mittler, 2002). The visible adaptive response depends on the severity of stress and can include leaf growth arrest, lesion formation, onset of leaf senescence and delayed or early flowering. In addition, plants can gauge mildly stressful conditions and respond by preparing for survival against future stressful conditions of the same kind in a process called hardening or priming (Tuteja and Gill, 2013). Exogenous application of osmoprotectants or priming agents prior to an expected stress can successfully be used to induce enhanced resistance to multiple abiotic stresses in plants and this strategy is being successfully used in agriculture to improve stress resistance of crop plants (Savvides et al., 2016). For example, natural or chemical compounds including putrescine, spermine, vitamins, hormones and oligosaccharides can be exogenously applied prior to the expected stress event (Aranega-Bou et al., 2014; Ebeed et al., 2017). Hence, plants have evolved effective mechanisms to cope with a variety of stresses and stress severities and these mechanisms can be manipulated to increase crop productivity.

1.3.1 Priming-induced abiotic stress tolerance in plants

Priming is an emerging field in the management of crops and produce against damaging effects of environmental stress (Savvides et al., 2016). The commercial storage of fruits at low temperature increases shelf life, but storage between 0-5 ˚C can cause chilling injuries or cold stress, especially in fleshy fruits. Recently, a study has shown that priming of peach fruits right after harvest by controlled, delayed cooling for 48-hours at 20 ˚C resulted in reduced chilling injuries as compared to fruits directly exposed to cold temperature (Tanou et al., 2017). In the field, soil salinity is a major agricultural problem because of decreased irrigation water quality and mineral weathering causing a slow increase in soil salinity (Flowers, 2004). Recent studies have shown that priming of *Triticum aestivum L.* plants

with 1 mmol ABA caused higher antioxidant activity and resistance to salt stress by protecting the photosynthetic electron transport chain (Wang et al., 2017). Also, pre-treatment of tomato plants with the proton pump inhibitor omeprazole increased ROS levels and resulted in improved shoot and root mass and plant nutritional status during salt stress (Van Oosten et al., 2017). Moreover, drought is a common abiotic stress to plants and priming has been confirmed by various studies to enhance the tolerance to water deficit conditions: the priming of *Medicago sativa* plants with the antioxidant melatonin enhanced the osmoprotection and antioxidant activity and conferred enhanced tolerance to a prolonged drought period (Antoniou et al., 2017). In addition, seed priming with salicylic acid, jasmonic acid or paclobutrazol significantly increased drought resistance in rice plants (Samota et al., 2017). Increased stress resistance as a result of priming resulted in marked improvements in shoot biomass compared to the non-primed plants. For example, maize seeds which were primed with silicon produced plants with significantly increased leaf size and fresh weight and after being exposed to alkaline stress as compared to plants developed from non-primed seeds (Abdel et al., 2016). Moreover, *Arabidopsis* plants pre-treated with 50 mM NaCl displayed enhanced tolerance to desiccation, resulting in plants with greener leaves and a larger rosette size than non-primed control plants (Sani et al., 2013). Thus, priming has proven to be an effective approach in the improvement of crops under stressed conditions because it not only improves survival, but also yield.

Priming is believed to increase stress tolerance because the priming induces an endogenous stress responses that allows the plants to handle future stress with greater tolerance (Gamir et al., 2014). It is suggested that in primed plants the protective effect is caused by increased ROS signalling, which activates several signalling cascades, hormones, small peptides and antioxidants (Borges et al., 2014; Colcombet and Hirt, 2008; Mittler et al., 2011). Indeed, exogenous application of H_2O_2 increased drought and salt stress resistance in plants by modulating multiple processes including photosynthetic activity, ROS scavenging and turgor (Hossain et al., 2015). An effect of the priming-induced increased ROS levels may be enhanced antioxidant activity, resulting in restricted overproduction of ROS as a result of subsequent stress (Afzal et al., 2011; Hussain et al., 2016; Rejeb et al., 2014). Therefore, priming induces increased stress resistance, without apparent negative effects on plant growth, primarily by controlling ROS overproduction in response to various subsequent stresses (Conrath, 2011).

1.3.2 Abiotic stress-induced programmed cell death as an adaptive response in plants

Under certain stressed conditions like UV or ozone, cells that are no longer needed commit suicide, which is mediated by a highly coordinated process known as PCD (Tuzhikov et al., 2008). During this process only specific cells are destroyed so that neighbouring cells can survive the adverse effect of the

environmental stress (Wang and Bayles, 2013). The overproduction of ROS mediates PCD in many cell types (Petrov et al., 2015). In plants different stress factors like, heat shock, water deficit and salinity can cause the initiation of PCD (Gaussand et al., 2011; Zuppini et al., 2010). UV-B radiation that reaches the earth's surface can also cause the activation of PCD and this is visible by the appearance of lesions or chlorotic areas (Nawkar et al., 2013). UV-B exposure results in reduced photosynthetic capacity and cessation of leaf growth because of delayed cell division and cell expansion (Hectors et al., 2010; Lo et al., 2005; Milchunas et al., 2004). Leaf growth resumes once the leaf's injury is repaired, but in the case of severe stress, it can lead to premature leaf senescence (Suchar and Robberecht, 2015). Ozone is a major photochemical oxidant and can also cause lesion formation in leaves. For example, ozone caused leaf lesions in ozone-sensitive *Arabidopsis* accession Wassilewskija, while ozone-tolerant accession Columbia was not affected by the same stress levels (Tamaoki et al., 2003), indicating that ozone-stress resistance is a genetically controlled trait.

Mild abiotic stress such as drought, salinity or heat rapidly reduces plant growth and development. The primary cause of stunted plant growth is stomatal closure which is useful in terms of reducing the transpiration rate, but the closed stomata also lead to a reduction in photosynthesis (Kaya et al., 2006; Manickavelu et al., 2006; Hancock et al., 2001; Sahoo et al., 2017). The reduced energy production, leading to delayed cell elongation and cell expansion restrict the plant growth (Munns and Termaat, 1986). Tolerance to mild osmotic stress can be achieved by accumulation of osmoprotectants such as proline which helps in adjusting the osmotic pressure as well as scavenging of various ROS radicals and this may cause only minor effects on plant growth (Nanjo et al., 1999; Saradhi et al., 1995). Nevertheless, more pronounced osmotic stress can adversely affect plant growth (Maggio et al., 2001; Fahad et al., 2017).

One of the most conspicuous consequences of abiotic stress is the onset of senescence in adult leaves (Munns et al., 1995; Petronia et al., 2011). Leaf senescence is a natural process that is a result of ageing or initiation of reproduction. It is the final stage of leaf development, which is usually marked by the yellowing and withering of leaves and ultimately leads to the death of a leaf (Buchanan-Wollaston, 1997; Diaz et al., 2006; Guo and Gan, 2014). Senescence is an essential process that allows the remobilisation of the nutrients within the old senescent leaf so these can used to support young growing tissues (Himelblau and Amasino, 2001). However, senescence as a result of abiotic stress can be considered unwanted as it may result in decreased plant growth and yield (Sharabi-Schwager et al., 2009). However, as stress may result in the shut-down of photosynthesis and growth, nutrients made available through the senescence of the older leaves may allow the plant to survive and reproduce. The apparent positive effect of abiotic stress-induced senescence of the older leaves on the survival of the whole plant can also be seen in a number of transgenic plant lines in which stress resistance was affected by the transgene. For example, in *Arabidopsis*, the autophagy-related mutants *atg5*, *atg7* and *nbr1* are

more sensitive to heat and drought stress as compared to wild type plants (Zhou et al., 2013). However, careful observation of plant phenotypes shows that the old leaves have undergone senescence and the young leaves remained green and viable. Similarly, drought stress on ascorbate and GSH-deficient mutants (*vtc-2* and *pad-2*) also displayed advanced yellowing in old leaves but young leaves remained green (Koffler et al., 2014).

The biosynthesis of ABA is upregulated during environmental stress and as part of the senescence program (Khan et al., 2013). Pyrabactin resistance1-like (PYL) belongs to the family of ABA receptors that function in ABA and drought-stress signalling. *Arabidopsis* lines overexpressing *PYL9* displayed a greater tolerance to drought stress and ABA-induced leaf senescence of old leaves in an ethylene-independent manner (Zhao et al., 2016). This example clearly indicates that ABA-induced senescence of the old leaves during water deficit is important for the survival of young tissues. Thus, premature leaf senescence as a result of stress affects productivity but it is also an important strategy adopted by plants to assure the survival of young leaves. Therefore, the stress response depends on leaf age and I propose that ROS is a factor linking the two. Consistent with this, *ARABIDOPSIS A-FIFTEEN* (*AAF*) modulates redox homeostasis in *Arabidopsis* and transgenic lines overexpressing *AAF* (*oxAAF*) displayed early senescence and stress sensitivity in an age-dependent manner (Chen et al., 2012). The physiological parameters used to monitor the progression of senescence in the third rosette leaves at 49 days after germination displayed accelerated senescence as compared to 28 days old leaves. Moreover, accelerated senescence was found during ozone exposure due to overproduction of ROS in *Arabidopsis* (Miller et al., 1999). In addition to this, research has shown that expression of ROS responsive genes are upregulated in fully expanded *Arabidopsis* rosette leaves, prior to the initiation of senescence (Breeze et al., 2011). This indicates that once leaves reach maturity, an increase in ROS production leads to the progressive onset of senescence and this is consistent with ROS playing a central role in the initiation of senescence in old leaves (Sedigheh et al., 2011; Schippers et al., 2008).

As described above, ROS, ABA and ethylene also function in plant survival during environmental stress. Here, I propose that (1) the dual role of ROS, ABA and ethylene in either leaf death or survival is ultimately determined by leaf age and (2) that stress-induced leaf senescence of old leaves benefits the survival of the whole plant. One purpose of early senescence in stressed plants is to complete the life cycle quickly thereby allowing early initiation of flower development and seed production (Buchanan-Wollaston, 1997; Lamb, 2012; Kazan and Lyons, 2016). However, whether plants can survive and complete reproduction depends on the severity of stress (Xu et al., 2010). Under severe stress, suppression of various biochemical and physiological processes eventually leads to the death of the whole plant (Munns et al., 1995; Pandey et al., 2017).

Altogether, plants' response to stress can have at least three different outcomes: mild stress may have limited impact on plant growth and development, but it can result in a priming effect, hardening the

plant for future stress of a similar kind. Secondly, intermediate stress will induce leaf senescence in the older leaves, allowing those leaves to continue to function as a nutrient and energy source and allowing the growing parts of the plant to survive. Finally, severe stress will lead to the death of the plant. These responses are illustrated in Figure 1.1, where *Arabidopsis* plants were treated with increasing periods of continued darkness, followed by a recovery period. Two days of dark treatment has limited effect on plant growth, while 4 days of darkness allowed the survival of the young leaves, at the expense of the older leaves. Here, the young leaves showed a strong survival response, while the older leaves died. Six days of darkness, did not allow the survival of the plant even though Figure 1.1 shows that the older leaves were completely wilted while the younger leaves still appeared pale green. Therefore, these three responses are more likely part of a continuum where initially a survival response is set in motion, but that depending on leaf age, continued stress will result in senescence of older leaves, with survival of young leaves for as long as possible.

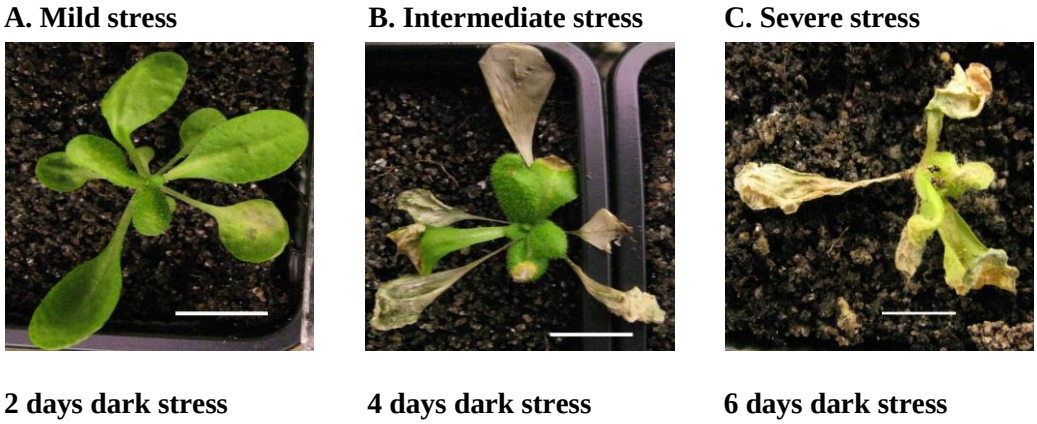

Figure 1.1. Distinct response to stress in *Arabidopsis* plants
18 days old *Arabidopsis* plants, grown under long-day conditions in a growth chamber were treated with 2 (A), 4 (B) or 6 (C) days of total darkness and were then allowed to recover for three days under long-day conditions. Representative plants where photographed. The bar represents 10 mm.

1.4 The occurrence of age-related changes determines the outcome of the stress response

A huge amount of research has been done to understand how plants adapt in response to environmental stress, with the aim of producing better performing crops under fluctuating and, as a result of climate change, more unpredictable environmental conditions. However, while relatively little is known about

how leaves of a different age respond to stress, a wide range of studies on abiotic stress responses and leaf senescence, allows a model correlating ageing and stress response of individual leaves to be proposed.

As part of the developmental ageing process of leaves, age-related changes (ARCs) will take place (Figure 1.2). Such ARCs include cell division, cell expansion, cell elongation, degradation of cellular components, developmental changes in hormone and ROS levels and many more. Finally, when leaves reach the final stage of development, this occurrence of ARCs leads to the decline in function of cells and onset of senescence (Caswell and Salguero-Gomez, 2013). In addition, stress can induce early senescence in mature, but not in young leaves, as discussed above. This has been clearly shown by ethylene treatment of *Arabidopsis* plants, where only the older leaves were able to respond to the senescence treatment with the onset of senescence (Grbic and Bleecker, 1995; Jing et al., 2002; Jing et al., 2005). Even prolonged ethylene treatment did not induce senescence in young leaves and the constitutive ethylene signalling mutant *ctr1* did not show early senescence (Grbic and Bleecker, 1995). This suggests that certain ARCs are required for a leaf to become competent to senesce (Jibran et al., 2013). Moreover, the phenotype of the *ctr1* mutant suggests that a stress treatment in young leaves can induce a strong survival response to that stress, resulting in old leaves that do not respond to the ethylene signalling with senescence. Thus I propose that young leaves are unable to respond to stress with the onset of senescence, while certain ARCs allow a mature leaf to senescence in response to abiotic stress (Jibran et al., 2013). Finally, the occurrence of further ARCs in old leaves cause senescence, even in the absence of environmental stress (Jibran et al., 2013). The above-described idea is supported by research dating more than 3 decades ago when a study showed that *Beta vulgaris* leaves undergoing cell division were not affected by salt stress while extending and fully extended leaves were found to be sensitive to salt treatment (Papp et al., 1983). Also, an experiment conducted on *Albizia* leaves described the effect of stress and age on the rhythmic frequency of opening and closure of leaves. The study showed that mature leaves closed slowly and incompletely as compared to young leaves when exposed to darkness, drought stress or ethylene (Lee and Satter, 1983).

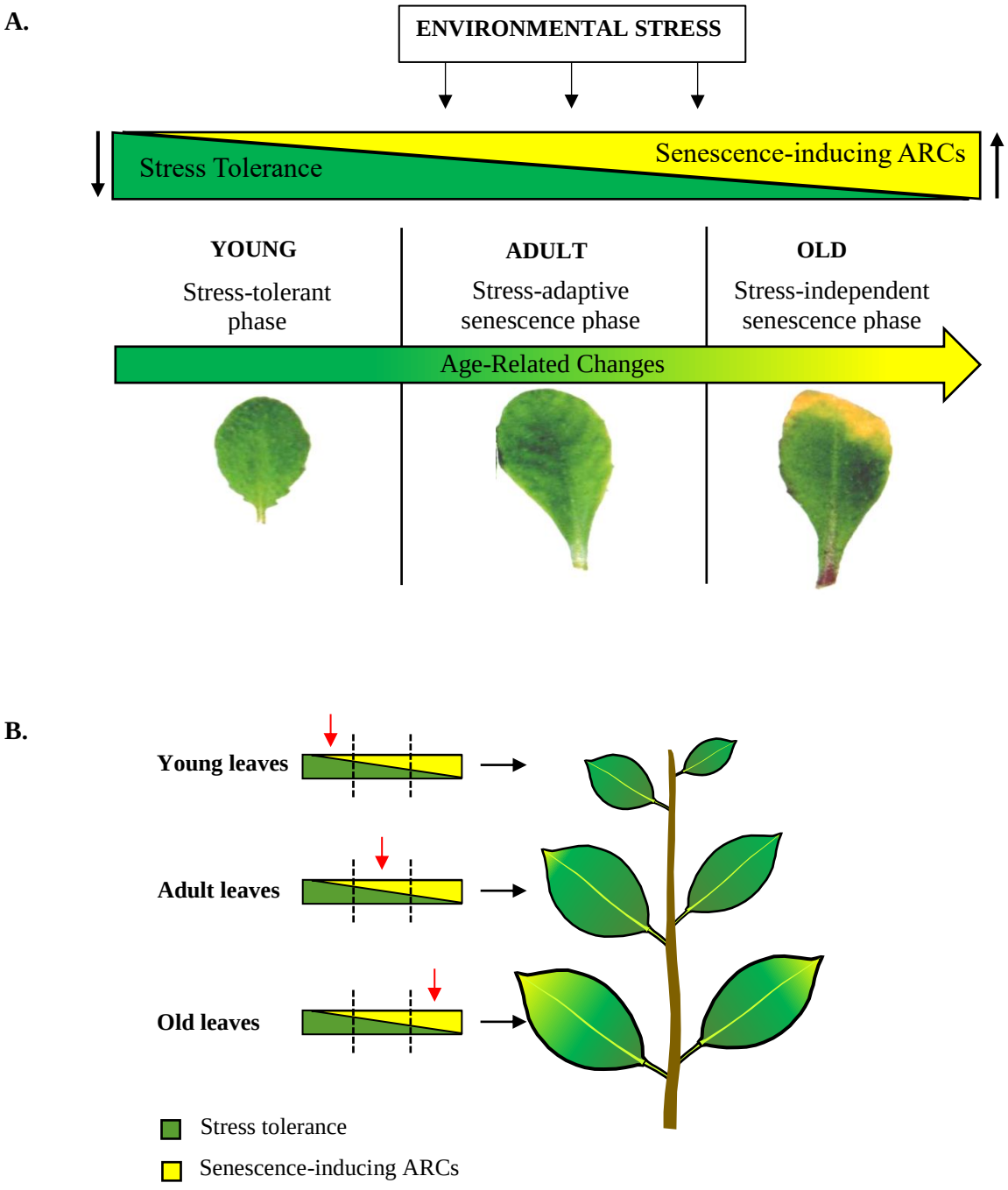

Figure 1.2. A tentative model showing stress response in different age of leaves.
A. Leaves undergo age-related changes (ARCs) throughout their development. These ARCs may include a gradual reduction in stress tolerance or the acquisition of senescence-inducing ARCs. Young leaves therefore are highly tolerant to stress, while mature leaves can respond to abiotic stress with the induction of leaf senescence. Old leaves will senesce because of senescence-inducing ARCs. **B.** Individual leaves of plants exposed to environmental stress show a distinct response depending on their age. Young leaves are in the stress tolerant phase because of negligible senescence-inducing ARCs, adult leaves are in the stress adaptive phase because of gradually occurred senescence-inducing ARCs, while old leaves senesce by default as a result of low stress tolerance and increase of senescence-inducing ARCs.

While the nature of the ARCs that allow a mature leaf to senesce in response to stress is unclear, some recent reports point to ARCs that coincide with decreased stress resistance of old leaves. In *Arabidopsis* leaves, DNA repair efficiency was highest in young leaves and lower in adult leaves (Golubov et al., 2010), suggesting that an age-related reduced ability to maintain genomic integrity may cause an old leaf to be more susceptible to stress and ROS-related DNA damage. In addition to this, the production of secondary metabolites is one of the strategies for protection against environmental stress and research conducted on *Cistus ladanifer* showed that the amount of flavonoids and terpenes in young leaves was greater than in mature leaves (Valares Masa et al., 2016). The greater amount of these compounds present in young leaves may allow for a higher resistance to stressful conditions than the mature leaves by keeping the antioxidant machinery active and by keeping ROS generation at acceptable levels (Fini et al., 2011; Loreto et al., 2004). Therefore, there is evidence to suggest that as a result of ARCs, leaves are programmed to become less tolerant to stress over time (Figure 1.2).

Figure 1.2A describes a model that explains how ARCs determine whether abiotic stress results in the survival or death of a leaf. The model is adapted from the senescence window concept model proposed by Jing et al., (2002). As described above, ARCs take place over the course of leaf development and some of these may decrease stress resistance over time. In addition, or as a result of these ARCs, the chance for a leaf to senesce increases over time. This leads to three distinct phases: the first where a leaf is highly resistant to stress, i.e. a leaf at this stage has not yet obtained the competence to senesce. Then, as time progresses, increased ROS, ABA and ethylene levels, together with a decline in cytokinins, DNA repair and antioxidant activity may be essential senescence-inducing ARCs. These ARCs result in the leaf to acquire the competence to senesce, but leaves only do so in the presence of stress. Finally, the leaf will die regardless of the presence of stress as a result of the occurrence of sufficient senescence-inducing ARCs.

The consequence of this model explains the whole plant response to stress (Figure 1.2B) where plants have leaves of a different age. The older, bottom leaves are more likely to senesce in response to stress than the younger leaves, while the reduced stress resistance of the middle leaves allow senescence to occur as a result of severe stress levels, but not in case of mild stress. The nutrients remobilised as a result of the senescence will then allow the highly stress-resistant young leaves to survive as long as possible.

The model has important shortcomings, including a lack of evidence that a decrease in stress resistance of individual leaves is actually programmed into the leaf developmental program. In addition, it is not clear if senescence-inducing ARCs actually exist or whether the chance to senesce is purely a result of reduced stress resistance. Moreover, what is the nature of the ARCs and how are they regulated? Nevertheless, I believe that it is a working model that explains certain aspects of the plant stress

response and highlights the importance of age in that response. I hope that future research into abiotic stress response will include the age factor and as such allow extension or modification of the model described here.

As sessile organisms, plants have evolved exceptional resistance mechanisms to cope with many abiotic stresses and most plants can survive a wide range of temperatures, water availabilities and light intensities. It is clear that ROS and phytohormones play important roles as stress sensors and signalling molecules in many abiotic stress responses. However, they play equally important roles in development and biotic stress responses. Recent omics approaches have helped reveal the complexity of the regulation of stress responses, yet we are still far away from fully understanding these. Nevertheless, it is clear that plants' ability to regulate the age-dependent life and death of individual organs is an important strategy to survive adverse environmental conditions. I hope that this review will stimulate future research to include the age factor as a hard-wired regulatory checkpoint for the life-death decision of plant organs in response to abiotic stress.

1.5 Thesis aims

Leaf senescence is a highly regulated and complex process involving a vast set of genes that interact through multiple signalling pathways (Breeze et al., 2011). So far, several studies have been performed to understand the processes that take place during senescence, however our knowledge is limited about the process that initiates senescence. In a number of research papers, it has been observed that leaves of different age show distinct responses to stress, however the biological mechanisms responsible for these different responses are poorly understood. The possible role of senescence-inducing age-related changes (ARCs) in stress resistance and senescence reviewed in the literature above, lead to my hypothesis that stress tolerance decreases in leaves with age due to gradual occurrence of senescence-inducing ARCs. The aim of study is also to find out genes that modulate senescence-inducing ARCs.

To test this hypothesis, the model plant *Arabidopsis thaliana* of Landsberg *erecta* (L*er*-0) accession was used to address the following aims:

1) Determine the occurrence of senescence-inducing ARCs by comparative transcriptome analysis of *Arabidopsis* early expanding, mid expanding and fully expanded first rosette leaves.

2) Determine the effect of senescence-inducing ARCs in *Arabidopsis* leaves of different ages. Plants in three different stages; when the first rosette leaves were in early expanding, mid expanding and fully expanded phase, will be exposed to drought, salinity shock and dark stress and the effects will be observed.

Transcriptomic results indicated that senescence-inducing ARCs gradually occur with age, leading to decreased stress resistance. The second objective of this thesis was to identify mutants regulating senescence-inducing ARCs. Previously, ***o****nset of* ***l****eaf* ***d****eath (old)* mutants were isolated using an ethylene-induced senescence screen which was found to cause stress sensitivity and early onset of senescence (Jing et al., 2005). Two of these mutants; *old13* and *old14*, were used in this study and characterised as to whether they are the regulators of senescence-inducing ARCs. My hypothesis was that the mutants regulating senescence-inducing ARCs will not show altered growth and development or early initiation of senescence, compared to the L*er*-0 plants, but will show sensitivity to stress treatments in an age-dependent manner.

To test these hypothesis, following objectives were established:

1) Identify altered growth and development of mutant plants compared to L*er*-0 by phenotypic analysis of plants grown in soil.

2) Determine whether the *old13* and *old14* mutants are regulators of senescence by performing physiological experiments and measuring the progression of senescence.

3) Determine whether the mutants are sensitive to stress by exposing plants to different stress conditions and observing the effects compared with the wild type L*er*-0.

The *old13* mutant which other than heightened stress sensitivity was not any different from L*er*-0, was selected for further studies. The third objective of this thesis was to determine the key senescence-inducing ARCs involved in stress sensitivity in *old13* plants and also identify the mutated *old13* gene using the next generation sequencing approach. It was hypothesized that mutation in the *old13* gene caused amplified senescence-inducing ARCs, making plants susceptible to stress conditions.

To test this hypothesis, the following aims were established:

1) Determine whether stress susceptibility increases with age in *old13* mutants by exposing plants of different developmental age: when first rosette leaves were in early expanding, mid expanding and fully expanded phase, to different stress conditions.

2) Determine the early occurring senescence-inducing ARCs in *old13,* by conducting transcriptomic studies in early expanding, mid expanding and fully expanded first rosette leaves, compared to the L*er*-0 leaves.

3) Identify the mutated gene causing early acquisition of ARCs in *old13* by next generation sequencing.

Chapter 2 Materials and Methods

2.1 Plant growth conditions for long and short-day photoperiods

The wild type (WT) *Arabidopsis thaliana* plants used in this study belong to the ecotype Landsberg *erecta* (L*er*-0). The ethyle methanesulfonate (EMS) mutant seeds were *old13* and *old14* both in L*er*-0 genetic background (Jing et al., 2005). The seeds were surface sterilized with 70% ethanol for 1 minute, followed by three rinses with sterile water for a minute each. For germination, the sterilized seeds were kept in 0.1% agarose and stratified at 4°C for 3 days. The seeds were sown in wet Seed Raising Mix® soil from Daltons. Relative humidity was maintained at 65%. Day length was 16-hours for long-day (LD) whereas, short-day (SD) experiments were carried out with 8-hours of light. Daytime and night-time temperature was maintained at 21°C. The average light intensity at the top of planted pots was around 180 µE.

2.2 RNA sequencing analysis

2.2.1 Sample harvest and RNA preparation

RNA sequencing dataset includes 3 time points of *Arabidopsis* L*er*-0 and *old13* first rosette leaves from 10 to 20 days after germination, at 5 day intervals. The first rosette leaves harvested 10, 15 and 20 DAG were in early expanding, mid expanding and fully developed phase, respectively. Three biological replicates were used for each time point. Samples were snap frozen in liquid nitrogen and RNA extraction was performed using an Ambion PureLink RNA-mini Kit (see https://www.thermofisher.com/ for the full protocol). Plant samples were ground to a fine powder using glass beads in a Precellys®24 homogenizer from Bertin instruments. A final volume of 30 µL RNA-containing solution was eluted from the spin cartridge tube. To maintain the integrity of the RNA, 0.25 µL RNase inhibitor (Thermo scientific) was added to the samples. To remove DNA from RNA samples, the Ambion TURBO DNA-free Kit was used. The reaction of 0.1 volume of 10 X TURBO DNase buffer, 1 µL of TURBO DNase and total RNA was mixed gently and incubated at 37 ºC for 20 minutes. DNase was deactivated by adding 0.1 volume of DNase inactivation reagent and incubating at room temperature for 5 minutes. The samples were centrifuged at 10,000 X g for 2 minutes and RNA was transferred to fresh tubes. A total of ~1 µg of RNA samples were sent to BGI Tech Solutions (Hong Kong) on dry ice for sequencing (HiSeq 4000 100 Paired end).

2.2.2 RNA sequencing analysis methodology

Raw sequencing reads were assessed for quality using FastQC and custom-made scripts (refer to Table 2.1). All the reads exhibited very high quality, and therefore did not require further filtering with respect to base quality. Reads were filtered for rRNA using SortMeRNA v2.1. Filtered reads were pseudoaligned to the *Arabidopsis thaliana* transcriptome (TAIR10), using kallisto v0.42.4 with 100 bootstraps. R-package Sleuth v0.28.1 was used for differential expression analysis. A gene was considered significantly differentially expressed if the $\log_2$ fold change >= 1 and q-value <= 0.1. Clustering of significantly differentially expressed genes was performed using pheatmap package in R/Bioconductor. Transcripts per million (TPM) values were used for plotting heat maps for selected set of genes. Saurabh Gupta from the University of Potsdam helped in the bioinformatics analysis of RNA-sequencing data.

Table 2.1 Read QC stats generated using an in-house script, after filtering for rRNA and pseudo alignment stats using kallisto v0.42.4.

Sample description	Reads	% reads having >= 75% bases >= Phred 20	rRNA filtered reads	% rRNA reads	Pseudo aligned reads	% Pseudo aligned reads
L*er*-0 10 days rep. 1	25,225,200	99.11	25,048,498	0.70	23,912,520	95.46
L*er*-0 10 days rep. 2	32,974,327	99.31	32,706,109	0.81	31,124,610	95.16
L*er*-0 10 days rep. 3	27,576,878	99.28	27,267,880	1.12	26,095,866	95.70
old13 10 days rep. 1	28,701,599	99.03	28,414,184	1.00	27,053,371	95.21
old13 10 days rep. 2	36,571,302	99.30	36,370,739	0.55	34,683,121	95.36
old13 10 days rep. 3	30,408,401	99.28	30,154,697	0.83	28,816,937	95.56
L*er*-0 15 days rep. 1	31,313,194	99.33	30,952,487	1.15	29,780,083	96.21
L*er*-0 15 days rep. 2	26,718,331	99.25	26,503,135	0.81	25,512,406	96.26
L*er*-0 15 days rep. 3	26,326,789	99.16	25,845,646	1.83	24,871,182	96.23
old13 15 days rep. 1	28,263,709	99.32	27,975,952	1.02	26,886,639	96.11
old13 15 days rep. 2	32,810,045	99.21	32,559,081	0.76	31,290,290	96.10
old13 15 days rep. 3	32,462,204	99.17	32,146,543	0.97	30,885,801	96.08
L*er*-0 20 days rep. 1	27,731,359	99.38	27,466,145	0.96	26,417,210	96.18
L*er*-0 20 days rep. 2	29,978,924	99.49	29,814,566	0.55	28,644,308	96.07
L*er*-0 20 days rep. 3	29,020,922	99.48	28,737,149	0.98	27,614,477	96.09
old13 20 days rep. 1	23,838,554	99.38	23,710,472	0.54	22,745,696	95.93
old13 20 days rep. 2	29,336,621	99.43	29,163,180	0.59	28,020,547	96.08
old13 20 days rep. 3	32,082,093	99.50	31,700,829	1.19	30,483,546	96.16

Rep. = Replicate.

Gene Ontology (GO) enrichment was performed by submitting the AGI codes of the selected genes into the Thalemine database (https://apps.araport.org/thalemine/begin.do). The following formula was used to calculate the ratio of enriched upregulated and downregulated genes specific to the functional groups shown in Figure 3.3, Figure 3.6 and Figure 5.8:

$$\text{Ratio of upregulated genes specific to the functional group} = \frac{\text{Number of upregulated genes}}{\text{Number of downregulated genes}}$$

$$\text{Ratio of downregulated genes specific to the functional group} = \frac{\text{Number of downregulated genes}}{\text{Number of upregulated genes}}$$

2.3 Transcript analysis using quantitative Real-Time PCR (qRT-PCR)

WT and *old13* plants were grown in LD photo cycles as described in section 2.1. The first rosette leaves were detached 10, 15 and 20 DAG and snap frozen in liquid nitrogen. Samples were ground to fine powder and total RNA was isolated using the Zymo Research Plant RNA Miniprep Kit (see http://www.zymoresearch.com/ for the full protocol), followed by DNase I treatment using a kit from Roche Applied Sciences. A reaction mixture containing 2.5 µg of RNA sample, 5 µL of 10 X incubation buffer and 10 units of recombinant RNase-free DNaseI was incubated at 37 ºC for 20 minutes. DNaseI was deactivated by adding 2 µL of 0.2M EDTA (pH 8.0) and incubating at 75 ºC for 5 minutes. The RNA samples were then converted to cDNA utilizing oligo (dT) primers, and using the transcription first strand cDNA synthesis Kit (Roche). Syber Green PCR master mix (Roche) was used for qRT-PCR reactions (Table 2.2) made up in LightCycler® 480 multi-well plates and for analysis, plates were placed into a LightCycler® 480 II instrument with a set programme outlined in Table 2.3.

Table 2.2 qRT-PCR reaction mixture

Component	Final Concentration
cDNA	10 ng
SYBR Green PCR master mix	5 µL
Reverse primer	10 pmol/µL
Forward primer	10 pmol/µL
Nuclease-free water	Up to 5 µL

Table 2.3 qRT-PCR programme

Steps	Temperature	Time	Cycle
Initial denaturation	95 ^{O}C	5 min	1
Amplification: Denaturation	95 ^{O}C	10 sec	
Annealing	60 ^{O}C	10 sec	35
Extension	72 ^{O}C	10 sec	
Melting curve	95 ^{O}C	5 sec	
	65 ^{O}C	1 min	1
	97 ^{O}C	4 min	
Cooling	40 ^{O}C	30 sec	1

EXOR software was used for raw data analysis and LinRegPCR software was used for primer efficiency measurements and calculating quantification cycles (Cq). The *ACTIN 2* (*ACT2*), *TUBULIN BETA-2* (*TUB2*) and *UBIQUITIN-PROTEIN LIGASE 7* (*UPL7*) genes were used as reference genes. The Quant prime (Arvidsson et al., 2008) tool was used to design the primers listed in Appendix 6. Relative mRNA expressions were determined using the following calculation (Pfaffl, 2004):

$$R = \frac{Eff^{(Cq_{calibrator} - Cq_{sample})}\ \text{Gene of interest}}{Eff^{(Cq_{calibrator} - Cq_{sample})}\ \text{Housekeeping gene}}$$

R = relative expression
Cq = qRT-PCR quantification cycle
Eff = primer efficiency

The relative expression of genes (*RBOHD, WRKY53* and *SAG13*) in L*er*-0 10, 15 and 20DAG leaf sample shown in Figure 3.7 (Chapter 3) and Figure 5.5 (Chapter 5) are same, as the qRT-PCR experiment was performed on the samples harvested same day and the same time.

2.4 Measurement of field capacity (FC)

For the drought stress treatment, FC of the pots was measured before planting. The weight of the pots with soil (total solid mass) was measured and then well saturated with water and left overnight. The next day, the pots with wet soil were weighed and recorded (total solid mass before drying). By the end of the drought stress the soil weight in the pots (total solid mass after drying) was measured again. The percentage of field capacity of the pots was measured using the formula:

$$FC\ \% = \frac{\text{Total solid mass before drying - Total solid mass after drying}}{\text{Total solid mass}} X100$$

2.5 Watering schedule during drought stress and salt shock treatments

For the drought stress experiments, germinated plants were well watered every alternate day but water was withheld after 10, 15 and 20 DAG, for 6 days. After 6 days of drought stress the samples were used for analyses.

For the salt shock experiments, before 10, 15 and 20 DAG, plants were watered normally, but on 10, 15 and 20 DAG, plants were watered with 300 mM NaCl every alternate day. After 6 days of salt shock, young, mature and adult plant samples were used for analyses.

2.6 Measurement of leaf relative water content (RWC)

To assess the water status of drought-stressed plants RWC was measured by the method from Yamasaki and Dillenburg (1999). The drought-stressed leaves were harvested and weighed immediately to obtain the fresh mass (FM). The leaves were then floated in distilled water and incubated for 4-hours to obtain the turgid mass (TM). After 4 hours the leaves were gently wiped with tissue paper and weighed. Then, samples were placed in a pre-heated oven at 80 °C for 24-hours to determine the dry mass (DM). The values of FM, TM and DM were used to calculate the RWC from the formula:

$$RWC\ \% = [(FM-DM)/(TM-DM)]\ X\ 100$$

The drought stress treatment on L*er*-0 and *old13* plants were performed as part of a single experiment. Therefore, data of FC and RWC measured together with the pictures taken of control and drought-stressed L*er*-0 is used in Chapter 3 (Figure 3.9) as well as in Chapter 5 (Figure 5.3).

2.7 Whole plant dark and recovery treatment

For the dark stress experiment mentioned in Chapter 4, the 20 DAG mutants and WT plants were shifted into a box to stimulate dark conditions at a temperature of 21 °C for 2, 4 and 6 days. After 2 and 4 days of dark stress, the plants were shifted into a LD photoperiod for a 3 day recovery, as mentioned in section 2.1.

For the dark experiment mentioned in Chapter 3 and Chapter 5, the WT and *old13* plants at 10, 15 and 20 DAG were shifted into a box to stimulate dark conditions at a temperature of 21 °C for 4 days. After 4 days of dark treatment, the plants were shifted into a LD photoperiod for a 3 day recovery period, as mentioned in section 2.1.

The dark stress treatment on L*er*-0 and *old13* plants were performed as part of a single experiment. Therefore, data of chlorophyll level measured together with the pictures taken of control and dark-stressed L*er*-0 is used in Chapter 3 (Figure 3.12) as well as in Chapter 5 (Figure 5.4).

2.8 Chlorophyll quantification

During pigment extraction, the most widely used chemicals; acetone or ethanol, cause artefactual chlorophyllide production. Therefore, they potentially generate erroneous results, by decreasing the content of chlorophyll in extracts (Hu et al., 2013). Hence, to measure the chlorophyll level, a method of Wellburn published in 1994 using DMF (N, N'-dimethylformamide) was adapted. The first rosette leaf pairs were ground in liquid N_2 and re-suspended into DMF solution. Plant material was homogenized and vortexed in 100 volumes (fresh weight basis) of DMF and incubated overnight in darkness at 4 °C. The samples were centrifuged at 2500 X g for 5 minutes and supernatant was used to quantify chlorophyll contents spectrophotometrically at 647 nm and 664 nm wavelengths. The formula used to measure chlorophyll was:

$$\text{Chl } b = \quad 20.7\ OD_{647} - 4.62\ OD_{664}$$

$$\text{Chl } a = \quad 12.7\ OD_{664} - 2.79\ OD_{647}$$

$$\text{Total Chl} = 17.9\ OD_{647} + 8.08\ OD_{664}$$

2.9 Electrolyte leakage measurement

First and second rosette leaf pairs were used to measure the cell membrane stability by the method adapted from Campos et al. (2003). Leaves were detached and rinsed three times with demineralized water for about 2-3 minutes. Then, in 50 mL falcon tubes, samples were immersed in 10 mL demineralized water and shaken at 180 rpm for 30 minutes at 25 °C. The electrolyte leakage in the solution was measured using a conductivity-meter model E527 (Motrohm Herisau). Total conductivity was measured after the sample boiled for 10 minutes. Results were expressed as the percentage of total conductivity, an indicator of membrane stability.

2.10 Histochemical detection of H_2O_2 by DAB staining

To detect hydrogen peroxide, first and second rosette leaves were stained with DAB (3, 3'-diaminobenzidine) according to the method adapted from Thordal-Christensen et al. (1997) and Daudi et al. (2012).

Preparation of 50 mL DAB staining solution in 0.05 M Tris acetate (pH 5): 0.302 g of Tris base was weighed and dissolved in 50 mL of distilled water. The pH was adjusted to 5 with glacial acetic acid. Fifty mg of DAB was dissolved in the above 50 mL 0.05 M Tris acetate solution. The solution was covered with aluminium foil as DAB is light sensitive. The solution was kept overnight on a stirrer to dissolve DAB.

Bleaching solution: Ethanol 200 mL, glycerol 50 mL, lactic acid 50 mL (4:1:1).
Staining leaves with DAB solution: The first and second rosette leaf pairs were detached and placed in 50 mL falcon tubes, and labelled accordingly. The DAB solution was added to the tubes, and the volume was adjusted to ensure that all the leaves were immersed. The leaves were vacuum-infiltrated by placing the falcon tubes in a desiccator and applying gentle vacuum pressure of about -25 kilopascals for 5-10 minutes. The tubes were placed on a standard laboratory shaker for 4-5 hours at 100 rpm. Following incubation, the DAB staining solution was replaced with bleaching solution. (Ethanol: glycerol: lactic acid 4:1:1). The falcon tubes were placed in a boiling water bath for 15 minutes. This bleaches the chlorophyll but leaves a brown precipitate formed by DAB reacting with hydrogen peroxide. After boiling, the bleaching solution was replaced with fresh bleaching solution and the DAB stained leaves were visualized under a microscope.

2.11 Leaf starch assay

To measure starch levels, a method from Yu et al. (2001) was adapted. The reagents used are:
Killing solution: Ethanol 160 mL, Formic acid 10 mL, distilled water 30 mL (Final concentration- ethanol 80%, formic acid 5%, distilled H_2O 15%).

Lugol's IKI solution: Iodine 5.7 mM, Potassium Iodide 43.3 mM (Reagent is light sensitive, bottle was wrapped with aluminium foil) and kept at 4 °C.

Ethanol 80%

The killing solution was added to the detached leaves and kept at 90 °C for 10 minutes. Then, the killing solution was replaced with 80% ethanol and incubated for 5 minutes at 90 °C. The leaves were then placed in a petri plates and to stain the starch in leaves Lugol's IKI solution was added for 5 minutes, and then finally washed with distilled H_2O.

2.11.1 Quantifying stained starch area by image J software

The percentage of total stained starch area in the leaf tissue was calculated by Image J software version 1.47v. The staining area was assessed by setting a "threshold" using the thresholding tool by selecting image >adjust> colour threshold. The total area was measured by adjusting the Hue and Saturation to full, and adjusting the Brightness bar to a point at which all tissue is selected. After this, the selected area was measured by selecting Analyse > Measure. The measured total area was recorded into an Excel sheet. To measure the stained area, without changing the brightness bar, the Hue bar was decreased until only the stained area was selected (the Saturation and Brightness bar was adjusted to fine tune). The selected area was then measured and recorded into an excel worksheet. The recorded total area and stained area were used to quantify the percentage of stained area. The formula used was:

Stained area/Total area X 100%

2.12 Metabolomic profiling and GC-MS analysis

First rosette leaf pairs were detached 10, 15 and 20 DAG from L*er*-0 and *old13* plants grown in LD photoperiod (section 2.1) and were then snap frozen in liquid nitrogen. Five biological replicates were used for each sample. Samples were ground to fine powder using glass beads in Precellys®24

homogenizer from Bertin instruments and 50 mg of ground tissue was sent in screw cap Eppendorf tubes stored at -80°C to Max Planck Institute (MPI) of Germany for Gas-Chromatography-Mass Spectrometry (GC-MS) analysis.

Plant material (50 mg) was extracted in 700 µL 100% methanol (+ 20 µL from the internal standard solution (Ribitol: 0.2 mg/mL)) at 70 °C for 15 minutes. Following centrifugation at 20,800 X g for 10 minutes, chloroform (375 µL) and water (750 µL) were added and mixed well with the supernatant. Following a second centrifugation at 15,300 g for 15 min., the clear supernatants (300 µL) were dried overnight under vacuum. Residues were then derivatized for 120 minutes at 37 °C in 40 µL of 20 mg/mL methoxyamine hydrochloride in pyridine, followed by 30-minutes treatment at 37 °C with 70 µL of MSTFA. The GC-MS system used was a gas chromatograph coupled to a time-of-flight mass spectrometer (Leco Pegasus HT TOF-MS). An auto-sampler (Gerstel Multi-Purpose system) injected the samples. Helium was used as carrier gas at a constant flow rate of 2 mL/s and gas chromatography was performed on a 30 m DB-35 column. The injection temperature was 230 °C and the transfer line and ion source were set to 250 °C. The initial temperature of the oven (85 °C) was increased at a rate of 15 °C/minute up to a final temperature of 360 °C. After a solvent delay of 180 s, mass spectra were recorded at 20 scans/s with m/z 70-600 scanning range (Kerchev et al., 2016). Chromatograms and mass spectra were evaluated by using Chroma TOF 4.5 (Leco), TagFinder 4.2 software (Luedemann et al, 2008) and Xcalibur 2.1 (Thermo Fisher Scientific, Waltham, MA, USA). MPI Golm Metabolome Database (GMD, http://gmd.mpimp-golm.mpg.de) was used for quantification and annotation of the peaks (Kopka et al, 2005). Metabolomic data was analysed and heat maps were produced using MeV software. Prof. Alisdair Fernie and Dr Maria Benina from MPI kindly helped in metabolomic profiling.

2.13 Sucrose and dark treatment on first rosette leaves

At 18 DAG, first rosette leaf pairs from WT and *old13* plants were detached using a scalpel and placed on Petri dishes layered with Whatmann-filter paper saturated with 2%, 4%, 6% sucrose and distilled water (as a control). The Petri dishes were placed in a closed box to maintain dark conditions for 2 days. The leaves were subsequently used for analyses.

2.14 Extraction of nuclear genomic DNA by the method of Lutz et al., (2011)

2.14.1 Nuclei extraction

0.2 g of plant tissue was flash frozen in liquid nitrogen and ground to a fine powder. Thirty mL of extraction buffer 1 (0.4 M sucrose, 10 mM Tris, pH 8, 10 mM $MgCl_2$, 5 mM β-mercaptoethanol) was added to the ground tissue and the solution was filtered through Mira cloth. The samples were centrifuged at 4000 rpm (1940 X g) for 20 minutes at 4 ºC. The supernatant was removed and pellet was re-suspended in 1 mL of chilled extraction buffer 2 (0.25 M sucrose, 10 mM Tris, pH 8, 10 mM $MgCl_2$, 1% Triton X-100, 5 mM β-mercaptoethanol) and centrifuged at 12,000 X g at 4 ºC for 10 minutes. The pellet was re-suspended in 300 µL of chilled extraction buffer 3 (1.7M sucrose, 10 mM Tris, pH 8, 2 mM $MgCl_2$, 0.15% Triton X-100, 5 mM b-mercaptoethanol), another 300 µL of chilled extraction buffer 3 was placed in a clean 1.5 mL Eppendorf tube. The pellet was then re-suspended by gentle pipetting and transferred to the new tube of extraction buffer 3, and centrifuged at 14,000 X g for 1 hour at 4 °C.

2.14.2 DNA precipitation

The nuclear pellet was re-suspended in 720 µL TE buffer (10 mM Tris-HCl, pH 8, 1 mM EDTA, pH 8) and the samples were treated with RNase by adding 16 µL of 5 M NaCl, 64 µL of water and 10 µL of 5 mg/mL RNase and incubated at 65 ºC for 30 minutes. The DNA samples were then treated with Proteinase K by adding 80 µL 10% SDS and 12 µL 10 mg/mL Proteinase K and incubated at 45 ºC for 1 hour. Next, the DNA was cleaned and precipitated by adding 800 µL phenol: chloroform to lysate and centrifuged for 2 minutes. To remove traces of phenol from the samples, chloroform extraction was performed by adding 1 volume of chloroform to the supernatant from above. For DNA precipitation, 80 µL of 3 M NaOAc (1/10 volume) and 880 µL of isopropanol (1 volume) was added to 800 µL of supernatant from above and centrifuged for 30 minutes at 13,000 rpm at 4 ºC. The pellet was washed with 70% ethanol two times by centrifuging for 10 minutes at 13,000 rpm at 4 ºC. DNA pellet was air-dried at room temperature for 10 minutes and re-suspended in 50 µL TE (10:0.1). The samples were run on 0.8% agarose gel against lambda DNA of known concentrations. To visualise DNA in agarose gel, 2 µL of 10 mg/mL ethidium bromide was added to the gel.

2.15 A hybrid method of CTAB and nuclear DNA extraction to isolate nuclear-enriched genomic DNA for the next generation sequencing of *Arabidopsis*

2.15.1 Solutions

Extraction Buffer 1 For 100 mL: 20 mL of 2 M sucrose, 1 mL of 1 M Tris-HCl (pH 8.0), 1 mL of 1 M $MgCl_2$, 35 µL of 14.3 M β-Mercaptoethanol (added before use) and the volume made up to 100 mL with sterile water.

Extraction Buffer 2 For 10 mL: 1.25 mL of 2 M sucrose, 100 µL of 1 M Tris-HCl (pH 8.0), 100 µL of 1 M $MgCl_2$, 100 µL 100% Triton X-100, 3.5 µL of 14.3 M β-Mercaptoethanol (added before use) and the volume made up to 10 mL with sterile water.

Extraction Buffer 3 For 10 mL: 8.5 mL of 2 M sucrose, 100 µL of 1 M Tris-HCl (pH 8.0), 20 µL of 1 M $MgCl_2$, 15 µL of 100% Triton X-100, 3.5 µL of 14.3 M β-Mercaptoethanol (added before use) and the volume made up to 10 mL with sterile water.

Sodium bisulfide extraction buffer For 1 litre solution: 100 mL of 1 M Tris HCl (pH 7.5), 10 mL of 0.5 M EDTA (pH 8.0) and 63.8 g sorbitol added to sterile water and made up to 1 litre. Just before use, add 38 mg of sodium bisulfide ($Na_2S_2O_5$) to 10 mL of extraction buffer (to make the solution of 20 mM sodium bisulfide).

CTAB Nuclear Lysis Buffer For 100 mL: 20 mL of 1 M Tris HCl (pH 7.5), 10 mL of 0.5 M EDTA (pH 8.0), 40 mL of 5 M NaCl and 2% CTAB (pH 7.5) added to the sterile water and made up to 100 mL. (CTAB does not solubilize well, so mix overnight on stirrer).

TE pH 8.0 10 mM Tris HCl/0.1 mM EDTA

Tris buffered phenol 250 g phenol crystals were dissolved in 100 mL water containing 0.25 g (0.1% w/v to phenol) of hydroxy quinoline. Hundred mL 0.5 M Tris HCl (pH 8.0) was mixed for ~15 min with the phenol. After phase separation, the upper layer was discarded and the procedure repeated with 0.1 M Tris HCl to produce ~1 cm layer of Tris on the top layer above the phenol, and the phenol stored at 4°C in the dark. The pH of buffer saturated phenol should be ≤ 7.5 for DNA extraction.

PCI Phenol: chloroform:isoamyl alcohol (25:24:1)

All extraction buffers were stored at 4 °C.

2.15.2 Procedure

Around 2 g of 20-day old fresh leaf material was snap frozen and ground to a very fine powder in liquid nitrogen (I preferred using fresh tissue for genomic DNA (gDNA) isolation as less shearing of the gDNA was observed). The tissues were transferred to 50 mL falcon tubes and 20 mL of chilled

extraction buffer 1 was added and vortexed to re-suspend the plant material, and then filtered through double-layered Mira cloth into a sterile 50 mL falcon tube. The crude extract was centrifuged at 1,940 X g for 20 minutes at 4 °C, and the supernatant was discarded. The pellet was re-suspended in 1 mL of extraction buffer 2, containing triton X-100 for preferential elimination of chloroplasts and spun at 12,000 X g for 10 minutes at 4 °C. The supernatant was discarded and the nucleus-containing pellet was re-suspended in 300 µL of chilled extraction buffer 3. Using a plastic pestle all the cell clumps were broken down and gently transferred into 300 µL of extraction buffer 3 in sterile 1.5 mL Eppendorf tubes followed by centrifugation at 14,000 X g for 1 hour at 4 °C. After discarding the supernatant, 200 µL sodium bisulfide extraction buffer, 300 µL CTAB nuclei lysis buffer and 100 µL 5% sarkosyl were added to the pellet and incubated at 65 °C for 1 h to lyse the nuclei. The viscous solution was mixed with a 1 mL pipette and vortexed for 10 seconds. After this step 600 µL of phenol, chloroform and isoamyl alcohol (25:24:1) were added to the lysate and mixed gently by inversion for ~2 minutes. This step was repeated followed by centrifugation at 21,980 X g for 2 minutes. The supernatant was then transferred to a new tube with 1 volume of chloroform and mixed for 2 minutes by inversion and centrifuged for 2 minutes to remove any traces of phenol. The supernatant containing DNA was digested with 5 µL of 10 mg/mL RNase A to remove RNA contamination and incubated at 37 °C for 1 hour. Then, the DNA was precipitated with an equal volume of chilled isopropanol and 1/10 volume of 3 M NaOAc followed by incubation for 30 minutes on ice, and finally centrifuged at 21,980 X g for 30 minutes at 4 °C. The DNA pellet was washed twice with 70% ethanol by centrifuging for 10 minutes at 19,350 X g at 4 °C. The DNA was air dried and then dissolved in 50 µL of TE (10:0.1). 1 µL of extracted gDNA was run on 0.8% agarose against lambda DNA of known concentration. To visualise DNA in agarose gel, 2 µL of 10 mg/mL ethidium bromide was added to the gel. The quantity of DNA was checked on a Nano-Drop 1000 spectrophotometer and sent for qubit florometer quantification to check the quality (by overnight courier in parafilm-sealed 1.5 mL Eppendorf tubes at 4 °C). Typically, 2-4 µg gDNA was obtained from 2 g leaf tissue.

2.16 Whole genome sequencing

2.16.1 *old13* and *old14* nuclear-enriched genomic DNA sample submission for Illumina sequencing

To identify the mutated gene in *old* mutants, gDNA extracted from *old13* and *old14* plants were sent for whole genome sequencing. Approx. 2.5 µg gDNA of *old13* and *old14* mutants, at a concentration of at least 20 ng/µl was prepared and sent to Massey Genome Service (MGS) to prepare an Illumina TruSeq DNA PCR-Free library of *old13*. This was then sent to the Otago Genomics and Bioinformatics

Facility (OGBF), to run on an Illumina HiSeq lane, on a 2 X 100 base PE run. DNA samples of *old14* were sent to OGBF for Illumina Nextera Mate Pair Library preparation with an insert size of 8 Kb.

2.16.2 Alignment and visualisation of sequenced reads

The genomic sequence of L*er*-0 was downloaded from TAIR. Bowtie 2 tool was used to map reverse and forward raw reads of the *old13* whole genome sequence to the reference genome of L*er*-0. Using Bowtie 2, L*er*-0 reference was indexed and then the PE sequences of *old13* were mapped separately to the index-generated reference sequence (Langmead and Salzberg 2012). The output file with aligned reads to L*er*-0 was in SAM (Sequence Alignment Map) format. Using samtools, the SAM file was converted to BAM (Binary Alignment Map) and BAM into the sorted BAM files. The command lines used to convert the files are shown below:

#samtools to convert sam to a bam file
samtools view –bT Reference file.name.sam > file.name.bam

#sort the file
samtools sort file.name.bam file.name.sorted

#index file
samtools index file.name.sorted.bam

To visualise the aligned genomic data, integrative genomics viewer (IGV) software was downloaded from https://software.broadinstitute.org/software/igv/download (Thorvaldsdóttir et al., 2013) and sorted.bam files were uploaded to detect the single nucleotide polymorphisms (SNPs) present in the *old13* genome. Dave Wheeler and Mauro Truglio from MGS kindly provided the bioinformatics support and the knowledge that helped in working with the whole genome data.

2.16.3 Processing NIKS script

The NIKS (needle in a K-stack) script (Hunter et al., 2018) was processed with the kind help of Mauro Truglio. NIKS created a list of contigs of around 100-200 base pair in size having SNPs which was used as a search template for nucleotide BLAST to detect the position on the chromosome and to identify whether the change in base pair is causing a mutation of a gene or not. For the SNPs present in the protein coding region, the stability of the protein was predicted using CUPSAT tool (http://cupsat.tu-bs.de/).

Chapter 3 Transcriptomic changes in *Arabidopsis* leaves suggest possible causes for loss of stress tolerance with age

3.1 Introduction

During normal plant development, sequential changes in development and metabolism occur during the transition from germination to senescence and death. The progressive changes that occur during plant development are termed age-related changes (ARCs) (Thomas, 2002). Examples of visible ARCs in plants are the transition of leaves from juvenile to adult phase, initiation of the reproductive phase, yellowing of senescing leaves etc. Endogenous ARCs include cell division, cell elongation, cell expansion, change in hormones, ROS overproduction, degradation of cellular components and many more. The growth stages that start from leaf emergence and go to expansion, maturation and eventually senescence, are all achieved through the action of ARCs. After the plants reach a certain level of growth, the gradual occurrence of ARCs leads to the progressive decline of cell and tissue function that results in leaf senescence (Caswell and Salguero-Gomez, 2013). Therefore, it is possible that some ARCs play specific roles in age and senescence and could be termed senescence-inducing ARCs.

Ageing is an irreversible and deleterious process where plants age and enter the last phase of life, known as senescence (Jing et al., 2003). Ageing can be initiated earlier in plants if they are exposed to unfavourable environmental conditions. For instance, during drought, salinity or nutrient deficiency, plant growth is rapidly reduced and the onset of senescence is initiated earlier than normal (Buchanan-Wollaston 1997). In such stressed environments, plant ageing is initiated earlier to ensure that reproduction is achieved, therefore early seed development is observed. However, in acute stress conditions, plants may not survive long enough to progress to seed development and may die without reproducing (Xu et al., 2010). Hence, ageing is a degenerative process driven by both endogenous and exogenous factors (Jibran et al., 2013).

While many studies have focused on transcriptomic and metabolomic changes during the senescence process, pre-senescence changes have not been well studied. Therefore, this research attempts to examine the occurrence of pre-senescence ARCs and their effects in *Arabidopsis* leaves of different ages. Firstly, the transcriptomic datasets of first rosette early expanding leaves (EEL) 10 days after germination (DAG), mid expanding leaves (MEL) 15 DAG and fully expanded leaves (FEL) 20 DAG were analysed to reveal the global picture of ARCs function/expression. The analysis of differentially expressed genes showed that leaf maturation coincides with a marked downregulation of genes involved in DNA repair, while genes involved in stress hormone biosynthesis and signalling and those indicative

of oxidative stress, were upregulated. Next, to identify the effect of senescence-inducing ARCs in different aged leaves, stress-induced experiments were performed on *Arabidopsis* plants after 10, 15 and 20 days after germination, before the initiation of flowering. The results of experiments suggest that plants lose stress tolerance as they get older, and indicate a role for senescence-inducing ARCs in stress resistance. This study suggests that 10 DAG plants are more tolerant to stress because of negligible senescence-inducing ARCs in EEL, whereas the gradual occurrence of senescence-inducing ARCs in MEL and FEL result in decreased stress tolerance. Moreover, reduction of DNA damage protection and stress tolerance, appear to be intrinsically coupled to ageing, ensuring a timely and certain death.

3.2 Results

3.2.1 The global picture of ARCs taking place in different aged *Arabidopsis* leaves

The extensive research performed on *Arabidopsis* has increased knowledge of the senescence process in monocarpic plants, however, the pre-senescence process is not well studied. Therefore, in this section the ARCs taking place in differentially aged *Arabidopsis* leaves prior to the onset of senescence, were identified. Comparative transcriptome analysis using RNA sequencing was performed to elucidate the global picture of ARCs in *Arabidopsis*.

For RNA sequencing, three developmental stages of *Arabidopsis* plants grown in a long-day (LD) photoperiod were selected at 10, 15 and 20 DAG, before the initiation of the reproductive phase. These different ages were selected based on the first rosette leaf growth, where 10 DAG EEL attained a size of 4 mm (Figure 3.1A, B). Whereas, MEL were selected 15 DAG (7 mm) based on the leaf size being twice the size of EEL, and half the size of FEL. The FEL were selected at 20 DAG because at this stage the first rosette leaf pair has reached its final size and will not exceed more than ~10 mm longitudinally (Figure 3.1A, B).

Total RNA was extracted from *Arabidopsis* WT, 10 DAG, 15 DAG and 20 DAG first rosette leaf samples (EEL, MEL, FEL) and sequenced using Illumina HiSeq 4000. Three replicates were used for each leaf stage. A comparison of 15 and 20 DAG leaf transcripts with 10 DAG leaf samples was performed to observe gene expression changes from EEL to MEL and FEL samples. The heat map (Figure 3.2) represents clusters of 4813 differentially expressed genes and shows significant differences in gene expression patterns between EEL, MEL, and FEL first rosette samples. Out of 4813 differentially expressed genes, 2230 were downregulated, while 2583 were upregulated. The heat map indicates that in 10 DAG leaves, the genes in clusters 1, 5, 6, 8, 9, 10, 15 and 18 were upregulated, while in 15 and 20 DAG leaf samples, these genes were downregulated. Similarly, the genes in clusters 7, 14, 4, 16 and 19 were initially downregulated in 10 DAG leaf samples, but were later upregulated in 15 and 20 DAG samples. The expression of genes in clusters 2, 3, 12, 13, 20, 11 and 17 are low in 10 DAG and 15 DAG leaf samples, but highly expressed in 20 DAG samples. Thus, these results suggest global patterns of ARCs taking place in first rosette EEL, MEL and FEL samples.

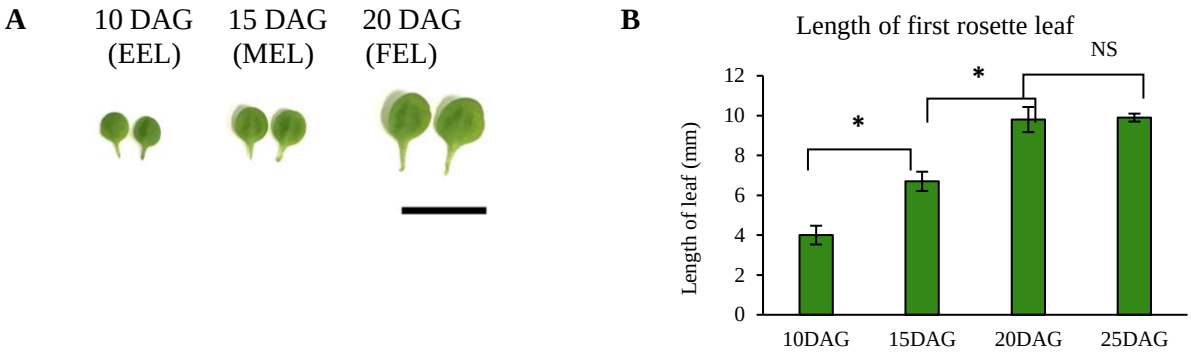

Figure 3.1. Age of first rosette leaf pair selection.
A. *Arabidopsis* wild type first rosette leaf pairs detached from plants after 10, 15 and 20 days after germination (DAG). Scale bar represents 10 mm. **B.** The length of first rosette EELs (Early Expanding Leaves), MELs (Mid Expanding Leaves) and FELs (Fully Expanded Leaves) were measured after 10, 15, 20 and 25 DAG respectively, and grown under LD photoperiod. * indicates the values are significant at $p \leq 0.05$ using a Student's t-test between the indicated values; NS- not significant.

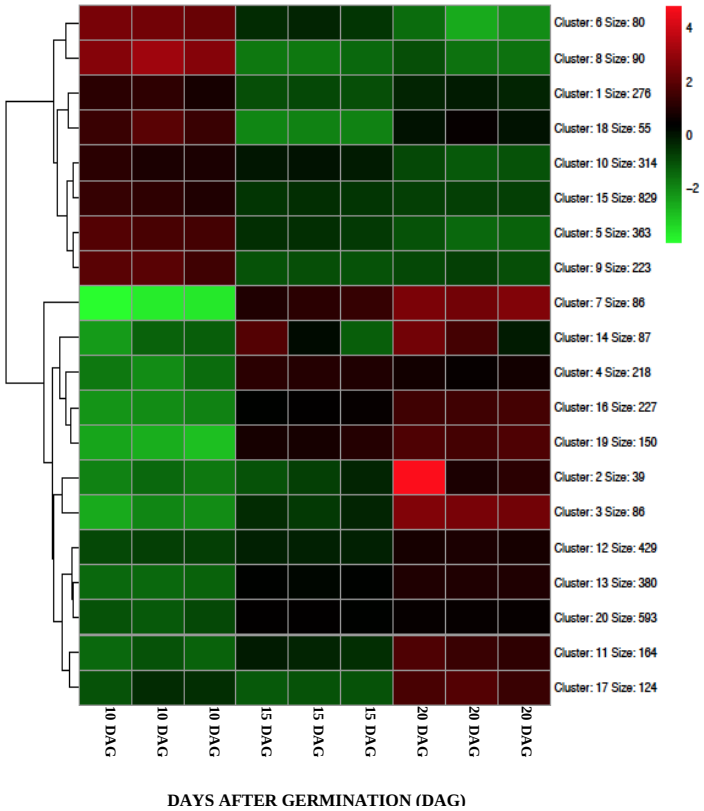

Figure 3.2. Heat map depicting gene expression of *Arabidopsis* WT EEL (10 DAG), MEL (15 DAG) and FEL (20 DAG) first rosette samples.
The heat map illustrates the expression profile of genes from leaf samples at 10, 15 and 20 days after germination (DAG). Three biological replicates were used for each sample. Red represents high gene expression, green represents low gene expression, and black or darker shades show intermediate levels of expression. Values of colour scale are in $\log_2$.

3.2.2 Gene Ontology enrichment of differentially expressed genes in *Arabidopsis* leaves

It was suggested that initiation of leaf senescence depends on the accumulation of ARCs (Jibran et al., 2013; H.C. Jing et al., 2005), and these ARCs could be termed as senescence-inducing ARCs. In the above section, the RNA sequencing data revealed global changes taking place in *Arabidopsis* first rosette leaves before the onset of senescence (section 3.2.1). Next, the differentially expressed gene profiles enriched in specific functions were identified to discover the senescence-inducing ARCs that accumulate with age. As the leaf grows, changes in expression of genes related to growth and development can be observed, furthermore, gradual changes in key biological pathways that lead up to senescence are also expected.

Gene Ontology (GO) enrichment was performed by submitting the AGI codes of the differentially expressed genes into the Thalemine database (https://apps.araport.org/thalemine/begin.do). The ratio of upregulated and downregulated genes of specific functional groups in 15 and 20 DAG leaf samples are shown in Figure 3.3. The functional groups that are significantly downregulated are associated with cell cycle, cellular component organisation, growth regulation, defense response, DNA repair, gene regulation and biosynthesis of cell constituents. While the functional groups enriched in the upregulated gene category are related to cell growth regulation, oxidation-reduction, stress response, photosynthesis, signal transduction, transport activity, hormone response pathway and antioxidant activity (Figure 3.3). Since my aim was to focus on senescence-inducing ARCs, further study will not include any detailed analysis on genes linked to growth and development of a leaf such as cell cycle, cell growth and maintenance, cell wall organisation, cellular component organization and degradation, growth and gene regulation, oxidation-reduction, photosynthesis, signal transduction, transcription factors, transport activity, biosynthesis of cell constituents, others and unknown genes.

The graph in Figure 3.3 shows that the highest ratio of downregulated genes is related to DNA repair mechanisms in 15 and 20 DAG first rosette leaves. In comparison, the highest ratio of upregulated genes is related to stress (700/741) in 15 and 20 DAG leaf samples. Notably, the ratio of upregulated genes associated with hormones is two-fold up. As plant hormones have a wide range of functions in growth and development, a detailed study on each class of hormones may suggest what changes are taking place in differentially aged leaves. Therefore, results from the GO enrichment analysis pinpoints the crucial functional gene categories of DNA repair, stress and hormones as senescence-inducing ARCs that gradually accumulate as the *Arabidopsis* leaves grow older.

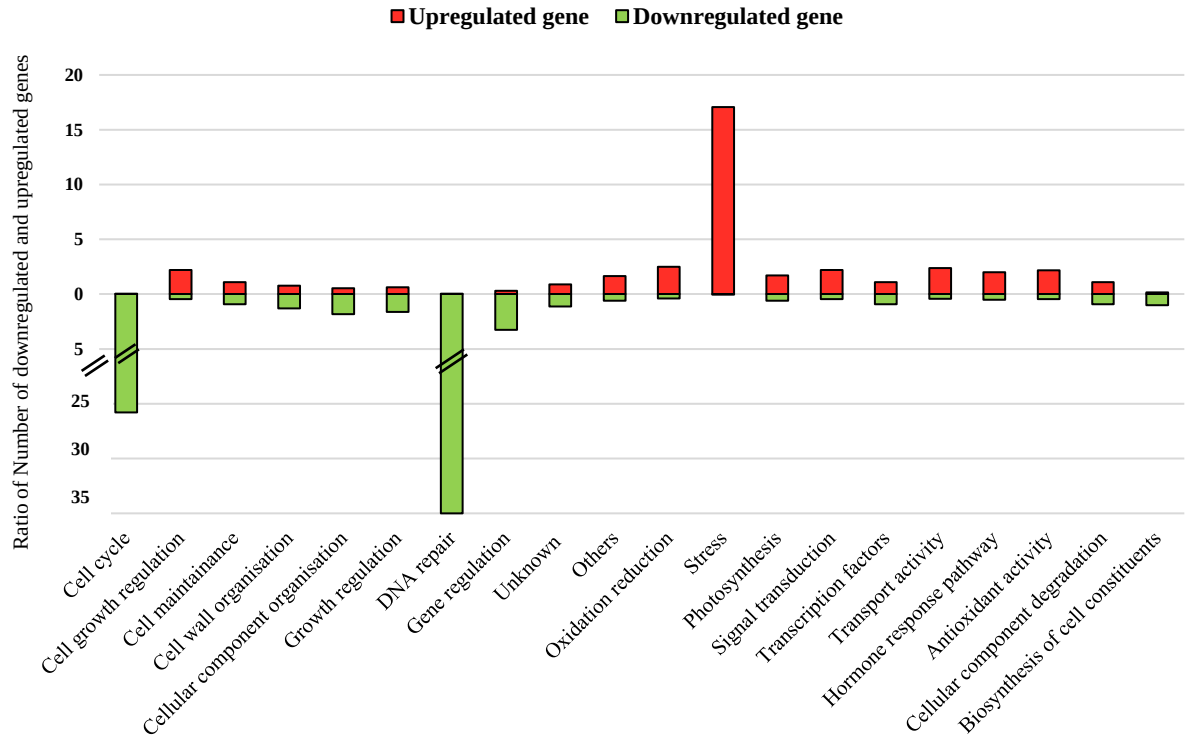

Figure 3.3. Gene Ontology (GO) enrichment of differentially expressed genes.
This graph illustrates the ratio of total up and downregulated genes enriched in specific biological functions. Green bars represent downregulated genes and red bars indicates upregulated genes. Black bars represent the axis break.

3.2.3 Examination of key senescence-inducing ARCs in *Arabidopsis*

In the previous section, overall gene expression changes of distinct biological functions were examined in three different leaf stages. A highly informative gene class screened from the broad group of downregulated genes was associated with DNA repair mechanisms. On the contrary, the large class of upregulated genes was found to be related to functions in stress and hormones. In this section, the genes associated with DNA repair, stress and hormones are studied in detail to identify possible regulatory genes and pathways involved in senescence-inducing ARCs.

3.2.3.1 Downregulation of DNA repair mechanisms with age in *Arabidopsis*

Spontaneous DNA damage caused by endogenous factors is protected by DNA repair mechanisms in plants (Singh et al., 2010). From RNA sequencing data, 34 differentially expressed genes were found to be involved in DNA repair mechanisms, and all showed decreased expression in MEL and FEL samples. The heat map in Figure 3.4 shows that genes linked to DNA repair are upregulated in 10 DAG samples, and downregulated in 15 and 20 DAG samples. Of these 34 DNA repair associated genes, two are associated with breast cancer suppressor proteins found in mammals; *BRCA2(IV)* and *BARD1*,

which both play an important role in DNA damage repair (Reidt et al., 2006; Siaud et al., 2004). Also, *RAD51* and a paralog, *RAD51B* which function in DNA repair via homologous recombination, were found to be downregulated in MEL and FEL samples (Li et al., 2007; Wang et al., 2014). Other important DNA repair genes that were downregulated in MEL and FEL samples are *DDB1B, MRE11, RECA2, WHY1, RPA70B* and *RPA70D* (Bernhardt et al., 2010; Bundock and Hooykaas, 2002; Miller-Messmer et al., 2012; Takashi et al., 2009; Yoo et al., 2007). Taken together, the gene transcripts associated with DNA repair mechanisms are high in 10 DAG leaves and their expression declines with age in 15 and 20 DAG leaves.

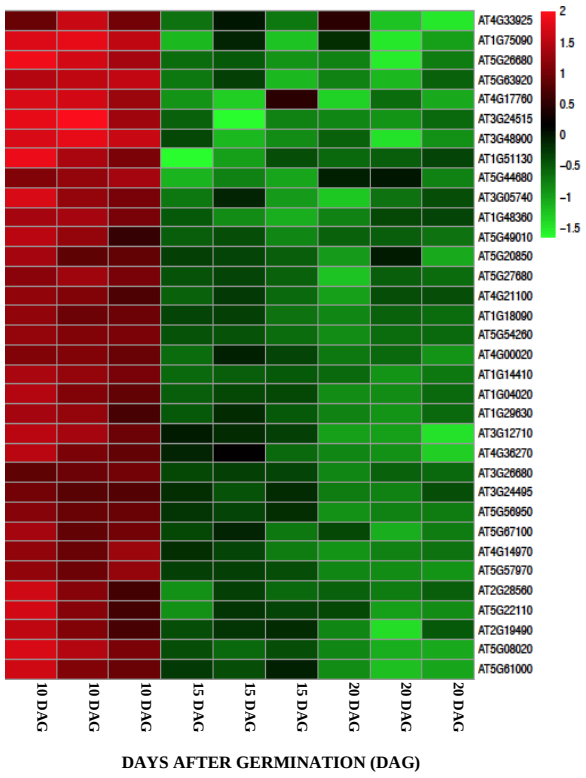

Figure 3.4. Differentially expressed genes involved in DNA repair mechanisms
Heat map of transcripts involved in DNA repair showing high expression in 10 days after germination (DAG) leaf samples and low expression in 15 and 20 DAG *Arabidopsis* leaf samples. Red represents high gene expression, green represents low gene expression, and black darker shades show intermediate levels of expression. Values on colour scale are in $\log_2$.

3.2.3.2 Upregulation of endogenous stress-related genes with age in *Arabidopsis*

The results from the above section suggest that DNA repair mechanisms decline as the leaf ages. It is also known that unrepaired DNA damage leads to ageing and eventual onset of senescence (Britt, 1996). Therefore, transcripts linked to ROS and senescence should also be elevated in 15 and 20 DAG leaves of *Arabidopsis*. As it was observed in the previous section, 700 stress-related genes are highly expressed

in 15 and 20 DAG leaf samples. Therefore, the upregulated stress-related genes that have biological functions in oxidative stress and senescence were examined.

The heat map in Figure 3.5A depicts the pattern of stress-related gene expression in 10, 15 and 20 DAG first rosette leaf pairs. The result shows that, among the 741 stress-related genes, 41 are downregulated, while 700 are upregulated in 15 and 20 DAG leaf samples. Examination of the biological function of these upregulated stress associated genes shows that 48 (7%) are linked to leaf senescence, 305 (43%) to oxidative stress and 347 genes (50%) are related to different stress conditions (Figure 3.5B). All of the upregulated genes in 15 and 20 DAG leaf samples are listed in Appendix 1. The genes modulating leaf senescence and oxidative stress include a large number of NAC and WRKY transcription factors (TFs) that are known to play a prominent role in response to stress during the onset of senescence (Balazadeh et al., 2008). The upregulated senescence associated genes include *SAG2*, *SAG13*, *SAG20*, *SAG21*, *SAG29* and *SAG113*. Genes belonging to mitogen activated signalling pathways (*MPK3*, *MPK11*, *MKK1* and *MAPKKK18*), strigolactone signalling (*MAX1*, *MXL6*, *MXL8*) and members of tetraspanin (*TET3*, *TET8*, *TET9*) are also upregulated. Taken together, these results suggest the elevation of endogenous stress in 15 and 20 DAG leaves. The upregulation of ROS and senescence linked genes supports the finding of reduced DNA damage repair associated gene expression in 15 and 20 DAG leaf samples.

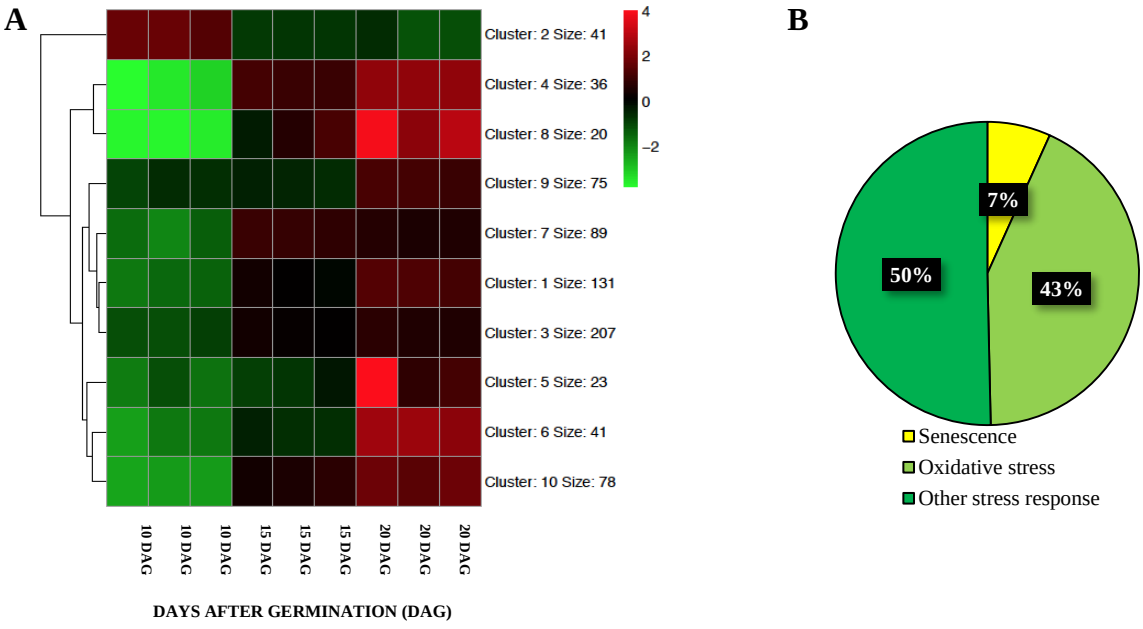

Figure 3.5. Differentially expressed genes involved in stress responses
A. Heat map depicting differentially expressed stress-responsive genes in 10, 15 and 20 days after germination (DAG) leaf samples. Red represents high gene expression, green represents low gene expression, and black darker shades show intermediate levels of expression. Values on colour scale are in $\log_2$. **B.** Pie chart representing the percentage of upregulated senescence, oxidative and other stress-responsive genes.

3.2.3.3 Hormonal networks in EELs, MELs and FELs *Arabidopsis*

In the previous section, stress-related genes appeared to be gradually upregulated with age in 15 and 20 DAG *Arabidopsis* leaves. In this section, differentially expressed genes related to hormones are studied to understand the regulatory pathway of hormones during development of EEL, MEL and FEL. Since senescence and stress responsive genes are highly expressed in MEL and FEL, it is expected that ethylene and stress-related hormones will be upregulated in 15 and 20 DAG leaf samples.

In total, 157 differentially expressed genes were found to be linked with different hormone signalling. The graph in Figure 3.6 presents the ratio of upregulated and downregulated genes in 15 and 20 DAG samples associated with specific hormones. This graph shows an almost equal ratio of upregulated and downregulated genes related to Auxin and Cytokinin. Therefore, only genes linked to Jasmonic acid (JA), Abscisic acid (ABA), Salicylic acid (SA), and Ethylene hormones were further studied as the gene expression of these hormones displayed significant changes in different ages of leaf.

In the class of stress hormones, genes involved in ABA signalling were overrepresented (21/26) in 15 and 20 DAG leaf samples (Figure 3.6). The key regulatory genes; *NCED3* (Nine-Cis-Epoxycarotenoid dioxygenase3), *ZEP* (Zeaxanthin Epoxidase) and *AAO3* (Abscisic Aldehyde Oxidase3) involved in ABA biosynthesis, (Endo et al., 2014) were upregulated in 15 and 20 DAG leaf samples, suggesting a high level of ABA activity in these tissues. Expression of *CYP707A4* (cytochrome P450, family 707), which plays a predominant role in the catabolism of ABA, especially in a stressed environment (Kushiro et al., 2004), was also upregulated. Furthermore, several other genes responsive to ABA specifically during stress, were found to be upregulated with age. This data confirms the activation of stress hormone ABA-related genes as the endogenous stress level is up in MEL and FEL.

JA is another hormone known to have an active role in plant growth, response to stress, and leaf senescence (Santino et al., 2013). The 10 DAG leaf samples showed low expression of genes regulating JA signalling, while, 14 out of 15 genes in this group displayed upregulation in 15 and 20 DAG leaf samples. These upregulated genes comprise of *AOS* (Allene Oxide Synthase), *AOC1*, *AOC2*, *AOC3* (Allene Oxide Cyclase) and *LOX1*, *LOX2*, *LOX3*, *LOX4* (Lipoxygenase), all of which catalyse an important step in the biosynthesis of JA (Stenzel et al., 2012). The other overrepresented genes that regulate chief roles in JA signalling are *JAZ1*, *JAZ3*, *JAZ5*, *JAZ6*, *JAZ7*, *JAZ9*, *JAZ10* (Jasmonate-ZIM domain), *MYC2* (bHLH transcription factor) and *COI1* (Coronatine Insensitive1). This data confirms that stress hormone JA-related genes are high in 15 and 20 DAG leaf samples.

Numerous genes related to SA, specifically in stressed conditions, were upregulated in 15 and 20 DAG leaves. Key regulatory genes involved in signalling and biosynthesis of SA were also upregulated in 15 and 20 DAG leaf tissues. These highly expressed SA-related genes included *ICS1*, *PBS3*, *EDS1* and

PAD4. This data collectively indicates that, similarly to ABA and JA-related genes, increased expression of SA-associated genes is also coupled with the elevated stress responsive genes in 15 and 20 DAG leaf tissues.

Ethylene is a well-known hormone for inducing ageing in plants (Jibran et al., 2013; Schaller, 2012). It was found that all differentially expressed ethylene regulatory genes (27/27) were upregulated in 15 and 20 DAG leaf tissues, when compared to 10 DAG leaf samples. Of these upregulated genes, those which have an important role in ethylene biosynthesis were *ACS2, ACS6, ACS8* and *ACS11* (Wang et al., 2002). Furthermore, 15 and 20 DAG leaf samples showed an overrepresentation of around 10 *ERF* (ethylene response factor) genes. Other genes with roles in the ethylene signalling pathway included *CEJ1, RAP2.10, MYB73, ESE3, RAN1, DEAR2,* as well as several others that displayed increased expression in 15 and 20 DAG leaf samples. Therefore, this data together with the upregulation of senescence-related genes (section 3.2.3.2), supports the hypothesis that the expression of genes linked to ethylene biosynthesis increases with age in 15 and 20 DAG leaf samples.

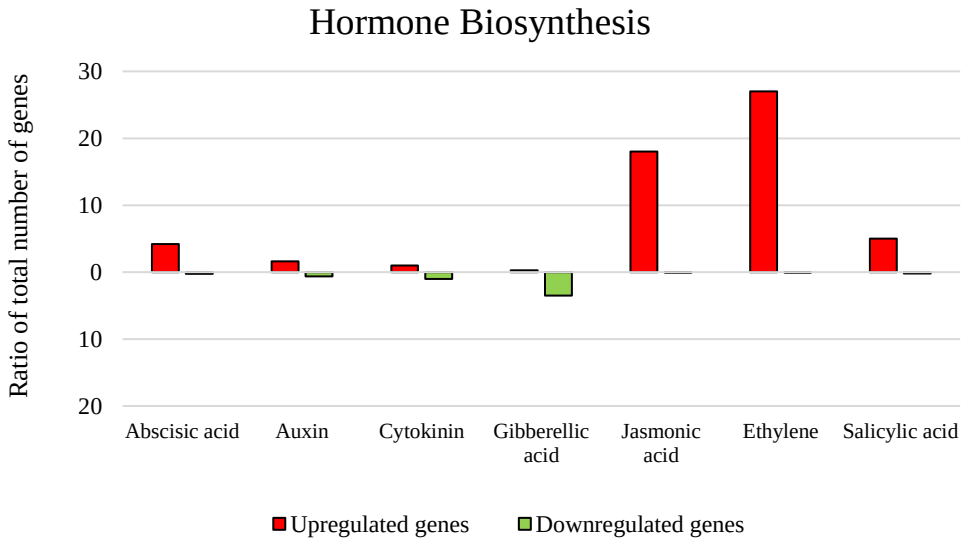

Figure 3.6. Differentially expressed genes involved in hormone signalling
Bar graph representing the ratio of total number of up and downregulated differentially expressed genes enriched to specific hormone signalling in MEL and FEL samples. Green bars represent downregulated genes and red bars indicate upregulated genes.

3.2.4 Confirmation of RNA sequencing data by qRT-PCR

A few genes were analysed by quantitative real-time polymerase chain reaction (qRT-PCR), to confirm the pattern of differentially expressed genes related to senescence-inducing ARCs, previously identified by RNA sequencing. The genes selected to measure expression level by qRT-PCR are associated to reactive oxygen species (ROS) (*RBOHD*, *WRKY53*), senescence (*SAG13*) and antioxidant activity (*FSD3*). WT *Arabidopsis* plants were grown in LD photoperiods and the first rosette leaves were harvested at 10, 15 and 20 DAG to measure the transcript level of the selected genes (Materials and method section 2.3).

The qRT-PCR results showed that transcript levels of ROS responsive gene function (*RBOHD*) increased ~14-fold in 15 and 20 DAG samples (Figure 3.7A), however in RNA sequencing data the expression of *RBOHD* in 20 DAG sample was higher than 15 DAG. Additionally, there was no significant difference observed in the expression of *WRKY53* in 10 and 15 DAG leaf samples but the transcript increased ~2-fold in 20 DAG (Figure 3.7B), while RNA sequencing data revealed that the expression of *WRKY53* constantly increased from EEL to MEL and FEL. Moreover, expression of the senescence-related gene (*SAG13*) was 7-fold higher in 15 DAG and 585-fold higher in 20 DAG leaf tissues (Figure 3.7C), which is similar to the pattern observed in the transcriptomic data set. Also, the antioxidant-related gene transcript (*FSD3*) was significantly higher in 10 DAG samples and the gene expression decreased by half in the 15 and 20 DAG first rosette leaf pair (Figure 3.7D). This data is also identical to the gene expression pattern observed in RNA sequencing. Taken together, the changes in expression of selected genes related to senescence-inducing ARCs found by qRT-PCR are similar to the expressions identified by RNA sequencing.

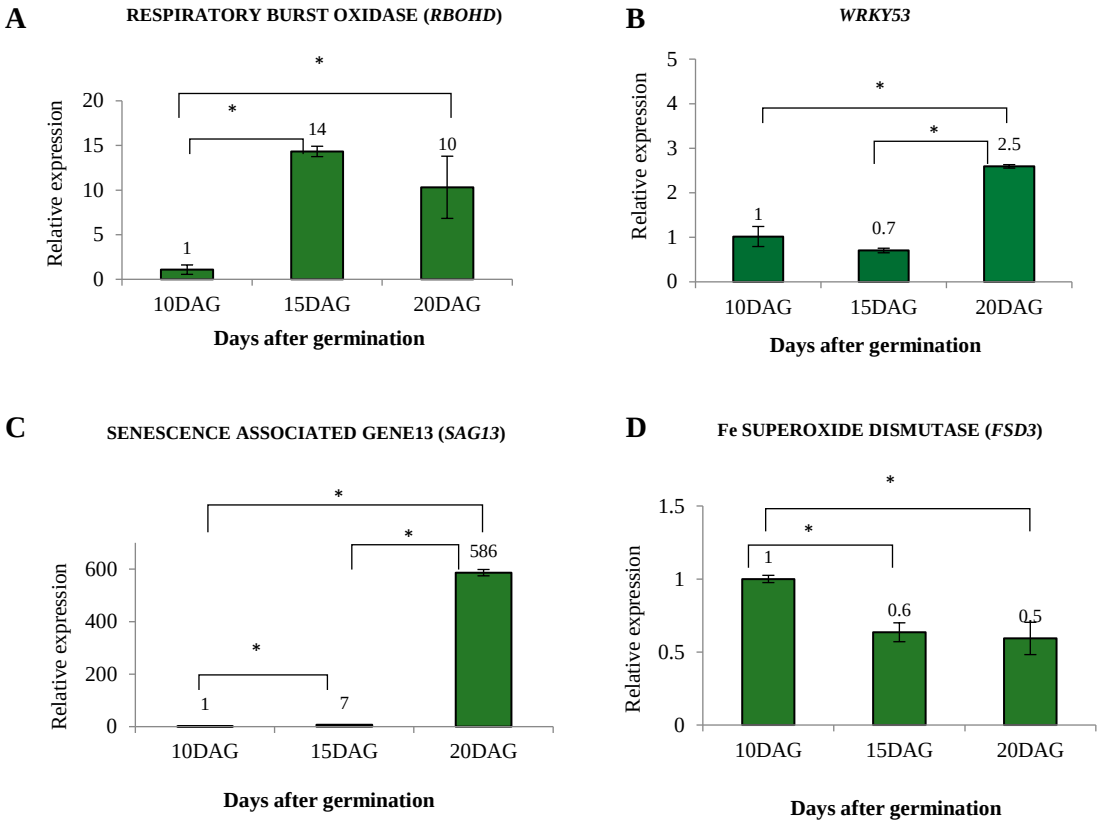

Figure 3.7. Expression of genes related to senescence-induce ARCs in *Arabidopsis* EEL, MEL and FEL
Expression profiles of *RBOHD, WRKY53, SAG13* and *FSD3* genes from *Arabidopsis* WT 10, 15 and 20 days after germination (DAG) first rosette leaf samples. The plants were grown under long-day photoperiod (16-hour light: 8-hour dark). Gene expression data represents mean values of three biological replicates. * indicates the values are significantly different at $p \leq 0.05$ using a Student's t-test between the indicated samples.

3.2.5 Tolerance to drought stress decreases with age in *Arabidopsis* leaves

The above transcriptomic studies confirm the gradual occurrence of senescence-inducing ARCs with increased age of the *Arabidopsis* leaves. The next question was, how does the gradual occurrence of senescence-inducing ARCs affect plants of different developmental ages? To answer this question, *Arabidopsis* plants of different ages were exposed to drought stress. Based on RNA sequencing data, the senescence-inducing ARCs gradually increased with leaf age, therefore it is expected that the leaves will become more drought stress-sensitive with age.

Arabidopsis WT plants were exposed to water deficit conditions and the effects on the first rosette EELs (10 DAG), MEL (15 DAG) and FEL (20 DAG) were examined. The plants were well-watered in equal volumes every alternate day until 8, 13 and 18 DAG for EEL, MEL and FEL respectively, after which

water was withheld for 6 days at 10, 15 and 20 DAG (Figure 3.8A). The initiation of drought stress was considered to start after two days of first water holding because at this point normally water was provided. After 6 days of drought-stress on 10+6, 15+6 and 20+6 DAG samples, pictures of the drought-stressed and well-watered rosettes were taken and the relative water content (RWC) was measured (Materials and methods section 2.6). The measured soil field capacity (SFC) of well-watered pots was around ~98%, whereas SFC of the drought-stressed pots was ~20% (Figure 3.8B). Drought stress responses of darker rosette colour and reduced leaf growth were observed in all three stages of *Arabidopsis* plants (Figure 3.9). Also, early leaf emergence was observed in dehydrated 10+6, 15+6 and 20+6 day old plants, but not in well-watered plants (Figure 3.9). Initiation of early flowering was observed in 20+6 DAG plant samples (data not shown). In Figure 3.9D, the percentage of leaf RWC in well-watered and drought-stressed *Arabidopsis* plants is presented. This graph shows that there is no significant difference in RWC between the control and drought-stressed 10 DAG+6 samples. No sign of wilting was observed in the EEL except for an apparent reduced leaf size compared to the control (Figure 3.9A iii, iv). Symptoms of drought stress were clearly visible in 15+6 samples, and they also showed a ~17% reduction in RWC compared to the control. This result supports the observation of the pronounced wilting sign in the MEL (first rosette leaf pair). The effect of drought stress on 20+6 DAG samples is exhibited as a substantial decrease in stress tolerance, as almost 22% RWC declined in water deficit samples compared to the well-watered plants. This result reflects the degree of wilting along with the initiation of senescence seen in the FEL (Figure 3.9C iv), and induced leaf curling/rolling in second rosette leaf pair (Figure 3.9C vi). Although plants in all three stages survived well and appeared tolerant to drought stress, close inspection of EEL, MEL, FEL samples, and the observed difference in RWC supports the hypothesis that leaves of different ages show distinct adaptive responses to stress. Therefore, these results suggest that because of negligible senescence-inducing ARCs, the 10 DAG leaves exhibit drought resistance, and as senescence-inducing ARCs accumulate, drought stress tolerance decreases in 15 and 20 DAG plants.

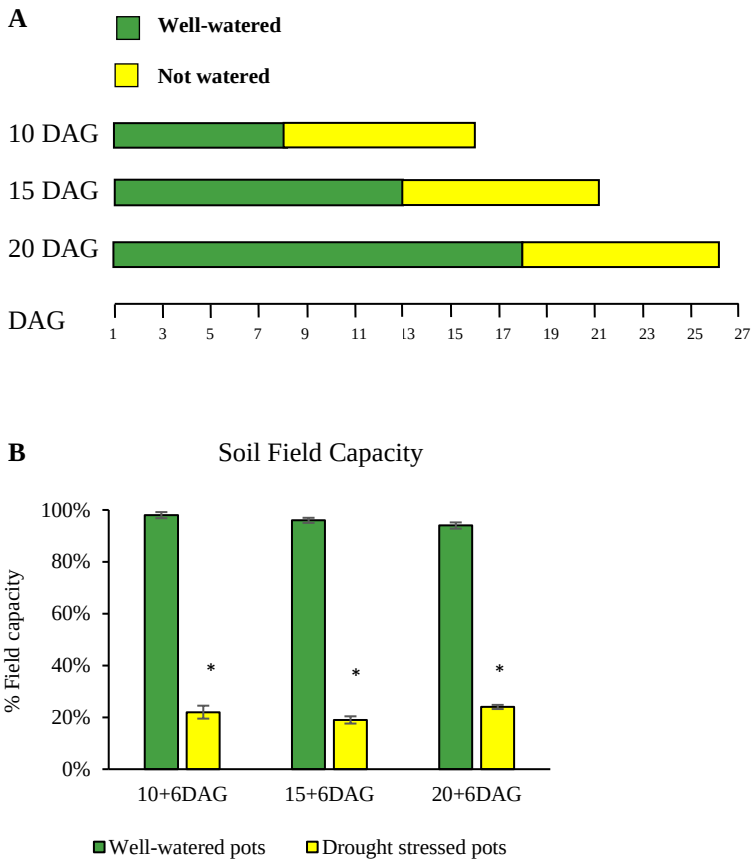

Figure 3.8. Watering schedule during drought stress.
A. After germination, WT plants were watered equally every alternate day and watering was stopped after 8, 13 and 18 DAG to initiate the drought stress after 10, 15 and 20 DAG respectively. Physiological measurements and pictures were taken after 6 days of drought stress in each time point. Watering was not stopped for the control plants. **B.** Measured soil field capacity (SFC) in well-watered pots and drought-stressed pots after 10+6, 15+6 and 20+6 days old plants. Green bar represents SFC in hydrated plants and yellow bar represents SFC in drought-stressed plants. Results are represented as means and standard deviations from 6 pots. * indicates the values are significantly different at $p \leq 0.05$ using Student's t-test, between the hydrated and drought-stressed plants.

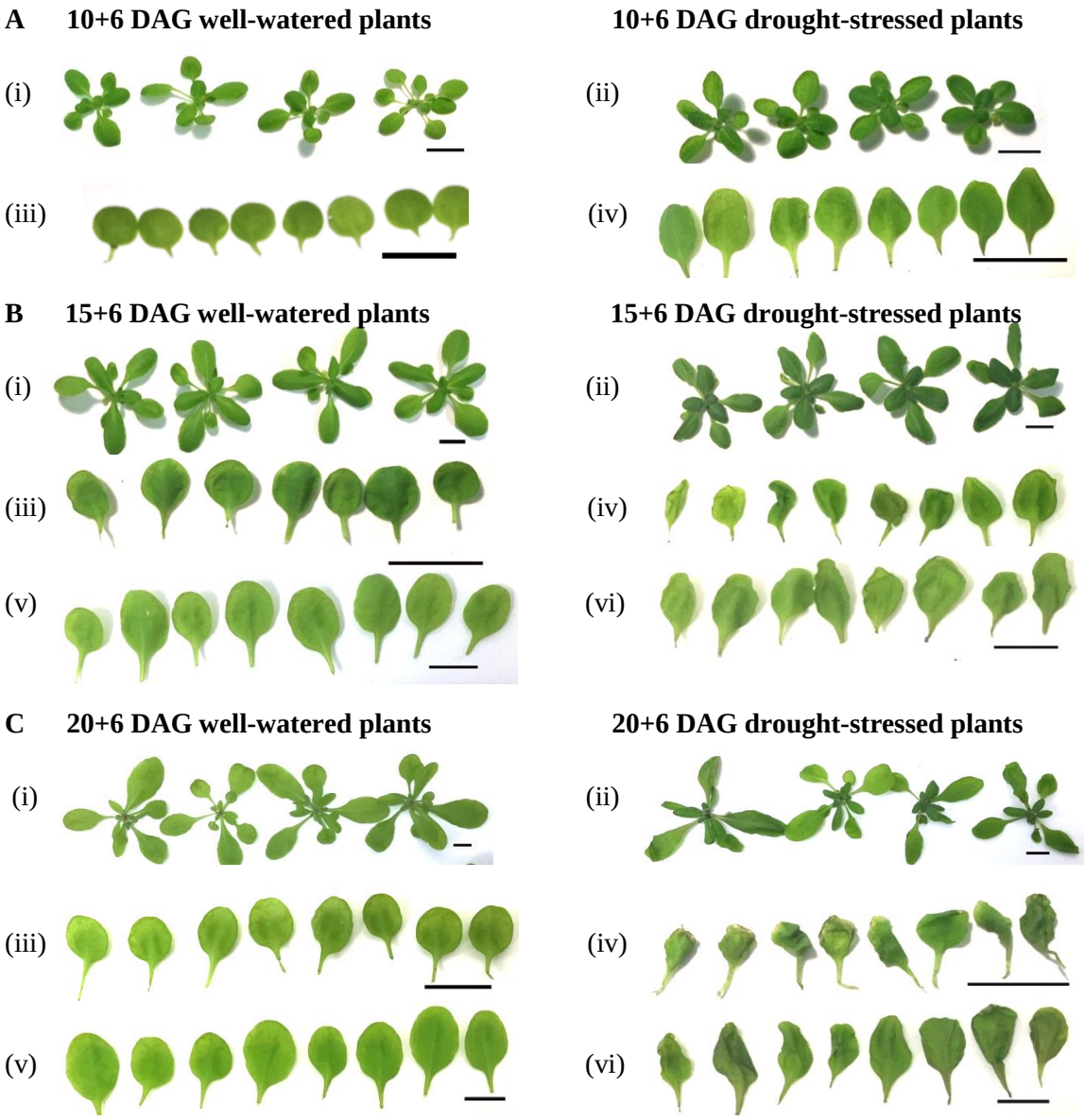

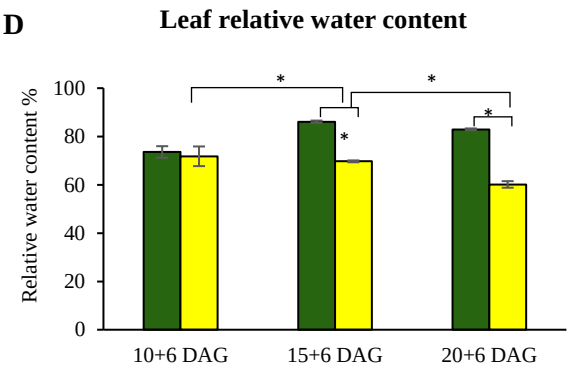

Figure 3.9. Effect of drought stress at three different stages of development in *Arabidopsis* WT plants. **A.** 6 days of drought stress on 10 days old WT plants. Photographs were taken of well-watered plants (i) as a control and drought-stressed plants (ii) at 10 DAG +6 days of drought period (10+6). First rosette EEL leaf pair was detached and photographed from both control (iii) and drought-stressed plants (iv). **B.** 6 days of drought stress on 15 days old WT plants. Photographs were taken of well-watered plants (i) as a control and drought-stressed plants (ii) at 15 DAG +6 days of drought period (15+6). First rosette MEL and second rosette leaf pair was detached and photographed from both WT (iii, v) and drought-stressed plants (iv, vi). **C.** 6 days of drought stress on 20 days old WT plants. Pictures were taken of plants at 20 DAG +6 days of drought period (20+6) (ii), well-watered plants were taken as control (i). First rosette FEL and second rosette leaf pair was detached and photographed from control (iii, v) and drought-stressed plants (iv, vi). **D** Estimation of relative water content (RWC) in well-watered and drought-stressed WT plants after 10+6, 15+6, and 20+6 DAG. Green bars

represent RWC in hydrated plants and yellow bars represent RWC in drought-stressed plants. Results are represented as means and standard deviations from 6 plants. * indicates the values are significantly different at $p \leq 0.05$ using Student's t-test between the indicated samples. Scale bar represent 10 mm. DAG- days after germination. 10+6 DAG- 6 days of drought period at 10 DAG. 15+6 DAG- 6 days of drought period at 15 DAG, 20+6 DAG- 6 days of drought period at 20 DAG.

3.2.6 Tolerance to salt shock decreases with age in *Arabidopsis* leaves

The above results have suggested that with an increase in senescence-inducing ARCs, tolerance to drought stress decreases in *Arabidopsis* leaves. In this section, to examine whether a similar effect is observed from a different stress, 10, 15 and 20 DAG plant samples were exposed to salt shock. It was expected that with increased age, *Arabidopsis* leaves will show decreased tolerance to salt shock, similar to the results from drought stress.

For this study, plants were exposed to salt shock after 10 DAG, 15 DAG and 20 DAG to see whether changes are evident in the three different stages. Plants were exposed to salt shock for 6 days by watering with 300 mM NaCl solution (Figure 3.10). After 6 days of salt shock, the stressed and control rosettes were detached and photographed at 10+6, 15+6 and 20+6 DAG. The chlorophyll level was quantified from the first rosette EEL, MEL and FEL leaves to measure the progression of senescence in control and salt shocked samples (Figure 3.11D). The overall effect of salt shock in all three developmental stages was observed as reduced leaf number, as well as decreased rosette leaf area compared to the well-watered plants (Figure 3.11). Apart from the reduced growth and number of leaves, salt induced senescence was not readily visible in the first rosette EEL sample (Figure 3.11A), but chlorophyll quantification showed substantial reduction in chlorophyll (2.06 mg/g FW) after the salt shock compared to the control plants (Figure 3.11D). The chlorophyll level greatly declined (0.74 mg/g FW) in salt shocked 15+6 DAG leaf samples, and this result corresponds to the leaf yellowing observed in the first rosette MEL samples (Figure 3.11B iv). In 20+6 DAG salt shocked leaves the chlorophyll level was extremely low (0.27 mg/g FW) and the first rosette FEL appeared dead (Figure 3.11C iv), while the second rosette leaves displayed significant yellowing (Figure 3.11C vi). These results conclude that the EEL samples were the less susceptible to salt shock, but this susceptibility increased in the MEL and FEL samples. These result are consistent with the previous conclusion that stress resistance decreases as plants age, because of gradual accumulation of senescence-inducing ARCs.

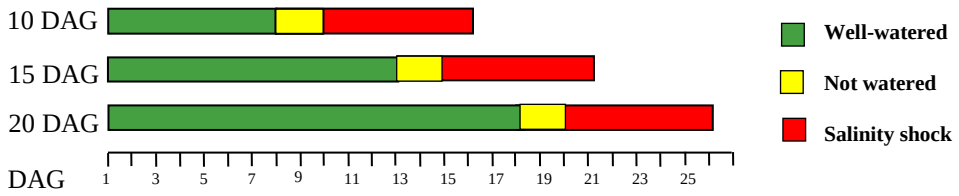

Figure 3.10. Watering schedule during salt shock

Arabidopsis plants were normally watered till 8, 13 and 18 DAG and then exposed to salt shock for 6 days by watering with 300 mM of NaCl solution in equal volume at 10, 15 and 20 DAG. Control plants were watered with water.

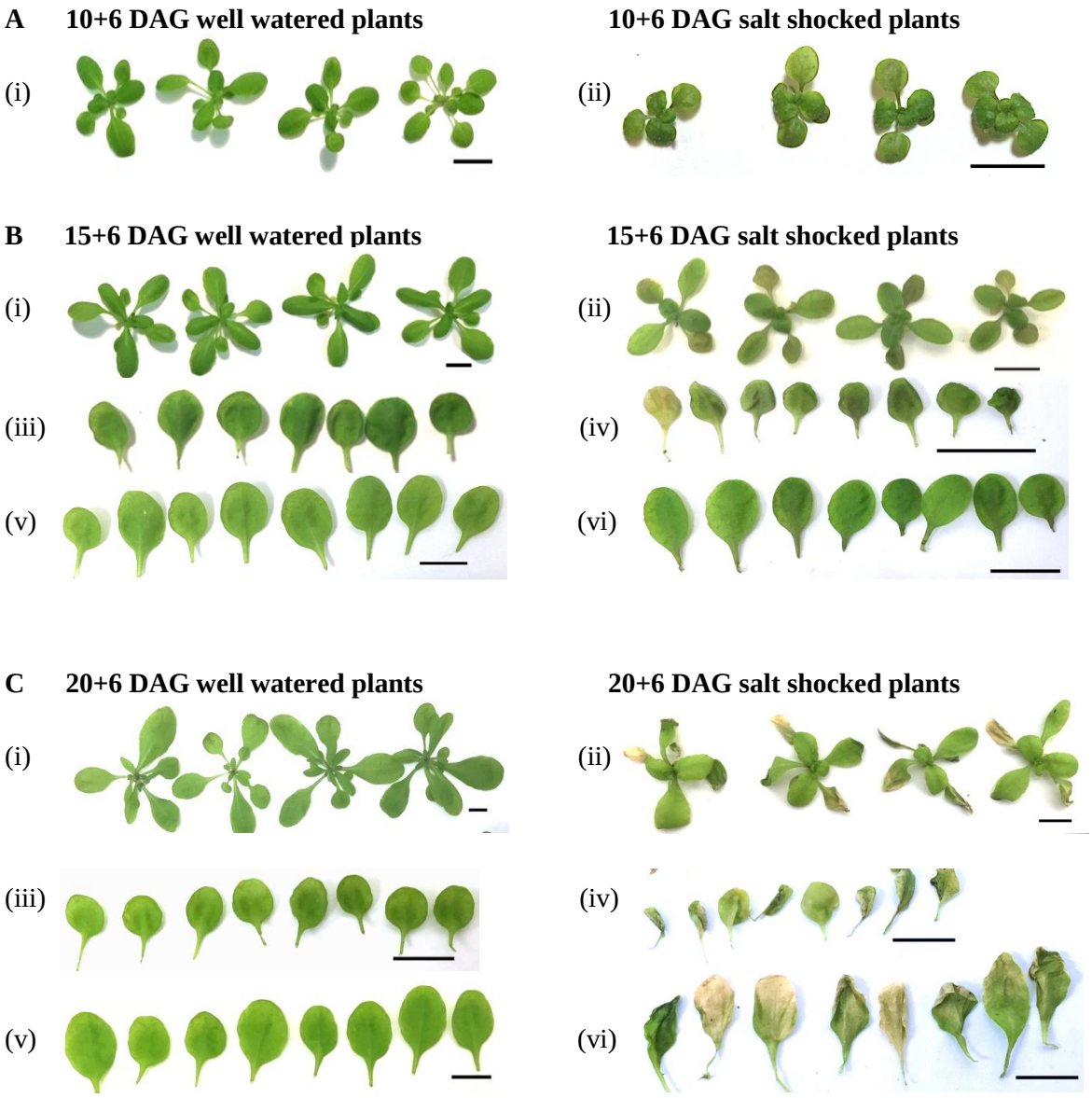

D

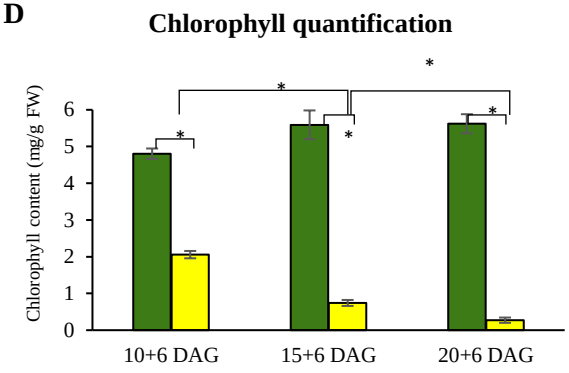

Figure 3.11. Effect of salt shock at three different stages of development in *Arabidopsis* WT plants. **A.** Effect of 6 days salt shock on 10 days old WT plants (10+6 DAG). Photographs were taken after plants were watered normally as a control (i) and plants were watered with 300 mM NaCl (ii) for 6 days at 10 DAG . **B**. Effect of 6 days salt shock on 15 days old WT plants (15+6 DAG). Photographs were taken after plants were watered normally as a control (i) and plants were watered with 300 mM NaCl (ii) for 6 days at 15 DAG. First rosette MEL and second rosette leaf pair from control (iii, v) and salt shocked plants (iv, vi) were detached and photographed. **C.** Effect of 6 days salt shock on 20 days old WT plants (20+6 DAG). Photographs were taken after plants watered normally as a control (i) and plants watered with 300 mM NaCl (ii) for 6 days at 20 DAG. First rosette FEL and second rosette leaf pair from control (iii, v) and salt shocked plants (iv, vi) were detached and pictures were taken. **D.** Chlorophyll quantification of well-watered and salt shocked first rosette leaf pairs from WT plants at 10+6, 15+6, and 20+6 DAG. Green bars represent chlorophyll content in hydrated plants and yellow bars represent chlorophyll content in salt shocked plants. Results are represented as means and standard deviations from 6 plants. * indicates the values are significantly different between the indicated samples at $p \leq 0.05$ using Student's t-test. Bar represent 10 mm. DAG- days after germination. 10+6 DAG- 6 days of salt shock at 10 DAG. 15+6 DAG- 6 days of salt shock at 15 DAG, 20+6 DAG- 6 days of salt shock at 20 DAG.

3.2.7 Tolerance to dark stress and ability to recover decreases with age in *Arabidopsis* leaves

In the previous sections treatments that provide, drought and salt shock stress confirmed that as senescence-inducing ARCs increase with age, the tolerance to stress decreases in plants. The next question was whether the plant recovery after stress also decreases with age. Therefore, it was expected that similar to drought and salt shock, at 10 DAG, leaves will be more tolerant to dark stress compared to leaves at 15 and 20 DAG. Also, it was expected that dark-stressed 10 DAG leaves will show better recovery, and this recovery will become weaker as the plant ages.

To determine the effect of dark stress and efficiency of recovery in different aged plants, 10, 15 and 20 DAG plants were exposed to darkness for 4 days and then returned to light with a 16-hour photoperiod, for a 3-day recovery (Materials and methods section 2.7). To understand the progression of senescence after 4 days of darkness, the total chlorophyll level was measured from the first rosette of EEL, MEL and FEL samples. To observe the ability of plants to recover after stress, the percentage of leaves present before the dark period, and the percentage of leaves that survived after the dark recovery, was counted. Chlorophyll content declined in all differently aged leaf samples that were exposed to darkness for 4 days (10+4, 15+4, 20+4 DAG). However, the chlorophyll content in EEL samples was 3.08 mg/g FW which is comparatively more than MEL and FEL dark-stressed samples (Figure 3.12D). In 15+4 MEL

samples the chlorophyll content was around 2.35 mg/g FW, whereas in the 20+4 FEL samples, the chlorophyll had degraded substantially, leaving a concentration of around 1.57 mg/g FW (Figure 3.12D). The survival rate after 4 days of dark and 3 days of recovery in 10+4+3 DAG plant samples was the highest with about 66% of leaves surviving. While in 15+4+3 DAG plant samples, 62% of leaves survived and only 54% of leaves recovered in 20+4+3 DAG plant samples (Figure 3.12E). Taken together, the percentage of leaf survival decreased with age after dark stress treatment. This study concludes that the tolerance to dark stress decreases with plant age, as does the ability of recovery, which was found to be the highest in 10 DAG, followed by 15 and 20 DAG leaf samples which had the lowest ability to recover.

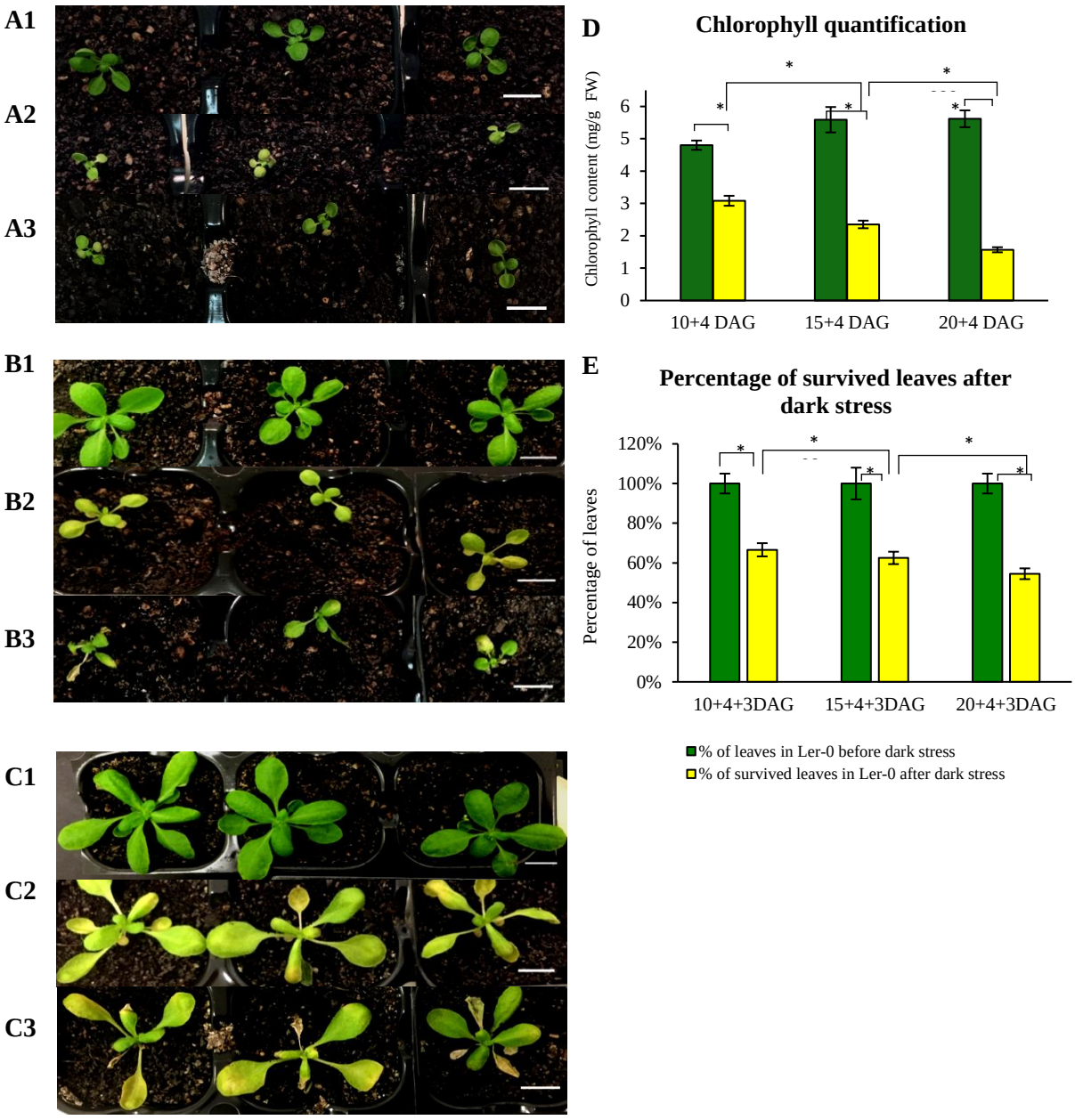

Figure 3.12. Effect of 4 days dark stress and 3 days recovery at three different stages of development in *Arabidopsis* WT plants.

A. At 10 DAG, plants were kept in the dark for 4 days (10+4). Pictures were taken of plants grown under normal photoperiod (A1), after 4 days of dark stress (A2) and 3 days of recovery after the dark period (A3). **B.** After 15 DAG, plants were kept in the dark for 4 days. (B) old WT plants (15+4). Pictures were taken of plants grown under normal photoperiod (B1), after 4 days of darkness (B2) and 3 days of recovery after the dark period (B3). **C.** At 20 DAG plants were kept in the dark for 4 days. Pictures were taken of plants grown under normal photoperiod as a control (C1), after 4 days of darkness (C2) and 3 days of recovery after dark period (C3). **D.** Chlorophyll was measured in first rosette leaf pairs in the control and 4 days dark stressed 10, 15 and 20 DAG WT plants. **E.** Bar graph showing the percentage of leaves present before dark stress and the percentage that survived after 4 days of dark + 3 days of recovery. Green bars represent the percentage of leaves in the control and yellow bars represent percentage of leaves that survived after 4 days of dark and 3 days of recovery. Data shown in graphs D and E represent the mean of 6 biological replicates. * indicates the values are significantly different between the indicated samples at $p \leq 0.05$ using Student's t-test. Scale bar represents 10 mm.

3.3 Discussion

3.3.1 Senescence-inducing ARCs gradually occur with increased age of *Arabidopsis* leaves

This research was performed to determine the senescence-inducing ARCs taking place during the pre-senescence process in *Arabidopsis* leaves of three different ages. Firstly, a transcriptomic study was carried out on the first rosette leaf pairs, which for *Arabidopsis* are the first true leaves after the cotyledons. Under the LD photoperiod (16 hours of light) growth conditions in our lab the first rosette leaf pair is the first to senesce, a process which allows immobilization of nutrients and senescence following the initiation of new leaves or reproduction (Himelblau and Amasino, 2001). Thus, from the vegetative phase, three developmental stages were selected for study; 10 DAG first rosette leaves in early expanding phase, 15 DAG leaves in mid expanding phase, and 20 DAG first rosette leaf pairs at their final size (Figure 3.1). The RNA sequencing data illustrated the global change taking place in gene expression from EEL to MEL to FEL (Figure 3.2). The change in overall gene expression patterns for distinct biological functions was examined in three different leaf stages. As the leaf samples selected were in the growing phase, changes in expression of genes related to growth and development were likely to be observed (Figure 3.3) such as cell cycle, cellular component organisation, gene regulation, biosynthesis of cell constituents, cell wall organisation etc. For instance, data shows that gene expression linked to the cell cycle was high in EEL and reduced in MEL and FEL, which was expected as during the cell cycle, complete division occurs prior to DNA replication and as the leave matures, cell division ceases (Johnson and Skotheim, 2013). The antioxidant defense system that protects plants against ROS toxicity appears moderately active, and most likely regulates ROS production, as most antioxidant-related genes (83/121) were overrepresented in both MEL and FEL samples. As expected, the photosynthesis-related genes are elevated in MEL and FEL, as photosynthetic machinery increases to support the growth of a leaf (Ferris et al., 2001; Gardner and Shao, 2001). Since the aim was to focus on senescence-inducing ARCs, further study will eliminate analysis on genes linked to growth and development of leaves. Furthermore, the downregulated DNA repair-related genes, and the upregulated stress-related genes were studied in detail to identify the key regulatory genes or pathways involved in the pre-senescence process that leads to decreased stress tolerance in aged plants. Also, the expression of genes linked to specific hormonal regulatory pathways were studied in detail to elucidate their possible function in the three different leaf stages.

3.3.1.1 DNA repair linked genes are significantly downregulated in *Arabidopsis* MEL and FEL

Under standard laboratory conditions, DNA errors can occur in plants during DNA replication (Spangenberg et al., 2015). Another primary cause of DNA damage is the overproduction of ROS in

response to environmental challenges (Roldán-Arjona and Ariza, 2009). DNA damage caused by ROS radicals produce lipid peroxidation and lesions within DNA. High absorption of UV-B radiation is another cause of DNA damage and therefore results in lower yield of certain crops (Krizek, 2004; Zavala et al., 2001). However, plants have evolved different DNA repair mechanisms such as excision repair, mismatch repair, and double-strand break repair, which detect and correct the damages within DNA (Britt, 1996; Gill et al., 2015). However, unrepaired DNA damage can induce mutations within the plant genome, and affect the growth, productivity and survival of stressed plants (Biedermann et al., 2011; Singh et al., 2010). Application of Helium-Neon (He-Ne) on crops is known to aid protection against several abiotic stresses by controlling oxidative stress and improving plant growth (Perveen et al., 2011; Qiu et al., 2013; Yang et al., 2012). Recently, a study has shown that He-Ne irradiation on salt stressed fescue seedlings enhanced salt tolerance by protecting cell wall materials, controlling overproduction of ROS, and inducing DNA repair (Limei et al., 2015). Since ROS accumulation increases the possibility of DNA damage, it is possible that the salt resistance of He-Ne irradiated fescue seedlings is due to regulation of ROS, which spontaneously reduces the frequency of DNA damage under stressed conditions. The *ddm1* (Decrease in DNA Methylation 1) mutant identified in *Arabidopsis* displayed developmental defects such as small leaf size, abnormal flowers, reduced fertility and increased cauline leaf number (Kakutani et al., 1996). Further research showed that the *ddm1* mutants are susceptible to salt stress and have reduced DNA repair capabilities (Yao et al., 2012). Also, it has been found that overexpression of DDB2 (Damaged DNA binding protein 2) in transgenic tomato enhanced tolerance to UV stress, suggesting a possible function for DDB2 in UV-induced DNA repair (Lanyang et al., 2015).

A study has shown that DNA repair efficiency in *Arabidopsis* was higher in young leaves and lower in adult leaves (Golubov et al., 2010). RNA sequencing data also show that the highest ratio of downregulated genes (34/34) related to DNA repair mechanisms in MEL and FEL. This research signifies that DNA repair mechanisms are developmentally regulated and therefore maintenance of genomic integrity decreases as the leaf ages. From transcriptomic data, the DNA repair-related genes includes *BRCA2(IV), BARD1, RAD51, RAD51B, DDB1B* (Damaged DNA Binding protein 1B), *MRE11* (Meiotic recombination11), *RECA2, WHY1* (Whirly1), *RPA70B* (Replication protein A 70B) and *RPA70D* (Replication protein A 70D), which all show decreased expression in MEL and FEL samples (Bernhardt et al., 2010; Bundock and Hooykaas, 2002; Li et al., 2007; Miller-Messmer et al., 2012; Reidt et al., 2006; Siaud et al., 2004; Takashi et al., 2009; Wang et al., 2014; Yoo et al., 2007). All these genes are very important to protect plant cells against damage and avoid lesions or mutations of the DNA strands (Britt, 1996). Taken together, DNA repair mechanisms appear to be highly active in EEL, but reduced in MEL and FEL. Unrepaired DNA damage can result in plant ageing, leading to weakened stress tolerance with age and onset of senescence.

3.3.1.2 Oxidative stress and senescence-related genes are upregulated in *Arabidopsis* MEL and FEL

Interestingly, stress-related genes were found to be the most enriched (711/752) among all other genes enriched in different biological functions in 15 DAG leaf samples. Studies have found that the onset of senescence results in activation of stress-related genes (Breeze et al., 2011), but from RNA sequencing data it is evident that this activation occurs earlier than previously thought; at the mature phase prior to initiation of senescence. Analysis of these upregulated stress-associated genes show that 7% are related to leaf senescence, 43% are responsive to oxidative stress and 50% are involved in other stress responses (Figure 3.5B). Upregulated genes linked to leaf senescence and oxidative stress include a large number of NAC and WRKY transcription factors (TFs), among other genes.

Several research studies have shown that a large number of TFs are involved in regulating the response to different stress factors and can also act as positive regulators of senescence. The study of NAC (*NAM/ATAF1, 2/CUC2*) and WRKY TFs in many species has shown a significant involvement in senescence processes (Balazadeh et al., 2008). TFs may interact with other signalling agents like plant hormones, protein kinases or other proteins that aid plant response to internal or external environmental factors (Gechev et al., 2006). In plants, WRKY TFs are a large family with important roles in internal and external stress responses (Rushton et al., 2010). There are 74 WRKY TFs identified with distinct association to senescence processes in *Arabidopsis* (Ulker and Somssich, 2004). Under stressed conditions, rapid induction of WRKY TFs expression activates signal transduction to activate stress responsive genes and ultimately result in adaption to stress tolerance (Chen et al., 2012). Of the many studies on WRKY involvement in response to abiotic factors, only a few WRKY genes were found to be enhanced in response to H_2O_2, dark, ethylene, salinity, cold and heat treatment, which are *WRKY6, WRKY22, WRKY25, WRKY33, WRKY34, WRKY39,* respectively (Chen et al., 2009, Zhou et al., 2011, Li et al., 2009, Jiang and Deyholos, 2009, Zou et al., 2010, Li et al., 2010). In addition, research on *Arabidopsis atwrky53* mutant lines showed a delayed senescence phenotype (Miao and Zentgraf, 2007). Moreover, the signal transduction of senescence-related *WRKY53* factor can be stimulated by H_2O_2, to regulate senescence specific gene expression (Miao et al., 2004). Thus, studies suggest that *WRKY53* act as a positive regulator of leaf senescence. Interestingly, transcriptomic data show that *WRKY53, WRKY57, WRKY25, WRKY33, WRKY27, WRKY25*, and many other WRKY TFs are already upregulated in MEL and FEL even before the completion of leaf growth, possibly in response to age-related changes.

There are approximately 135 NAC coding genes that have been identified in *Arabidopsis. BnNAC2, BnNAC5, AtNAP, OsNAP, ORESARA1,* and *ORESARA1SISTER1* are few examples of genes identified in species such as *Brassica napus, Arabidopsis thaliana, Oriza sativa* that encode NAC TFs and induce

accelerated leaf senescence under stressed conditions (Zhong et al., 2012, Zhou et al., 2013, Balazadeh et al., 2011). Among several NAC-coding genes, *ORESARA1* is probably the best gene characterised that regulates senescence. The isolated mutants in *Arabidopsis; oresara1*, *oresara3* and *oresara9*, all show greater stress tolerance and increased leaf longevity (Hye et al., 2004a). A further study done by Kim et al. (2009) showed that NAC TF *ORE1* gene expression increased with age in plants, and proposed that *ORESARA1*, *EIN2* (Ethylene Insensitive 2) and *miR164* (micro RNA164) are positive regulators of age-dependent senescence (Kim et al., 2009). The leaf senescence signalling cascade is further regulated by direct suppression of *miR164* through *EIN3*, working downstream of *EIN2*, which subsequently promotes the expression of *ORE1* (Li et al., 2013). Results from RNA sequencing illustrate that several NAC TFs, together with *ORE1*, are upregulated in 15 and 20 DAG leaf samples. In addition to this, a study has shown that the expression of the Zinc finger protein Zat12, increases in response to biotic and abiotic stress and plays a crucial role in regulation of ROS and stress signalling (Davletova et al., 2005b). However, results show that *Zat12* gene expression was already increased in MEL and FEL samples even before the initiation of senescence and absence of stress.

In monocarpic plants, around 800 senescence-associated genes (*SAG*) were isolated (Gepstein et al., 2003), out of which, *SAG12* and *SAG13* are both considered as the preferable senescence marker genes. The expression of *SAG12* is particularly stimulated by progressive senescence (Noh and Amasino, 1999) whereas, *SAG13* expression is visible before the senescence process starts, and can be observed to increases with leaf age (Swartzberg et al., 2006). Stress-induced treatments such as exposing plants to ethylene, darkness and leaf detachment eventually promote senescence processes and upregulate *SAG13* expression (Weaver et al., 1998). Furthermore, *WRKY53* TF expression level was also found to be increased during early leaf maturation, even before *SAG12* became noticeable (Zentgraf, 2001). In addition, rice plants grown in darkness exhibit over-expression of three *SAGs* under dark-induced senescence, but not during natural leaf senescence (Lee et al., 2001). Senescence acceleration was also found during ozone exposure, due to overproduction of ROS, which induced approximately eight *SAG* in *Arabidopsis* (Miller et al., 1999). Interestingly, *SAG* expression under different stressed conditions was not found to be associated with normal senescence processes, suggesting a specificity for *SAG* upon different senescence-inducing factors. RNA sequencing data showed increased expression of *SAG13* in MEL and FEL samples. Previous research together with these results clearly shows that *SAG13* is an age-related gene which possibly indicates the gradual ageing and senescence of leaves. Also, five other senescence-associated genes; *SAG2*, *SAG20*, *SAG21*, *SAG29* and *SAG113* all showed early overrepresentation in MEL and FEL tissues. Studies have shown that the expression of these genes increases with ageing in plants.

Moreover, genes related to strigolactone signalling (*MAX1, MXL6, MXL8*), mitogen activated signalling pathways (*MPK3, MPK11, MKK1* and *MAPKKK18*) and members of the tetraspanin family (*TET3, TET8, TET9*) are also upregulated in 15 and 20 DAG leaf samples. All these genes are studied to induce

ageing and senescence, and are responsive to stressed environments. It is surprising to observe the upregulation of oxidative stress and senescence-related genes before the completion of leaf growth and initiation of senescence. Upregulation of the large set of oxidative stress-related genes indicates that the cellular ROS level is high in 15 and 20 DAG samples, possibly because of highly active metabolic pathways in growing leaves. Although the antioxidant mechanism appears to be high (Figure 3.3) to keep ROS under control, the overproduction of ROS is perhaps beyond the threshold level. Upregulation of other stress-related genes supports the hypothesis that ROS stress is higher. Another possible reason of elevated oxidative and senescence-related genes, is the reduction of active DNA repair mechanisms in MEL and FEL (Roldán-Arjona and Ariza, 2009). However, it is not clear whether a poor DNA repair mechanism leads to oxidative stress or *vice versa*. But, RNA sequencing data explains well that leaf maturation coincides with poor DNA repair and increased oxidative stress, perhaps leading to the onset of senescence after the completion of a leaf growth. Together, the transcriptomic data set provides an informative set of genes (Appendix 1) that are possibly involved in senescence-induced ARCs.

3.3.1.3 Hormonal networks in EELs, MELs and FELs of *Arabidopsis*

Transcriptomic data illustrates a significant upregulation of differentially expressed genes related to JA, ABA, SA, Ethylene and Gibberellic acid (GA) hormones in MEL and FEL samples. As the stress responsive genes are upregulated in MEL and FEL samples, it is likely to see the upregulation of stress-related hormones in 15 and 20 DAG leaf samples.

ABA is not only known for its influence on plant growth but also in stress responses (Raghavendra et al., 2010). ABA-related genes upregulated in MEL and FEL samples included genes involved in ABA biosynthesis such as, *NCED3, ZEP* and *AAO3* (Endo et al., 2014). This suggests that biosynthesis of ABA is comparatively high in 15 and 20 DAG leaf tissue, compared to 10 DAG leaves. A study has shown that expression of the ABA catabolism gene, *CYP707A4*, increases during stressed conditions. *CYP707A4* expression is also found to be upregulated in 15 and 20 DAG leaf samples (Kushiro et al., 2004). Furthermore, genes involved in JA biosynthesis such as *AOS, AOC1, AOC2, AOC3* and *LOX1, LOX2, LOX3, LOX4* are low in EEL tissues, but upregulated in MEL and FEL samples (Stenzel et al., 2012). Other JA signalling genes upregulated in MEL and FEL tissues are *JAZ1, JAZ3, JAZ5, JAZ6, JAZ7, JAZ9, JAZ10, MYC2* and *COI1*. *COI1* is an F-box protein receptor that mediates JA signalling in response to cues that produce highly bioactive hormonal signals by degrading the JAZ repressor proteins (negative regulators of Jasmonate responsive genes) (Sheard et al., 2010). Degradation of JAZ proteins result in the release of the MYC2 transcription factor, which further regulates different JA-dependent functions (Melotto et al., 2009). Moreover, genes involved in SA biosynthesis and many SA-related genes responsive to stressed conditions are also upregulated in MEL and FEL. *ICS1*

(Isochorismate synthase 1) encodes a key enzyme in the SA biosynthesis pathway which synthesizes the precursor isochorismate from chorismate (Chen et al., 2009). *ICS1* was found to be highly expressed in 15 and 20 DAG samples. Also, it was found that *PBS3* (AVRPPHB Susceptible 3), *EDS1* (Enhanced Disease Susceptibility1) and *PAD4* (Phytoalexin Deficient 4), all of which are important genes required for disease resistance, were upregulated. A study has shown that the expression of these genes is induced by the accumulation of SA (Feys et al., 2001). Increased expression of *EDS5* (Enhanced Disease Susceptibility 5), which is localised to the chloroplast envelope, functions in transporting SA into the cytoplasm from its site of production (Yamasaki et al., 2013). Together, this data suggests that the increased activity of stress hormones ABA, JA and SA in MEL and FEL samples is due to enhanced cellular stress.

The expression profile of GA hormone-related genes reveals that expression is enhanced in EEL tissues, while in MEL and FEL samples, 7 out of 9 genes are downregulated (Figure 3.8C). GA is a hormone which suppresses senescence, and the active forms are decreased as plants age (Schippers et al., 2007). Another study showed that *GAST1* (GA-stimulated transcript1) and the members of the gene family *GASA1-14* (GST1 protein homolog), are involved in the early GA signalling pathway (Rubinovich and Weiss, 2010). The transcriptomic data shows that the expression of *GASA4, GASA6, GASA14, TRM13* and three other unknown genes were consistently downregulated from EEL to FEL tissues. Moreover, the gene expression of *GA20X1* (Gibberellin 2-oxidase 1), which has known involvement in the mechanism of GA inactivation, is upregulated in both MEL and FEL samples (Thomas et al., 1999). However, the genes involved in biosynthesis of GA were not differentially expressed in any of the leaf samples, clearly indicating that the functional form of GA is still active in EEL, MEL and FEL tissues. Studies have shown that *GASA4* and *GASA14* are responsive to ROS levels (Rubinovich and Weiss, 2010; Sun et al., 2013), and that *GASA4* and *GASA6* are both down-regulated by the stress hormones JA, ABA and SA (Qu et al., 2016). These studies together with RNA sequencing data suggest that downregulation of GA in MEL and FEL tissues is an outcome of increased stress hormone production (JA, ABA and SA). The transcriptomes have shed light on key regulatory genes involved in GA signalling, particularly when endogenous ROS or stress levels increase with leaf age.

Interestingly, all differentially expressed ethylene-related genes were upregulated in MEL and FEL tissues, as compared to EEL samples. These upregulated genes included *ACS2, ACS6, ACS8* and *ACS11* (1-amino-cyclopropane-1-carboxylate synthase), ACS is a key enzyme involved in ethylene biosynthesis, and converts S-AdoMet to 1-amino-cyclopropane-1-carboxylic acid (ACC) (Wang et al., 2002). *MKK9* is another highly expressed gene, suggested to be involved in ethylene biosynthesis through activation of *ACS2, ACS6* and several other ethylene response factor (*ERF*) genes (Xu et al., 2008). ERFs are transcription factors and the main mediators of ethylene signalling, in response to various stress conditions (Müller and Munné-Bosch, 2015). The MEL and FEL samples showed overrepresentation of 10 ERFs, likely due to elevated endogenous stress, (Thirugnanasambantham et

al., 2015). Several other genes involved in the ethylene signalling pathway such as *CEJ1*, *RAP2.10*, *MYB73*, *ESE3*, and *RAN1* are overrepresented in MEL and FEL samples. It is known that ROS overproduction and DNA damage responses contribute in the onset of leaf senescence (Gan and Amasino, 1997). Furthermore, results from 15 and 20 DAG leaf samples show upregulation of oxidative stress and senescence-associated genes, and downregulation of DNA repair-related genes. Therefore, upregulation of ethylene-related genes is well supported, and together the results provide strong evidence that senescence-inducing ARCs gradually occur in *Arabidopsis* leaves as they age.

3.3.2 Senescence-inducing ARCs decrease tolerance to stress with increased age of *Arabidopsis* leaves

To study the effects of senescence-inducing ARCs in EEL, MEL and FEL, *Arabidopsis* WT plants were exposed to drought stress at 10, 15 and 20 DAG, and the RWC was measured after a 6-day drought period. The percentage of RWC in drought-stressed plants decreased more with age, when compared to the well-watered plants (Figure 3.9D). Also, the first and second rosette leaves were detached from the control and stressed plants to observe the influence of drought stress in leaves of distinct ages. This was chosen because the first rosette leaf that emerges is older than the second rosette leaf, so it was likely that age-related symptoms would be observed primarily on the first rosette leaf pair and later in the second rosette leaf pair. The water deficit in 10+6 DAG first rosette leaf pairs did not show any wilting, while the drought-stressed 15+6 DAG first rosette leaves displayed moderate level of wilting, and the 20+6 DAG stressed samples showed the greatest display of wilting. The same results were found on the second rosette drought-stressed leaves, where wilting was only visible on the 20+6 DAG leaves (Figure 3.9). Altogether, these results clearly show that as *Arabidopsis* leaves age, the occurrence of senescence-inducing ARCs cause reduced desiccation tolerance.

Salt shock was another experiment used to examine the consequence of stress on different aged *Arabidopsis* leaves. Plants can be exposed to salt stress in two ways, either by exposure to mild salt levels causing osmotic stress, or by sudden exposure to concentrated salt that leads to osmotic shock (Shavrukov, 2013). In this study plants were exposed to osmotic shock by watering with 300 mM NaCl solution for 6 days at 10, 15 and 20 DAG, and the progression of senescence was recorded by measuring the chlorophyll content from the first rosette leaf pair (Figure 3.11D). The obvious effect of salt was viewed in all three stages (10, 15 and 20 DAG), where plant samples showed darker colour and diminished leaf growth (small rosette), likely due to reduced photosynthetic capacity, affected cell division and cell enlargement (Osakabe et al., 2014). However, the results showed a significant difference between the salt shocked samples of different ages, where leaf yellowing was more pronounced in 20+6 DAG first rosette leaves than 15+6 DAG samples (Figure 3.11). This result

correlates with the observation that the chlorophyll level declined progressively with age. Hence, this experiment also suggests that tolerance to stress decreases with leaf age because of gradual occurrence of senescence-inducing ARCs. Additionally, the effect of darkness was examined in different aged plants by exposing them to dark conditions (Figure 3.12D). It was also determined whether plant recovery was affected by increased leaf age (Figure 3.12E). The results of this experiment were consistent with the previous observation where chlorophyll degraded progressively with age, and leaf recovery also decreased with age.

It has previously been found that young plants are more tolerant to stress than mature plants. For example, detached *Xanthium* young leaves did not show wilting after drought stress, but mature leaves showed signs of leaf dryness and stress-induced ABA accumulation (Cornish and Zeevaart, 1984). Also, young cucumber leaves were shown to display remarkable resistance to sulphur dioxide (SO_2) stress, whereas mature leaves were more susceptible (Sekiya et al., 1982). The research conducted by Wang et al., (2012) also revealed that young rice leaves adapt well to alkaline stress, but the cell membranes of adult rice leaves were severely injured, and showed reduction in chlorophyll pigment. Moreover, recent research has shown that paraquat sprayed on young *Arabidopsis* leaves results in reduced ROS accumulation due to higher antioxidant activity, while adult leaves exhibited damage from high ROS abundance and reduced ROS scavenging activity (Moustaka et al., 2015). The results of these studies confirm that decreased stress tolerance with age is a consequence of developmental senescence-inducing ARCs. Thus, young seedlings were resistant to stress because of reduced senescence-inducing ARCs, whereas adult leaves displayed sensitivity because of elevated senescence-inducing ARCs. In plants, ageing itself does not lead to death under stress but causes the decrease in stress tolerance in plants and therefore later increases a susceptibility to death (Mueller-Roeber and Balazadeh, 2014).

Altogether, these findings justify the hypothesis that EEL are more tolerant to stress because of highly active DNA repair mechanisms and reduced endogenous stress. Low expression of oxidative stress and senescence-related genes signify that EEL have negligible levels of endogenous stress at this age. On the contrary, the expression of genes linked to DNA repair are reduced, and genes associated to oxidative stress and senescence are increased in MEL and FEL. Here, I propose that, this is one of the reasons the first rosette MEL and FEL samples display poor stress tolerance. The downregulation of genes linked to stress is well supported by the elevated stress hormones and ROS accumulation in first rosette MEL and FEL samples. Whereas, the constant increase in endogenous oxidative stress, senescence, stress hormones and ethylene-related genes is a finding that strengthens our understanding that reduced resistance to stress increases in leaves with age.

I propose that, in a stressed environment the occurrence of senescence-inducing ARCs causes death of the oldest leaves with remobilisation of nutrients to the young growing tissues for the survival.

Therefore, together the transcriptomic study presented here suggests that occurrence of senescence-inducing ARCs is an intrinsic process that causes timely and certain death in plants.

Chapter 4 Characterisation of mutants modulating age-related changes that regulate senescence in *Arabidopsis thaliana*

4.1 Introduction

Leaf senescence is the final stage of leaf development, during which nutrients within the senescent leaf are recycled to the other growing parts of the plants (Hörtensteiner, 2006). The process of senescence is evolutionary advantageous to plants, but early leaf senescence due to adverse environmental conditions contributes to postharvest loss of vegetables and reduced yield in certain crops (Gan and Amasino, 1997). Research has been done during the last five decades with the aim to have a better quality and increased production of fruits, vegetables and crops all around the world. Along with the research in improving the quality of food and studying the physiology of plants, understanding leaf senescence is also one of the primary interests of plant biologist with the aim of expanding the lifespan of plants in stressed environments. To understand the basic conserved biological processes, various strategies such as reverse and forward genetic approach used so far, have enabled us to gain knowledge about the regulation of developmental senescence (Alonso and Ecker, 2006; Chardon et al., 2014; Xi et al., 2013).

To identify genes that are involved in plant ageing, a forward genetic approach was applied. From *Arabidopsis* Landsberg *erecta* (L*er*-0) background, eight *onset of leaf death (old)* mutants have been previously isolated by exposing plants to stress using ethylene gas (Jing et al., 2005). The L*er*-0 seedlings were treated with ethylene gas for three days at 11, 21 and 27 DAG. The *old* mutant plants were divided into three classes based on their phenotypic response before and after ethylene stress treatment (Jing et al., 2002). The class 1 mutants comprised of *old1, old5* and *old14* showed premature senescence symptoms in the air and further enhanced senescence after ethylene treatment. *old13* is a class 2 mutant, that displayed normal growth in the air but enhanced symptoms of senescence when treated with ethylene. *old12* and *old3* mutants belong to class 3, displaying accelerated senescence in air that could not be further enhanced by ethylene (Jing et al., 2005).

In this chapter I sought to identify mutants that modulate senescence-induced Age-Related Changes (ARCs). In chapter 3, it is shown that the occurrence of ARCs reduces stress tolerance with an increased age of *Arabidopsis* leaves. Therefore, mutants showing enhanced susceptibility to stress treatments as a cause of early occurrence of ARCs should be chosen modulating senescence-induced ARCs. For this, the *old13* and *old14* mutants were characterised to ascertain if these genes have a function in controlling senescence-induced ARCs in plants. These mutants were selected because the *old13* mutant is the same

as the WT and *old14* which shows early ageing symptoms when grown under standard laboratory conditions. Nevertheless, both mutants displayed early onset of senescence when exposed to ethylene stress. This chapter describes the growth disorders and stress responses observed in *old13* and *old14* mutant plants as compared to the wild type.

4.2 Results

4.2.1 Phenotypic characterisation of the *old13* and *old14* mutants in long-day photoperiod

In this section, the phenotype of *old13* and *old14* mutants was determined under standard growth conditions. Growth stage-based phenotypic analysis using the BBCH (BASF, Bayer, Ciba-Geigy, Hoechst) scale was carried out to interpret phenotypic differences in *old13* and *old14* mutants compared to the *Arabidopsis* wild type (WT) L*er*-0 plants (Boyes et al., 2001; Hess et al., 1997).

Phenotypic differences were observed in the *old13* and *old14* mutants compared to the WT plants, when grown on soil in a long-day (LD) photoperiod (16-hours of light). Emerged rosette leaves in *old13* and *old14* mutants were very similar to the WT in appearance (Figure 4.1) but, after comprehensive observation there were one or two-days difference in the emergence of rosette leaves at 10 DAG as shown in Appendix 2 (from stage 1.05) and in Figure 4.2A. However, clear abnormalities in the mutants were observed after initiation of bolting in plants. In contrast to L*er*-0, *old13* and *old14* mutants show early and late inflorescence emergence, respectively. The elongated inflorescence in *old13* was higher than L*er*-0 as shown in Figure 4.2B, where it reached 316 mm in height at 45 DAG. The *old14* late flowering mutant only reached 241mm in height when compared to the WT plants, which measured 301mm (Figure 4.2B). The results in Figure 4.2C indicate that emergence of inflorescence in *old13* occurs two days earlier than WT, and in *old14*, one day later than WT (Figure 4.2D). Thus, under a LD photoperiod, these mutants, although appearing visibly normal, are slightly altered in stages of plant development.

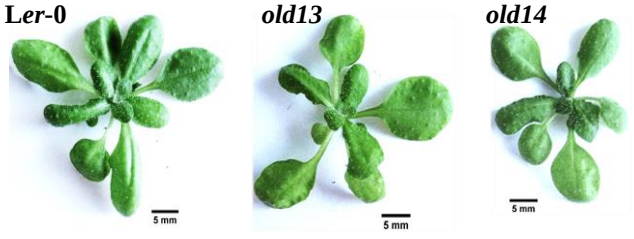

Figure 4.1. *Arabidopsis* wild type (WT) L*er*-0 and *old* mutants grown under long day (LD) photoperiod. Photographs were taken at 22 days after germination. Bar represents 5mm.

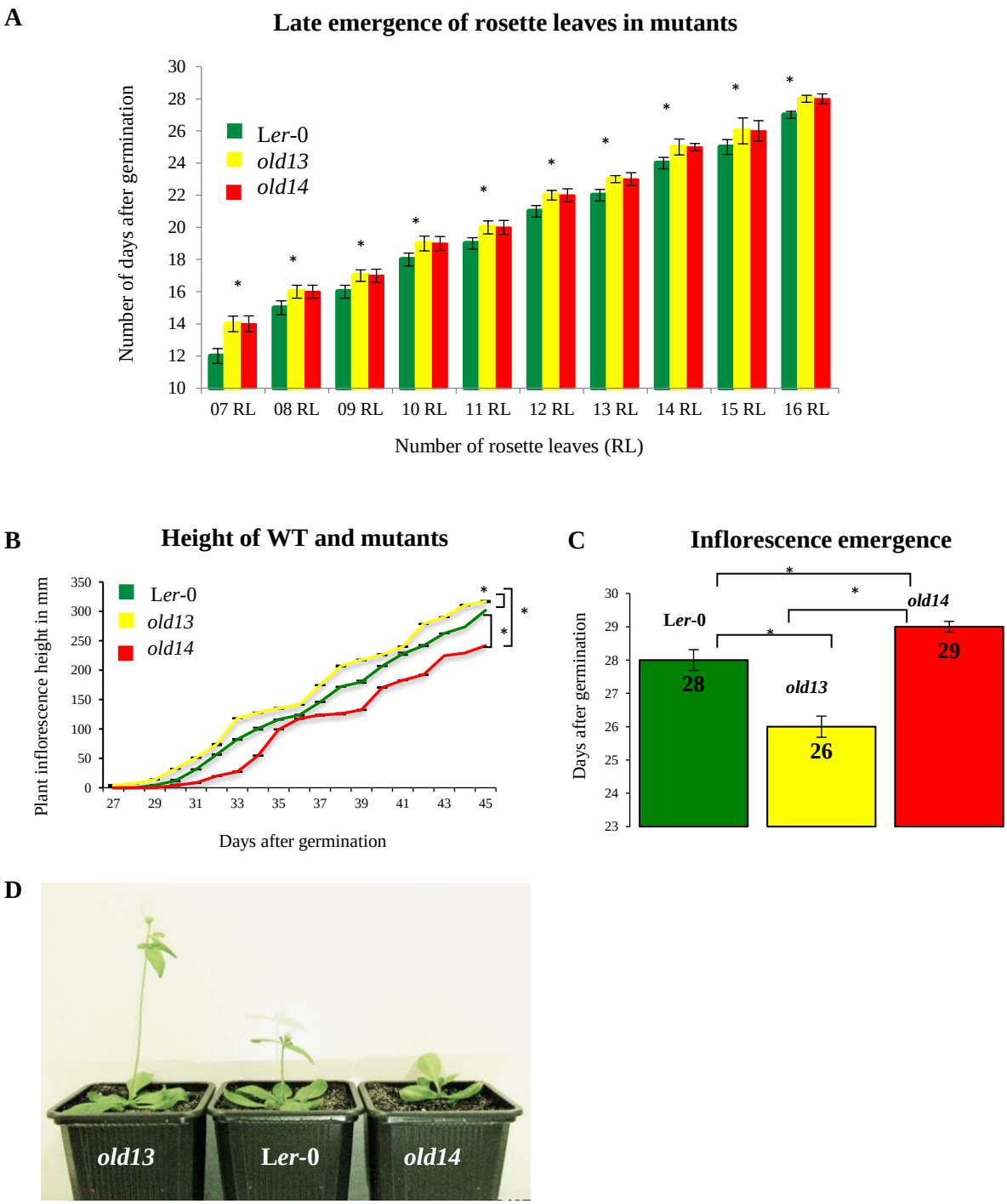

Figure 4.2. Phenotypic differences between wild type (WT) L*er*-0 and *old* mutant plants in long day (LD) light conditions.

A. Number of emerged rosette leaves between L*er*-0 and mutants. Twenty biological replicates were used, represented as mean ± standard deviation. Green, yellow and red bars represent L*er*-0, *old13* and *old14*, respectively. **B.** Comparison of height over time between L*er*-0 and mutants. Three biological replicates were used for each data point. Data in green, yellow and red colour indicate L*er*-0, *old13* and *old14* respectively. **C.** Comparison of early and late inflorescence in *old13* and *old14* compared to WT. Data are averages and standard deviation was calculated using 20 plants. **D.** Early flowering in *old13* and late flowering in *old14*. Picture was taken on 31 DAG. In Figure B, * indicates the values are significantly different between each indicated samples from 30 DAG onwards. In Figures A and C, * indicates the values are significantly different between the indicated samples at $p \leq 0.05$ using Student's t-test.

4.2.2 Phenotypic characterisation of the *old13* and *old14* mutants in short-day photoperiod

Since *Arabidopsis* growth is regulated by light duration and intensity (Roden et al., 2002), it was next investigated whether changes in light period length would amplify the subtle phenotype observed in mutants under LD photoperiod. Therefore, growth parameters were recorded for plants grown on soil under short-day (SD) conditions (8-hours light). At 15 DAG, rosette leaf emergence in *old13* and *old14* mutants was similar to the WT, but at 16 DAG, a difference in the rosette leaf emergence was observed in both the mutants (Appendix 3, Figure 4.4A). The *old13* mutant plants displayed late emergence of rosette leaves, but only by one or two days as compared to L*er*-0. The inflorescence emergence in WT plants was observed 69 DAG in SD light, whereas in *old13* plants early inflorescence appearance was recorded at 65 DAG (Figure 4.4C). The graph in Figure 4.4B shows that the length of inflorescence was higher in *old13* mutant compared with the WT plants. Also, flower emergence was 4 days earlier in *old13* mutants compared to WT plants grown in SD photoperiod (Figure 4.4 D). On the contrary, the *old14* mutants displayed a much smaller rosette size (Figure 4.3) and delayed inflorescence appearance and flowering (Figure 4.4C, D; Appendix 3). The emergence of rosette leaves in *old14* was delayed by 2-3 days in SD conditions while in LD it was delayed by just 1-2 days (Figure 4.4A). Interestingly, the emergence of inflorescence was delayed 5 days in *old14* plants under SD, and grew to only 102 mm in height at 89 DAG, compared to L*er*-0 where the inflorescence reached 178 mm (Figure 4.4C). Therefore, the *old14* mutant plants grown under a SD photoperiod revealed noteworthy morphological divergences.

The differences observed in growth stages by phenotypic analysis suggests that the *old13* mutant is less sensitive to the day length, as there was little difference between the LD and SD photoperiod treatments. On the contrary, it appears that the *old14* mutant is sensitive to the day length as the reproductive phase was significantly delayed in SD, compared to the LD conditions.

Figure 4.3. *Arabidopsis* wild type (WT) L*er*-0 and *old* mutants grown under short day (SD) photoperiod. Photographs were taken at 32 days after germination. Bar represents 10 mm.

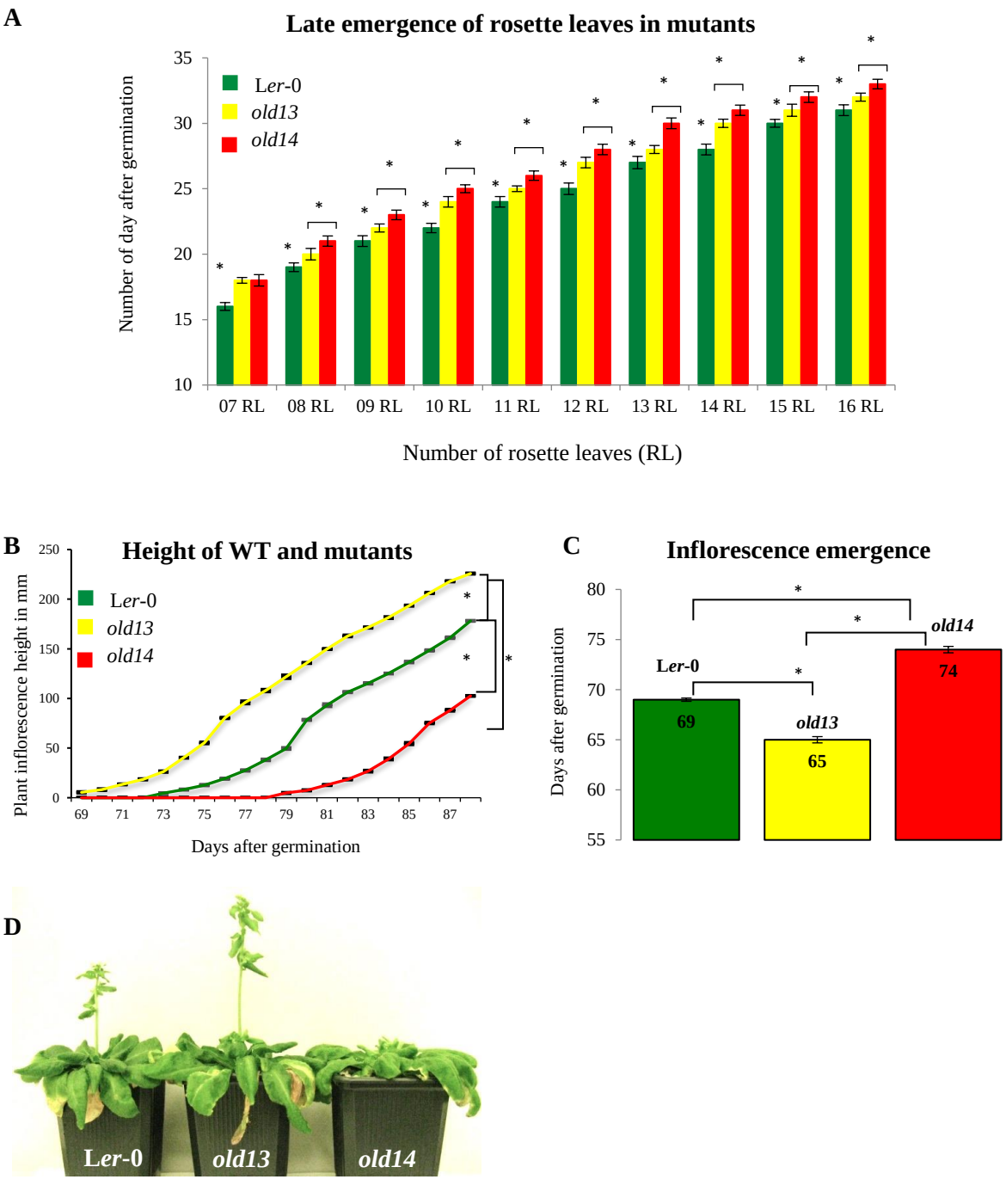

Figure 4.4. Phenotypic differences between wild type (WT) L*er*-0 and *old* mutant plants in short day (SD) photoperiod.

A. Number of emerged rosette leaves between L*er*-0 and mutants. Twenty biological replicates were used, represented as mean ± standard deviation. Green, yellow and red bars represent L*er*-0, *old13* and *old14* respectively. **B.** Comparison of height over time between L*er*-0 and mutants. Three biological replicates were used for each data point. Data in green, yellow and red colour indicate L*er*-0, *old13* and *old14* respectively. **C.** Comparison of early and late inflorescence in *old13* and *old14* compared to WT plants. Data for this are averages and standard deviation was calculated using 20 plants. **D.** Early flowering in *old13* and late flowering in *old14*. Picture was taken at 80 DAG. In Figure A, * indicates the values are significantly different between WT and mutants (*old13* and *old14*), * indicated by inverted brackets shows the values are significantly different between the *old13* and *old14*. In figure B, * indicates the values are significantly different between each indicated samples from 69 DAG onwards. In Figure C, * indicates the results are significantly different between the indicated samples at $p \leq 0.05$ using Student's t-test.

4.2.3 Physiological characterisation of mutants in standard growth conditions

Next it was investigated whether the *OLD13* and *OLD14* genes are potential regulators of senescence under standard growth conditions. If these genes function in suppressing the onset of senescence, then the mutants should display early onset of senescence when grown in standard laboratory conditions compared to the WT. To monitor the progression of senescence in the *old13* and *old14* mutants, the first rosette leaf pair was used to measure membrane integrity and chlorophyll level. Plants were grown at 21°C with 65% humidity and 16-hour day length. Electrolyte leakage was calculated by the percentage of leaked ions from samples before boiling and after boiling (Materials and method section 2.9). The results show that the percentage of ion leakage in *old13* is similar to the WT plants, with no significant difference at any of the time points after germination (Figure 4.5A). In contrast to the WT, the percentage of leaked ions increased in the *old14* mutant from 32 DAG. In addition to this, the chlorophyll content declined in *old14* from 28 DAG while no apparent sign of chlorophyll reduction was observed in *old13* and L*er*-0 plants (Figure 4.5B). The *old13* mutant appeared normal with no noteworthy reduction in chlorophyll content or leaked ions (Figure 4.5A, B). Thus, the results for each experiment outlined above show that the progression of senescence in the *old13* mutant is similar to that in WT, confirming that the *OLD13* gene is not a regulator of senescence in plants grown under standard conditions. However, in the *old14* mutant, initiation of early chlorophyll degradation coupled with increased ion leakage suggests that the *OLD14* gene is a negative regulator of senescence.

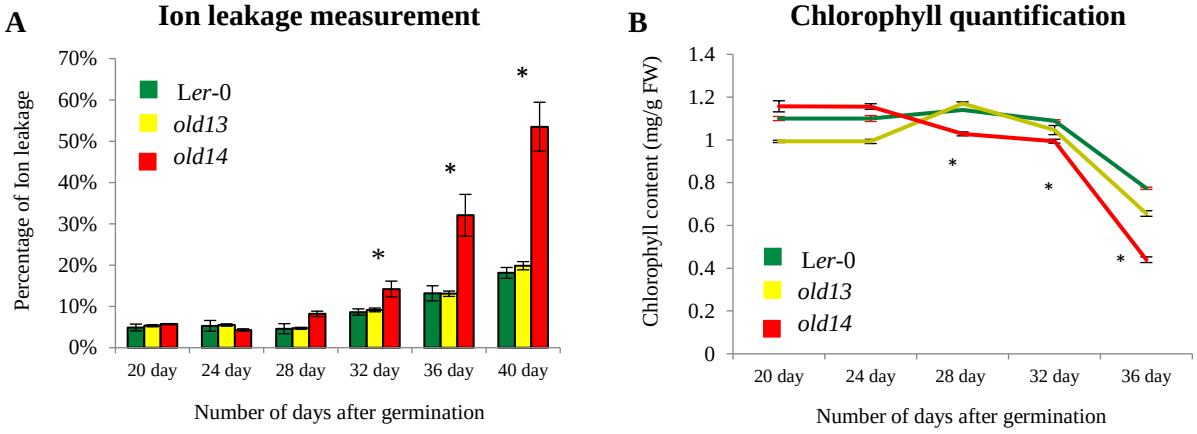

Figure 4.5. Physiological characterisation of mutants in normal air grown conditions.
A. Measurement of ion leakage in first rosette leaves from 21 until 40 DAG for physiological characterisation of the *old13* and *old14* mutants. Green, yellow and red colour represents L*er*-0, *old13* and *old14* respectively. * indicates the results are significant at p≤0.05, between L*er*-0 and *old14*. Data represent the mean and standard deviation of three independent measurements. **B.** Measurement of chlorophyll content of the first pair of rosette leaves from 20 till 36 DAG, for physiological classification of the *old13* and *old14* mutants. Green, yellow and red colour represents L*er*-0, *old13* and *old14* respectively. * indicates the values are significantly different at p≤0.05 using Student's t-test, between WT and *old14*. Data represents the mean and standard deviation of three independent replicates.

4.2.4 Physiological characterisation of mutants grown in stressed environments

4.2.4.1 Effect of drought stress on the *old13* and *old14* mutants

Previous results suggest that the *OLD13* gene is not involved in the regulation of senescence but that the *OLD14* gene functions in controlling the onset of senescence under standard growth conditions. Next, it was examined whether the *OLD13* and *OLD14* genes function in controlling the senescence-inducing ARCs in plants. If these genes function in controlling the ARCs, then the mutated genes will cause early or late occurrence of ARCs. If the mutation in *old13* and *old14* genes have caused late occurrence of ARCs then the mutants will be tolerant to stress treatments, whereas early occurrence of ARCs in these mutants will cause enhanced susceptibility to the stress. Therefore, it was expected that the *old13* and *old14* plants would be either more tolerant or susceptible to stressed environments compared to the WT plants. To investigate stress responses in the *old13* and *old14* mutants, the plants were exposed to drought stress.

WT, *old13* and *old14* plants grown in a LD photoperiod were exposed to water deficit conditions. Watering was stopped 18 DAG, and after 5 days of drought, the relative water content (RWC) was measured. The results show that WT plants are tolerant to the water deficit conditions, as no significant reduction in RWC was detected between well-watered and drought-stressed plants (Figure 4.6A, B). It can be seen in Figure 4.6A, that after 5 days of drought stress the RWC has reduced to 58% and 22% in *old13* and *old14* respectively. The measured RWC reflects the wilting observed in drought-stressed *old13* and *old14* plants (Figure 4.6C, D). Therefore, these results illustrate the sensitivity of these mutants to water deficit conditions, especially in *old14* which was most sensitive to the drought stress. Taken together, these results suggest that the mutated *OLD13* and *OLD14* genes cause early occurrence of ARCs in plants under water deficit conditions.

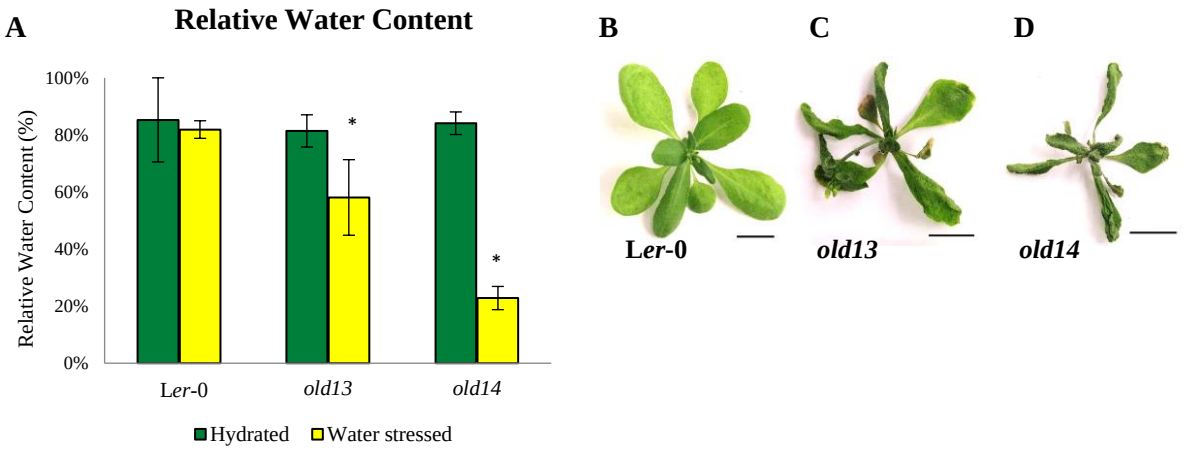

Figure 4.6. Susceptibility of *old* mutants to drought stress.
A. Estimation of relative water content (RWC) during the imbibition period for hydrated and drought-stressed plants. Green bars represent hydrated plants, whereas yellow bars indicate drought-stressed plants. Results are represented as means and standard deviations from 6 plants for each line. * indicates the values are significantly different at $p \leq 0.05$ using Student's t-test between the hydrated and drought-stressed *old13* and *old14* plants. Photographs were taken after 5 days of drought treatment **B** L*er*-0, **C** *old13* and **D** *old14*. Bar represent 10 mm.

4.2.4.2 Effect of dark stress on the *old13* and *old14* mutants

Results from the previous experiment show that the *old13* and *old14* mutants are susceptible to water deficit conditions, suggesting that the mutated genes have possible roles in early occurrence of ARCs in plants. Next, another stress experiment was carried out to ascertain if mutant susceptibility is restricted to only drought stress, or whether other stresses have a greater impact as well. Therefore, to investigate similar impact of different stresses in the *old13* and *old14* mutants, the plants were exposed to dark stress. If the *OLD13* and *OLD14* genes function in controlling the ARCs in plants, then it is expected that mutants will be susceptible to dark stress treatment as well.

To determine the effect of dark stress, plants were first grown for 20 days in LD conditions and subsequently the plants were shifted to complete darkness for 2, 4, 6 and 8 days. The progression of senescence was monitored by quantifying the chlorophyll content of the first rosette leaf pair. The results show that with increased days in darkness, the chlorophyll content declined in WT, *old13* and *old14* leaf samples. However, in contrast to L*er*-0, the chlorophyll content decreased more in *old13* samples (Figure 4.7). The *old14* leaves showed significant yellowing (Figure 4.9) followed by a comparatively large reduction in chlorophyll compared to the WT samples after dark stress. Taken together these result confirm that the susceptibility to dark stress observed in the *old13* and *old14* mutants is consistent with the reduced tolerance to drought stress, supporting the hypothesis that the mutants have early occurrence of ARCs.

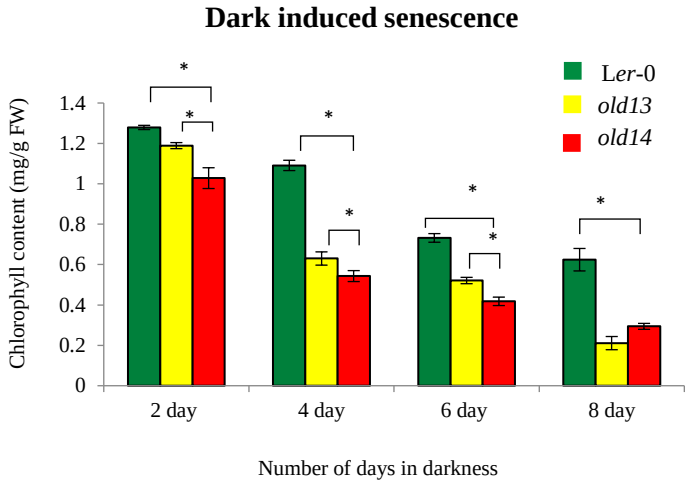

Figure 4.7. Dark induced early leaf senescence in *old* mutants.
At 20 days after germination (DAG) plants were kept in the dark for 2, 4, 6 and 8 days. Total chlorophyll content was calculated from the first pair of rosette leaves. Green, yellow and red bars indicate WT, *old13* and *old14*, respectively. Three biological replicates were used for each data point, represented as mean ± standard deviation. * indicates the values are significantly different between the indicated samples at $p \leq 0.05$ using Student's t-test.

4.2.4.3 Light independent early senescence and high ROS level of *old* mutants

ROS overproduction has been suggested to constitute one of the causes of ageing and senescence in plants (Biesalski, 2002; Schieber and Chandel, 2014). Therefore, if the mutated *OLD13* and *OLD14* genes cause early occurrence of ARCs, then after stress treatment the mutants should also have high ROS levels leading to early senescence. To investigate ROS levels, 20 DAG *old13* and *old14* plants were kept in darkness for two days. The hydrogen peroxide (H_2O_2) content was detected histochemically by staining the leaves with 3,3 ′-diaminobenzidine (DAB) solution after dark stress. DAB in the presence of H_2O_2 oxidises and generates a dark brown precipitate within plant tissues (Thordal-Christensen et al., 1997). The experiment was conducted by DAB staining the WT and *old* mutant second rosette leaves before and after 2 days of dark treatment. Before dark incubation the level of H_2O_2 appears to be low in both WT and mutant leaves as no apparent brown precipitation was observed (Figure 4.8A). But, after 2 days of darkness, increased H_2O_2-induced staining was observed in *old13* second rosette leaf pairs compared to the WT (Figure 4.8B), and pronounced staining was found in the *old14* leaves. The results support the hypothesis that upon stress treatments, the *old13* and *old14* mutants display high ROS levels.

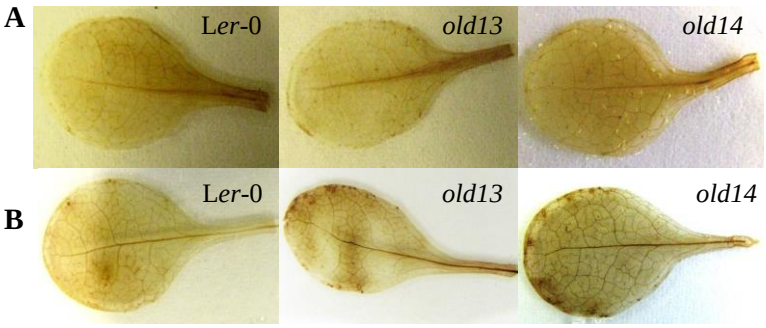

Figure 4.8. Histochemical detection of elevated ROS level in *old* mutants after dark stress
A. DAB-stained second rosette leaves of WT and *old* mutants before dark incubation. B. DAB-stained second rosette leaves of WT and *old* mutants after 2 days of dark incubation. Three replicates were used for each plant and a picture of a representative leaf is shown.

4.2.4.4 Early starch turnover in the *old13* and *old14* mutants

From the above results it is confirmed that *old13* and *old14* mutants showed susceptibility to stressed treatments, possibly because of early occurrence of senescence-inducing ARCs. Also, in chapter 3, it was confirmed that, with age, the occurrence of senescence-inducing ARCs reduces the recovery in plants after dark stress (section 3.2.3). Based on this, I hypothesise that the *old13* and *old14* mutant plants will show poor recovery after dark stress treatment. Plant recovery was recorded by staining starch in leaves before and after the dark treatment. If the mutants show poor recovery, then it is expected that after dark stress and a recovery period, the *old* mutants will show reduced or no starch in the leaves compared to the WT plants.

To determine the dark stress recovery in WT and *old* mutants, plants grown in LD photoperiod were shifted to darkness for 2 and 4 days at 20 DAG. After the dark treatment, plants were returned to a LD photoperiod at 21°C and harvested three days later to assay for starch recovery. The iodine staining method was used to detect the presence of starch in leaves, which is based on colour development after iodine binds to starch polymers. After 2 days of darkness and a 3 day of recovery period, the WT rosette displayed staining of 81% of the leaf area (Table 4.1, Figure 4.9A), measured by image J (see section 2.11.1). In contrast, 39% and 27% (Table 4.1) of leaf area was stained in 2 days dark stressed *old13* and *old14* rosette respectively (Figure 4.9A) after 3 days of recovery in light. Additionally, after 4 days of prolonged darkness and 3 days of recovery, 41% of leaf area was stained in WT plants, but in *old13* and *old14* samples only 26% and 14% leaf was stained respectively (Table 4.1, Figure 4.9B). Also, the *old* mutant plants displayed significant yellowing after 4 days of darkness and bleached leaves after 3 days of recovery. Thus, the result shows that along with the early dark-induced senescence, the mutants showed poor recovery after the dark stress treatment, further supporting the hypothesis of early occurrence of senescence-inducing ARCs in the *old13* and *old14* mutants.

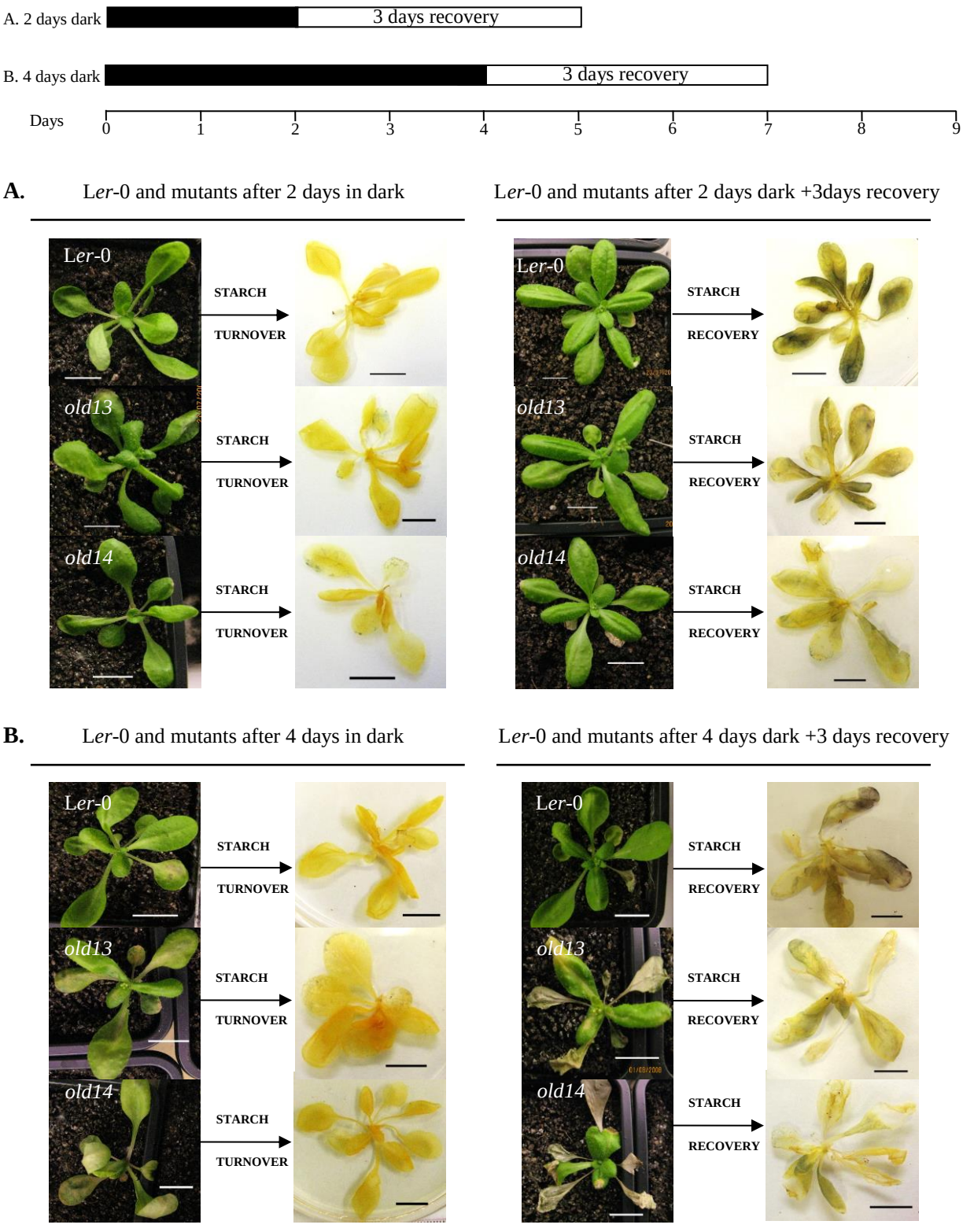

Figure 4.9. Early starch turnover effect in the *old13* and *old14* mutants.
Plants were stained with Lugol's IKI solution to visualize the presence of starch at the end of the dark period and after three days of recovery. Blue-black colour indicates presence of starch in leaves. Three biological replicates were used for each experiment and representative plants are shown. **A.** Iodine-stained WT and mutants after 2 days in dark and 3 days of recovery. **B.** Iodine-stained W.T and mutants after 4 days in dark and 3 days of recovery. Leaves were photographed after dark incubation and after staining. The bar represents 10 mm.

Table 4.1 Percentage of stained leaf area calculated by Image J software

Dark + Recovery	Stained leaf area in L*er*-0	Stained leaf area in *old13*	Stained leaf area in *old14*
2 Days dark + 3Days recovery	80.70%	39.10%	27.10%
4 Days dark + 3Days recovery	41.10%	26.30%	13.50%

4.3 Discussion

4.3.1 Growth disorders in the *old13* and *old14* mutants

The integration of data from phenotypic analyse provided information about the developmental alterations occurring in the *old13* and *old14* mutant plants under non-stressed conditions as a result of mutated genes. These phenotypic analyse of mutants in contrast to L*er*-0 revealed noteworthy morphological differences.

It is well studied that stress-induced early flowering is an adaptive mechanism ensuring survival of a plant (Takeno, 2012). The seeds produced from stressed plants could carry adaptive genes that enable better survival under stress (Takeno, 2016). Extensive research has been done to understand the flowering mechanism in plants during stress, which involves a set of genes regulating flowering time such as, *FLOWERING LOCUS T*, *SUPPRESSOR OF OVEREXPRESSION OF CONSTANS 1*, *TWIN SISTER OF FT*, *FLOWERING LOCUS C*, *miR169* and many more (Kardailsky, 1999; Sheldon, 2000; Wada et al., 2013; Xu et al., 2014). Delayed or early flowering time is one of the important strategies plants adapt in response to abiotic stress tolerance. It was shown that the overexpression of transcription factor *CDF3*, which regulates flowering time-induced tolerance to drought, heat and salt by promoting late flowering in transgenic *Arabidopsis* plants (Kazan and Lyons, 2016). It has also been proven that an increase in ROS during stressed conditions promotes reproductive growth in plants (Kotchoni et al., 2008a; Riboni et al., 2014; Zimmermann et al., 2006). Also, an antioxidant ascorbic-acid deficient mutant flowered earlier than WT, possibly due to uncontrolled ROS production (Kotchoni et al., 2008b). The morphological characterisation of *old13* shows that during vegetative growth, the rosette leaf emergence is delayed by 1 to 2 days as compared to the WT (Appendix 2 and 3). Although *old13* plants display late rosette leaf emergence, they are early during the reproductive phase (Figures 4.2 and 4.4). Additionally, Schippers et al., (2008) confirmed that the mutated *old13* gene is a positive regulator of senescence with an increased level of ROS. The results of the experiments described in this chapter also show that *old13* plants are susceptible to stress, and display accumulation of ROS (Figure 4.8). Taken together, these data suggest that *old13* plays a role in altering a pathway that results in a slight but significant early flowering phenotype in the mutant.

The growth stage-based phenotypic analysis of the *old14* mutant illustrated delayed inflorescence together with reduced plant size and delayed flower formation under LD photoperiod (Appendix 2 and Figure 4.2). The late-flowering phenotype in *old14* was much more conspicuous under a SD photoperiod (Appendix 3 and Figure 4.4). The *old14* mutant was only half the size of L*er*-0 as measured by the length of the stem in the SD photoperiod (Figure 4.4C). Premature exhaustion of starch results

in a carbon deficit at night, which causes inhibition of growth and premature senescence in plants (Pantin et al., 2011; Tetley and Thimann, 1974; Yazdanbakhsh et al., 2011). It has been reported that mutants deficient in starch synthesis (*pgi1, pgm1* and *adg1*) grown in a SD photoperiod show delayed initiation of flowering because of insufficient starch synthesis (Yu et al., 2000). Moreover, the early senescence symptoms were rescued in *egy1* (ethylene-dependent gravitropism-deficient and yellow-green 1) mutants after treating the plants with glucose (Chen et al., 2015), suggesting that sugar starvation was the cause for premature leaf senescence. It is possible that the late flowering in *old14* was due to reduced starch metabolism, where sufficient starch cannot be accumulated as a carbon source for growth during short-day conditions. Additionally, the *old14* mutants show early senescence symptoms in normal growth conditions (Figure 4.5). It could also be possible that the *old14* mutant displays premature ageing due to sugar starvation and induced accumulation of ROS. Together, the growth disorders in *old14* suggest that the increase in flowering time in SD, as well as in LD conditions, is not caused by a specific defect in one of the flowering pathways, but by a more general defect in plant growth, which simultaneously leads to late flowering in *old14*.

In conclusion, it is evident that on one side *old13* plants display an early flowering phenotype whereas, on the other side *old14* plants show delayed flowering symptoms. As, mutated *old13* and *old14* genes are positive regulators of senescence during stressed conditions, the variation of flowering time suggests that the premature ageing symptoms are independent of an early or late reproductive phase. Thus, based solely on the phenotypic analysis, the *old13* and *old14* mutants have provided informative evidence in relation to their growth disorders.

4.3.2 The mutated *old14* gene is a positive regulator of senescence in *Arabidopsis*

Leaf senescence has been suggested to begin when the photosynthetic rate drops below a certain threshold, therefore the leaf no longer contributes in carbon fixation (Hensel et al., 1993). To identify whether the mutants are positive regulators of senescence, chlorophyll quantification is one of the essential parameters which can provide basic information related to the physiological condition of plants. Additionally, membrane degradation is another classic feature of senescing cells. The electrolytes that are contained within the membranes of the plant cells leak when plants are exposed to severely stressed conditions or during the onset of senescence (Leopold et al., 1981). To determine the intactness of cell membranes, measuring the leaked solutes from plant tissue is a very common physiological method (Bajji et al., 2001). In this chapter, estimation of chlorophyll content and the percentage of electrolyte leakage signify that the onset of senescence starts 28 DAG in *old14* compared to 32 DAG in WT plants. Also, it was previously described that the *old14* mutant shows early onset of

senescence in normal growth conditions (Jing et al., 2005). Thus, results in this chapter confirmed that the *old14* plants enter the senescence phase earlier than the WT plants (Figure 4.5).

Leaf senescence can be induced by different internal and environmental stress signals (Li et al., 2012). It was found that *old14* plants showed enhanced yellowing of leaves when treated with ethylene gas (Jing et al., 2005). Therefore, the *old14* mutant was further characterised to test whether the early ageing symptoms increase susceptibility to drought and dark stress in *old14* plants. To drought stress, *old14* plants showed to be hypersensitive with completely wilted leaves (Figure 4.6). The dark experiment conducted on the *old14* mutant displayed rapid chlorophyll loss and enhanced senescence symptoms (Figure 4.7). Moreover, after two days of dark treatment, *old14* leaves stained with DAB exhibited pronounced H_2O_2 accumulation compared to the WT leaves, suggesting enhanced sensitivity to dark stress (Figure 4.8). Studies have shown that H_2O_2 is involved in normal growth and development of a plant, but excess H_2O_2 accumulation causes early ageing and increased susceptibility to stressed environments (Mittler et al., 2004). In addition to this, the *old14* mutant plants also showed poor recovery with reduced starch stained leaf area after 2 and 4 days of dark treatment as compared to WT plants (Figure 4.9). Delayed flowering, dark-induced early senescence, elevated H_2O_2 and poor starch recovery in *old14* leaves together indicates that the *old14* mutant is defective in starch metabolism.

Thus, all together the results show that early ageing in *old14* mutants enhances senescence symptoms under stress-induced treatments, and is probably due to altered starch metabolism and an uncontrolled oxidative burst. These results confirm the role of the *OLD14* gene as a negative regulator of senescence that modulates plant fitness under stressed environments. Moreover, it has been found in several transgenic lines, that early ageing symptoms increase plant's susceptibility to the stressed environments (Jalil et al., 2016; Jing et al., 2008). This supports the results where *old14* plants show enhanced susceptibility to stress treatments because of premature ageing.

Many studies have been done to understand what exactly happens during the onset of senescence, but we lack information about what happens during the pre-senescence process. With the aim to identify mutants regulating senescence-inducing ARCs the *old14* mutant was characterised, but the results show *old14* plants display early onset of senescence. Detailed studies on *old14* mutant display the events of senescence rather than just the ARCs involved in initiation of senescence, therefore the *old14* mutant was not further selected to study pre-senescence processes.

4.3.3 A mutation in *OLD13* causes early occurrence of senescence-inducing age-related changes in *Arabidopsis*

The *old13* mutants grown under standard laboratory conditions were characterised and the progression of senescence was monitored by estimating chlorophyll content and percentage of electrolyte leakage. In monocarpic plants, the progression of ageing starts after plants enters into the reproductive phase (Davies and Gan, 2012). Since *old13* plants show early initiation of flowering it was expected that the mutant will exhibit an early ageing pattern. Interestingly, the results illustrated that the *old13* mutants are similar to the WT and show no significant difference when grown under standard growth conditions (Figure 4.5).

Plants display early senescence symptoms when they are exposed to environmental stresses such as drought, darkness, an extremely low or high temperatures, salinity and many others. Extensive research done through stress treatments on plants has provided us a wealth of knowledge about their adaptive and stress-induced senescence responses (Jajic et al., 2015). The stress-induced experiments were designed to examine whether the *old13* mutation causes increased sensitivity to stress in plants. The *old13* mutants exposed to drought stress displayed high sensitivity and exhibited poor maintenance of tissue water potential compared to WT plants (Figure 4.6). Additionally, after dark stress, the *old13* mutants displayed enhanced senescence symptoms, exemplified by early chlorophyll loss, when compared to WT plants (Figure 4.7). The effect of both drought and dark treatments clearly shows that the *old13* mutant is more susceptible to the stress-inducing treatments than WT plants. In addition, the *old13* first rosette leaves stained with DAB after 2 days of dark treatment illustrated an increased level of H_2O_2 accumulation (Figure 4.8). Also, the *old13* plants showed poor recovery after 2 and 4 days of dark treatment. The sensitivity to stress-induced treatments in *old13* plants shows that the *OLD13* gene plays an important role in maintaining fitness of a plant under stressful conditions. It is expected that overexpression of the *OLD13* gene may result in greater tolerance to environmental stress.

As confirmed in chapter 3, occurrence of senescence-inducing ARCs as plant leaves age causes reduced stress tolerance and concomitant induction of senescence. The results shown here and in chapter 3 suggest that the mutation in the *old13* gene is directly involved in the early occurrence of senescence-inducing ARCs. *old13* is an appropriate mutant to use to study the regulatory pathway of senescence-inducing ARCs because it is undisguisable from the WT when grown under standard laboratory conditions, but is more susceptible to the stressed conditions. Detailed studies on the *old13* mutant to understand the pre-senescence process should include key genes or pathways involved in senescence-inducing age-related factors, and exclude the factors involved in senescence. Thus, *old13* mutants will be used to study and identify the key senescence-inducing ARCs leading to decreased stress resistance

as the plant ages. Further study and gene identification would shed light on the age-related factors that are involved in stress responses in plants.

Chapter 5 Early acquisition of senescence-inducing ARCs causes poor stress tolerance in *old13* plants

5.1 Introduction

Senescence is a natural part of development in a plants life and is provoked by both internal and external factors (Jibran et al., 2013). There are various senescence-inducing factors and senescence-retarding factors that have been studied, and suggested to induce or delay the senescence process respectively in plants. Studies have confirmed that various senescence-inducing factors like abscisic acid, jasmonic acid, ethylene, sugar and overproduction of reactive oxygen species (ROS), promote senescence in plants (Arrom and Munné-Bosch, 2012; Jing et al., 2005; Oliver et al., 1987). Whereas, various senescence-retarding factors like auxin, cytokinin, gibberellic acid and antioxidants, could slow down the senescence process (Barth et al., 2006; Khan et al., 2013; Zwack and Rashotte, 2013). The progression of age-dependent senescence is primarily driven by endogenous, developmental factors and varies substantially from species to species (Guo and Gan, 2005).

Age-dependent senescence is a gradual degenerative process that not only progressively activates the onset of senescence, but also decreases plant tolerance to stressed environments (Sharabi-Schwager et al., 2009; Chapter 3). Thus, stress resistance also depends on age, as plants show distinct responses to stress, depending on stress severity and leaf age (Clauw et al., 2015; Cornish and Zeevaart, 1984; Valares et al., 2016; Wang et al., 2012; Zhao et al., 2016). For example, this is shown in Figure 1.1, where mild stress leads to the inhibition of plant growth as a result of coping with the stress, while intermediate stress results in senescence of the oldest leaves to enable survival of the young leaves. In chapter 3, it is shown that when *Arabidopsis* leaves are young, they are more tolerant to stresses like drought or darkness, but in the adult stage, they show greater sensitivity. This study verifies that with age, the occurrence of senescence-inducing ARCs decreases stress tolerance in *Arabidopsis* leaves. Together, the study conducted in chapter 3 confirmed that age is involved in the stress response pathway.

My aim was to identify genes that are involved in 'measuring' the age of a leaf, and regulate the integration of age into the stress responses. If the function of such genes was disrupted, then the phenotypic effect in plants could be observed in four different ways; as shown in Figure 5.1. Either the effect of the wild type gene would be to positively regulate integration of age into the stress response; in the case this gene is mutated, all the leaves would be measured as young by having negligible senescence-inducing ARCs and plants would show enhanced tolerance to stress at all stages (Figure 5.1

B). Or, the effect of the wild type gene would be to negatively regulate integration of age into the stress responses; plants in which this gene is mutated will have all the leaves to be determined as old by having exaggerated senescence-inducing ARCs, this would lead to activation of leaf senescence due to stress, in all stages of the plant (Figure 5.1 C). Another possibility is that a gene could affect its regulation, resulting in the age of the leaf being overestimated as old or underestimated as young when the gene is mutated; resulting in enhanced stress sensitivity or enhanced stress tolerance respectively, but in an age-dependent way (Figure 5.1 D, E).

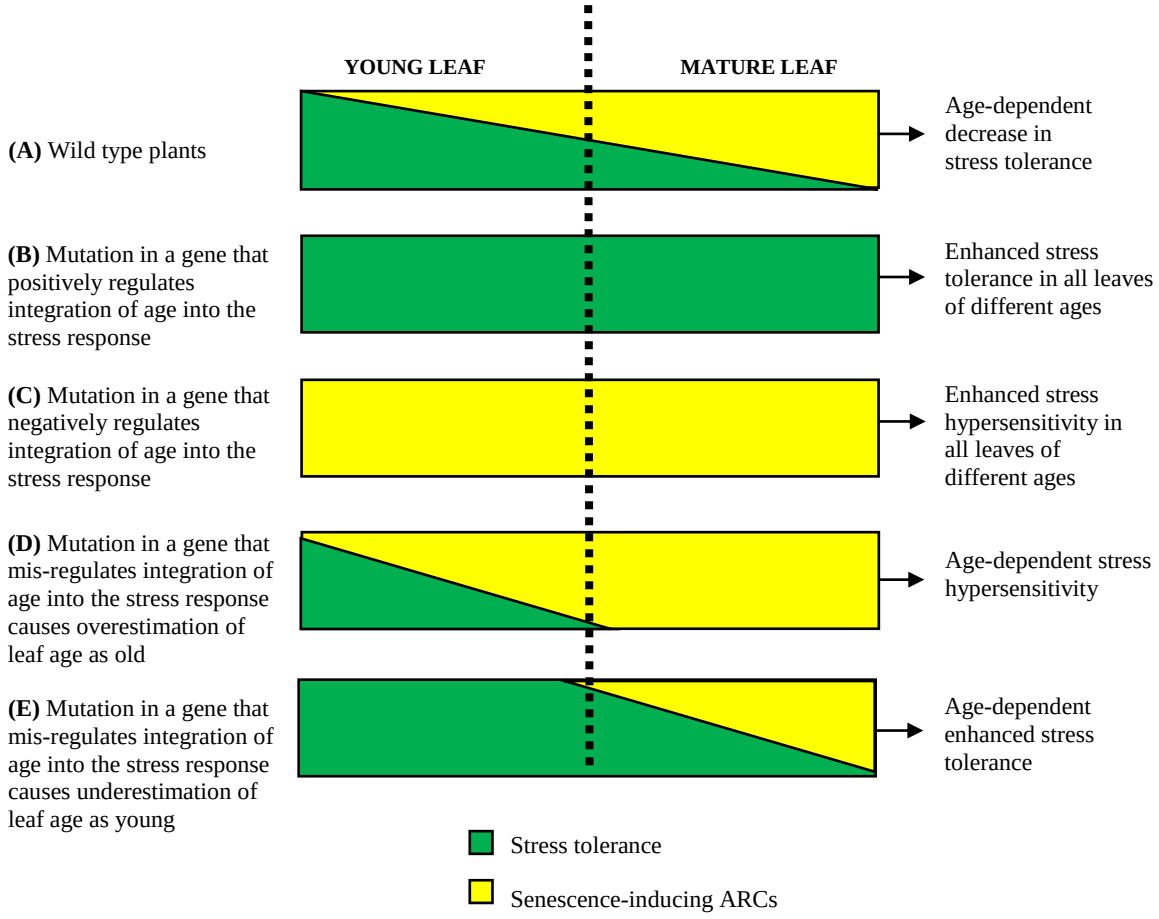

Figure 5.1 Model representing the impact of a disrupted gene having function in integration of age into the stress response

(A) Gradual occurrence of senescence-inducing ARCs causes reduction in stress tolerance as the leaf ages. (B) Mutation in a gene that positively regulates integration of age into the stress response will induce enhanced stress tolerance in leaves of all ages having negligible senescence-inducing ARCs (C) Mutation in a gene that negatively regulates integration of age into the stress response will induce enhanced stress hypersensitivity in leaves of all ages having negligible stress tolerance. (D) Mutation in a gene that mis-regulates integration of age into the stress response causes overestimation of the leaf age as old, resulting in plants displaying age-dependent hypersensitivity. (E) Mutation in a gene that mis-regulates integration of age into the stress response causes underestimation the leaf age as young will show enhanced stress tolerance in an age-dependent way.

Therefore, to investigate how stress is integrated into the plant ageing process, the *old13* mutant was selected for study (Chapter 4). Interestingly, the *old13* mutant is very similar to WT, and while it did not show early initiation of senescence, it was hypersensitive to stress (section 4.2.4). The results in chapter 4 showed that *old13* plants are stress-sensitive, therefore eliminating the possibility of mutants displaying enhanced tolerance to stress. Therefore, if the *OLD13* gene has been mutated in a way that integration of age into the stress response becomes dysfunctional, then there are two possibilities of how *old13* plants would react to stressed conditions: 1) Either, *old13* plants will have amplified senescence-inducing ARCs that make the leaves act as if they are old, causing the hypersensitive response to stress in all ages (Figure 5.1 C). 2) Or, the *old13* gene is mis-regulated and the age of leaves is overestimated as old, causing stress sensitivity in an age-dependent manner (Figure 5.1 D). Therefore, together the hypothesis is that the mutation in *OLD13* causes early occurrence of senescence-inducing ARCs, which make plants hypersensitive to stressed conditions. It will also be determined if *old13* plants show the hypersensitive response in all stages of growth, or whether the susceptibility increases with the age of a leaf. In this chapter, I aim to test the hypothesis that the stress susceptibility of *old13* mutants is due to amplified senescence-inducing ARCs (As shown in Figure 5.1 C, D). The age-dependent stress responses and transcriptomes of *old13* first rosette EEL, MEL and FEL were studied to explore the key senescence-inducing ARCs that are involved in stress responses and plant ageing.

5.2 Results

5.2.1 Drought stress susceptibility increases with age in *old13* mutant plants

To test whether *old13* plants show a hypersensitive response to stress in all developmental stages or that the stress susceptibility increases with age, *old13* plants were first treated to drought stress at three different ages; 10, 15 and 20 DAG (before the initiation of reproductive phase). It is expected that the severity to drought stress will increase with age in 10, 15 and 20 DAG *old13* plant samples.

To determine the drought stress susceptibility in different aged *old13* mutants, plants at 10, 15 and 20 DAG were exposed to water deficit conditions. These three developmental stages (10, 15 and 20 DAG) were selected as described in chapter 3 section 3.2.1. The watering schedule was the same as mentioned in Figure 3.8A (Chapter 3), where plants were drought-stressed for 6 days at 10, 15 and 20 DAG. After 6 days of dehydration on 10+6, 15+6 and 20+6 days old WT and *old13* samples, the drought-stressed, and well-watered rosettes were photographed and the relative water content (RWC) measured (Materials and methods section 2.6). The soil field capacity (SFC) measured in well-watered pots was around 98%, whereas the drought-stressed pots were near 20% (Figure 5.2). The drought-stressed WT plants in all three stages displayed better stress tolerance than *old13*, however, this resistance decreased with age, and was confirmed by measured RWC (Figure 5.3D) and visible wilting in drought-stressed 15+6 and 20+6 DAG first rosette leaf pairs (Figure 5.3B, C). On the contrary, the *old13* mutants showed greater sensitivity in all three stages of vegetative growth, compared to the WT plants. But, wilting of drought-stressed *old13* first rosette leaf pairs were more intense in 15+6 and 20+6 DAG samples, compared to the 10+6 DAG leaves (Figure 5.3). This observation is further supported by RWC measurements, which show a decrease with age; down to 53% in 10+6 DAG, 37% in 15+6 DAG and 23% in 20+6 DAG showing young leaves are more resistant to drought stress than old leaves (Figure 5.3A, B, C). Moreover, Figure 5.3E shows age-dependent reduction in RWC measured between 10, 15 and 20 DAG well-watered and drought-stressed samples. The relative reduction in RWC increases from 0% to 14% and 26% in WT, whereas the RWC reduction proliferates significantly in *old13* samples, increasing by 19%, 31% and 36%. The *old13* plants respond to drought stress more strongly than the WT plants. These results support the hypothesis that drought stress sensitivity in *old13* mutants increases with age in 10, 15 and 20 DAG plants.

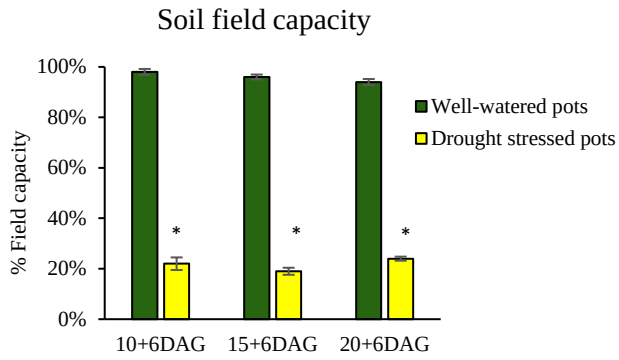

Figure 5.2. Measured soil field capacity (SFC) in well-watered pots and drought-stressed pots at 10+6, 15+6 and 20+6 days after germination (DAG). Green bars represent SFC in hydrated plants and yellow bars represent SFC in drought-stressed plants. Results are represented as means and standard deviations from 6 pots. * indicates the values are significantly different at $p \leq 0.05$ using Student's t-test, between the hydrated and drought-stressed plants.

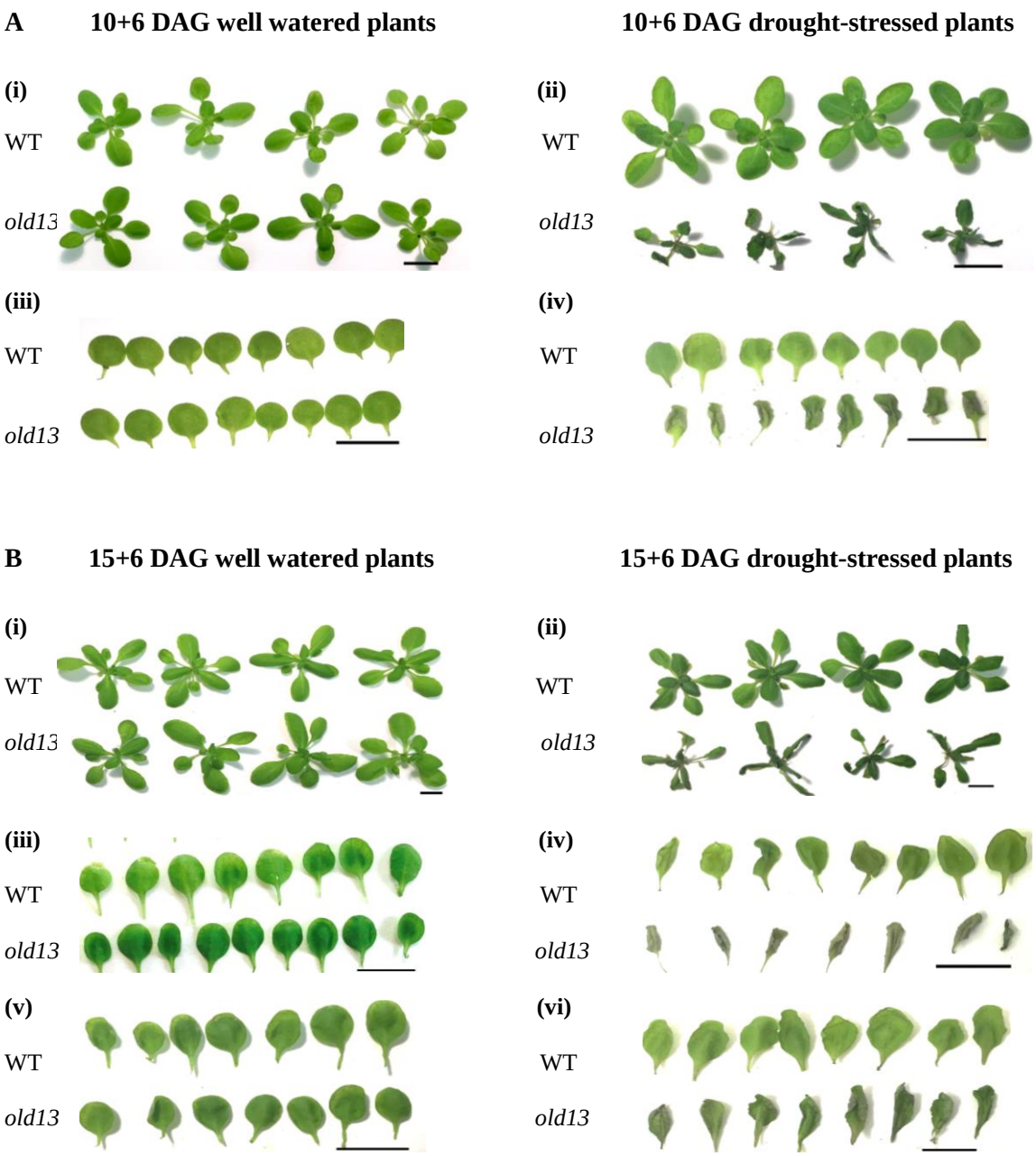

C **20+6 DAG well watered plants** **20+6 DAG drought-stressed plants**

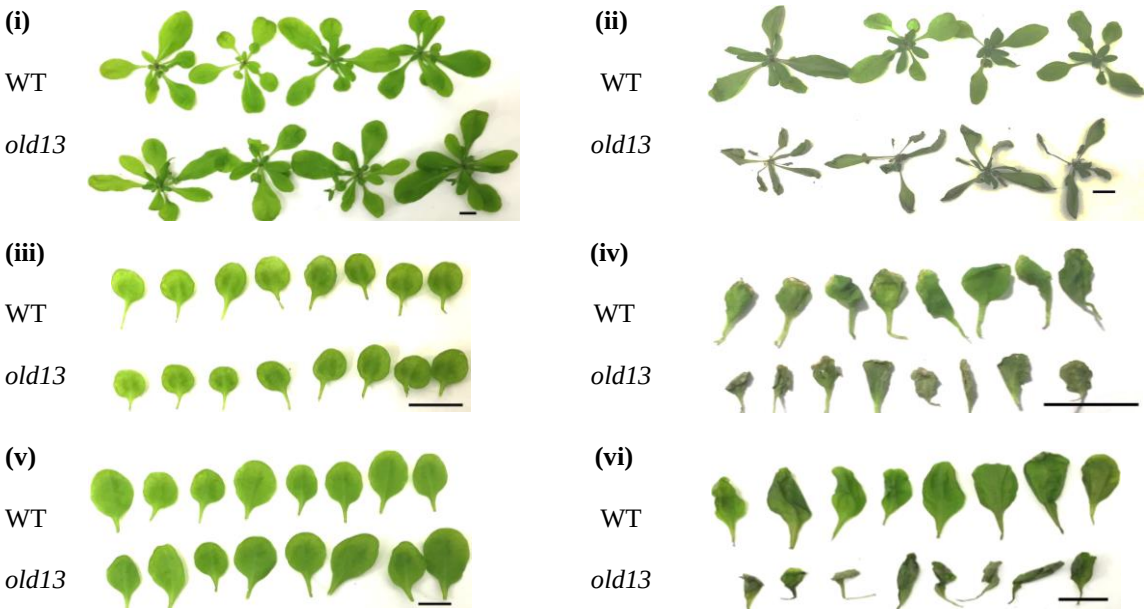

D

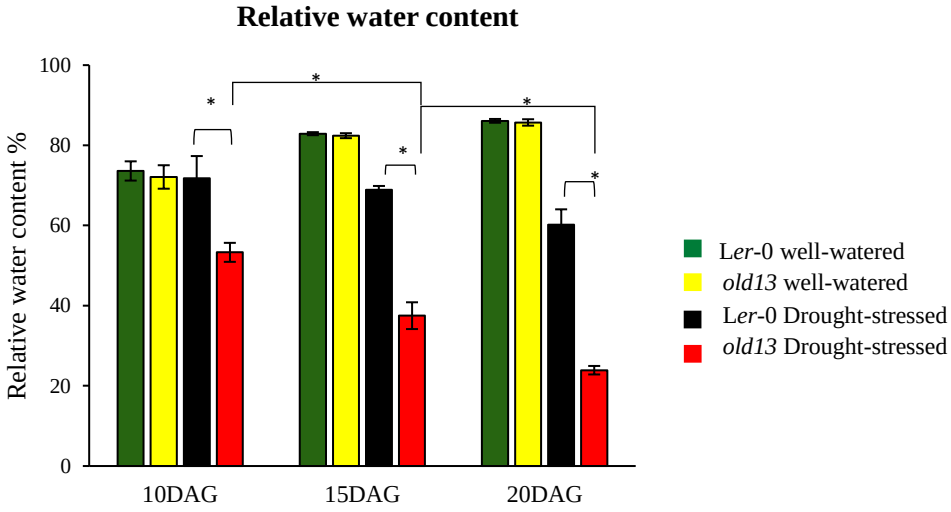

E

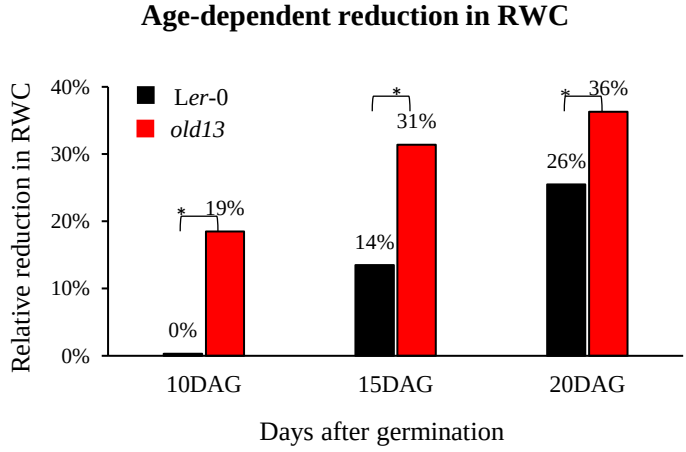

Figure 5.3. Effect of drought stress at three different stages of development in *Arabidopsis* WT and *old13* plants.
A. Drought stress imposed on 10 day old WT and *old13* mutant plants. Photographs were taken of well-watered (i) and drought-stressed plants (ii) at 10 days after germination (DAG) + 6 days of drought (10+6 DAG). First rosette leaf pairs were detached and photographed from both control (iii) and drought-stressed plants (iv). Bar represents 10 mm. **B.** Well-watered (i) and drought-stressed (ii) WT and *old13* plants were photographed at 15 DAG + 6 days of drought (15+6 DAG). First and second rosette leaf pairs were detached and photographed from both well watered (iii, v) and drought-stressed plants (iv, vi). Bar represents 10 mm. **C.** WT and *old13* plants at 20 DAG + 6 days of drought (20+6 DAG) were photographed (i, ii). First and second rosette leaf pairs were detached and photographed from both well watered (iii, v) and drought-stressed plants (iv, vi). Bar represents 10 mm. **D.** The RWC was measured from well-watered and drought-stressed WT and *old13* plants at 10+6, 15+6 and 20+6 DAG. Green and yellow bars represent RWC in hydrated L*er*-0 and *old13* plants respectively, whereas black and red bars represent RWC in drought-stressed WT and *old13* samples. Results are represented as means and standard deviations from 6 plants for each line. **E.** Age-dependent reduction in RWC was measured from 10, 15 and 20 DAG WT and *old13* plants. * indicates the values are significantly different between the indicated samples at $p \leq 0.05$ using Student's t-test.

5.2.2 Impaired dark stress tolerance and poor recovery in the *old13* mutant

The above results showed that drought stress susceptibility in *old13* plants increases with age. To further validate that the *old13* response to stress increases with leaf age, *old13* plants were exposed to darkness for 4 days and then recovered and examined. It is hypothesized that *old13* will have an age-dependant susceptibility to dark stress, and its response will be stronger than WT.

For this study, the *old13* and WT plants were exposed to darkness for 4 days at 10, 15 and 20 DAG, and then exposed to LD photoperiod for 3 days of recovery (Materials and methods section 2.7). Progression of senescence was recorded by measuring total chlorophyll level after 4 days of darkness from the first rosette EEL, MEL and FEL samples. The ability of plants to recover was measured by counting the percentage of leaves that survived, following the dark treatment and recovery. It was observed that the chlorophyll level declined in both WT and *old13* dark-stressed plants in all three different leaf ages (Figure 5.4D). But, the degradation of chlorophyll was more pronounced in *old13* samples compared to WT. The chlorophyll content declined consistently in *old13* plants, containing around 1.88 mg/g FW in EEL tissues, 1.23 mg/g FW in MEL samples and 1.19 mg/g FW in FEL samples (Figure 5.4D). The percentage of survived leaves recorded after 4 days of dark and 3 days of recovery in WT 10, 15 and 20 DAG samples was 66%, 62% and 54% respectively (Figure 5.4A(v), B(v), C(v), E). Interestingly, the percentage of survived leaves after 4 days of dark period in *old13* mutants was only ~6%, and there was negligible recovery observed in all three leaf stages (Figure 5.4A(vi), B(vi), C(vi), E). These results show that *old13* plants are hypersensitive to dark stress but don't display an age-dependant increase in stress susceptibility. Moreover, chlorophyll reduction in *old13* 15 DAG dark stressed sample is significantly more than 10 DAG dark-stressed plants, however, no significant difference could be observed between 15 and 20 DAG *old13* dark stressed samples.

Hence, this data partly supports the hypothesis that the stress susceptibility in *old13* mutant is age-dependent.

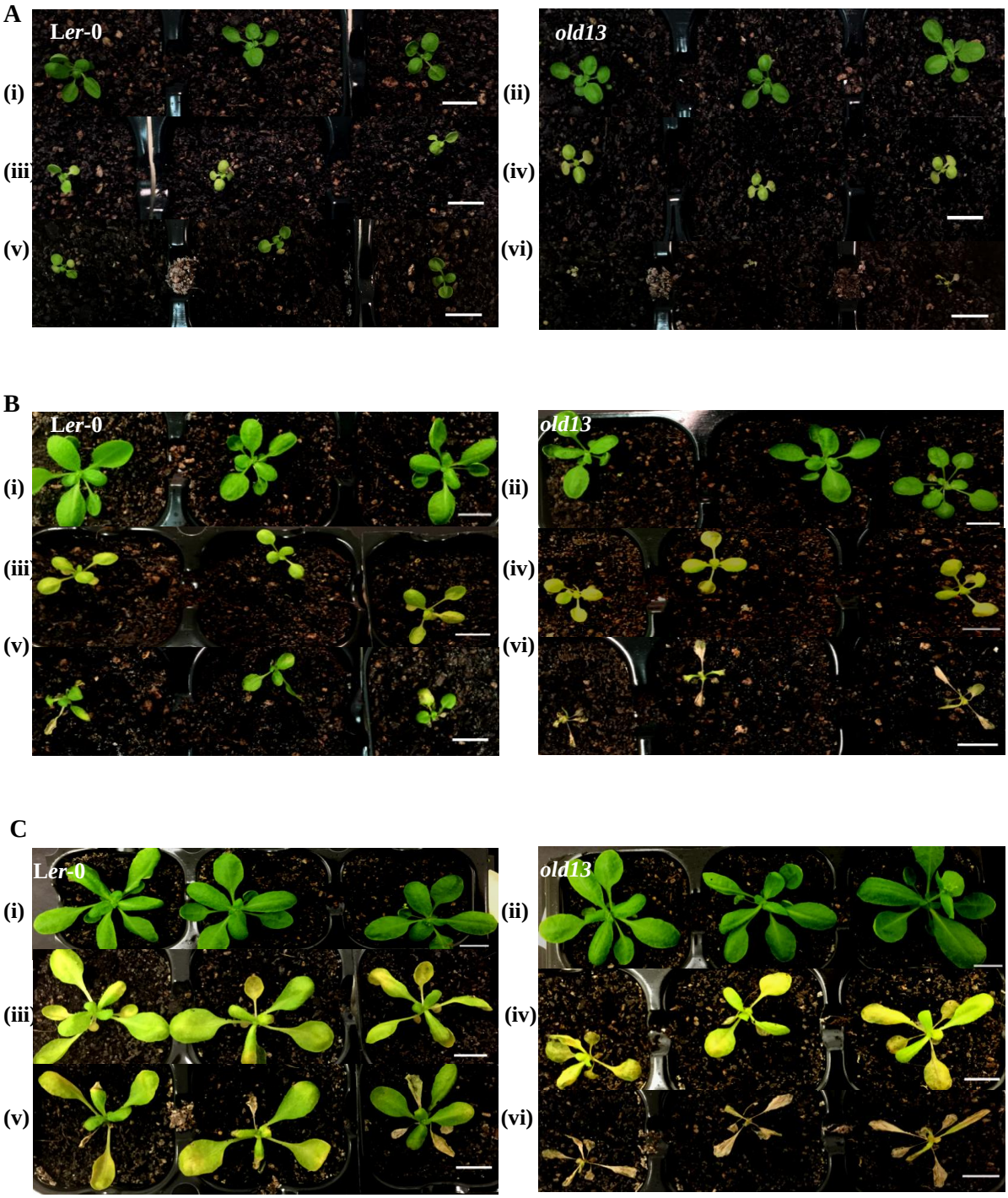

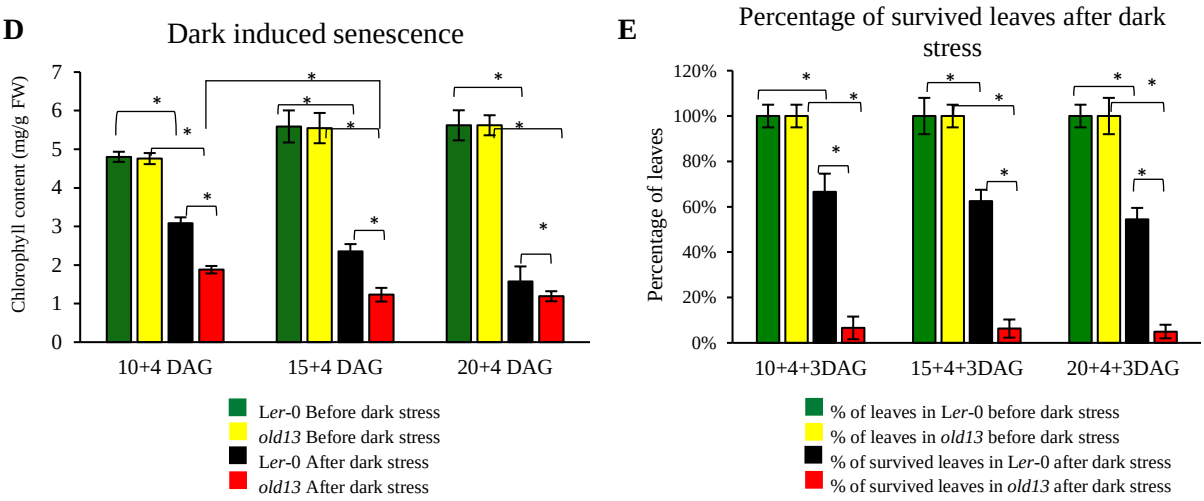

Figure 5.4. Effect of 4 days dark stress and recovery in young, mature and adult *old13* plants. A. At 10 days after germination (DAG), plants were kept in the dark for 4 days (10+4). Pictures were taken of WT and *old13* plants grown under normal photoperiod (i, ii), after 4 days of dark stress (iii, iv) and 3 days of recovery (v, vi). **B.** 4 days of dark period on 15 day old WT and *old13* plants (15+4). Pictures were taken of plants grown under normal photoperiod (i, ii), after 4 days of darkness (iii, iv) and 3 days of recovery (v, vi). **C.** 4 days of dark period on 20 day old WT and *old13* plants (20+4). Pictures were taken of plants grown under normal photoperiod as a control (i, ii), after 4 days of darkness (iii, iv) and 3 days of recovery (v, vi). **D.** Chlorophyll was quantified from 10, 15 and 20 DAG first rosette leaf pairs of WT and *old13* plants before dark stress and after 4 days of darkness. **E.** The percentage of leaves that survived 4 days of darkness + 3 days of recovery. Green and yellow bars represent percentage of leaves in WT and *old13* before dark stress, whereas, black and red bars represent percentage of leaves that survived after 4 days of dark and 3 days of recovery. Data shown in graph D and E signify the mean of 6 biological replicates. * indicates the values are significantly different between the indicated samples at $p \leq 0.05$ using Student's t-test. Scale bar represents 10 mm.

5.2.3 Analysis of stress resistance gene markers in three developmental stages of *Arabidopsis* leaves

From the stress experiments in the previous section, it was partially confirmed that the susceptibility to stress increases with age in *old13* plants. Therefore, gene markers for stress resistance were tested in the first rosette EEL, MEL and FEL of L*er*-0 and *old13* plants, to investigate whether stress-responsive genes increase with age in *old13* or not. If stress resistance gene markers increase with age in *old13*, then the results will support that stress hyper-susceptibility in *old13* is age-dependent. Genes that are involved in processes that regulate stress resistance in plants such as ROS (*RBOHD*), *WRKY53*, senescence (*SAG13*) and antioxidant activity (*SOD1*) were selected as gene markers and their expression levels were measured by quantitative real-time PCR. To measure the transcript level of selected genes, the first rosette leaf pairs were detached at 10, 15 and 20 DAG from L*er*-0 and *old13* plants and grown in a LD photoperiod (Materials and method section 2.3).

Figure 5.5 illustrates that expression of antioxidant gene *SOD1* gradually decreases with age in both WT and *old13* 10, 15 and 20 DAG first rosette leaves. However, compared to WT, *SOD1* gene transcript levels were significantly higher in *old13* leaf samples. There was no significant difference in *RBOHD* expression between WT and *old13* 10 and 20 DAG samples, however, expression increased up to 30-fold higher in 15 DAG leaf tissues of *old13*, whereas in WT 15DAG, the *RBOHD* gene expression is only 14-fold up. Moreover, the senescence-related gene expression of *WRKY53* is 2-fold higher in 15 DAG leaf samples and 4.5-fold higher in 20 DAG leaf samples of *old13* compared to WT. However, the relative expression of *SAG13* significantly increased with age, as at the EEL stage *old13* samples had 5-fold higher expression in 10 DAG leaves, 35-fold higher in 15 DAG leaves, and elevation of transcript levels up to 946-fold in 20 DAG leaf tissues. Thus, 3 out of 4 gene markers in *old13* compared to WT did not show a significant difference in young leaves (10 DAG), while their expression was generally higher in older tissues (20 DAG). These results support the hypothesis that *old13* plants are susceptible to stress in an age-dependent manner.

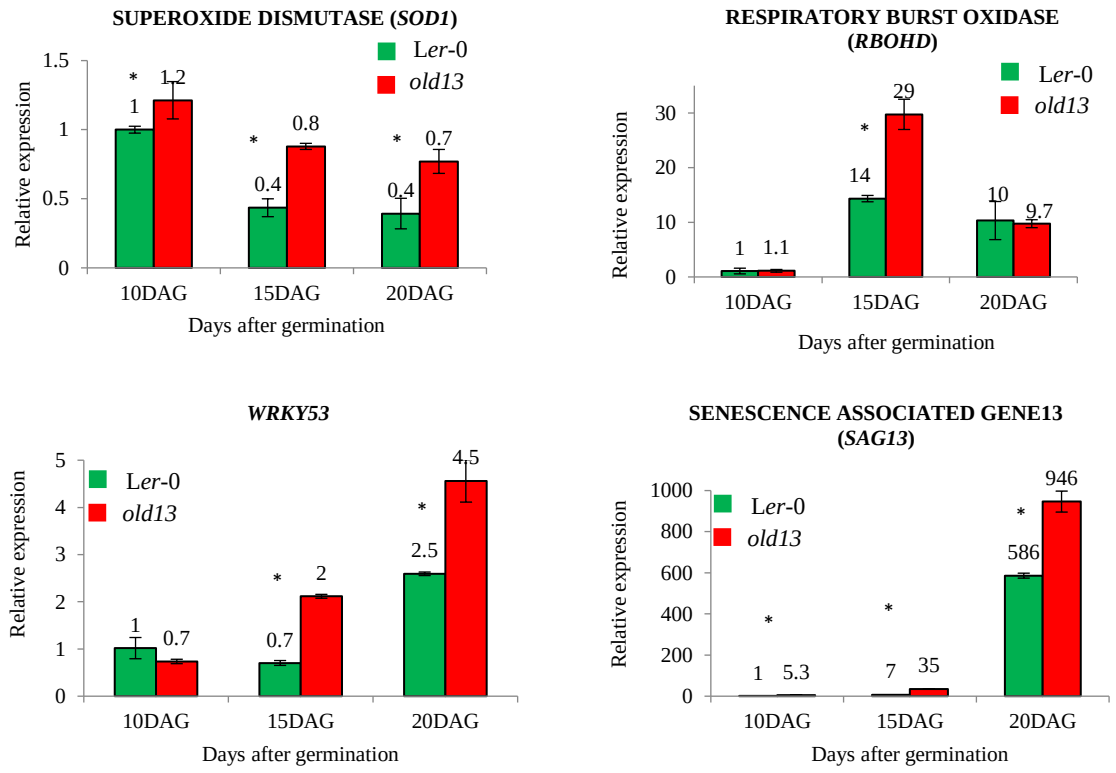

Figure 5.5. Expression of age-related gene markers in young, mature and adult *Arabidopsis* WT and *old13* leaf samples. Expression profiles of *SOD1*, *RBOHD*, *WRKY53* and *SAG13* genes from WT and *old13* first rosette leaf pairs at 10, 15 and 20 days after germination (DAG) under LD photoperiod (16-hour light: 8-hour dark). Gene expression data represents mean values of three biological replicates. * indicates the values are significantly different between L*er*-0 and *old13* at $p \leq 0.05$ using Student's t-test.

5.2.4 Transcriptomic footprints of early age-related changes in the *old13* mutant

The transcript level of four stress responsive genes in the above section provided evidence that *old13* plants are susceptible to stress in an age-dependent way, but the whole transcriptomic analysis would provide a better view of the differences in age-related changes between *old13* and WT leaves. Therefore, transcriptomes were analysed to determine the differences between WT and *old13* in EEL, MEL and FEL samples. It was hypothesized that an increased number of differentially expressed genes in older *old13* leaves would be identified.

Plants were grown in LD photoperiod, and total RNA was extracted from first rosette leaf pairs at 10, 15 and 20 DAG, and sequenced using Illumina HiSeq 4000. Three replicates were used for all three different leaf ages. Transcriptomes of each leaf sample; EEL, MEL and FEL, were compared between *old13* and WT to identify the differences in *old13* mutants. A Venn diagram in Figure 5.6 shows that only 2 differentially expressed genes were identified in *old13* EEL samples, 22 in MEL, and 768 in FEL compared to WT. It is noteworthy that there is no overlap of genes between the samples of different age.

The heat map in Figure 5.7A indicates the expression pattern of 2 differentially expressed genes in WT and *old13* 10 DAG leaf samples that have functions in polygalacturonse activity and oxidative stress. The heat map in Figure 5.7B depicts the expression pattern of 22 differentially expressed genes in 15 DAG leaf tissues, where out of 22 genes, 6 were upregulated, while 16 were downregulated, in *old13* MEL. The heat map in Figure 5.7C shows the pattern of 768 differentially expressed genes in *old13* 20 DAG leaf tissues, displaying upregulated genes in clusters 2, 3, 6, and 7, and downregulated genes in cluster 1, 4, 5, 8, 9, and 10. Thus, these results support the hypothesis that the number of differentially expressed genes increases with age in *old13* first rosette EEL, MEL and FEL in comparison to WT samples. These results also support the hypothesis that there is an age-dependent difference in *old13*.

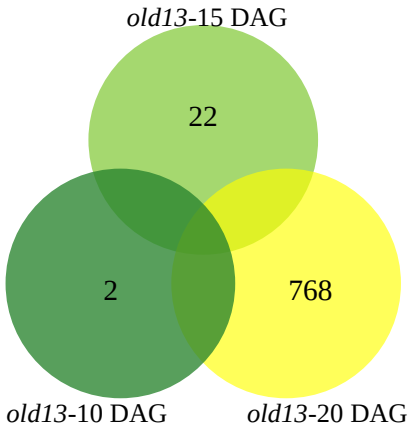

Figure 5.6. Venn Diagram showing the differentially expressed genes in 10, 15 and 20 DAG *old13* leaf samples compared with the WT samples.

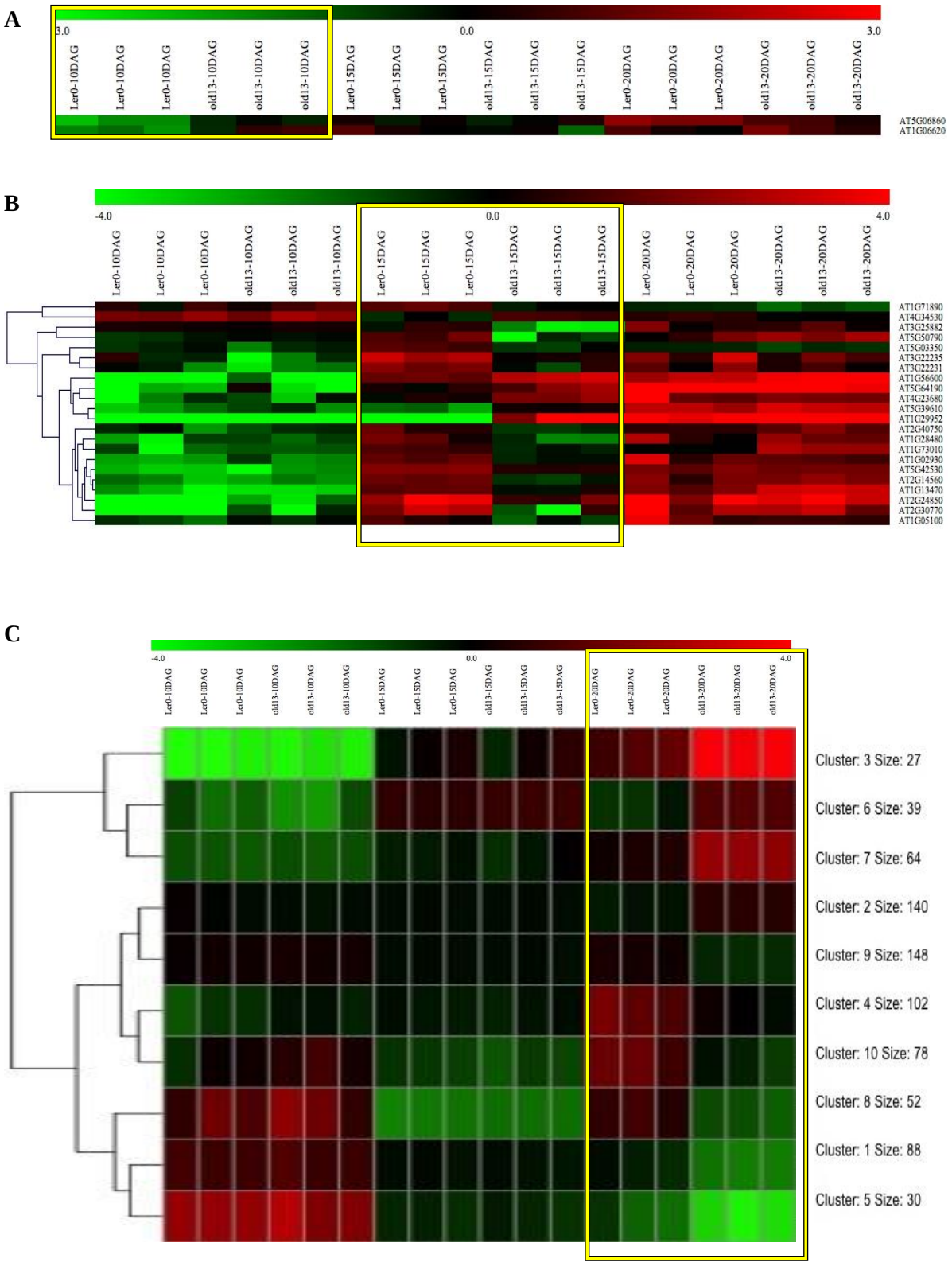

Figure 5.7. Heat map showing the increase or decrease in expression trends of total differentially expressed genes from WT and *old13* first rosette leaf pairs.

Yellow box highlights differentially expressed genes in WT and *old13* samples 10 DAG (A), 15 DAG (B) and 20 DAG (C). Three biological replicates were used for each sample. Red represents high gene expression, green represents low gene expression, and black or darker shades show intermediate levels of expression. Values of colour scale are in $\log_2$

5.2.5 Identification of differentially expressed genes governing early senescence-inducing ARCs in the *old13* mutant

In the previous section, RNA sequencing data revealed changes in gene expression taking place in *old13* EEL, MEL and FEL samples. At the physiological level, *old13* is similar to WT under standard laboratory conditions (chapter 4), therefore, it is expected that any differential gene expression in *old13* would be of genes involved in stress sensitivity. To discover genes that increase stress susceptibility in *old13* plants, differently expressed gene profiles enriched in specific functions were identified.

Gene function was identified from the web link of Araport (https://www.araport.org/). The two differentially expressed genes that are upregulated in 10 DAG leaf tissues of *old13* were assigned to the functional roles of oxidative stress and polygalacturonse activity. Additionally, amongst 22 genes found in *old13* 15 DAG leaf samples, downregulated genes were associated with defence response (5/5), antioxidant (3/4), sucrose transport (2/2), stress response (2/3), kinase activity and unknown function (3/4). Whereas, upregulated genes had functional roles in senescence (*NAC6*), flower development, oxidative stress, antioxidant (1/4) and 2 other unknown functions.

Gene Ontology (GO) enrichment was performed by submitting the AGI codes of 767 differentially expressed genes of 20 DAG *old13* leaf samples into Thalemine database (https://apps.araport.org/thalemine/begin.do). Figure 5.8 presents the ratio of upregulated and downregulated genes of specific function in *old13* 20 DAG leaf samples. Genes that were significantly downregulated in 20 DAG leaf samples of *old13* were associated to the functional groups of stress tolerance (42/46), biosynthesis of cell constituents (35/42), cell maintenance (29/40), cell-wall (CW) organisation (49/50), growth regulation (32/35), oxidation reduction (26/27), signal transduction (13/19), transcription factors (30/47), and sugars (10/11). While the most highly upregulated genes were found to be enriched in functional groups associated with stress response (69/91), transport activity (34/54) and unknown genes (159/231) (Figure 5.8). Gene categories that could have potential roles in causing age-dependent stress sensitivity in *old13* plants were selected for further study. The genes that were selected for detailed analysis from the highest downregulated categories includes; stress tolerance, CW organisation, hormones and sugars. Whereas, the highest ratio of upregulated gene categories selected were related to stress responses. Altogether, the results from GO enrichment analysis pinpoints the important functional gene categories of stress tolerance, CW organisation, sugars, stress and hormones.

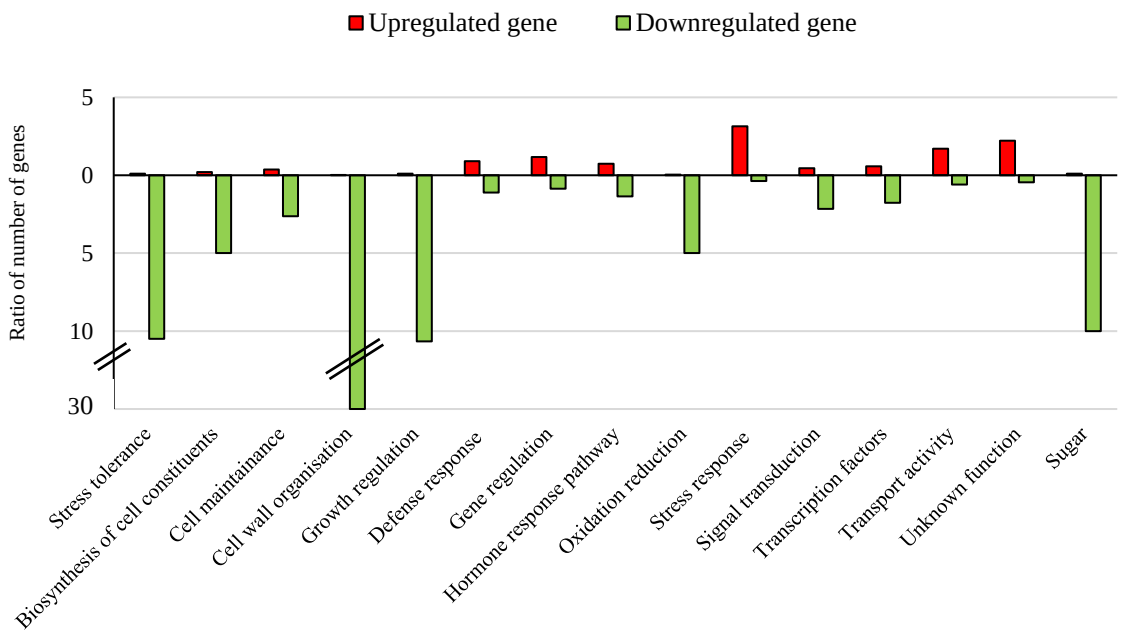

Figure 5.8. GO enrichment of differentially expressed genes in *old13* 20 DAG leaf samples.
Ratios of total up and downregulated genes enriched in specific biological functions in *old13* FEL. Green bars represent downregulated genes and red bars indicate upregulated genes enriched in different biological function groups. Black bars represent axis breaks.

5.2.6 Examination of key senescence-inducing ARCs in *old13* fully expanded leaves

In the previous section, the change in overall expression pattern of genes with distinct biological functions were examined in three developmental stages of *old13* leaves. In this section, the highest ratio of downregulated and upregulated gene categories (stress tolerance, CW organisation, sugars, stress and hormones) identified in *old13* FEL samples, are further studied. Detailed analysis of gene categories will help identify possible regulatory genes and pathways involved in early occurrence of senescence-inducing ARCs in *old13* mutants, and increased susceptibility to stress.

5.2.6.1 Upregulation of stress and hormone-related genes in *old13* FEL

Since *old13* mutants are sensitive to unfavourable environmental conditions, my hypothesis is that genes related to stress hormones and other stress-related genes will be more highly expressed in *old13* 20 DAG than the WT samples. RNA sequencing results showed that 69 out of 91 differentially expressed stress-related genes were upregulated in *old13* 20 DAG samples. The genes known to be

involved in the stress response include several transcription factors (TFs) such as 6 *NAC* TFs, 7 *MYB* TFs, *WRKY46*, *WRKY22* and *WRKY6*, which function in the senescence process, and many other genes of unknown function.

Moreover, RNA sequencing data also showed that among 26 hormone-related differentially expressed genes in *old13* 20 DAG samples, 15 genes are downregulated, while 11 genes are upregulated. Eleven out of 15 downregulated genes were found linked to the hormone auxin, in *old13* FEL. As auxin is a growth hormone, it was expected to observe downregulation of auxin-related genes in fully developed *old13* leaves (20 DAG) (Ljung et al., 2005). Other downregulated genes function in cytokinin and gibberellin signalling. Interestingly, 8 out of 11 upregulated genes were found to have a function in ethylene and ABA signalling. Taken together, these results support the hypothesis that genes associated to stress hormones and other stress responsive genes are upregulated in *old13* 20 DAG leaf samples.

5.2.6.2 Downregulation of stress tolerance, cell-wall and sugar-related genes in *old13* FEL

The results of the previous section show that stress, senescence and ethylene-related genes are upregulated in *old13* FEL. Also, *old13* mutants are sensitive to stress conditions, therefore, it was expected that transcripts linked to stress tolerance would be changed in *old13* FEL samples. From RNA sequencing data analysis, a total of 42 out of 46 genes related to stress tolerance were downregulated in *old13* FEL. Of these 42 stress tolerance genes, 24 genes have a function in antioxidant activity, while others are involved in inducing tolerance to stress. This data confirms that the large set of genes involved in stress tolerance are downregulated in *old13* 20 DAG first rosette leaf samples.

The CW consists of a complex network of components that play distinct roles in CW development, signalling, and stress tolerance (Tenhaken, 2015). Of the 50 genes involved in CW organisation, 49 were found to be downregulated in *old13* 20 DAG leaf samples. Among these downregulated transcripts, 10 genes were suggested to have a biological function in xyloglucan metabolic processes, 13 are linked to arabinogalactan proteins, 8 are involved in pectinesterase activity, 5 are related to expansin, 7 are involved in biosynthesis of CW protective layer, and 6 other genes are related to CW development. These CW components all have important roles in providing stress resistance, strength and structure to the cell (Gall et al., 2015).

In plants, sugars are the primary product of photosynthesis, and are transported from source tissues to sink organs via a number of sugar transporters (Chen, 2014). The RNA sequencing data showed a decrease in the expression of 5 genes involved in sugar transport activity, along with downregulation of 5 genes whose expression decreases in response to high sugar levels. This data confirms that genes associated with sugar transportation and responsiveness to high sugar levels are downregulated in fully

expanded first rosette *old13* leaf samples. These results might indicate that the sugar level is high in 20 DAG *old13* leaves.

5.2.7 Increased sensitivity of *old13* FEL to sugar

High sugar concentration can lead to the initiation of leaf senescence (Wingler et al., 2017; Yuanyuan et al., 2010). If *old13* leaves have high sugar levels, then it is expected that *old13* leaves will be sensitive to supplemented sugar and show early onset of senescence compared to WT leaves. In this section, to confirm whether *old13* are sensitive to high sugars levels, first rosette fully expanded WT and *old13* leaves were exposed to different sugar concentrations and kept in darkness to accelerate senescence. To test sugar sensitivity, first rosette leaves were detached from WT and *old13* plants at 20 DAG and placed on Whatman-filter paper saturated with 2%, 4% and 6% sucrose solution. To accelerate the senescence process, samples were kept in darkness for 2 days and senescence progress was monitored by measuring the chlorophyll content. Pictures in Figure 5.9 clearly illustrate that sugar sensitivity increases with greater sucrose percentage in *old13* leaves, by observation of leaf yellowing compared to WT (Figure 5.9A). Although a progressive decline in chlorophyll content was observed in both WT and *old13* leaves, as a result of sugar and dark treatment, this decline was stronger in the *old13* leaves exposed to 2%, 4% and 6% sucrose (Figure 5.9B). Together, these results suggest that *old13* FEL are more sensitive to sucrose treatment than WT FEL.

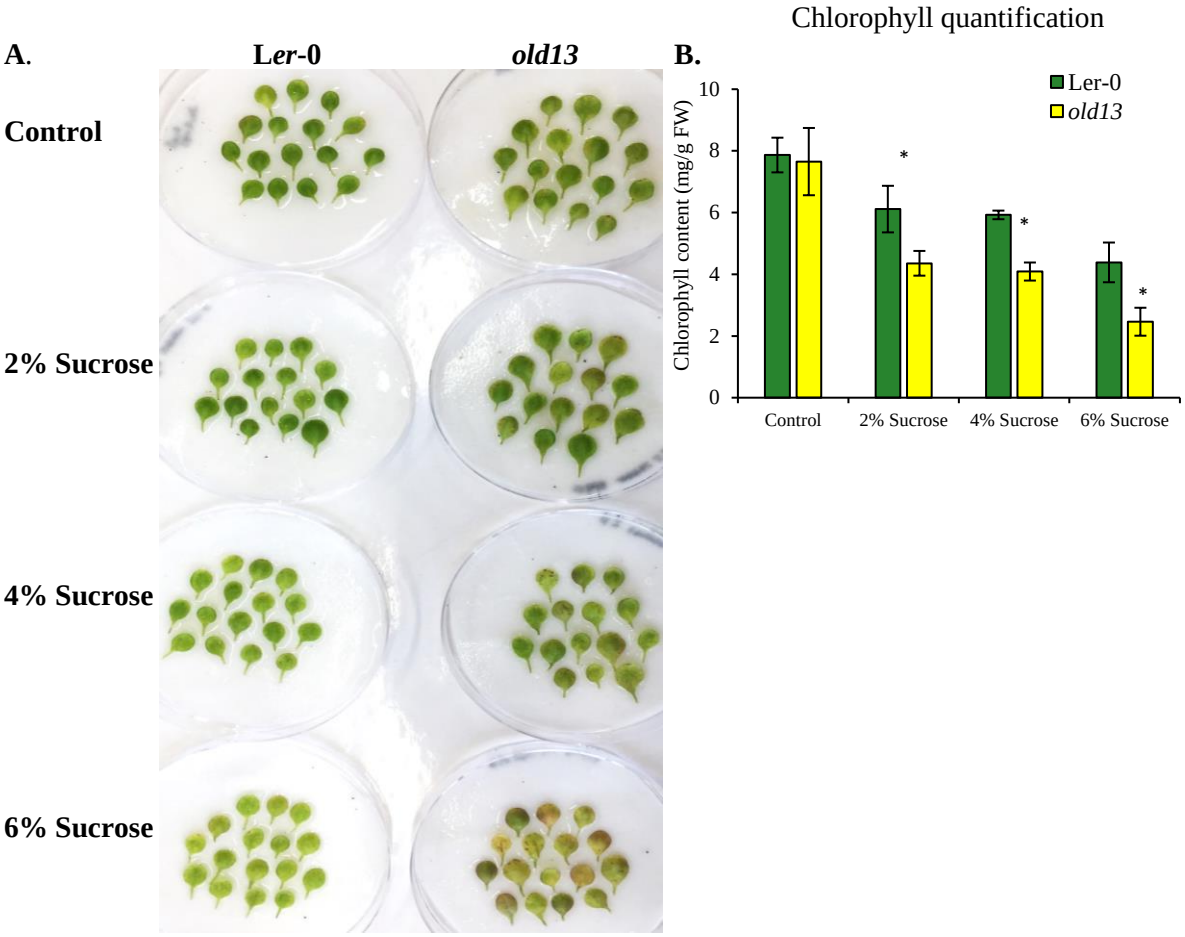

Figure 5.9. Effect of sucrose on detached L*er*-0 and *old13* first rosette leaves.
A. Twenty DAG first rosette leaves of WT and *old13* were placed on Whatman-filter paper saturated with 2%, 4%, and 6% sucrose, and kept in darkness for two days. **B.** Chlorophyll content was measured after 2 days of darkness from control and sucrose-treated WT and *old13* first rosette leaves. Green bars represent chlorophyll content in WT leaves and yellow bars represent chlorophyll content in *old13* leaves. Results are represented as means and standard deviations from 6 plants. * indicates the values are significantly different between the WT and *old13* samples at $p \leq 0.05$ using Student's t-test.

5.2.8 Metabolomic analysis reveals high sugar content in *old13* FEL

It was confirmed that *old13* mutants are sensitive to stressed conditions. The results from the previous section illustrate that *old13* FEL are also susceptible to sucrose treatment. Next, I hypothesise that *old13* mutants are more susceptible to sugar because the *old13* cellular sugar levels are higher than those of the WT. Therefore, to determine if sugars are high in *old13*, primary metabolite profiling of *old13* EEL, MEL and FEL using Gas Chromatography-Mass Spectrometry (GC-MS) was performed. If *old13* mutants contain high concentrations of sugars, then it is expected to see increased sugar metabolites in *old13* leaf samples compared to the WT.

For primary metabolic profiling, samples were extracted from WT and *old13* first rosette EEL, MEL and FEL, as described in methods section 2.12. To observe the difference between metabolites, 10, 15, and 20 DAG *old13* samples were compared with WT samples. Among the 60 metabolites analysed, only sugar metabolites (23 in number) are shown in the heat map (Figure 5.10). The heat map shows that most of the sugar metabolites (15/23) are low in *old13* 10 DAG samples compared to the *old13* 15 and 20 DAG samples. Interestingly, raffinose and galactinol which were undetectable in *old13* 10 DAG samples, significantly increased in 15 and 20 DAG *old13* leaf samples. Also, the heat map and data bars clearly illustrate that most of the sugar-related metabolites are significantly higher while some sugars like maltose and threitol are considerably lower in 20 DAG *old13* leaf samples, compared to *old13* 10 and 15 DAG samples. The $\log_2$ values of significantly different carbohydrates in *old13* 10, 15 and 20 DAG leaf samples are listed in Appendix 4. These results confirm that sugar levels are high in *old13* FEL leaf samples and are generally low in *old13* EEL.

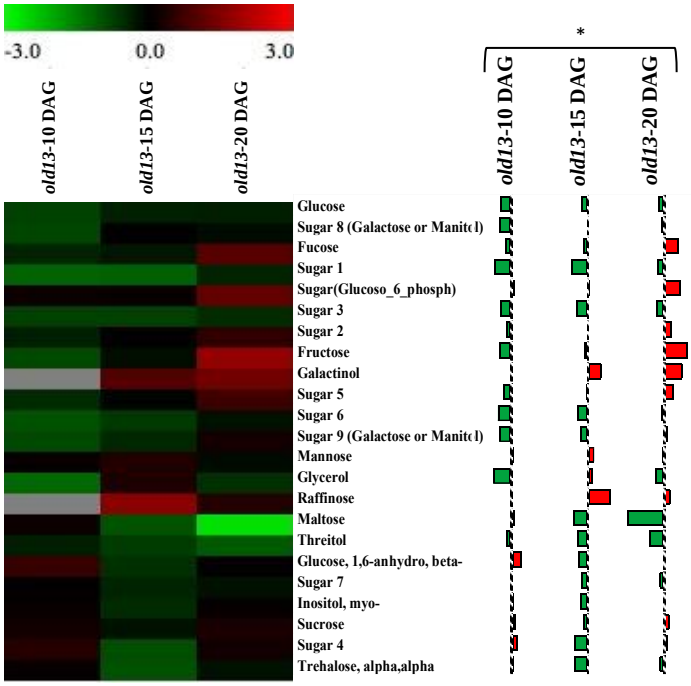

Figure 5.10. Primary sugar metabolite profiling of *old13* first rosette EEL, MEL and FEL
(A) Heat map representing changes in primary metabolite content quantified by GC-MS. Metabolite levels were determined in *old13* first rosette leaf pairs 10, 15 and 20 DAG. The samples are expressed as $\log_2$. Scale bar represents red maximum (between 0.0 and 3.0) and green minimum (between 0.0 and -3.0). **(B)** The data bars represent $\log_2$ transformed fold changes. * indicates the values are significantly different between 10 DAG WT and *old13*, 15 DAG WT and *old13*, 20 DAG WT and *old13* samples at $P < 0.05$ using Student t-test. Values were obtained from five biological replicates.

5.3 Discussion

Research performed on various plant species such as *Arabidopsis thaliana*, *Oriza sativa*, *Solanum lycopersicum*, *Zea mays* and *Nicotiana tabacum* provide information about the number of genes involved in regulating senescence processes (Lim et al., 2007). It has been shown that mutant plants with delayed developmental growth, flowering and extended longevity, often exhibit greater stress resistance. Whereas, phenotypes showing early growth, reproductive phase and premature ageing, often show sensitivity to stressed environments. This suggests that when plants are young, they show enhanced resistance to stress, but as they age, they become more susceptible. For instance, transgenic plants overexpressing the *JUB1* NAC transcription factor, exhibited extended leaf longevity, strongly delayed reproductive growth, and greater tolerance to stress inducing treatments (Wu et al., 2012). As a result, young *JUB1*-overexpressers might display increased tolerance to stress factors and a delayed senescence phenotype. Similarly, recent research on *Arabidopsis* lines overexpressing *AtERF019*, showed enhanced drought tolerance compared to wild type (WT) plants (Scarpeci et al., 2017). Overexpression of *AtERF019* resulted in delayed vegetative and reproductive growth, along with delayed natural senescence. These studies also support the concept that improved tolerance to stress in transgenic plants is because of extended leaf longevity. The function of very few genes have been identified that display leaf longevity and increased stress resistance, without altering the growth and development of a plant. In *Arabidopsis*, mutants like *drd1*, *ddm1* and *oresara1* are well characterised, and show an association with plant ageing. These mutants show greater stress tolerance and longevity without alterations to developmental growth (Cho et al., 2016; Hye et al., 2004b). Results shown in chapter 3 also confirm that young leaves are more tolerant to stress compared to mature and old leaves. Also, it is confirmed that stress tolerance decreases with age in *Arabidopsis* because of gradual occurrence of senescence-inducing ARCs. In chapter 4, it was confirmed that *old13* shows no early ageing when grown in standard laboratory conditions, but displays early initiation of senescence when exposed to stress. In this chapter, the *old13* mutant was selected to better understand the ageing and stress responses because it is highly similar to the WT when grown in standard laboratory conditions, and is hypersensitive to stressed environments. To test whether the hypersensitive response to stress in *old13* is observed in all developmental stages, or whether the susceptibility increases with age, stress-induced experiments, followed by transcriptomic and metabolomic studies were carried out.

5.3.1 *old13* plants display age-dependent stress susceptibility

To understand how plants respond to stress at different developmental ages, *old13* mutants were selected and treated to different stresses. Firstly, *old13* and WT plants were exposed to water deficit

conditions for 6 days at 10, 15 and 20 DAG. The results in Figure 5.3D show that RWC consistently decreased in both WT and *old13* drought-stressed plants as their age increased. However, the reduction in RWC was stronger in *old13* samples, confirming that drought sensitivity in *old13* is age-dependent. It can be seen from Figure 5.3 that *old13* first rosette leaves show more severe wilting than second rosette leaf pairs, supporting the hypothesis that stress sensitivity in *old13* is age-dependent. Also, Figure 5.3E illustrates the percentage of age-dependent reduction in RWC between well-watered and drought-stressed samples, and confirms that the effect of drought stress becomes greater with age. For instance, in *old13* 10, 15 and 20 DAG samples, relative reduction in RWC is 19%, 31% and 36% respectively, which is higher than WT samples. Although, *old13* shows no signs of early ageing and appears similar to WT in non-stressed conditions, these data suggest that senescence-inducing ARCs are amplified in *old13* leaves, making these mutants more sensitive to stressed conditions than WT plants.

To further confirm the observation of age-dependent stress sensitivity, *old13* and WT plants were shifted to darkness for 4 days and then recovered for 3 days. The chlorophyll content declined in all the samples as a result of the dark treatment, but chlorophyll declined more strongly in *old13* samples. The reduction in chlorophyll content consistently declined with increased leaf age. Also, after the dark treatment, *old13* plants showed no recovery when shifted to LD photoperiod. This is possibly because of intense damage and poor tolerance to stress in plants, due to mutation in *OLD13* gene. In chapter 3, Figure 3.12 shows that recovery in WT plants after dark stress decreases with age. It is possible that 4 days dark period is a saturating stress on *old13* that makes it impossible to observe the age-dependent stress sensitivity. Perhaps, a reduced dark period would reveal an age-dependent stress effect in *old13* plants. Together, it appears that senescence-inducing ARCs have likely occurred in early stages, leading to stress susceptibility and poor recovery in *old13* plants.

Since *old13* age-dependent stress sensitivity could not be confidently confirmed by stress-inducing experiments, this hypothesis was further validated by qPCR results. Expression of genes related to stress resistance (*SOD1*, *SAG13* and *WRKY53*) showed no significant difference in 10 DAG but were elevated in 15 and 20 DAG *old13* samples. Plants have different adaptation strategies to cope with stressed environments, involving the interaction of a number of signalling pathways and changes in expression of various stress resistance genes (Pandey et al., 2015). The expression of *SOD1, SAG13, WRKY53* and *RBOHD* are also found to be changed during the events of senescence or in aged leaves (Balazadeh et al., 2008; Dhindsa et al., 1981; Koo et al., 2017). Thus, qPCR results strongly support that stress sensitivity in *old13* plants are age-dependent. Also, RNA sequencing was performed to examine the transcriptomic variation between WT and *old13* EEL, MEL and FEL. With increased age of *old13* leaves, the gene transcripts also increased from 2 to 22 and 767 in EEL, MEL and FEL, respectively (Figure 5.6), which confirms that stress susceptibility in *old13* is age-dependent. It is surprising that none of the differentially expressed genes overlap between the two samples. However, in RNA

sequencing data there are several multireads that originated from repetitive regions or gene duplications which may result in false positives (Consiglio et al., 2016). There are several other errors in RNA sequencing techniques that may lead to uncertainty in gene expression. Hence, it is possible that there are overlapping genes that could not be detected by statistical methods used to determine significant differences in RNA transcript level.

5.3.2 Comparative transcriptomic analysis revealed an important functional gene category causing stress sensitivity in *old13* plants

Gene function of differentially expressed genes were identified from the web link of Araport (https://www.araport.org/). Interestingly, there were only 2 genes identified that showed significant difference between 10 DAG WT and *old13* samples. These two genes were found to be upregulated, and function in oxidative stress (*AT1G06620*) and hydrolysis of pectin (*PGIP1*), which is a cell-wall component.

Moreover, 22 genes were differentially expressed in *old13* 15 DAG samples. Amongst the 22 genes, the biological function of genes that could play important roles in stress susceptibility of *old13* plants include antioxidant activity, sucrose transport, oxidative stress responses and senescence. Three antioxidant-related genes belonging to the thioredoxine superfamily; *GRX480*, glutathione S-transferase (*GSTF6*) and tyrosine aminotransferase 3 (*TAT3*), which play important roles in ROS scavenging, were found to be downregulated in *old13* MEL (Lu and Holmgren, 2014; Noctor et al., 2012). The stress-responsive *ORE1* and *WRKY54* genes, which are positive regulators of senescence, are upregulated in *old13* MEL samples (Besseau et al., 2012; Hye et al., 2004a). Studies have also shown that plants with mutations in the *ore1* and *wrky54* genes exhibit oxidative stress tolerance (Chen et al., 2017; Hye et al., 2004a; Li et al., 2013). Moreover, from the transcriptomic results shown in chapter 3, *WRKY54* and *ORE1* are both highly expressed in WT FEL, whereas in *old13*, the expression is high initially from the MEL stage (Appendix 1).

5.3.3 Up- and down-regulated genes in FEL reveal essential pathways contributing to stress susceptibility in *old13* plants

The transcriptomic data showed 768 differentially expressed genes in *old13* FEL. Several gene categories were found to be highly or lowly expressed (Figure 5.8) and those with biological functions in stress tolerance, stress responses, senescence, cell-wall modification, sugar and stress hormones were

selected for detailed analysis. These gene categories were selected based on a possible role in inducing stress susceptibility in *old13* plants.

Stress responses: The detailed analysis of 69 differentially expressed stress-related genes identified in 20 DAG *old13* samples included genes responsive to oxidative stress, senescence and other stress conditions. Excessive generation of ROS as a result of exposure to environmental stress has been proposed to induce leaf senescence (Bhattacharjee, 2012). Upregulation of 69 stress-related genes in *old13* FEL included 6 NAC TFs (*NAC036*, *NAC047*, *NAC048*, *NAC055*, *NAC090*, *NAC100*) and 3 WRKY TFs (*WRKY46*, *WRKY22* and *WRKY6*) that are directly associated to oxidative stress and senescence (Kim et al., 2014; Zhou et al., 2011b). Expression of most of the upregulated stress-related genes that were responsive to oxidative stress and senescence in *old13* FEL were already found to increase with age in WT leaves (Chapter 3). These genes included *NAC036, NAC047, NAC055, NAC099, HSFA2* (*Heat shock transcription factor A2*), *RPL20* (*RECEPTOR LIKE PROTEIN 20*), and *PCR2* (*PLANT CADMIUM RESISTANCE 2*). Also, various MYB TFs known to be involve in regulation of multiple stress responses, such as *MYB34*, *MYB48*, *MYB29*, *MYB32*, *MYB13*, *MYB59*, and *MYB31*, are upregulated in *old13* FEL (Roy, 2016). The upregulation of stress-related genes is possibly due to enhanced cellular stress in *old13* leaves.

Because stress- and senescence-related genes are upregulated in 20 DAG *old13* leaves, a detailed study on genes related to hormones was carried out to identify whether genes related to stress and senescence hormones, are elevated in *old13* FEL. The well-known hormone ethylene plays an important role in various stages of plant growth, and is also a key hormone in regulating leaf senescence (Zacarias and Reid, 1990). In addition to ethylene, the level of abscisic acid (ABA) also increased in response to various stresses, and both hormones are suggested to play a role in the senescence process (Xiong and Zhu, 2003, Glazebrook, 2001). Detailed analysis of hormone-related genes displayed 8 out of 11 upregulated genes are associated to ethylene and ABA signalling in *old13* FEL samples. Upregulated genes include ethylene response factors *ERF1* and *ERF15*, which are both known to mediate ethylene signalling in response to various stressed conditions (Müller and Munné-Bosch, 2015b). *ERF15* is also known to positively regulate ABA responses and its expression has been found to increase with age in WT samples (Chapter 3; Lee et al., 2015). Together, the increase in expression of stress hormones, oxidative stress and senescence associated genes, is consistent with the hypothesis that stress susceptibility in *old13* leaves is a cause of early senescence-inducing ARCs. Also, a few stress-related genes elevated in *old13* FEL also shown a constant increase in expression with age in WT leaves from EEL to MEL and FEL (results shown in chapter 3); this result is indicative of amplified senescence-inducing ARCs in *old13.*

Stress tolerance: Since plants are sessile in nature, they cannot move to escape from unfavourable environmental factors. Thus, to protect themselves from stressed conditions, plants evolved various

adaptive mechanisms that involve the interaction of multiple signalling pathways, large sets of stress tolerant genes, antioxidant machinery, etc. (Ciarmiello and Woodrow, 2011). Transcriptomic results showed decreased expression of 42 out of 46 differentially expressed genes that are associated to stress tolerance in *old13* FEL. Amongst 42 genes, 21 function in antioxidant activity in *old13* FEL. Out of 21 antioxidant-related genes, 10 belong to the thioredoxin protein superfamily, 4 to the glutaredoxin protein family and 3 are associated with the peroxidase protein superfamily. All these families are known to play important roles in redox regulation and antioxidant defence (Caverzan et al., 2012; Meyer et al., 2008). Antioxidant defence systems are actively involved in stress tolerance by keeping ROS under tight control (Suzuki et al., 2012). Reduced activity of ROS scavengers leads to the overproduction of ROS radicals, thus making plants susceptible to stressed environments (Halliwell, 2006). Antioxidants are overproduced in plant cells when ROS levels increase, and severe stress leads to the overabundance of ROS that cannot be controlled by antioxidant machinery (Foyer and Shigeoka, 2011). This data suggests that in *old13* plants, the antioxidant activity is low, leading to an increase in cellular stress. Moreover, 21 downregulated genes in *old13* FEL are associated with stress tolerance and are involved in inducing tolerance to various abiotic stress factors. Genes such as *LTI78, LTI65* (*LOW-TEMPERATURE-INDUCED*), *MSRB6* (*METHIONINE SULFOXIDE REDUCTASE B6*), and *CIPK3* (*CBL-INTERACTING PROTEIN KINASE 3*), are known to protect plants against drought, salinity, low temperature, and oxidative stress (Kanwar et al., 2014; Rouhier et al., 2006; Sukweenadhi et al., 2015), and are lowly expressed in *old13* FEL. Stress tolerance-related genes also include transcription factors like *WRKY11*, *WRKY28*, and *MYB102* (Babitha et al., 2013; Denekamp and Smeekens, 2003; Liu et al., 2011). Interestingly, the transcriptomic results shown in chapter 3 illustrate that expression of *MYB102*, *WRKY11*, and *LTI65* are high in WT FEL, but low in *old13* FEL. Together, these data, along with elevated genes responsive to oxidative stress, senescence and other stresses, illustrate that the stress tolerance mechanism is reduced in *old13* FEL, which explains why *old13* plants are hypersensitive to stress.

Cell-wall: For survival under stressed conditions, plants have evolved various adaptive mechanisms. Reduced growth is the first event visible in plants exposed to abiotic stress (Basu et al., 2016). Reduction in plant size under stress is primarily governed by modification of cell-wall (CW) structure (Gall et al., 2015). Plant CWs are also considered as protective barriers against stressed environments. From RNA sequencing data, only one CW-related gene was upregulated in *old13* EEL, and this gene functions in pectin hydrolysis (*PGIP1*) (Nguema-Ona et al., 2013). Whereas, no differentially expressed CW-related genes were identified in *old13* MEL samples. However, in FEL samples, decreased expression of 49 genes related to CW organisation was found. The 49 differentially expressed genes were associated with xyloglucan, pectin, expansin, and pectinesterase activity, arabinogalactan proteins and the CW protective layer. Xyloglucan is the major hemicellulose component found in the primary CW (Malinovsky et al., 2014). Xyloglucan endo-β-transglucosylases/hydrolases (XET/XTH) are

responsible for hydrolysis of xyloglucans, and thus function in CW loosening and therefore cell expansion (Rose et al., 2002). From the transcriptomic data, a total of 14 genes involved in xyloglucan metabolism were found to be downregulated in *old13* FEL samples. These genes included *XTH4*, *XTH16, XTR4, XTH33, XTH9, XTR6, XTH22* and *XTH18,* which all function in CW loosening (Hayashi and Kaida, 2011; Kaku et al., 2004). Several studies have suggested that increased expression of *XTH* or *XET* genes provide enhanced tolerance to osmotic stresses, through adjustment of CW composition, which allows further growth of stressed organs (Dong et al., 2011; Nishiyama et al., 2012). The downregulation of these genes illustrate that the cell wall of *old13* FEL is probably stiff but this needs to be confirmed experimentally.

Additionally, pectin is another important CW component linked to hemicellulose that forms a gel phase, providing cell adhesion and strength to the wall (Voragen et al., 2009). Interestingly, the pectin-modifying enzyme, pectin methyl esterase (PME), which contributes in cell wall loosening, fruit softening, defence response, and leaf senescence (Giovane et al., 2004), was observed to have low expression in *old13* adult leaf tissues, with around 13 genes functioning in pectinesterase activity. Expansin is another CW protein involved in CW extension. The expression of these proteins, are generally higher in growing cells and ripened fruits (Cho and Cosgrove, 2000). Several studies have shown that overexpression of expansin-related genes in transgenic plants results in better salt or drought stress resistance (Dai et al., 2012; Han et al., 2012; Lü et al., 2013). The transcriptomic data highlights the low expression of expansin-related genes (*EXPA16*, *EXPL2*, *EXPL1*, *EXPL3*, *EXPB1*) in *old13* 20 DAG samples when the leaf was fully developed. The downregulated genes also include those that encodes Arabinogalactan proteins (AGP), which are involved in several biological processes such as cell division, cell expansion, biotic and abiotic stress responses, and reproductive development (Ellis et al., 2010). These proteins are also known to interact with CW polysaccharides and form a network with components of the CW, providing strengthening against stressed conditions (Knoch et al., 2014). In total, 13 AGP encoding genes showed decreased expression in *old13* 20 DAG leaf samples. Moreover, genes involved in cutin biosynthesis processes such as, *CER1*, *CER4* (*ECERIFERUM*), *GPAT8,* and *GPAT3* (Glycerol-3-phosphate acyltransferase), are downregulated in *old13* FEL samples. In plants, the cuticle acts as a barrier against stressed conditions and is also essential in reducing water loss in drought-stressed plants (Aarts et al., 1995; Chen et al., 2011; Kosma et al., 2009). The other genes involved in suberin synthesis; *RWP1* and *ABCG2* (ABC-2 type transporter family protein), are also lowly expressed in mature leaf tissues of *old13* (20 DAG). Suberin is found at the inside of the CW and protects plants against various environmental stresses (Gou et al., 2009). Together, it appears that the CW protective layer is weak in 20 DAG *old13* plants and makes plants susceptible to stressed conditions.

Plants show distinct responses to stress depending on the severity, for example, plants will show tolerance to mild stress without restricting growth, where the CW continues to elongate and expand

(Tenhaken, 2015). On other hand, plant growth is reduced under intermediate stress, mediated by CW stiffening as an adaptive mechanism for the survival of plants (Zhu, 2016). In the view of present data, downregulation of CW loosening components in *old13* FEL hint towards rigidity of the CW. Although the leaf size of *old13* is not different from WT, it is possible that *old13* FEL sense prolonged endogenous stress even before the completion of leaf growth, leading to stiffening of the CW. High expression of genes involved in oxidative stress, senescence, ABA and ethylene, support the prediction that endogenous stress is high in mature *old13* leaves, which likely leads to the activation of CW strengthening as an adaptive mechanism in plants. Since cell growth demands high energy in form of sugars (O'Hara et al., 2013), CW stiffening results in restriction of cell growth, leading to accumulation of more sugars, because of growth limitations (Lemoine et al., 2013). Transcriptomic and metabolomic results both strongly illustrate that sugars are high in 20 DAG *old13* leaves (discussed below), which could be due to restricted CW growth.

5.3.4 High sugar causes stress susceptibility in *old13* fully expanded leaves

Plants collectively require light from the sun, water absorbed through roots, and carbon dioxide from the air, to produce nutrients in the form of sugars (Poorter, 1993). In the light, sugars are converted to starch which is remobilised at night to support the metabolism and growth of a plant (Zeeman et al., 2010). Soluble sugars function in various processes such as cell signalling, metabolism, stress responses, growth, and development (Eveland and Jackson, 2012; Rosa et al., 2009). Stressed conditions such as drought, high or low light and temperature, and pathogen attack, limit photosynthesis, which then induces sugar depletion in plants, restricting the supply of soluble sugars to sink tissues (Rosa et al., 2009). In such conditions, sugars from source tissues (old leaves) are transferred to the sink tissues (young leaves) for the survival of the plant (Figure 1.1). It has been suggested that sugar starvation due to limited photosynthesis leads to the onset of leaf senescence (Morkunas et al., 2012; Tetley and Thimann, 1974). Plants exposed to darkness or leaves under shade are more prone to age quickly because of depleted sugar (Moore et al., 2003). It has been found that when a whole *Arabidopsis* plant is kept in darkness, the attached leaves do not display significant yellowing compared to detached leaves, which showed severe yellowing when kept in the dark for the same amount of time (Louis et al., 1998). Moreover, it was observed that senescence is induced in individual *Arabidopsis* leaves that were kept in darkness, by wrapping in aluminium foil, but were attached to an otherwise light grown plant (Weaver and Amasino, 2001). These observations suggest that delayed progression of dark-induced senescence on attached leaves is endogenously controlled by the whole plant, possibly by sacrificing stored starch in older leaves and distributing it to the young leaves for their survival (Figure 1.1). Studies have shown that early starch turnover initiates premature leaf senescence whereas, it is also known that high sugars initiate the senescence process (van Doorn,

2004). Several experiments involving detached tobacco, barley, and *Arabidopsis* leaves on sucrose solutions show accelerated leaf senescence, confirming that high sugar levels promote the onset of senescence (Van Doorn, 2008; Parrott et al., 2005). However, it is still not clear how high sugars are primarily involved in early initiation of senescence.

To understand and identify the senescence-inducing ARCs involved in stress responses and ageing in plants, the *old13* mutant was used. The transcriptomic studies indicated differences in several sugar-related genes compared to the WT samples. In the RNA sequencing data, none of the sugar-related genes are differentially expressed in *old13* EEL but in the MEL leaf samples, two sugar transport-related genes (*SUC5* and *SWEET10*) were found to be downregulated. Both these genes are involved in sucrose transport (Durand et al., 2017), and downregulation of *SUC5* and *SWEET10* suggests that less sugars are transported in *old13* MEL. Moreover, in *old13* FEL, 10 out of 11 sugar-related genes are downregulated. In *old13* FEL, decreased expression of genes that function in sugar transportation are *ATCWI1* (*ARABIDOPSIS THALIANA CELL WALL INVERTASE 1*), *PMT6* and *PMT5* (*POLYOL TRANSPORTER*). The sugar-sensitive genes that are downregulated in *old13* FEL are *BT2* (*TAZ DOMAIN PROTEIN* 2), *BZIP1* (*BASIC LEUCINE-ZIPPER 1*), *STP1* (*SUGAR TRANSPORTER PROTEIN 1*) and *DIN10* (*DARK INDUCIBLE 10*). All these genes are found to be strongly suppressed in the presence of high sugars (Cordoba et al., 2015; Fujiki et al., 2000; Kang et al., 2010; Mandadi et al., 2009). Thus, together these data indicate that *old13* FEL exhibit a high sugar level, possibly because of poor sugar transportation, which leads to the accumulation of sugars and results in decreased expression of sugar sensitive genes.

Since high sugar accelerates leaf senescence, *old13* FEL were placed in darkness supplemented with 2%, 4% and 6% sucrose to test whether *old13* FEL show accelerated senescence compared to the WT. These results together with sugar metabolomic data of *old13* 20 DAG samples show that increased sugar sensitivity is consistent with high sugar levels. First rosette leaf pairs from WT and *old13* 10, 15 and 20 DAG were subjected to GC/MS based metabolic profiling. A total of 23 sugar metabolites were analysed in *old13* samples. Firstly, the results reveal that most of the carbohydrate content was low in *old13* 10 DAG samples compared to WT samples. The carbohydrate metabolites that were low in *old13* 10 DAG samples comprised glucose, fucose, fructose, threitol, galactinol, raffinose, glycerol and 8 other unidentified sugars. It is known that sugar starvation is a direct cause of leaf senescence (Van Doorn, 2008). For instance, in *Arabidopsis*, expression of the *sen1* gene (*senescence-associated gene1*), was strongly induced in naturally senescencing leaves and detached dark-stressed senescencing leaves (Oh et al., 1996). Detached leaves placed in darkness supplemented with sugar prevented the increase of *sen1* transcript abundance of *sen1* gene, suggesting that low sugar levels induces the leaf senescence process (Oh et al., 1996). In addition to this, the expression of the leaf senescence-specific gene *SAG12* is also increased by low sugar levels (Noh and Amasino 1999). In several experiments it has been shown

that leaves held in darkness have increased expression of various senescence-related genes (van Doorn, 2004). In addition to this, studies have also shown that sugar starvation enhances the production of ROS (Morkunas et al., 2003, 2012). These results suggest that the early carbohydrate deficiency and high cellular ROS in 10 DAG *old13* likely triggers the stress susceptibility that results in initiation of early onset of senescence under stressed conditions.

Secondly, in *old13* 15 DAG leaves the levels of most sugars, including maltose, threitol, glucose 1,6, anhydro-beta, Inositol-myo, α,α-trehalose and 6 other unidentified sugars, were lower than in WT leaves. Whereas, mannose and glycerol, are found in considerably high levels in 15 DAG *old13* leaves. Mannose and glycerol which are both known to improve abiotic stress tolerance in plants (He et al., 2017; Lai et al., 2015), were also found at higher levels in *old13* leaves as compared to the WT leaves. It is also noteworthy that galatinol and raffinose, which were both undetectable in 10 DAG *old13* leaves, had significantly increased in 15 DAG *old13* leaves. Galactinol and raffinose belong to the Raffinose family of oligosaccharides (RFOs). The accumulation of galactinol and raffinose has been intensively studied in drought, salinity, cold and heat tolerance, and they have been shown to play a role in defense against oxidative stress in plants (Sengupta et al., 2015). It is possible that *old13* MEL senses increased levels of endogenous stress, leading to increased levels of mannose, glycerol, galactinol and raffinose (Kempa et al., 2008).

Thirdly, the majority of sugar metabolites like fucose, fructose, galactinol, raffinose, sucrose and 8 other unidentified sugars were shown to increase in abundance in *old13* FEL samples. Maltose is a degraded product of starch and known to protect cell membranes and proteins in plants when exposed to salinity, heat or freezing stress (Kaplan and Guy, 2004; Kempa et al., 2008). In *old13* FEL it was found that maltose levels were significantly lower than in WT. This observation is consistent with the results shown in chapter 4, where after the dark treatment, *old13* leaves displayed minimal staining of starch in leaves (Figure 4.9), suggesting that *old13* FEL has high sugars but possibly less starch conversion. Decreased maltose content was also accompanied by decreased threitol, glycerol and 2 other unidentified sugars. All these components play important roles in stress resistance (Shen et al., 1999), and were found to be lower in *old13* FEL leaves compared to the WT . The metabolomic profile shows that most of the sugars are high in *old13* FEL. It has been extensively studied that increased levels of soluble sugars provide osmotic stress tolerance in plants (Boriboonkaset et al., 2012). But looking at the results in Figure 5.3, 20+6 drought-stressed *old13* leaves showed hypersensitive response and severe wilting of leaves. If increased levels of soluble sugars induce tolerance to stress in plants, then drought-stressed 20+6 DAG *old13* plants should have shown enhanced resistance. Accumulation of imbalanced sugars in *old13* FEL could be one of the reasons for drought stress susceptibility. Thus, together the results suggest that age-dependent senescence and stress responses also depend on the sugar balance. Here I speculate that, for the survival of young leaves from stress, elevated sugars likely act as crucial

osmoprotectants, but in adult leaves, high sugar levels have an antagonistic effect, leading to early initiation of senescence under stressed conditions.

During a plants life cycle, sugar levels fluctuate, and plants respond differently to stressed conditions depending on this sugar level (Rosa et al., 2009). For the survival of plant organs during stressful conditions, source-sink partitioning is one of the essential adaptive mechanisms in plants (Paul and Driscoll, 1997). Studies on several microRNAs like *miR172* and *miR156*, show that they are regulators of the transition from juvenile to adult phase, and progress ageing traits. (Lauter et al., 2005; Wu et al., 2009). A delayed juvenile phase was observed in *miR156* overexpression lines, while on the contrary, reduced expression of *miR156* stimulates the occurrence of features corresponding to the adult phase in plants (Wu and Poethig, 2006). In addition to this, recent research has confirmed that sugar accumulation reduces and sugar deprivation increases the abundance of *miR156* (Yu et al., 2013). For this reason, low sugar levels in young leaves (sink) and high sugar levels in mature leaves (source) act as one of the signals that trigger the transition from juvenile to adult phase (Thomas, 2013). Perhaps, in *old13* leaves, low sugar levels signal a longer juvenile phase, while high sugar levels result in a quick change from juvenile to mature phase. Based on results from transcriptomic data, metabolomic data, and previous research, I propose that sugar is one of the important senescence-inducing ARCs which signals how plants respond to stressed conditions, depending on the age of a leaf.

Various metabolic process such as photosynthetic activity, mitochondrial respiration, and the pentose-phosphate pathway are directly involved in increasing the sugar and ROS levels in plants (Couee, 2006; Rolland and Sheen, 2005). Although sugars have been found to be involved in ROS-producing metabolic pathways under stressed conditions (Couée et al., 2006), the connection between sugar sensing and ROS signalling is extremely complex and not yet clear. These results show that *old13* FEL have both high sugar and endogenous oxidative stress levels. From the above discussion it appears that increased cellular stress and high sugar levels are most likely two important mechanisms that have caused stress susceptibility in *old13* plants.

5.3.5 Biological pathways in *old13* affected by amplified senescence-inducing ARCs

As shown in chapter 3, upregulation of oxidative stress, senescence and other stress-related genes coincides with downregulation of antioxidant activity and increased age of *Arabidopsis* leaves. The transcriptomic data in this chapter also shows that the expression of genes associated with stress are already elevated and stress tolerance genes have declined in *old13* leaves, confirming that senescence-inducing ARCs are amplified. The early acquisition of senescence-inducing ARCs leads to the sensing of endogenous cellular stress in *old13*, affecting biological pathways mainly involved in stress

responses. Based on the results, a hypothetical model in Figure 5.11 shows how amplified senescence-inducing ARCs in *old13* FEL have resulted in disrupting the signals causing stress susceptibility in an age-dependent manner. Firstly, the sugars generated in *old13* young leaves by photosynthesis are considerably low, and low antioxidant activity has possibly lead to intensified ROS generation. At this stage, *old13* 10 DAG leaves are most likely under mild stress which still allows plant growth under standard laboratory conditions, but causes heightened stress sensitivity. The stress sensitivity in young *old13* leaves was considerably lower compared to the old leaves, because of differences in amplified senescence-inducing ARCs. Secondly, the *old13* mature leaves sense intermediate cellular stress, and activate the adaptive mechanism of CW stiffening. The restricted CW process possibly results in accumulation of more sugars in mature *old13* leaves. The high sugar level and cellular stress together makes *old13* mature leaves respond like old leaves when exposed to stress, displaying the hypersensitive stress response. It was assumed that *old13* would display stress responses and senescence-inducing ARCs as shown in Figure 5.1C and E. However, *old13* plants displayed neither enhanced hypersensitivity to stress in all the stages (Figure 5.1 C), nor showed tolerance to stress at a young age and hypersensitivity in later stages (Figure 5.1 E). Instead, *old13* plants showed stress susceptibility in an age-dependent way, which leads to the model shown in Figure 5.11, where senescence-inducing ARCs are amplified and stress tolerance is reduced in *old13* leaves. Taken together, the results from this chapter conclude that high cellular stress, reduced antioxidant activity, high sugar and CW structure play important roles in contributing to the early acquisition of senescence-inducing ARCs in *old13*. The studies shown in this chapter prove that the mutation in *old13* causes early occurrence of senescence-inducing ARCs and makes plants hypersensitive to stressed conditions in an age-dependent way.

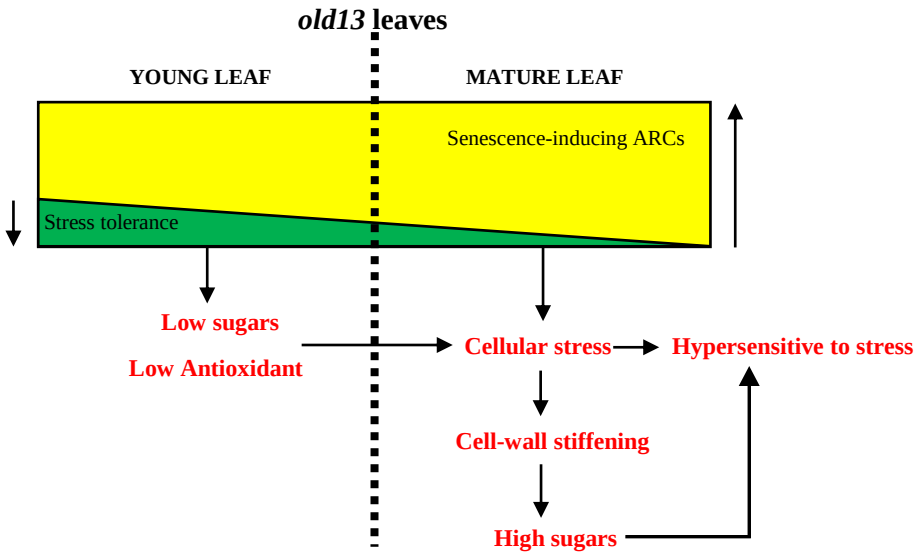

Figure 5.11. A tentative model showing biological pathways in *old13* affected by amplified senescence-inducing ARCs

Amplified senescence-inducing ARCs in *old13* young leaves are comparatively lower than in mature leaves, which causes *old13* plants to respond to stress in an age-dependent manner. Young leaves are susceptible to stress because of low sugar and low antioxidant activity. In mature leaves, intermediate cellular stress causes stiffening of the CW that results in accumulation of sugars, together inducing the hypersensitive response to stress because of amplified senescence-inducing ARCs.

Chapter 6 Attempted identification of *old13* by whole genome sequencing of nuclear-enriched DNA

6.1 Introduction

Before the year 2000, mutant identification in *Arabidopsis thaliana* was a lengthy process because of the unavailability of a whole genome sequence. In 2000, the publication of a complete genome sequence of *Arabidopsis* accession Columbia (Col-0) made it easier to study plant comparative genomics and to identify unknown gene functions (*Arabidopsis* Genome Initiative, 2000). Later in 2002, an *Arabidopsis* Landsberg *erecta* (L*er*-0) genome was published, but the sequence of L*er*-0 contains several InDels and single nucleotide polymorphism (SNPs) throughout the genome (Jander, 2002). The reason for the structural variation observed in L*er*-0 is because it is a draft sequence assembled from the previously sequenced genome of Col-0. The comparison of L*er*-0 and Col-0 sequence allows researchers to identify SNPs and design DNA markers for known positions. These markers are further used to map the position of mutations on chromosomes, which allows the identification of mutated regions in the genome sequence.

Mutant identification by next generation sequencing (NGS) of the whole genome has become increasingly popular and now is a powerful tool used widely by researchers. For gene identification, the sequenced reads produced from the mutant strain are compared with the reference genome to find the mutated region (Candela et al., 2015). In all *Arabidopsis* accessions, except Col-0, the whole genome sequence is available in the draft form, therefore finding a mutation in the background of a draft genome becomes challenging. As the draft genome consists of structural variations, the identification of a mutation within the missing regions (gaps) becomes impossible. Mutant recognition within the gaps can be resolved by using methods such as Iterative mapping and MutMap-Gap which fills the missing region within the genome by using de-novo assembly (Lai et al., 2011; Takagi et al., 2013; Tsai et al., 2010). Also, several reference free methods are proposed that do not require the reference genome and that compares the sequencing data from two different mutant lines. An example of a reference-free methods is needle in the K-stack (NIKS) which directly compares the whole genome of multiple mutant samples to identify the mutations (Nordström et al., 2013).

For successful sequencing, the extraction of high quality genomic DNA (gDNA) is particularly important (Simbolo et al., 2013). The incomplete removal of contaminants such as polysaccharides, proteins, RNA, salts etc. from DNA samples may hinder sequencing performance and library preparation (Shendure and Ji, 2008). Additionally, to obtain high quality assemblies from nuclear DNA,

it is important to extract nuclear-enriched gDNA with reduced contamination of chloroplast and mitochondrial DNA. Although there are several DNA extraction protocols and kits available that enable isolation of good quality gDNA, not all of them assure the extraction of highly nuclear-enriched gDNA. This chapter describes a hybrid approach combining the nuclear DNA enrichment technique of Lutz et al. (2011), and a CTAB extraction method to obtain nuclear-enriched gDNA from *old13* and *old14* plants and whole genome sequence analysis to identify the mutation in *old13*. While using the reference-free method for *old13* gene identification, the *old13* sequenced reads were then compared with the sequenced reads of *old14*.

6.2 Results

6.2.1 Nuclear-enriched genomic DNA isolation by method of Lutz et al. (2011)

Before attempting to identify the *old13* mutation by comparing genomic sequence, nuclear-enriched gDNA isolation was carried out. The foremost purpose of isolating nuclear-enriched gDNA for high throughput sequencing was to attain increased coverage of the nuclear genome. Therefore, for the isolation of high-quality nuclear-enriched gDNA from *old13* and *old14* plants, the protocol published by Lutz et al., (2011) was adapted. This methodology results in the isolation of high quality nuclear gDNA, therefore it was expected that the *old13* and *old14* gDNA would have reduced contaminants and be of high quality.

The detailed steps involved in this protocol are mentioned in the method section of chapter 2. The *old13* gDNA obtained by using the method of Lutz et al. (2011), had several problems. Firstly, during the extraction, a thick transparent jelly-like pellet was observed along with the isolated gDNA pellet, which was likely due to contamination with polysaccharides. Secondly, the isolated DNA was found to be of very low concentration and poor quality. A total amount of 0.2 g leaf tissue was used in this method, and resulted in the extraction of extremely low concentration of gDNA (~20 ng/µL, Figure 6.1) which does not fulfil the requirement for next generation sequencing. Thirdly, the quality of gDNA observed through spectrophotometric analysis showed an absorbance ratio between 2.52- 2.20, when measured at two different wavelengths (A_{260}/A_{280}). A ratio of ~1.8 is generally accepted as pure for DNA, and the higher A_{260}/A_{280} ratios obtained in the samples suggested the presence of contamination. Also, shearing of DNA was notably observed in the gel pictures (Figure 6.1). Thus, in my hands, the protocol published by Lutz et al (2011), for the nuclear gDNA extraction did not provide a high quality and quantity of gDNA.

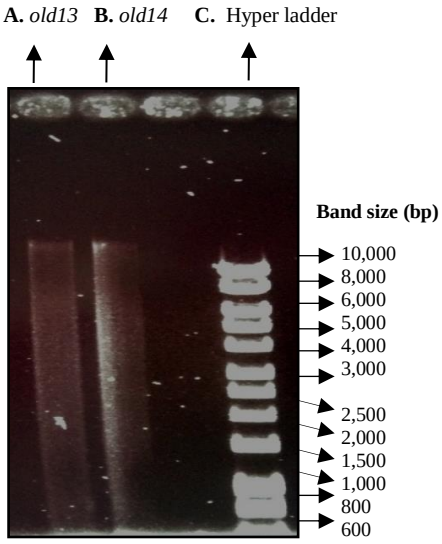

Figure 6.1. Agarose gel analysis of genomic DNA isolated using the Lutz et al. (2011) method.
1 µL of gDNA loaded onto a 0.8% agarose gel, stained with ethidium bromide. Lane A and B is gDNA obtained from leaf tissues of *old13* and *old14*, respectively. Lane C contains 5 µL hyper ladder1.

6.2.2 Hybrid method of CTAB by Dellaporta et al. (1983) and nuclear DNA by Lutz et al. (2011)

CTAB (cetyl trimethylammonium bromide) extraction buffer, which efficiently removes polysaccharides, is widely used for the purification of DNA from plant samples (Porebski et al., 1997). Therefore, to overcome the problems obtained using the Lutz et al. (2011) gDNA extraction protocol, various steps were modified including the incorporation of a CTAB gDNA extraction step (Dellaporta et al., 1983). The use of CTAB during DNA extraction should help reduce the contamination in the gDNA samples.

Firstly, to obtain a higher concentration of DNA, around 1.5-2 g of leaf tissue was used. This greatly increased the concentration of gDNA (~2.5 µg, Figure 6.2). Secondly, to improve the quality of gDNA, DNA was isolated from the nuclei containing pellet using an extraction buffer containing sodium bisulfite and nuclear lysis buffer containing CTAB. Subsequently, isolated DNA was precipitated with isopropanol and 3 M NaOAc. All together, these steps helped eliminate polysaccharide contamination as no jelly-like pellet was observed, and DNA smearing was notably reduced (Figure 6.2). The quality of extracted gDNA was observed through spectrophotometric analysis which showed an absorbance ratio between 2.1-2.5 and 2.1-2.48 in *old13* and *old14* samples, respectively, when measured at two different wavelengths (A_{260}/A_{280}). The concentration of gDNA was 200 ng/µL and 216 ng/µL in the samples. Hence, the modified steps, along with the adaptation of the CTAB gDNA method, improved the quality of gDNA. However, the increased RNA contamination and DNA smearing visible in the gel picture still remained to be solved (Figure 6.2).

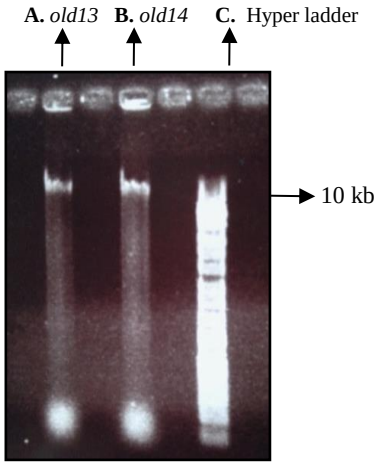

Figure 6.2. Agarose gel analysis of genomic DNA isolated with a modified step.
1 µL of gDNA loaded onto a 0.8% agarose gel, stained with ethidium bromide. Lane A and B is gDNA sample obtained from leaf tissues of *old13* and *old14*, respectively. Lane C contains 5 µL hyper ladder1 (Picture was overexposed to show the amount of shearing).

6.2.3 Elimination of RNA and DNA smearing

In the above section, the quality of gDNA was improved by adapting the CTAB method, but the sample still showed RNA contamination and DNA smearing in the gel picture. It was observed that the addition of RNase A was not very active for the removal of RNA contamination in the combined viscous solution of sarkosyl, CTAB nuclear lysis and extraction buffer (Materials and methods section 2.15). Therefore, for the removal of RNA contamination, RNase A was added after cleaning the DNA with phenol:chloroform:isoamyl alcohol. This successfully removed the RNA contamination from the isolated nuclear gDNA (Figure 6.3). In addition to this, a significant change was noted while using the fresh leaf tissue as compared to the frozen leaf tissue for the nuclear-enriched gDNA extraction. The gDNA extracted from frozen leaves displayed slight shearing in the gel picture (Figure 6.2), on the contrary, the gDNA extracted from fresh leaf tissue showed no shearing in the gel picture (Figure 6.3). The quality of gDNA obtained was observed through spectrophotometric analysis, and showed an absorbance ratio between 1.76- 2.0 and 1.79-2.0 in *old13* and *old14*, respectively, when measured at two different wavelengths (A_{260}/A_{280}). The concentration of gDNA was 107 ng/µL and 104 ng/µL in the two samples. Thus, the modified step used in this section helped in removing the RNA contamination and DNA smearing from the nuclear-enriched gDNA sample.

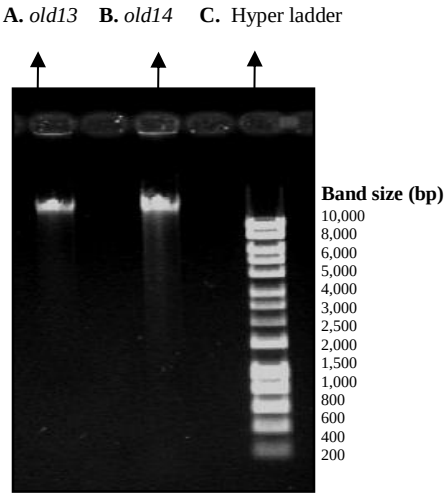

Figure 6.3. Agarose gel analysis of genomic DNA, isolated using a hybrid CTAB and nuclear DNA extraction approach.
1 µL of gDNA loaded onto a 0.8% agarose gel, stained with ethidium bromide. Lane A and B are gDNA samples obtained from leaf tissues of *old13* and *old14* respectively. Lane C contains 5 µL hyper ladder1.

6.2.4 Examination of genomic DNA quality

After optimising several steps, good quality gDNA was obtained from the hybrid approach of CTAB and nuclear DNA extraction. Next, the integrity and concentration of gDNA was examined spectrophotometrically using a Nano-Drop 1000, Qubit florometer and running the samples on a 0.8% agarose gel. A clear thick band in the gel picture (Figure 6.3) as well as the absorbance at A_{260}/A_{280} of 1.76/2.0 in *old13* and 1.79/2.0 in *old14*, signifies the purity of gDNA with high concentration (107 ng/µL and 104 ng/µL, respectively). The reading of qubit fluorometer quantification confirmed the elimination of protein, and only 7% of total RNA was found in the gDNA (Table 6.1). Around 10% of RNA in the gDNA samples is usually acceptable for high-throughput next generation sequencing (Lorraine Berry, personal communication). Therefore, taken together, these results confirm that the gDNA extracted from the leaf tissues of *old13* by the hybrid approach is of good enough quality and quantity for NGS.

Table 6.1 Qubit fluorometer readings

gDNA Sample	DNA Concentration (µg/mL)	RNA Concentration (µg/mL)	Protein Concentration (µg/mL)	% RNA Contamination	% Protein Contamination
old13	68.9	5.10	<1.0	7.4	N
old14	63.6	5.64	<1.0	8.8	N

N- Not detected.

6.2.5 Chloroplastic and nuclear gene abundance in DNA samples isolated by hybrid approach and CTAB method

To validate whether the hybrid method had preferentially reduced the chloroplast DNA and enriched the nuclear DNA, an abundance analysis of a nuclear gene and a chloroplastic gene was carried out. The relative abundance of the nuclear gene *Gigantea* (*Gi, AT1G22770*) and the chloroplastic gene *ribosomal protein S18* (*RPS18, ATCG00650*) was quantified by quantitative PCR on gDNA extracted by the CTAB method and hybrid method.

The graph in Figure 6.4A shows that the relative abundance of the *RPS18* gene is ~4-fold less in gDNA extracted using the hybrid approach, compared to the CTAB method. Moreover, the significant increase in abundance of *Gigantea* shows that hybrid DNA sample contains 2-fold higher nuclear genome compared to the CTAB method (Figure 6.4B). Taken together these results confirm that the hybrid method of gDNA isolation reduced chloroplastic DNA and yielded two-fold higher nuclear DNA, which should result in 2 X better coverage of the nuclear genome for the same sequencing price.

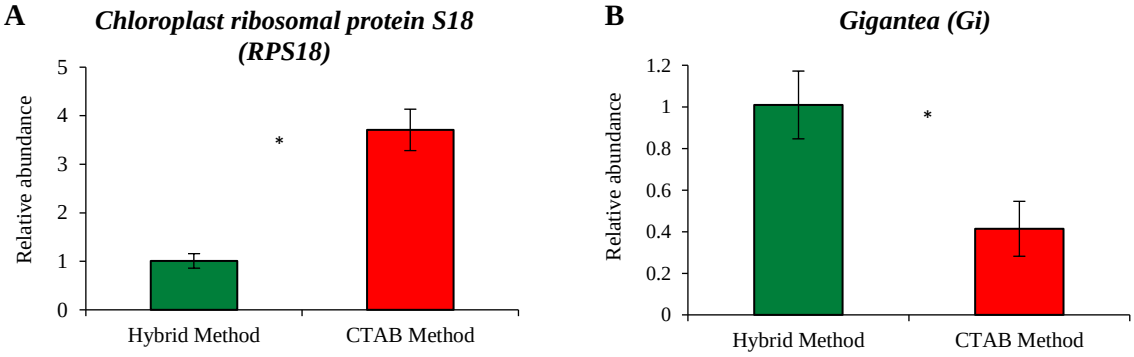

Figure 6.4. Gene abundance analysis of a chloroplastic and a genomic gene in DNA samples extracted using CTAB and a hybrid method.
Relative abundance of (A) a chloroplastic gene (*ribosomal protein S18 RPS18*) and (B) a nuclear gene (*Gigantea Gi*) obtained from DNA samples extracted using a hybrid or CTAB method. Green bars and red bars represent hybrid and CTAB gDNA samples, respectively. * indicates the values are significantly different between the samples at $P \leq 0.05$ using Student t-test.

6.2.6 Alignment of sequenced *old13* reads to the reference genome

Next generation sequencing technologies have become increasingly popular for mutation identification. The DNA sample of *old13* was sequenced with 200 bp insert size, whereas the *old14* DNA sample was sequenced with an insert size of 7 Kb. The sequenced reads from *old14* were used as a reference genome for the unique SNP identification specific to *old13*. Genetic analysis showed that the *old13* mutation segregates as a single monogenic recessive trait originally in the background of L*er*-0 (Schippers et al., 2008). The mutated *old13* locus was narrowed down to an ~23 Mb region on chromosome 5 by Shippers et al., (2008). In this section, the *old13* sequence obtained from nuclear-enriched gDNA was analysed to determine the genetic lesions causing the *old13* phenotype.

To identify the SNP causing the mutation in the *OLD13* gene, the genomic sequence obtained was firstly analysed by aligning the sequenced reads to the reference sequence of L*er*-0, downloaded from TAIR. The alignment of reads to the L*er*-0 genome was performed with Bowtie 2 software, which is a memory efficient tool used for mapping sequences against a large reference genome in a short period of time. The alignment by Bowtie 2 was followed by first indexing the L*er*-0 reference sequence and then mapping the paired-end sequences of *old13* separately to the index-generated reference sequence. The aligned reads to L*er*-0 is in the format of a SAM (Sequence Alignment Map) file, this is a file that contains the data in the form of text. Using samtools, the SAM file was converted to BAM (Binary Alignment Map) and from BAM into the sorted BAM files. BAM is the binary form of a SAM file, whereas a sorted BAM file is useful for having the huge alignment of data in a compressed form. The coverage of *old13* reads aligned to the L*er*-0 reference was found to be 96%.

6.2.7 Mapped *old13* reads reveal structural variations in the L*er*-0 reference genome

The BAM files created in the above section, containing the aligned *old13* sequenced reads to the reference genome, were further used to detect the mutated gene causing the *old13* phenotype. As the *old13* mutant was previously mapped to chromosome 5 at ~23 Mb loci, it was expected that the SNP-causing mutation in *OLD13* would be located in the respective mapped region.

The aligned genomic data was visualised by the user friendly Integrative Genomics Viewer (IGV) tool (Thorvaldsdóttir et al., 2013). Surprisingly, sequence analysis revealed no SNPs in the region where *old13* was mapped earlier. Instead, I noticed that there were several insertions and deletions present within the region. The picture in Figure 6.5, is an example of a region containing an insertion and deletion observed in the L*er*-0 reference sequence. Also, around 13 gaps were identified on chromosome 5 in the 20 Mb - 26 Mb region shown in Figure 6.6. The Illumina reads of *old13* sequenced

with an insert size of 200 bp, along with the sequenced *old14* library with an insert size of 7 Kb, was used to identify the size of the gap present within the mapped region. The mate-pair of the *old13* library, which was 200 bp apart, indicated that several gaps were less than 200 bp size. While, for a few gaps, the mate-pair of *old13* did not align anywhere, showing that the gaps were more than 200 bp. In that case the insert size of the gap was estimated using the *old14* library which was prepared with an average of 7 Kb inserts. Therefore, because of the structural variations in the reference sequence, the mutated *old13* loci could not be identified by aligning the sequenced reads to the L*er*-0 reference genome.

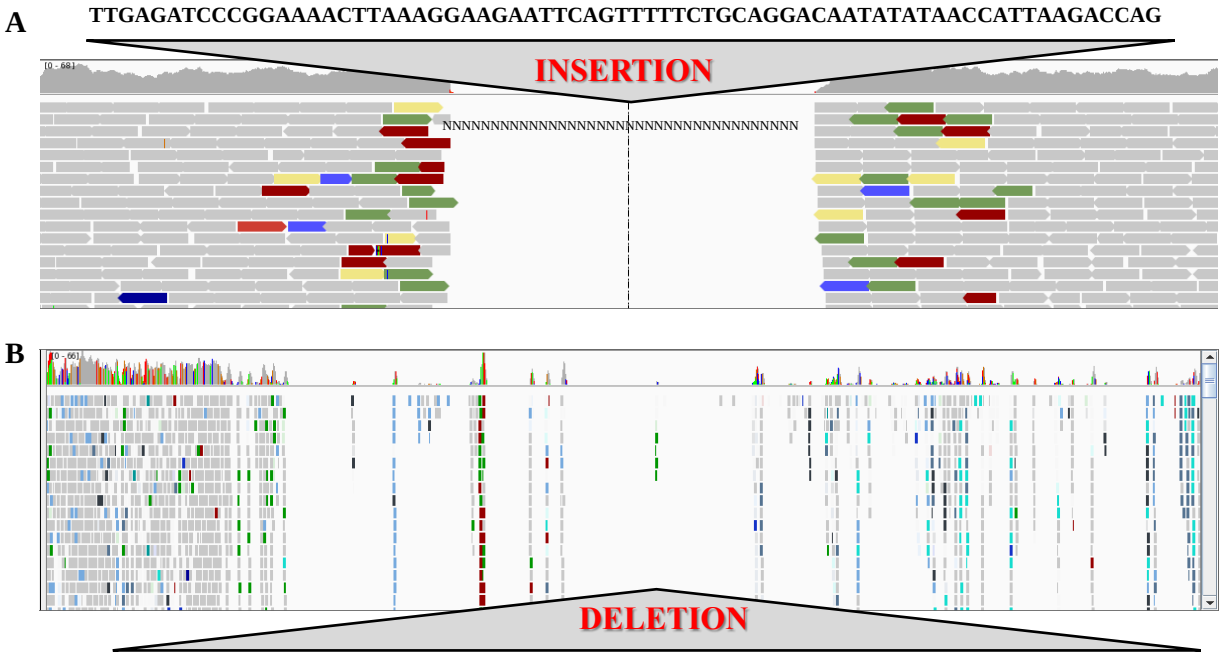

Figure 6.5. Misassembled sites observed in draft L*er*-0 reference sequence on IGV
A. Reads aligned to the L*er*-0 draft on IGV illustrating a region containing an insertion site.
B. Reads aligned to a region in the L*er*-0 draft on IGV, which is possibly deleted.

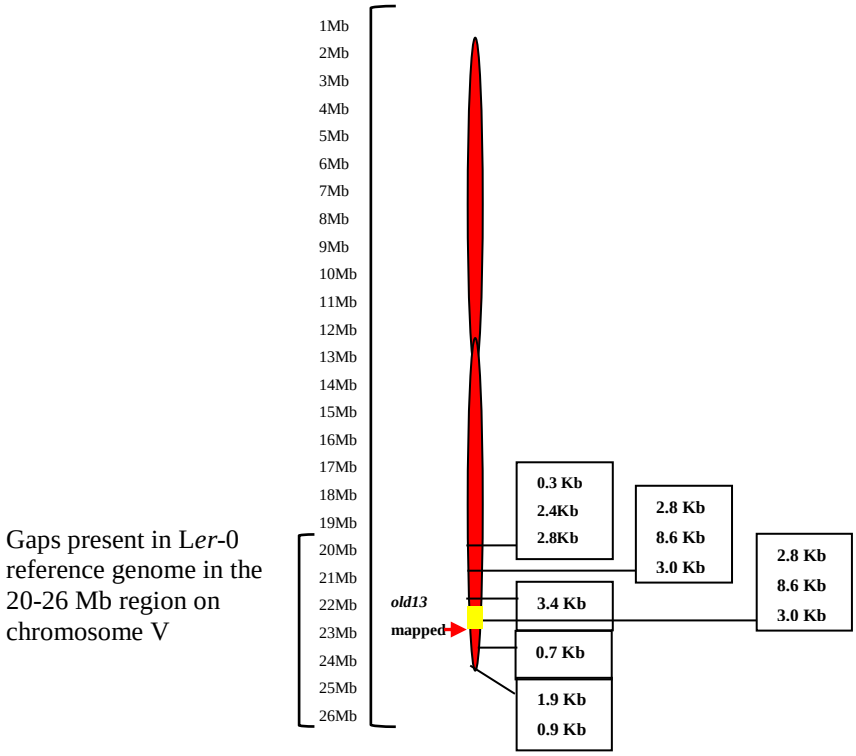

Figure 6.6. Number of gaps identified in the 20-26 Mb region in the L*er*-0 reference genome.
The approximate position and size of 13 gaps identified on chromosome V in the 20 Mb – 26 Mb region in the L*er*-0 genome. Size of gaps are shown in Kb (Kilobases). The yellow highlighted region on chromosome V signifies the region where the *old13* mutant was previously mapped (~23 Mb). Mb= Megabases.

6.2.8 Bridging the gaps in the L*er*-0 draft by iterative mapping

Variations in a reference genome can be determined by several methods. PCR amplification is one such method that could easily resolve the small insertions or misassembled regions however, this limits the identification of a sequence when the insertion in the draft genome is large (Alberts et al., 2002). Iterative mapping is another approach which helps fill in gaps by aligning the reads to the misassembled flagged region, then selecting the left and right flanking sequences and adding them to the reference (Lai et al., 2011; Tsai et al., 2010). Therefore, to identify the mutated gene in *old13,* resolution of the gaps present within the mapped region was attempted using iterative mapping.

Of the 13 gaps shown in Figure 6.6, the gap at ~23 Mb of 8.6 Kb size was selected and iterative mapping was carried out using a Geneious assembler by aligning the reads to the reference. The picture in Figure 6.7. shows Ns as a gap in the reference sequence, and newly added nucleotides assembled at the border of the flank. It can be observed in Figure 6.7 that the contigs added are from two different populations and have a lot of ambiguity that resulted in an unreliable final consensus. Therefore, in my hands next iteration and gap filling could not be resolved by iterative mapping.

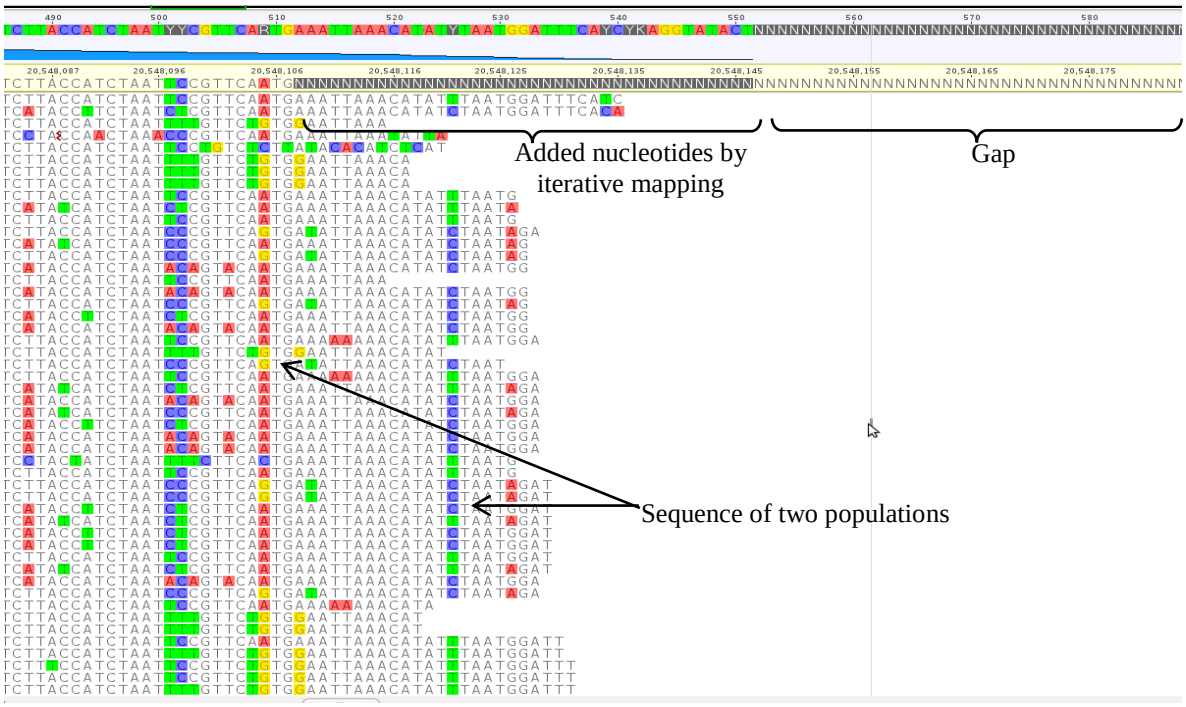

Figure 6.7. Bridging a gap in draft L*er*-0 sequence by iterative read mapping
The addition of contigs from two different populations give ambiguous data during the iterative mapping. The region selected is estimated to have a gap of around 2 Kb based on distance between the mate pairs.

6.2.9 Comparison of whole genome sequence of *old13* and *old14* by NIKS

Since the identification of the mutation in *old13* was unsuccessful because of variations in the reference sequence, the alternative reference-free method, NIKS was used to find the genetic lesions causing *old13* traits (Hunter et al., 2018; Nordström et al., 2013). NIKS compares the frequency of K-mers and creates a list of contigs of around 100-200 bp having SNPs specific to the sample genome. Since NIKS is a reference-free method, the whole genome of *old13* was compared with the *old14* sequence to obtain a list of SNPs specific to the *old13* mutant. For this, the contigs containing SNPs were searched using BLAST that resembles the *Arabidopsis* genes based on similarity of sequence. The workflow of NIKS is presented in Figure 6.8, in a diagrammatic form. NIKS created a list of around 246 contigs with SNPs which were further analysed by nucleotide BLAST to detect their position on a chromosome and check whether the SNP is causing a change in the function of a candidate *OLD13* gene. Therefore, the comparison of the *old13* whole genome sequence with *old14* by running the NIKS script aided identification of the SNPs specific to the *old13* mutant.

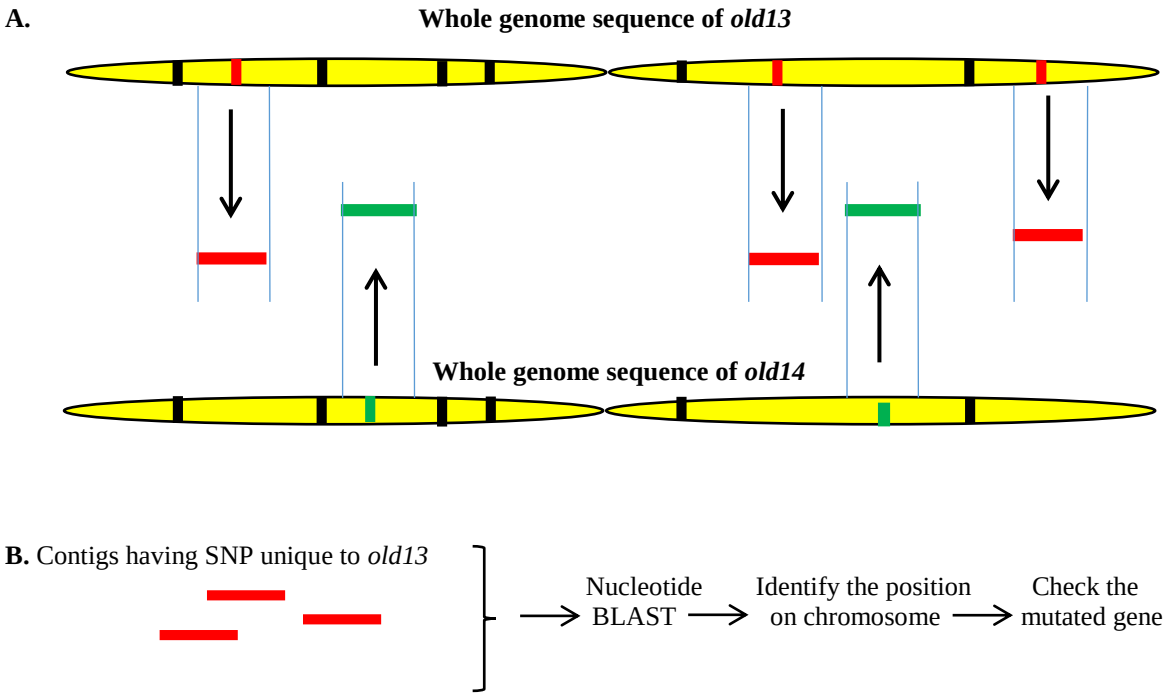

Figure 6.8. The workflow of NIKS to identify mutations in *old13* and *old14* without the reference sequence
A. Comparison of *old13* and *old14* whole genomes. Black bars in both the genomes represents the EMS-induced change in nucleotides. Red bars are the unique SNPs identified by NIKS in *old13* genome whereas, green bars signify the unique SNPs recognised in *old14.* B. Contigs of around 100-200 base pairs containing SNPs specific to *old13* were run through nucleotide BLAST to identify the position on the chromosome and the SNP causing the change in gene function.

6.2.10 Distribution of SNPs on chromosomes created by NIKS

In the above section, the NIKS script was found to have generated 246 contigs with SNPs specific to the *old13* sequence. In this section detailed analysis of a contig list was performed and it was expected to find SNPs on chromosome 5 at the mapped region of *old13*. If the analysis showed no SNPs on the mapped locus, then the *old13* mutant is either mapped to the wrong region or is present in the InDel.

The distribution of SNPs on the five chromosomes in *old13* is illustrated in Figure 6.9 and a detailed list of base pair changes in the *old13* genome is displayed in Appendix 5, including the position of the SNP on the chromosome, the location of SNPs in the reference genome, the change in nucleotide and the gene identity. Unexpectedly, none of the SNPs were found at or around the mapped regions of *old13*. This observation is consistent with previous results where alignment of mutant reads to the L*er*-0 genome displayed no SNPs at the mapped region, suggesting the mutant is mapped to the wrong region.

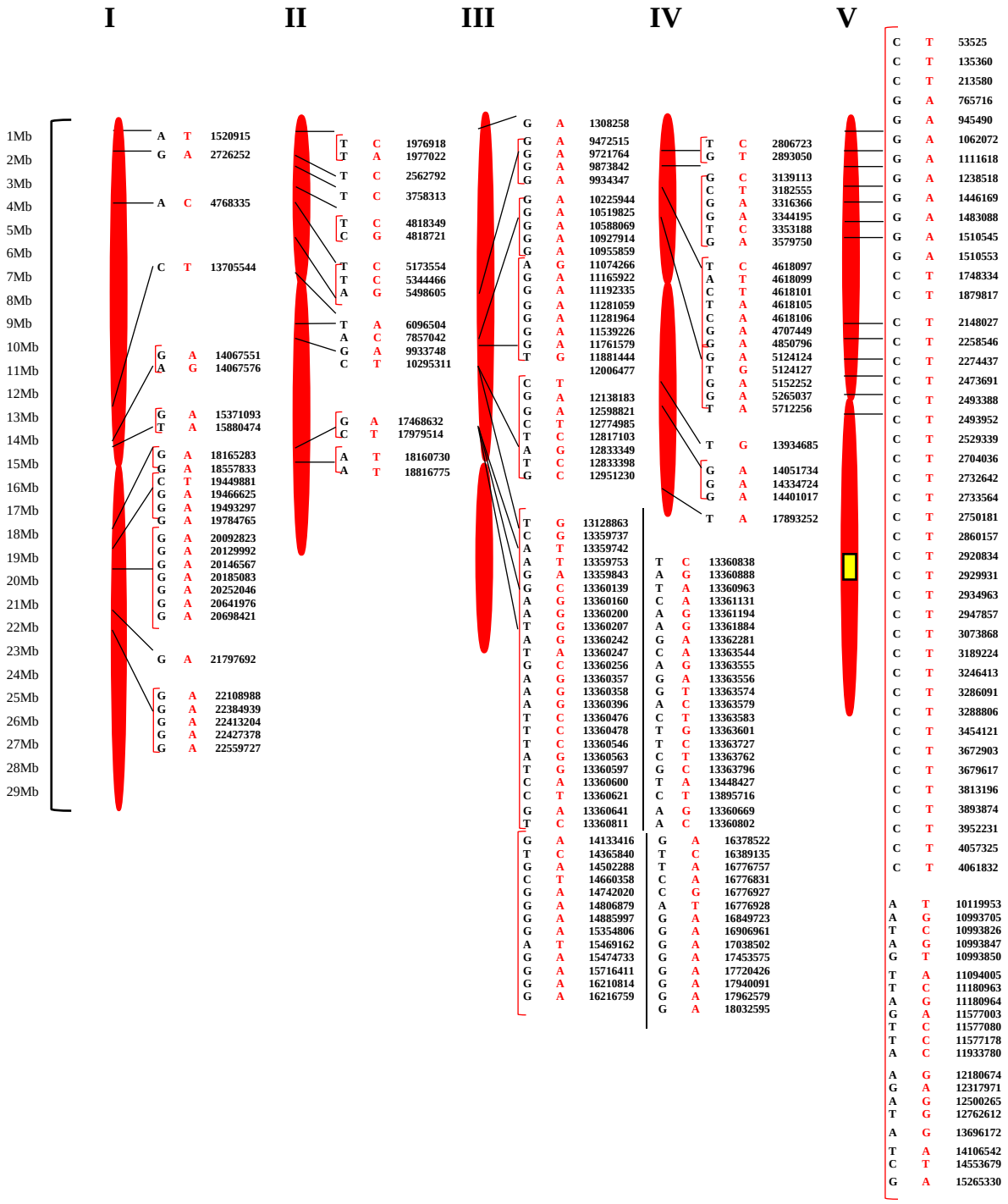

Figure 6.9. Distribution of SNPs on chromosomes identified in *old13* genome using NIKS

The approximate position of 246 SNPs on chromosome I, II, III, IV and V in the *old13* genome, identified by the NIKS protocol. The nucleotides in the L*er*-0 reference genome are written in black, and the red colour signifies the base pair change observed in the *old13* genome at specific locations on the reference genome. The yellow section on chromosome V shows the absence of SNPs around the region where the *old13* mutation was previously mapped (~23 Mb). Mb= Megabases.

6.2.11 Analysis of SNPs created by NIKS for *old13* mutant identification

As none of the SNPs were found on the mapped region of *old13*, the SNPs identified on other regions of the chromosomes were analysed with the aim to identify the *old13* mutation. The list of 246 SNPs recognised by NIKS in the *old13* genome was examined to determine whether any of them are causing a mutation in an annotated gene. Amongst 246 SNPs, 25 SNPs on chromosome 1, 3 and 5 were found in a protein coding region. Most of the single nucleotide changes in the protein coding region have been found to cause a synonymous amino acid change, whereas 7 were predicted to cause a genetic lesion in a conserved domain of a protein, causing a non-synonymous amino acid change as well as an unstable protein structure (Table 6.2). The stability of a protein after an amino acid change was predicted using the CUPSAT tool (http://cupsat.tu-bs.de/). Since there are seven identified genetic lesions in the conserved domain of a proteins distributed on chromosome 1, 3 and 5, future work would include the fine mapping of the *old13* mutant using the SNP targeted markers to confirm the identity of the mutated gene in *old13*.

Table 6.2 List of SNPs identified in RNA coding region that possibly contains *old13* mutation

Chr.	SNP position	Ref.	SNP	Gene ID	Amino acid change	Protein domain	Possibility of mutated *old13* gene
Chr.1	2726252	G	A	AT1G08600	Alanine → Threonine	Conserved domain	POSSIBLE
Chr.1	19784765	G	A	AT1G53840	Alanine → Threonine	Conserved domain	Stable protein
Chr.1	20129992	G	A	AT1G54820	Arginine → Lysine	Not in a conserved domain	
Chr.1	20252046	G	A	AT1G55140	Leucine → Phenylalanine	Conserved domain	Stable protein
Chr.3	9472515	G	A	AT3G26040	Glycine → Glutamic acid	Conserved domain	POSSIBLE
Chr.3	10519825	G	A	AT3G28345	Proline → Serine	Not in a conserved domain	
Chr.3	10955859	G	A	AT3G29070	Aspartic acid → Asparagine	Not in a conserved domain	
Chr.3	11192335	G	A	AT3G29400	Leucine → Phenylalanine	Conserved domain	POSSIBLE
Chr.5	53525	C	T	AT5G01150	Leucine → Phenylalanine	Not in a Conserved domain	
Chr.5	213580	C	T	AT5G01590	Alanine → Valine	Not in a conserved domain	
Chr.5	765716	G	A	AT5G03270	Alanine → Threonine	Conserved domain	POSSIBLE
Chr.5	1510545	G	A	AT5G05160	Glutamic acid → Lysine	Conserved domain	Stable protein
Chr.5	2473691	C	T	AT5G07810	Glycine → Glutamic acid	Not in a conserved domain	
Chr.5	2860157	C	T	AT5G09300	Glycine → Aspartic acid	Conserved domain	Stable protein
Chr.5	2929931	C	T	AT5G09500	Glycine → Glutamic acid	Not in a conserved domain	
Chr.5	2947857	C	T	AT5G09580	Arginine → Tryptophan	Not in a conserved domain	
Chr.5	3454121	C	T	AT5G11000	Alanine → Threonine	Not in a conserved domain	
Chr.5	3679617	C	T	AT5G11540	Glycine → Serine	Conserved domain	POSSIBLE
Chr.5	3952231	C	T	AT5G12290	Arginine → Histidine	Not in a conserved domain	
Chr.5	4317921	C	T	AT5G13530	Proline → Leucine	Not in a conserved domain	
Chr.5	4658359	C	T	AT5G14550	Arginine → Histidine	Conserved domain	POSSIBLE
Chr.5	5303979	C	T	AT5G16300	Proline → Serine	Not in a conserved domain	
Chr.5	6253125	C	T	AT5G18900	Serine → Asparagine	Conserved domain	POSSIBLE
Chr.5	6637828	C	T	AT5G19810	Proline → Serine	Not in a conserved domain	
Chr.5	7705729	G	A	AT5G23110	Glycine → Glutamic acid	Not in a conserved domain	

List of 25 single base pair changes found in protein coding region identified by NIKS in the *old13* genome. The 7 SNPs highlighted in red are deemed to be good candidates responsible for the *old13* phenotype under stressed conditions, as these SNPs are in conserved protein domains are predicted to cause an unstable protein structure. Chr. = Chromosome number, SNP position= position of altered base pair in L*er*-0 reference genome, Ref. = base pair in reference sequence, SNP= single nucleotide polymorphism in *old13*. Stability of protein was predicted using the CUPSAT tool.

6.3 Discussion

Plant cells consist of three genomes- nuclear, plastid and mitochondrial therefore, total isolated cellular DNA also includes chloroplastic and mitochondrial DNA. To identify mutations in the nuclear genome it is important to extract nuclear-enriched gDNA, so that sequenced reads will have high coverage of nuclear DNA and improve bioinformatic analysis of the nuclear genome. Therefore, for the isolation of high-quality nuclear-enriched gDNA from *old13* plants, a method combining nucleus purification (Lutz et al., 2011) with CTAB DNA extraction (Dellaporta et al., 1983) was used. In my hands, the gDNA sample isolated by the method of Lutz et al, (2011) was of poor quality and low concentration. It also contained a jelly-like substance that likely was made up of polysaccharides (Webb and Knapp, 1990). To obtain purified DNA, some steps were modified by adapting the CTAB method, as it efficiently removes polysaccharide and polyphenol contamination from plant DNA (Porebski et al., 1997). The CTAB-containing nuclear lysis buffer aided the preferential separation of polysaccharides from the nucleic acids. Moreover, the buffer containing sodium bisulfite helped in the prevention of phenol contamination and gDNA degradation. At every consecutive step of the extraction, a significant reduction in green colour was observed in the pellet containing DNA. After the sucrose gradient step, the appearance of a white pellet containing the nuclei signified the reduction in chloroplast contamination. The Phenol: chloroform: isoamyl alcohol mixture, as used in the hybrid protocol are universally used in many DNA purification methods for efficient protein removal (Kang and Yang, 2004). The results from gel pictures, spectrophotometer and Qubit fluorometer confirmed that gDNA extraction by the hybrid approach was of higher quality (section 6.2.4, Table 6.1). Additionally, in my hands, I observed that fresh and young leaf material allowed isolation of good quality gDNA with little shearing (Figure 6.3). Moreover, the reduced abundance of the *RPS18* gene confirmed that the hybrid method of gDNA extraction considerably reduces the chloroplastic DNA (Figure 6.4). Thus, the optimised hybrid DNA isolation method is suitable for extracting pure and high quality nuclear-enriched gDNA, appropriate for further use in next generation sequencing. This will result in the generation of more nuclear DNA reads and can improve the quality of the sequencing library.

Sequenced reads from *old13* nuclear-enriched gDNA were obtained by next generation sequencing. Since, the *old13* mutant is in the L*er*-0 accession genetic background, it is challenging to identify the mutated genes because of structural variations with the reference L*er*-0 genome (Figure 6.5 and 6.6). Research conducted by Lai et al (2011), identified around sixty-one misassembled regions present in the L*er*-0 draft sequence in the 15-17 Mb region on chromosome 3 (Lai et al., 2011). This becomes a problem for the successful identification of mutated genes especially when the genes are mapped to the region that does not have a good reference sequence. Therefore, for the successful identification of a mutated gene, the availability of a good reference sequence is extremely important.

However, the results from aligned reads to the reference sequence as well as use of the reference-free method (NIKS) did not show any genetic lesions at or around the previously mapped location of the *old13* mutation (Figure 6.7). Taking this into consideration, one possibility is that the *old13* phenotype is the outcome of an epistatic effect of the background mutations in the *old13* genome (Table 3). For example- the *ABP1* (*Auxin Binding Protein 1*) gene was first identified in maize plants as having an essential role in auxin hormone signalling and plant development (Jones, 1994). Several other studies using antisense or mutant lines also examined *ABP1* gene function in *Arabidopsis* and also suggested a role in cell division, cell elongation and as a key component in auxin signalling (Braun et al., 2008; Chen et al., 2001, 2014; Xu et al., 2014). However, the *abp1* null mutants recovered using CRISPR editing technology in *Arabidopsis* surprisingly did not displayed any defects and were indistinguishable from the wild type plants (Gao et al., 2015). Later, whole genome sequencing performed on an EMS generated *abp1-5* mutant showed several background mutations, suggesting an additional cause for the phenotypic differences observed in *abp1-5* mutant plants (Enders et al., 2015). Also, it has been found that the *coil-16* (*Coronatine-insensitive*) mutant also carries an additional mutation in the *PEN2* (*PENETRATION2*) gene, causing a phenotypic effect in *Arabidopsis* (Westphal et al., 2008). Therefore, these studies suggest that background mutations could also be a cause for the *old13* phenotype. The NIKS protocol identified 25 SNPs on chromosome 1, 3 and 5 in a protein coding region (Table 6.2). Amongst 25 SNPs, 11 were found in a conserved protein domain causing a non-synonymous amino acid change. The CUPSAT tool predicted that 7/11 SNPs caused unstable protein structure. However, even small changes in proteins can effect protein activity, therefore, 11 genetic lesions in a conserved protein domain may contain the mutated *old13* gene, and should be confirmed in future work.

The *old13* mutant was originally in a L*er*-0 background which was backcrossed with Col-0 and mapped on chromosome 5 at ~23 Mb locus in the Col-0 accession (Schippers et al., 2008). Another possible explanation for the unidentified *old13* gene is that the mapped *old13* region in Col-0 is not at the ~23 Mb location in the L*er*-0 background. The previous mapping data was not available in the records, making it impossible to match the mapped regions of Col-0 and L*er*-0 check if they are the same or not. To confirm the mapped locus of *old13*, and successfully identify the *old13* mutated gene, future work should include remapping of the mutant locus, using the SNP markers identified using the NIKS protocol (Table 3). The list of 25 SNPs identified are specific to the *old13* mutant and these SNPs were also confirmed by sequencing of PCR products (data not shown). Moreover, transcription factors binding to the promoter region of genes have crucial roles in determining gene function, and a mutation in a promoter may alter transcription factor binding and hence affect the activity of the gene (Hernandez-Garcia and Finer, 2014). Therefore, future work should also investigate mutations in promoter regions as a possible cause of the *old13* phenotype.

Chapter 7 Outlook, summary and future work

7.1 Senescence is integrated into the plant developmental program

Leaf senescence is a natural process of ageing. It is the final stage of leaf development that leads to the death of a leaf; therefore it brings the life expectancy of a plant to a limit (Lim et al., 2007). Forward and reverse genetic approaches have been used to understand the senescence process. Several studies have suggested possible models of regulation for senescence-associated genes in transgenic plants, that show early or delayed leaf senescence. However, most of the transgenic lines display early or delayed onset of senescence by altered growth of a plant. One example is a study on one of the early auxin-responsive genes, *SAUR36* (Small Auxin Up RNA gene 36). The researchers suggested that *SAUR36* is a positive regulator of senescence in *Arabidopsis.* The *SAUR36* overexpressor lines exhibited early senescence phenotypes, whereas knockout lines showed late senescence symptoms (Hou et al., 2013). However, the knockout *saur36* plants displayed larger leaf area compared to the control plants, suggesting a role for this functional gene in inhibiting cell enlargement. In reference to this study, it is widely known that auxin plays an important role in plant growth and development, including initiation of reproductive organs (Cheng and Zhao, 2007) and controlling cell expansion (Perrot-Rechenmann, 2010). Reduced auxin levels can prevent ethylene biosynthesis (Franklin and Morgan, 1978), failure of flower formation, and induce leaf elongation. Therefore, the phenotypes observed in the knockout *saur36* transgenic plants could have also resulted from low auxin levels. Similarly, overexpression of the *CBF2* (C-repeat/dehydration responsive element binding factor 2) gene in *Arabidopsis* resulted in delayed onset of senescence standard laboratory conditions and stressed conditions, by ~2 weeks (Sharabi-Schwager et al., 2010). Also, irrespective of the developmental stage, the whole rosette leaves appeared dwarf, suggesting a possible role for the *CBF2* gene in maintaining vegetative growth (Sharabi-Schwager et al., 2010). These findings imply that even a single gene, involved in early developmental processes, can alter later plant growth, by either early or delayed development, leading to premature or late senescence, respectively. This suggests that genes responsible for negatively regulating development may delay developmental stages in plants, including growth of rosette leaves, flowering, cell proliferation and enlargement. Delayed growth in a plant also delays the factors involved in ageing such as ethylene, jasmonic acid, abscisic acid, and overproduction of reactive oxygen species, hence resulting in delayed onset of leaf senescence. Alternatively, the genes responsible for positively regulating development may give early leaf development and reproductive growth. This eventually increases the factors involved in ageing thus, promoting progression of leaf senescence. Therefore, not all, but presumably many genes, may act as negative regulators of senescence, because those genes have control over development. This gives an indication that perhaps most of the genes we consider as

negative or positive regulators of senescence actually regulate growth and development of a plant, which alters the timing of leaf senescence. Thus, senescence can be controlled by overexpressing the genes involved in development of a plant. The younger the plant, the greater tolerance it will have to stress, and therefore, delayed leaf senescence will also be apparent. From the commercial point of view, these transgenic plants may show a greater tolerance to environmental stresses through their disrupted growth and development, but this may also result in delayed crop maturation.

7.2 Senescence-inducing ARCs reduce stress tolerance in *Arabidopsis* leaves

Past studies have provided vast information on the genes that regulate ageing in plants, but most of these genes also regulate growth and development. The mechanism that directly regulates the ageing process without disrupting growth has yet to be studied in detail. Therefore, in my thesis (chapter 3) I have studied the pre-senescence process to determine how the ageing process is initiated. *Arabidopsis thaliana* was used in this study because it is widely used by researchers for studies of the molecular and cellular biology of flowering plants (Wienkoop et al., 2010). It has been commonly observed in *Arabidopsis* that once leaf elongation stops, ageing events such as reproduction and initiation of leaf senescence proceed (Breeze et al., 2011). Therefore, to observe the global picture of transcriptomic changes taking place during the growth of a leaf (before the onset of senescence), I selected early expanding leaf (EEL), mid expanding leaf (MEL) and fully expended leaf (FEL) samples for RNA sequencing. The transcriptomic studies confirm that, as the leaf ages, decreased DNA repair mechanisms coincide with elevated endogenous cellular stress. These results show that, signals transmitted during the development from young to adult leaves, are senescence-inducing age-related signals. Thus, the RNA-sequencing data presented in this thesis provides evidence that the ageing process in *Arabidopsis* begins with the gradual occurrence of senescence-inducing ARCs (Chapter 3). The discovery of senescence-inducing ARCs provides new insights to better understand the pre-senescence changes taking place that lead to the activation of leaf senescence processes. The research shown in Chapter 3 contributes to our understanding that the initiation of senescence starts from a young age in *Arabidopsis* leaves, even before the completion of leaf elongation.

To further understand the effect of senescence-inducing ARCs in different aged leaves, plants were exposed to stressed conditions. Several studies have shown that plant organs of different ages show distinct responses to stress (Chapter 1); however, the cellular processes that result in these different responses are still poorly understood. The results in Chapter 3 clearly show that as the leaf ages, the plant's tolerance to stress decreases, which is likely due to the gradual occurrence of senescence-inducing ARCs. This study concludes that young leaves (10 DAG) are more tolerant to stress because of negligible senescence-inducing ARCs. Whereas, the gradual accumulation of senescence-inducing

ARCs, such as reduced DNA repair and tolerance to stress in the mature phase (15 DAG), activates senescence under stress-inducing conditions. In adult leaves (20 DAG), the senescence-inducing ARCs amplify to a level that enables plants to undergo senescence during environmental stress. This work contributes valuable research towards the understanding of why plants loose tolerance to stress as they develop. Together, this study suggests that initial senescence processes begin right from the young growth stage of *Arabidopsis* leaves and is accompanied by the gradual occurrence of senescence-inducing ARCs. Hence, ageing is a continuous process that starts with the birth of a leaf.

The model in Figure 7.1 illustrates how the age of a leaf is integrated into the stress responses. A plant's reaction to stress is primarily determined by the age of the leaf. Thus, ageing is a checkpoint that regulates plant survival or death under stressed environments. This checkpoint includes the presence of senescence-inducing ARC's, if they are low, then a leaf may show enhanced tolerance to stress, but if the senescence-inducing ARCs are elevated, then a leaf may undergo senescence. The misregulation of a gene involved in integration of age into the stress responses will wrongly estimate the age of a leaf. For example, the *old13* mutant appears the same as wild type plants but is sensitive to stress in an age-dependent way (Chapter 4). The results shown in Chapter 5 illustrate that stress susceptibility in the *old13* mutant is because of amplified senescence-inducing ARCs. This means that misregulation of the *old13* gene causes overestimation of the age of the leaf, therefore interpreting it as being old, resulting in enhanced stress susceptibility in an age-dependent way.

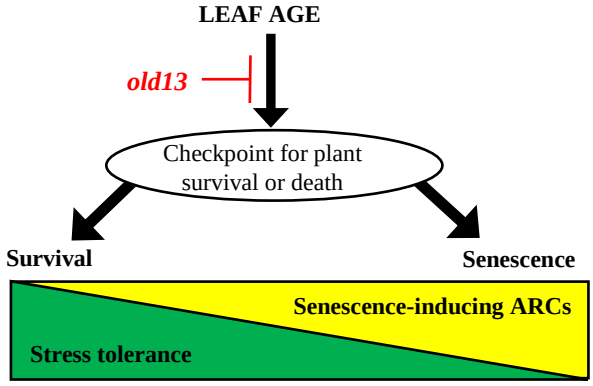

Figure 7.1 A tentative model depicting integration of age into the stress responses.
Model showing that leaf survival or death under stress is determined by the age of a leaf. Through the checkpoint, the age of a leaf is determined based on the occurrence of senescence-inducing ARCs. Decreased senescence-inducing ARCs could be one of the checkpoints for young leaves that will show resistance to stress, whereas, elevated senescence-inducing ARCs could be one of the checkpoints for old leaves that will undergo senescence under stressed conditions. Misregulation of the mutated *old13* gene overestimates the age of leaves as old and causes plants to be more sensitive to stress.

The findings from this thesis give new direction to the field of plant senescence and suggest that the genes involved in ageing or growth of a plant should be critically analysed for their involvement in senescence. This finding is useful to plant physiology in two different ways. If a gene functions in ageing of a plant, then mutation or overexpression of that gene should induce stress susceptibility or stress resistance respectively, in an age-dependent manner. This study also encourages the plant physiologist to carefully consider the age of a plant while performing stress experiments, as plants of different age show distinct stress responses.

7.3 Amplified senescence-inducing ARCs cause a hypersensitive response to stress

The characterisation of *old13* mutants in Chapter 4 and 5 verified that the *OLD13* gene functions in regulating senescence-inducing ARCs. The stress-induced experiments confirmed that *old13* displays stress susceptibility in an age-dependent manner. Also, the increase in misregulated genes with increased age of *old13* leaves confirmed that stress sensitivity in *old13* is a result of amplified senescence-inducing ARCs. The stress susceptibility in *old13* appeared to be caused by misbalanced sugar, elevated oxidative stress and impaired cell-wall morphology. This study also suggests that mutants with normal growth but distinct responses to stress could be involved in regulating plant ageing. The differentially expressed genes associated to oxidative stress, senescence and other stress responses listed in Appendix 1 and Chapter 5 will be of great use for future studies on the pre-senescence mechanism and responses to stress. Also, the *old13* gene identification would be a contribution in understanding the stress responses in plants in an age-dependent way. The SNPs listed in Table 6.2 will be used for future work in the successful identification of the *OLD13* gene.

7.4 Implications for plant improvement

In an attempt to produce more stress-tolerant plants, researchers should aim to understand and control the ageing process first. Even though a number of genes specific for senescence have been identified, we still lack information about the genes regulating integration of age into the stress responses. Mutants like *ore1, ore9, drd1,* and *ddm1* show delayed ageing and senescence and enhanced stress tolerance, without altered plant growth (Cho et al., 2016; Hye et al., 2004b). Thus, only a few studies have discovered age-related genes and biological processes that trigger ageing and are not involved in plant growth and development. It is a scientific challenge to find genes that control senescence, and can be used to increase the life span and tolerance of plants against external environmental stress. Therefore, further research on gene recognition associated to senescence-inducing ARCs needs to be carried out.

This knowledge can then be used in biotechnological applications to increase plant survival, growth, development and production under fluctuating unfavourable environmental conditions.

Transgenic plants with altered genes regulating senescence-inducing ARCs may show greater tolerance to stress and delayed ageing without disrupted growth. This could result in development of more productive crops under fluctuating environmental conditions. Although manipulation of the senescence-inducing ARCs could lead to the production of crops with better yield under stressed conditions, this may also develop unexpected stress resistance changes. For instance, the adaptive mechanism in plants under intermediate stress is followed by the initiation of senescence in the oldest leaves, which remobilises nutrients for the survival of young growing tissues. If senescence-inducing ARCs are delayed in transgenic plants exposed to intermediate stress, senescence may not be initiated in the oldest leaves. Therefore, the old leaves would not be able to function as a source of essential nutrients for the young leaves and this may result in the ultimate death of both old and young leaves. Under continuous environmental stress young and old leaves may die because the adaptive mechanism for the survival of young developing organs will no longer be activated. Thus, transgenic plants may show longer lifespan and enhanced tolerance to stress under mild stress, but intermediate stress will result in death of the whole plant. Such consequences need to be considered by researchers because while controlling the ageing of plants may be advantageous for improving crop yield under mild stress, it may also damage crops when exposed to intermediate stress.

Collectively, this thesis has contributed to understanding the process underlying ageing in plants and has also shed light on the integration of age into the stress responses. The knowledge provided in this thesis could be of use to develop crops with better fitness and survival under fluctuating environmental conditions.

Chapter 8 Appendices

Appendix 1. Up regulated leaf senescence, oxidative stress and other stress-related genes in mature and adult leaves of *Arabidopsis thaliana* before the initiation of the senescence process.

AGI ID	Gene name	Biological Function
AT1G05100	*MAPKKK18*	Leaf senescence
AT1G69490	*ANAC029*	Leaf senescence
AT3G04060	*NAC046*	Leaf senescence
AT3G10985	*WI12*	Leaf senescence
AT3G45600	*TET3*	Leaf senescence
AT4G30430	*TET9*	Leaf senescence
AT5G60360	*SAG2*	Leaf senescence
AT1G70530	*CRK3*	Leaf senescence
AT5G13170	*SAG29*	Leaf Senescence
AT5G39610	*NAC6; ORE1*	Leaf senescence
AT1G32870	*NAC13*	Leaf senescence
AT1G34180	*NAC016*	Leaf senescence
AT1G56010	*NAC1*	Leaf senescence
AT1G69310	*WRKY57*	Leaf senescence
AT1G73680	*ALPHA*	Leaf senescence
AT1G76680	*OPR1*	Leaf senescence
AT1G77450	*NAC032*	Leaf senescence
AT2G13790	*SERK4*	Leaf senescence
AT2G13810	*EDTS5*	Leaf senescence
AT2G17040	*NAC036*	Leaf senescence
AT3G04070	*NAC047*	Leaf senescence
AT3G15500	*NAC055*	Leaf senescence
AT3G15510	*NAC2*	Leaf senescence
AT3G15730	*PLD*	Leaf senescence
AT3G19290	*AREB2*	Leaf senescence
AT3G29035	*ANAC059*	Leaf senescence
AT3G44350	*NAC061*	Leaf senescence
AT3G49530	*ANAC062*	Leaf senescence
AT3G52430	*PAD4*	Leaf senescence
AT3G53280	*CYP71B5*	Leaf senescence
AT3G56400	*WRKY70*	Leaf senescence
AT4G02380	*SAG21*	Leaf senescence
AT4G05320	*UBQ10*	Leaf senescence
AT4G30270	*XTH24*	Leaf senescence
AT4G32940	*GAMMAVPE*	Leaf senescence
AT5G08790	*ATAF2*	Leaf senescence
AT5G24110	*WRKY30*	Leaf senescence
AT5G52310	*RD29A*	Leaf senescence
AT5G52830	*WRKY27*	Leaf senescence
AT1G03380	*ATG18G*	Leaf senescence
AT2G13800	*SERK5*	Leaf senescence
AT2G23810	*TET8*	Leaf senescence
AT2G29350	*SAG13*	Leaf senescence
AT2G30250	*WRKY25*	Leaf senescence
AT2G39200	*MLO12*	Leaf senescence
AT2G43570	*CHI*	Leaf senescence
AT5G22380	*NAC090*	Leaf senescence
AT5G24590	*ANAC091*	Leaf senescence
AT1G01140	*CIPK9*	Oxidative stress response
AT1G01470	*LEA14*	Oxidative stress response
AT1G01560	*MPK11*	Oxidative stress response
AT1G01720	*ANAC002*	Oxidative stress response
AT1G03940	*NA*	Oxidative stress response
AT1G05340	*NA*	Oxidative stress response
AT1G05575	*NA*	Oxidative stress response
AT1G05680	*UGT74E2*	Oxidative stress response
AT1G05690	*BT3*	Oxidative stress response
AT1G07200	*SMXL6*	Oxidative stress response
AT1G08930	*ERD6*	Oxidative stress response
AT1G10585	*NA*	Oxidative stress response
AT1G11210	*NA*	Oxidative stress response
AT1G13440	*GAPC2*	Oxidative stress response
AT1G14200	*NA*	Oxidative stress response
AT1G14790	*RDR1*	Oxidative stress response
AT1G14870	*PCR2*	Oxidative stress response
AT1G16370	*OCT6*	Oxidative stress response
AT1G18390	*NA*	Oxidative stress response
AT1G18890	*CPK10*	Oxidative stress response
AT1G20160	*ATSBT5.2*	Oxidative stress response
AT1G20440	*COR47*	Oxidative stress response
AT1G20450	*ERD10*	Oxidative stress response
AT1G20823	*NA*	Oxidative stress response
AT1G21100	*IGMT1*	Oxidative stress response
AT1G21250	*WAK1*	Oxidative stress response
AT1G21270	*WAK2*	Oxidative stress response
AT1G21520	*NA*	Oxidative stress response
AT1G21910	*DREB26*	Oxidative stress response
AT1G22190	*RAP2.4*	Oxidative stress response
AT1G22500	*ATL15*	Oxidative stress response
AT1G23140	*NA*	Oxidative stress response
AT1G26960	*HB23*	Oxidative stress response
AT1G27730	*ZAT10*	Oxidative stress response
AT1G32640	*MYC2*	Oxidative stress response
AT1G33560	*ADR1*	Oxidative stress response
AT1G35210	*NA*	Oxidative stress response
AT1G35720	*OXY5*	Oxidative stress response
AT1G36370	*SHM7*	Oxidative stress response
AT1G42990	*BZIP60*	Oxidative stress response
AT1G43910	*NA*	Oxidative stress response
AT1G47128	*RD21A*	Oxidative stress response
AT1G51700	*DOF1*	Oxidative stress response
AT1G52200	*NA*	Oxidative stress response
AT1G52400	*BGLU18*	Oxidative stress response
AT1G52890	*NAC019*	Oxidative stress response
AT1G54100	*ALDH7B4*	Oxidative stress response
AT1G55280	*NA*	Oxidative stress response
AT1G56280	*DI19*	Oxidative stress response
AT1G57630	*NA*	Oxidative stress response
AT1G59590	*ZCF37*	Oxidative stress response
AT1G61210	*DWA3*	Oxidative stress response
AT1G61340	*FBS1*	Oxidative stress response
AT1G63720	*NA*	Oxidative stress response
AT1G63840	*NA*	Oxidative stress response
AT1G65690	*NA*	Oxidative stress response
AT1G65790	*RK1*	Oxidative stress response
AT1G66160	*CMPG1*	Oxidative stress response
AT1G66180	*NA*	Oxidative stress response
AT1G67360	*NA*	Oxidative stress response
AT1G68010	*HPR*	Oxidative stress response
AT1G68670	*NA*	Oxidative stress response
AT1G69260	*AFP1*	Oxidative stress response
AT1G69270	*RPK1*	Oxidative stress response
AT1G69780	*ATHB13*	Oxidative stress response
AT1G71040	*LPR2*	Oxidative stress response
AT1G71960	*ABCG25*	Oxidative stress response
AT1G72300	*PSY1R*	Oxidative stress response
AT1G72770	*HAB1*	Oxidative stress response
AT1G73010	*PS2*	Oxidative stress response
AT1G73260	*KTI1*	Oxidative stress response
AT1G73330	*DR4*	Oxidative stress response
AT1G74020	*SS2*	Oxidative stress response
AT1G74360	*NA*	Oxidative stress response
AT1G74430	*MYB95*	Oxidative stress response
AT1G75280	*NA*	Oxidative stress response
AT1G75750	*GASA1*	Oxidative stress response
AT1G76180	*ERD14*	Oxidative stress response
AT1G76600	*NA*	Oxidative stress response
AT1G76800	*NA*	Oxidative stress response

AGI ID	Gene name	Biological Function
AT1G76930	*EXT4*	Oxidative stress response
AT1G77120	*ADH1*	Oxidative stress response
AT1G78410	*NA*	Oxidative stress response
AT1G79410	*AtOCT5*	Oxidative stress response
AT1G80130	*NA*	Oxidative stress response
AT1G80840	*WRKY40*	Oxidative stress response
AT2G04450	*NUDT6*	Oxidative stress response
AT2G05520	*GRP3*	Oxidative stress response
AT2G05710	*ACO3*	Oxidative stress response
AT2G06050	*OPR3*	Oxidative stress response
AT2G14560	*LURP1*	Oxidative stress response
AT2G17290	*CPK6*	Oxidative stress response
AT2G17520	*IRE1A*	Oxidative stress response
AT2G18690	*NA*	Oxidative stress response
AT2G19310	*NA*	Oxidative stress response
AT2G20560	*NA*	Oxidative stress response
AT2G22660	*NA*	Oxidative stress response
AT2G22880	*NA*	Oxidative stress response
AT2G23320	*WRKY15*	Oxidative stress response
AT2G24570	*WRKY17*	Oxidative stress response
AT2G24850	*TAT3*	Oxidative stress response
AT2G25000	*WRKY60*	Oxidative stress response
AT2G25735	*NA*	Oxidative stress response
AT2G26150	*HSFA2*	Oxidative stress response
AT2G26530	*AR781*	Oxidative stress response
AT2G30020	*NA*	Oxidative stress response
AT2G32030	*NA*	Oxidative stress response
AT2G32240	*NA*	Oxidative stress response
AT2G33150	*KAT2*	Oxidative stress response
AT2G33380	*RD20*	Oxidative stress response
AT2G33580	*LYK5*	Oxidative stress response
AT2G33590	*CRL1*	Oxidative stress response
AT2G34810	*NA*	Oxidative stress response
AT2G35930	*PUB23*	Oxidative stress response
AT2G37170	*PIP2B*	Oxidative stress response
AT2G37770	*AKR4C9*	Oxidative stress response
AT2G38470	*WRKY33*	Oxidative stress response
AT2G39030	*NATA1*	Oxidative stress response
AT2G39800	*P5CS1*	Oxidative stress response
AT2G39940	*COI1*	Oxidative stress response
AT2G40000	*HSPRO2*	Oxidative stress response
AT2G40130	*SMXL8*	Oxidative stress response
AT2G40140	*CZF1*	Oxidative stress response
AT2G41380	*NA*	Oxidative stress response
AT2G41640	*NA*	Oxidative stress response
AT2G43060	*IBH1*	Oxidative stress response
AT2G46270	*GBF3*	Oxidative stress response
AT2G46680	*ATHB7*	Oxidative stress response
AT2G47770	*TSPO*	Oxidative stress response
AT2G47780	*NA*	Oxidative stress response
AT2G47800	*MRP4*	Oxidative stress response
AT3G02130	*RPK2*	Oxidative stress response
AT3G02480	*NA*	Oxidative stress response
AT3G02800	*PFA-DSP3*	Oxidative stress response
AT3G02840	*NA*	Oxidative stress response
AT3G04110	*GLR1*	Oxidative stress response
AT3G05200	*ATL6*	Oxidative stress response
AT3G05500	*NA*	Oxidative stress response
AT3G08720	*S6K2*	Oxidative stress response
AT3G10930	*NA*	Oxidative stress response
AT3G11280	*NA*	Oxidative stress response
AT3G11410	*PP2CA*	Oxidative stress response
AT3G11820	*SYR1*	Oxidative stress response
AT3G11840	*PUB24*	Oxidative stress response
AT3G12580	*HSP70*	Oxidative stress response
AT3G14050	*RSH2*	Oxidative stress response
AT3G14440	*NCED3*	Oxidative stress response
AT3G15356	*NA*	Oxidative stress response

AGI ID	Gene name	Biological Function
AT3G16470	*JAL35*	Oxidative stress response
AT3G16530	*NA*	Oxidative stress response
AT3G16720	*TL2*	Oxidative stress response
AT3G17510	*CIPK1*	Oxidative stress response
AT3G18490	*ASPG1*	Oxidative stress response
AT3G19380	*PUB25*	Oxidative stress response
AT3G19580	*ZF2*	Oxidative stress response
AT3G20470	*GRP5*	Oxidative stress response
AT3G21780	*UGT71B6*	Oxidative stress response
AT3G23250	*MYB15*	Oxidative stress response
AT3G23400	*FIB4*	Oxidative stress response
AT3G23920	*BAM1*	Oxidative stress response
AT3G24500	*MBF1C*	Oxidative stress response
AT3G28210	*SAP12*	Oxidative stress response
AT3G28740	*CYP81D11*	Oxidative stress response
AT3G45640	*MPK3*	Oxidative stress response
AT3G46080	*NA*	Oxidative stress response
AT3G46090	*ZAT7*	Oxidative stress response
AT3G46600	*NA*	Oxidative stress response
AT3G46620	*RDUF1*	Oxidative stress response
AT3G46930	*NA*	Oxidative stress response
AT3G48090	*EDS1*	Oxidative stress response
AT3G48650	*NA*	Oxidative stress response
AT3G48850	*MPT2*	Oxidative stress response
AT3G49580	*LSU1*	Oxidative stress response
AT3G50060	*MYB77*	Oxidative stress response
AT3G50480	*HR4*	Oxidative stress response
AT3G50930	*BCS1*	Oxidative stress response
AT3G50970	*XERO2*	Oxidative stress response
AT3G51430	*YLS2*	Oxidative stress response
AT3G51440	*NA*	Oxidative stress response
AT3G51450	*NA*	Oxidative stress response
AT3G51920	*CML9*	Oxidative stress response
AT3G52400	*SYP122*	Oxidative stress response
AT3G52800	*NA*	Oxidative stress response
AT3G53420	*PIP2A*	Oxidative stress response
AT3G55610	*P5CS2*	Oxidative stress response
AT3G55980	*SZF1*	Oxidative stress response
AT3G57530	*CPK32*	Oxidative stress response
AT3G61190	*BAP1*	Oxidative stress response
AT3G61890	*ATHB12*	Oxidative stress response
AT3G63060	*EDL3*	Oxidative stress response
AT4G02280	*SUS3*	Oxidative stress response
AT4G03450	*NA*	Oxidative stress response
AT4G04490	*CRK36*	Oxidative stress response
AT4G05100	*MYB74*	Oxidative stress response
AT4G05590	*NA*	Oxidative stress response
AT4G10500	*NA*	Oxidative stress response
AT4G11360	*RHA1B*	Oxidative stress response
AT4G11890	*CRK45*	Oxidative stress response
AT4G12720	*NUDT7*	Oxidative stress response
AT4G13510	*AMT1*	Oxidative stress response
AT4G14390	*NA*	Oxidative stress response
AT4G14400	*ACD6*	Oxidative stress response
AT4G15975	*NA*	Oxidative stress response
AT4G16890	*SNC1*	Oxidative stress response
AT4G17230	*SCL13*	Oxidative stress response
AT4G18880	*HSF*	Oxidative stress response
AT4G19810	*ChiC*	Oxidative stress response
AT4G21440	*MYB102*	Oxidative stress response
AT4G21840	*MSRB8*	Oxidative stress response
AT4G21850	*MSRB9*	Oxidative stress response
AT4G21990	*PRH26*	Oxidative stress response
AT4G23130	*CRK5*	Oxidative stress response
AT4G23140	*CRK6*	Oxidative stress response
AT4G23150	*CRK7*	Oxidative stress response
AT4G23170	*CRK9*	Oxidative stress response
AT4G23260	*CRK18*	Oxidative stress response

AGI ID	Gene name	Biological Function
AT4G23450	*AIRP1*	Oxidative stress response
AT4G23810	*WRKY53*	Oxidative stress response
AT4G24160	*NA*	Oxidative stress response
AT4G24380	*NA*	Oxidative stress response
AT4G24570	*DIC2*	Oxidative stress response
AT4G24960	*HVA22D*	Oxidative stress response
AT4G25490	*CBF1*	Oxidative stress response
AT4G26070	*MEK1*	Oxidative stress response
AT4G26120	*NA*	Oxidative stress response
AT4G27410	*ANAC072*	Oxidative stress response
AT4G29110	*NA*	Oxidative stress response
AT4G31550	*WRKY11*	Oxidative stress response
AT4G31800	*WRKY18*	Oxidative stress response
AT4G31920	*RR10*	Oxidative stress response
AT4G33050	*EDA39*	Oxidative stress response
AT4G34000	*DPBF5*	Oxidative stress response
AT4G34390	*XLG2*	Oxidative stress response
AT4G34410	*RRTF1*	Oxidative stress response
AT4G34710	*SPE2*	Oxidative stress response
AT4G35480	*RHA3B*	Oxidative stress response
AT4G37370	*CYP81D8*	Oxidative stress response
AT4G37760	*SQE3*	Oxidative stress response
AT4G39030	*SID1*	Oxidative stress response
AT4G39400	*DWF2*	Oxidative stress response
AT5G01410	*PDX1*	Oxidative stress response
AT5G03350	*NA*	Oxidative stress response
AT5G04140	*GLUS*	Oxidative stress response
AT5G04340	*ZAT6*	Oxidative stress response
AT5G04950	*NAS1*	Oxidative stress response
AT5G05190	*NA*	Oxidative stress response
AT5G05410	*DREB2A*	Oxidative stress response
AT5G06760	*LEA4-5*	Oxidative stress response
AT5G07460	*PMSR2*	Oxidative stress response
AT5G10380	*RING1*	Oxidative stress response
AT5G14760	*FIN4*	Oxidative stress response
AT5G15860	*PCME*	Oxidative stress response
AT5G15960	*KIN1*	Oxidative stress response
AT5G19875	*NA*	Oxidative stress response
AT5G20910	*AIP2*	Oxidative stress response
AT5G23010	*IMS3*	Oxidative stress response
AT5G24530	*DMR6*	Oxidative stress response
AT5G27420	*CNI1*	Oxidative stress response
AT5G28630	*NA*	Oxidative stress response
AT5G37770	*TCH2*	Oxidative stress response
AT5G38710	*NA*	Oxidative stress response
AT5G38900	*NA*	Oxidative stress response
AT5G40890	*CLCA*	Oxidative stress response
AT5G41790	*CIP1*	Oxidative stress response
AT5G42380	*CML37*	Oxidative stress response
AT5G42650	*DDE2*	Oxidative stress response
AT5G45340	*CYP707A3*	Oxidative stress response
AT5G48570	*ROF2*	Oxidative stress response
AT5G48850	*ATSDI1*	Oxidative stress response
AT5G49520	*WRKY48*	Oxidative stress response
AT5G50200	*NRT3.1*	Oxidative stress response
AT5G50915	*NA*	Oxidative stress response
AT5G51190	*NA*	Oxidative stress response
AT5G51440	*NA*	Oxidative stress response
AT5G52050	*NA*	Oxidative stress response
AT5G52640	*HSP83*	Oxidative stress response
AT5G52760	*NA*	Oxidative stress response
AT5G52900	*MAKR6*	Oxidative stress response
AT5G54380	*THE1*	Oxidative stress response
AT5G54490	*PBP1*	Oxidative stress response
AT5G54610	*BDA1*	Oxidative stress response
AT5G56550	*OXS3*	Oxidative stress response
AT5G57220	*CYP81F2*	Oxidative stress response
AT5G57710	*SMAX1*	Oxidative stress response

AGI ID	Gene name	Biological Function
AT5G58940	*CRCK1*	Oxidative stress response
AT5G59450	*NA*	Oxidative stress response
AT5G59550	*RDUF2*	Oxidative stress response
AT5G59820	*ZAT12*	Oxidative stress response
AT5G61210	*SNP33*	Oxidative stress response
AT5G61900	*CPN1*	Oxidative stress response
AT5G62020	*HSFB2A*	Oxidative stress response
AT5G62470	*MYB96*	Oxidative stress response
AT5G63160	*BT1*	Oxidative stress response
AT5G64510	*TIN1*	Oxidative stress response
AT5G64660	*CMPG2*	Oxidative stress response
AT5G64810	*WRKY51*	Oxidative stress response
AT5G66070	*NA*	Oxidative stress response
AT5G66210	*CPK28*	Oxidative stress response
AT5G66400	*RAB18*	Oxidative stress response
AT5G67030	*ABA1*	Oxidative stress response
AT5G67300	*MYB44*	Oxidative stress response
AT1G01060	*LHY1*	Stress response
AT1G01520	*ASG4*	Stress response
AT1G01680	*PUB54*	Stress response
AT1G02820	*LEA3*	Stress response
AT1G03220	*NA*	Stress response
AT1G03230	*NA*	Stress response
AT1G03380	*ATG18G*	Stress response
AT1G03970	*GBF4*	Stress response
AT1G04440	*CKL13*	Stress response
AT1G07180	*NDA1*	Stress response
AT1G07720	*KCS3*	Stress response
AT1G08450	*PSL1*	Stress response
AT1G09080	*BIP3*	Stress response
AT1G09560	*PDGLP1*	Stress response
AT1G10920	*LOV1*	Stress response
AT1G11910	*ATAPA1*	Stress response
AT1G12200	*FMO*	Stress response
AT1G12210	*RFL1*	Stress response
AT1G12280	*SUMM2*	Stress response
AT1G15010	*NA*	Stress response
AT1G16110	*WAKL6*	Stress response
AT1G16130	*WAKL2*	Stress response
AT1G16850	*NA*	Stress response
AT1G17290	*AlaAT1*	Stress response
AT1G17600	*NA*	Stress response
AT1G17610	*CHS1*	Stress response
AT1G19210	*NA*	Stress response
AT1G19450	*NA*	Stress response
AT1G19660	*BBD2*	Stress response
AT1G20510	*OPCL1*	Stress response
AT1G22280	*PAPP2C*	Stress response
AT1G23120	*NA*	Stress response
AT1G23130	*NA*	Stress response
AT1G25560	*TEM1*	Stress response
AT1G28380	*NSL1*	Stress response
AT1G31540	*NA*	Stress response
AT1G31580	*ECS1*	Stress response
AT1G32920	*NA*	Stress response
AT1G33610	*NA*	Stress response
AT1G33960	*AIG1*	Stress response
AT1G35140	*EXL1*	Stress response
AT1G37130	*NR2*	Stress response
AT1G42470	*NA*	Stress response
AT1G49050	*NA*	Stress response
AT1G50180	*NA*	Stress response
AT1G51760	*IAR3*	Stress response
AT1G52690	*LEA7*	Stress response
AT1G53350	*NA*	Stress response
AT1G55920	*SAT1*	Stress response
AT1G56510	*WRR4*	Stress response
AT1G56520	*NA*	Stress response

AGI ID	Gene name	Biological Function
AT1G56540	*NA*	Stress response
AT1G57650	*NA*	Stress response
AT1G59620	*CW9*	Stress response
AT1G61190	*NA*	Stress response
AT1G63350	*NA*	Stress response
AT1G63360	*NA*	Stress response
AT1G63740	*NA*	Stress response
AT1G63750	*NA*	Stress response
AT1G64610	*NA*	Stress response
AT1G65800	*RK2*	Stress response
AT1G66090	*NA*	Stress response
AT1G66200	*GSR2*	Stress response
AT1G66980	*SNC4*	Stress response
AT1G67865	*NA*	Stress response
AT1G67970	*HSFA8*	Stress response
AT1G68740	*PHO1*	Stress response
AT1G69550	*NA*	Stress response
AT1G69850	*NTL1*	Stress response
AT1G70000	*NA*	Stress response
AT1G70660	*MMZ2*	Stress response
AT1G70890	*MLP43*	Stress response
AT1G71697	*CK1*	Stress response
AT1G72060	*NA*	Stress response
AT1G72890	*NA*	Stress response
AT1G72900	*NA*	Stress response
AT1G72910	*NA*	Stress response
AT1G72920	*NA*	Stress response
AT1G72930	*TN10*	Stress response
AT1G72940	*NA*	Stress response
AT1G73805	*SARD1*	Stress response
AT1G74450	*NA*	Stress response
AT1G74710	*SID2*	Stress response
AT1G76650	*CML38*	Stress response
AT1G77640	*NA*	Stress response
AT1G77760	*NR1*	Stress response
AT1G77920	*TGA7*	Stress response
AT1G78290	*SRK2C*	Stress response
AT1G78830	*NA*	Stress response
AT1G79900	*BAC2*	Stress response
AT1G80460	*GLI1*	Stress response
AT1G80820	*CCR2*	Stress response
AT2G01180	*PAP1*	Stress response
AT2G05940	*RIPK*	Stress response
AT2G14080	*NA*	Stress response
AT2G14960	*GH3.1*	Stress response
AT2G15080	*RLP19*	Stress response
AT2G15220	*NA*	Stress response
AT2G15480	*UGT73B5*	Stress response
AT2G16430	*PAP10*	Stress response
AT2G16870	*NA*	Stress response
AT2G17120	*LYP1*	Stress response
AT2G17480	*MLO8*	Stress response
AT2G18660	*PNP-A*	Stress response
AT2G20142	*NA*	Stress response
AT2G20340	*AAS*	Stress response
AT2G22240	*MIPS2*	Stress response
AT2G22300	*CAMTA3*	Stress response
AT2G24540	*AFR*	Stress response
AT2G25090	*SnRK3.18*	Stress response
AT2G25440	*RLP20*	Stress response
AT2G27500	*NA*	Stress response
AT2G27690	*CYP94C1*	Stress response
AT2G29110	*GLR2.8*	Stress response
AT2G30360	*CIPK11*	Stress response
AT2G30750	*CYP71A12*	Stress response
AT2G31865	*PARG2*	Stress response
AT2G31880	*OBIR1*	Stress response
AT2G32140	*NA*	Stress response

AGI ID	Gene name	Biological Function
AT2G32680	*RLP23*	Stress response
AT2G33550	*NA*	Stress response
AT2G33770	*UBC24*	Stress response
AT2G34930	*NA*	Stress response
AT2G35940	*EDA29*	Stress response
AT2G35960	*NHL12*	Stress response
AT2G37180	*RD28*	Stress response
AT2G37760	*AKR4C8*	Stress response
AT2G38170	*CAX1*	Stress response
AT2G39050	*EULS3*	Stress response
AT2G39210	*NA*	Stress response
AT2G40750	*WRKY54*	Stress response
AT2G40970	*MYBC1*	Stress response
AT2G41010	*CAMBP25*	Stress response
AT2G41100	*TCH3*	Stress response
AT2G42010	*PLDBETA1*	Stress response
AT2G43620	*NA*	Stress response
AT2G43710	*SSI2*	Stress response
AT2G45760	*BAP2*	Stress response
AT2G46440	*CNGC11*	Stress response
AT2G46450	*CNGC12*	Stress response
AT2G46830	*CCA1*	Stress response
AT2G47060	*PTI1-4*	Stress response
AT2G47130	*SDR3*	Stress response
AT2G48010	*RKF3*	Stress response
AT3G01290	*HIR2*	Stress response
AT3G01500	*SABP3*	Stress response
AT3G02360	*NA*	Stress response
AT3G03520	*NPC3*	Stress response
AT3G04210	*NA*	Stress response
AT3G06510	*SFR2*	Stress response
AT3G07700	*NA*	Stress response
AT3G07780	*OBE1*	Stress response
AT3G09600	*LCL5*	Stress response
AT3G09830	*NA*	Stress response
AT3G10800	*BZIP28*	Stress response
AT3G11010	*RLP34*	Stress response
AT3G11080	*RLP35*	Stress response
AT3G11480	*BSMT1*	Stress response
AT3G11660	*NHL1*	Stress response
AT3G12040	*NA*	Stress response
AT3G12360	*ITN1*	Stress response
AT3G13065	*SRF4*	Stress response
AT3G13100	*MRP7*	Stress response
AT3G13330	*PA200*	Stress response
AT3G13790	*ATCWINV1*	Stress response
AT3G14420	*GOX1*	Stress response
AT3G15353	*MT3*	Stress response
AT3G16460	*JAL34*	Stress response
AT3G17800	*NA*	Stress response
AT3G19550	*NA*	Stress response
AT3G19710	*BCAT4*	Stress response
AT3G20600	*NDR1*	Stress response
AT3G21150	*BBX32*	Stress response
AT3G21240	*4CL2*	Stress response
AT3G21890	*BBX31*	Stress response
AT3G22231	*PCC1*	Stress response
AT3G22460	*OASA2*	Stress response
AT3G22840	*ELIP*	Stress response
AT3G23000	*CIPK7*	Stress response
AT3G23110	*RLP37*	Stress response
AT3G23120	*RLP38*	Stress response
AT3G23430	*PHO1*	Stress response
AT3G24900	*RLP39*	Stress response
AT3G25010	*RLP41*	Stress response
AT3G25510	*NA*	Stress response
AT3G26170	*CYP71B19*	Stress response
AT3G26180	*CYP71B20*	Stress response

AGI ID	Gene name	Biological Function
AT3G26210	*CYP71B23*	Stress response
AT3G26230	*CYP71B24*	Stress response
AT3G26280	*CYP71B4*	Stress response
AT3G28270	*NA*	Stress response
AT3G28450	*NA*	Stress response
AT3G28890	*RLP43*	Stress response
AT3G29575	*AFP3*	Stress response
AT3G29670	*PMAT2*	Stress response
AT3G44260	*CAF1a*	Stress response
AT3G44400	*NA*	Stress response
AT3G44480	*RPP1*	Stress response
AT3G44630	*NA*	Stress response
AT3G44670	*NA*	Stress response
AT3G44880	*ACD1*	Stress response
AT3G45290	*MLO3*	Stress response
AT3G46530	*RPP13*	Stress response
AT3G47090	*NA*	Stress response
AT3G47570	*NA*	Stress response
AT3G48080	*NA*	Stress response
AT3G48520	*CYP94B3*	Stress response
AT3G48990	*AAE3*	Stress response
AT3G50470	*MLA10*	Stress response
AT3G50740	*UGT72E1*	Stress response
AT3G50840	*NA*	Stress response
AT3G50950	*ZAR1*	Stress response
AT3G51240	*TT6*	Stress response
AT3G53810	*LecRK-IV.2*	Stress response
AT3G54420	*EP3*	Stress response
AT3G54950	*PLP7*	Stress response
AT3G55840	*NA*	Stress response
AT3G55880	*SUE4*	Stress response
AT3G56710	*SIB1*	Stress response
AT3G57240	*BG3*	Stress response
AT3G57330	*ACA11*	Stress response
AT3G57520	*SIP2*	Stress response
AT3G59060	*PIL6*	Stress response
AT3G59700	*LECRK1*	Stress response
AT3G61060	*PP2-A13*	Stress response
AT3G61220	*SDR1*	Stress response
AT4G00970	*CRK41*	Stress response
AT4G01070	*UGT72B1*	Stress response
AT4G02420	*LecRK-IV.4*	Stress response
AT4G02520	*GSTF2*	Stress response
AT4G03460	*NA*	Stress response
AT4G04020	*PGL35*	Stress response
AT4G04500	*CRK37*	Stress response
AT4G04510	*CRK38*	Stress response
AT4G04570	*CRK40*	Stress response
AT4G04830	*MSRB5*	Stress response
AT4G10270	*NA*	Stress response
AT4G12000	*NA*	Stress response
AT4G13810	*RLP47*	Stress response
AT4G13830	*DJC26*	Stress response
AT4G13920	*RLP50*	Stress response
AT4G14370	*NA*	Stress response
AT4G17250	*NA*	Stress response
AT4G19520	*NA*	Stress response
AT4G19840	*PP2-A1*	Stress response
AT4G20830	*NA*	Stress response
AT4G21380	*RK3*	Stress response
AT4G23160	*CRK8*	Stress response
AT4G23180	*CRK10*	Stress response
AT4G23220	*CRK14*	Stress response
AT4G23230	*CRK15*	Stress response
AT4G23320	*CRK24*	Stress response
AT4G23600	*CORI3*	Stress response
AT4G23680	*NA*	Stress response
AT4G25110	*MC2*	Stress response

AGI ID	Gene name	Biological Function
AT4G25470	*CBF2*	Stress response
AT4G26090	*RPS2*	Stress response
AT4G26160	*ACHT1*	Stress response
AT4G26850	*VTC2*	Stress response
AT4G30440	*GAE1*	Stress response
AT4G31000	*NA*	Stress response
AT4G31390	*PGR6*	Stress response
AT4G32770	*VTE1*	Stress response
AT4G33300	*ADR1-L1*	Stress response
AT4G34131	*UGT73B3*	Stress response
AT4G34150	*NA*	Stress response
AT4G34180	*NA*	Stress response
AT4G35985	*NA*	Stress response
AT4G36040	*J11*	Stress response
AT4G36990	*TBF1*	Stress response
AT4G37150	*MES9*	Stress response
AT4G37310	*CYP81H1*	Stress response
AT4G37320	*CYP81D5*	Stress response
AT4G38740	*ROC1*	Stress response
AT5G01840	*OFP1*	Stress response
AT5G02020	*SIS*	Stress response
AT5G02490	*Hsp70-2*	Stress response
AT5G03210	*DIP2*	Stress response
AT5G03545	*ATIPS2*	Stress response
AT5G04720	*PHX21*	Stress response
AT5G05110	*NA*	Stress response
AT5G06320	*NHL3*	Stress response
AT5G06860	*PGIP1*	Stress response
AT5G06870	*PGIP2*	Stress response
AT5G07440	*GDH2*	Stress response
AT5G09440	*EXL4*	Stress response
AT5G09590	*MTHSC70-2*	Stress response
AT5G09990	*PROPEP5*	Stress response
AT5G10300	*MES5*	Stress response
AT5G10760	*NA*	Stress response
AT5G11250	*NA*	Stress response
AT5G13160	*PBS1*	Stress response
AT5G13320	*WIN3*	Stress response
AT5G13930	*TT4*	Stress response
AT5G14200	*IMD1*	Stress response
AT5G14780	*FDH*	Stress response
AT5G15450	*CLPB3*	Stress response
AT5G15850	*COL1*	Stress response
AT5G16910	*CSLD2*	Stress response
AT5G17000	*NA*	Stress response
AT5G17050	*UGT78D2*	Stress response
AT5G18360	*NA*	Stress response
AT5G22250	*CAF1b*	Stress response
AT5G24770	*VSP2*	Stress response
AT5G24780	*VSP1*	Stress response
AT5G25120	*CYP71B11*	Stress response
AT5G25130	*CYP71B12*	Stress response
AT5G25140	*CYP71B13*	Stress response
AT5G25250	*FLOT1*	Stress response
AT5G25610	*RD22*	Stress response
AT5G26030	*FC1*	Stress response
AT5G26920	*CBP60G*	Stress response
AT5G35450	*NA*	Stress response
AT5G40170	*RLP54*	Stress response
AT5G41550	*NA*	Stress response
AT5G41740	*NA*	Stress response
AT5G41750	*NA*	Stress response
AT5G44070	*PCS1*	Stress response
AT5G45380	*DUR3*	Stress response
AT5G45440	*NA*	Stress response
AT5G45490	*NA*	Stress response
AT5G46260	*NA*	Stress response
AT5G46270	*NA*	Stress response

AGI ID	Gene name	Biological Function
AT5G46830	*NIG1*	Stress response
AT5G48380	*BIR1*	Stress response
AT5G48620	*NA*	Stress response
AT5G49480	*CP1*	Stress response
AT5G49660	*XIP1*	Stress response
AT5G52250	*RUP1*	Stress response
AT5G52300	*RD29B*	Stress response
AT5G53120	*SPDS3*	Stress response
AT5G54110	*MAMI*	Stress response
AT5G54730	*G18F*	Stress response
AT5G57685	*LSB1*	Stress response
AT5G58120	*NA*	Stress response
AT5G59220	*SAG113*	Stress response
AT5G59310	*LTP4*	Stress response
AT5G59320	*LTP3*	Stress response
AT5G61640	*PMSR1*	Stress response
AT5G62570	*CBP60a*	Stress response
AT5G63020	*NA*	Stress response
AT5G65010	*ASN2*	Stress response
AT5G67450	*ZF1*	Stress response
ATCG00420	*NDHJ*	Stress response
AT1G18570	*MYB51*	Stress response
AT1G29340	*PUB17*	Stress response
AT1G29690	*CAD1*	Stress response
AT2G02220	*PSKR1*	Stress response
AT3G11650	*NHL2*	Stress response
AT3G16030	*RFO3*	Stress response
AT5G45110	*NPR3*	Stress response

Genes highlighted with green colour have been found to be involved during the senescence process identified using Araport. but the function of these genes have not been characterised yet.

APPENDIX 2. SOIL BASED PHENOTYPIC ANALYSIS FOR GROWTH STAGES OF L*er*-0, *old13* and *old14* IN LONG-DAYS

		L*er*-0		*old13*		*old14*	
PRINCIPAL GROWTH STAGE 1	LEAF DEVELOPMENT	[1]DAYS	SD	DAYS	SD	DAYS	SD
1.02	1 and 2 rosette leaves	1	0	1	0	1	0
1.03	3 and 4 rosette leaves	6	0.717	6	0.804	6	0.804
1.04	5 and 6 rosette leaves	10	0.872	10	0.804	10	0.872
1.05	7 rosette leaves	12	0.462	14	0.483	14	0.497
1.06	8 rosette leaves	15	0.436	16	0.402	16	0.402
1.07	9 rosette leaves	16	0.402	17	0.358	17	0.402
1.08	10 rosette leaves	18	0.402	19	0.462	19	0.436
1.09	11 rosette leaves	19	0.358	20	0.402	20	0.436
1.10	12 rosette leaves	21	0.358	22	0.300	22	0.402
1.11	13 rosette leaves	22	0.358	23	0.218	23	0.402
1.12	14 rosette leaves	24	0.358	25	0.497	25	0.218
1.13	15 rosette leaves	25	0.462	26	0.804	26	0.636
1.14	16 rosette leaves	27	0.218	28	0.218	28	0.300
PRINCIPAL GROWTH STAGE 5	INFLORESENCE EMERGENCE						
5.1	First flower bud visible	28	0.413	26	0.418	29	0.462
PRINCIPAL GROWTH STAGE 6	FLOWER PRODUCTION						
6	First flower open	30	0.366	29	0.315	32	0.412
6.1	10% of flowers open	39	0.321	38	0.387	40	0.345
6.2	20% of flowers open	42	0.219	41	0.401	45	0.329

1 Days after germination, SD- Standard deviation. Seeds were stratified at 4°C to synchronize germination. Plants were grown on seed-raising soil mix, under a long-day photo period (16 light: 8 dark) at 21°C with 65% relative humidity. Rosette leaf emergence, inflorescence and flowering time was recorded as the number of days after germination (DAG).

APPENDIX 3. SOIL BASED PHENOTYPIC ANALYSIS FOR GROWTH STAGES OF L*er*-0, *old13* and *old14* IN SHORT-DAYS

		***Ler*-0**		***old13***		***old14***	
PRINCIPAL GROWTH STAGE 1	LEAF DEVELOPMENT	[1]DAYS	SD	DAYS	SD	DAYS	SD
1.02	1 and 2 rosette leaves	1	0	1	0	1	0
1.03	3 and 4 rosette leaves	8	0.615	8	0.820	8	0.732
1.04	5 and 6 rosette leaves	13	0.888	13	0.732	13	0.447
1.05	7 rosette leaves	16	0.300	18	0.218	18	0.436
1.06	8 rosette leaves	19	0.332	20	0.437	21	0.392
1.07	9 rosette leaves	21	0.410	22	0.307	23	0.366
1.08	10 rosette leaves	22	0.358	24	0.402	25	0.300
1.09	11 rosette leaves	24	0.402	25	0.218	26	0.358
1.10	12 rosette leaves	25	0.436	27	0.402	28	0.402
1.11	13 rosette leaves	27	0.470	28	0.307	30	0.410
1.12	14 rosette leaves	28	0.410	30	0.315	31	0.392
1.13	15 rosette leaves	30	0.300	31	0.462	32	0.402
1.14	16 rosette leaves	31	0.410	32	0.307	33	0.366
PRINCIPAL GROWTH STAGE 5	INFLORESENCE EMERGENCE						
5.1	First flower bud visible	69	0.582	65	0.494	74	0.502
PRINCIPAL GROWTH STAGE 6	FLOWER PRODUCTION						
6	First flower open	76	0.218	72	0.306	82	0.282
6.1	10% of flowers open	81	0.804	77	0.497	87	0.402
6.2	20% of flowers open	85	0.462	81	0.218	90	0.358

[1] Days after germination, SD- Standard deviation. Seeds were stratified at 4°C to synchronize germination. Plants were grown on seed-raising soil mix, under a short-day photo period (8 light: 16dark) at 21°C with 65% relative humidity. Rosette leaf emergence, inflorescence and flowering time was recorded as the number of days after germination (DAG).

Appendix 4. The log_2 values of carbohydrate metabolite content quantified by GC-MS in *old13* leaf samples.

Carbohydrates	*old13*-10 DAG	*old13*-15 DAG	*old13*-20 DAG
Fructose	-0.884	-0.170	1.747
Fucose	-0.413	-0.276	1.040
Galactinol	-	0.983	1.324
Glucose, 1,6-anhydro, beta-	0.680	-0.568	0.021
Glucose	-0.795	-0.404	-0.367
Glycerol	-1.266	0.344	-0.564
Inositol, myo-	0.086	-0.509	0.076
Maltose	0.145	-1.005	-2.682
Mannose	0.099	0.409	-0.126
Raffinose	-	1.637	0.427
Sucrose	0.220	-0.222	0.310
Sugar(Glucoso_6_phosph)	0.173	0.120	1.186
Sugar 1	-1.177	-1.160	-0.425
Sugar 2	-0.367	0.029	0.558
Sugar 3	-0.760	-0.776	-0.524
Sugar 4	0.455	-0.920	0.217
Sugar 5	-0.511	-0.064	0.733
Sugar 6	-0.954	-0.690	-0.209
Sugar 7	0.027	-0.414	-0.219
Sugar 8 (Galactose or Manitol)	-0.833	0.008	-0.151
Sugar 9 (Galactose or Manitol)	-0.874	-0.485	0.238
Threitol	-0.358	-0.718	-1.075
Trehalose, alpha,alpha	0.080	-0.964	-0.219

Red colour represents maximum value, green minimum value and white represent intermediate values. DAG-Days after germination.

Appendix 5. List of SNPs in *old13* whole genome identified by NIKS.

Chromosome	SNP position	Ref.	SNP	Gene ID and description
Chr.1	1520915	A	T	Non-coding DNA
Chr.1	2726252	G	A	AT1G08600
Chr.1	4768335	A	C	Non-coding DNA
Chr.1	13705544	C	T	Non-coding DNA
Chr.1	14067551	G	A	Transposable element gene
Chr.1	14067576	A	G	Transposable element gene
Chr.1	15371093	G	A	Non-coding DNA
Chr.1	15880474	T	A	Transposable element gene
Chr.1	18165283	G	A	Non-coding DNA
Chr.1	18557833	G	A	Non-coding DNA
Chr.1	19449881	C	T	Non-coding DNA
Chr.1	19466625	G	A	Non-coding DNA
Chr.1	19493297	G	A	AT1G53160 (Squamosa promoter-binding-like protein 4)
Chr.1	19784765	G	A	AT1G53840 (Pectinesterase 1)
Chr.1	20092823	G	A	AT1G54680 (unknown protein)
Chr.1	20129992	G	A	AT1G54820 (Protein kinase superfamily protein)
Chr.1	20146567	G	A	Non-coding DNA
Chr.1	20185083	G	A	AT1G54970 (Proline-rich protein 1)
Chr.1	20252046	G	A	AT1G55140 (Ribonuclease III family protein)
Chr.1	20641976	G	A	AT1G56050 (GTP-binding protein-related)
Chr.1	20698421	G	A	Non-coding DNA
Chr.1	21797692	G	A	AT1G60072 (MIR859a; miRNA)
Chr.1	22108988	G	A	AT1G60990 (Glycine cleavage T-protein family)
Chr.1	22384939	G	A	AT1G61630 (Equilibrative nucleotide transporter 7)
Chr.1	22413204	G	A	AT1G61680 (S-(+)-linalool synthase, chloroplastic)
Chr.1	22427378	G	A	AT1G61700 (DNA-directed RNA polymerase subunit 10-like)
Chr.1	22559727	G	A	AT1G62020 (Coatomer subunit alpha-1)
Chr.2	1976918	T	C	Non-coding DNA
Chr.2	1977022	T	A	Non-coding DNA
Chr.2	2562792	T	C	AT2G06645 (unknown protein)
Chr.2	3758313	T	C	AT2G10170 (transposable element gene)
Chr.2	4818349	T	C	AT2G12305 (transposable element gene)
Chr.2	4818721	C	G	AT2G12305 (transposable element gene)
Chr.2	5173554	T	C	Non-coding DNA
Chr.2	5344466	T	C	Non-coding DNA
Chr.2	5498605	A	G	Non-coding DNA
Chr.2	6096504	T	A	AT2G14650 (transposable element gene)
Chr.2	7857042	A	C	Non-coding DNA
Chr.2	9933748	G	A	Non-coding DNA

Chr.2	10295311	C	T	Non-coding DNA
Chr.2	17468632	G	A	AT2G42810 (Serine/threonine-protein phosphatase 5)
Chr.2	17979514	C	T	AT2G44380 (Cysteine/Histidine-rich C1 domain family protein)
Chr.2	18160730	A	T	AT2G44890 (cytochrome P450, family 704, subfamily A)
Chr.2	18816775	A	T	Non-coding DNA
Chr.3	1308258	G	A	Non-coding DNA
Chr.3	9472515	G	A	AT3G26040 (HXXXD-type acyl-transferase family protein)
Chr.3	9721764	G	A	AT3G26600 (armadillo repeat only 4)
Chr.3	9873842	G	A	Non-coding DNA
Chr.3	9934347	G	A	Non-coding DNA
Chr.3	10225944	G	A	Non-coding DNA
Chr.3	10519825	G	A	AT3G28345 (ABC transporter B family member 15)
Chr.3	10588069	G	A	Non-coding DNA
Chr.3	10927914	G	A	AT3G29032 (Transposable element gene)
Chr.3	10955859	G	A	AT3G29070 (Transmembrane emp24 domain containing protein)
Chr.3	11074266	A	G	AT3G29210 (Transposable element gene)
Chr.3	11165922	G	A	Non-coding DNA
Chr.3	11192335	G	A	AT3G29400 (Exocyst subunit exo70 family protein)
Chr.3	11281059	G	A	Non-coding DNA
Chr.3	11281964	G	A	Non-coding DNA
Chr.3	11539226	G	A	Non-coding DNA
Chr.3	11761579	G	A	Non-coding DNA
Chr.3	11881444	T	G	AT3G30413 (transposable element gene)
Chr.3	12006477	C	T	AT3G30570 (transposable element gene)
Chr.3	12138183	G	A	Non-coding DNA
Chr.3	12598821	G	A	Transposable element gene
Chr.3	12774985	C	T	AT3G31945 (Transposable element gene)
Chr.3	12817103	T	C	AT3G32010 (Transposable element gene)
Chr.3	12833349	A	G	AT3G32022 (Transposable element gene)
Chr.3	12833398	T	C	AT3G32022 (Transposable element gene)
Chr.3	12951230	G	C	AT3G32118 (Transposable element gene)
Chr.3	13128863	T	G	Non-coding DNA
Chr.3	13359737	C	G	Non-coding DNA
Chr.3	13359742	A	T	Non-coding DNA
Chr.3	13359753	A	T	Non-coding DNA
Chr.3	13359843	G	A	Non-coding DNA
Chr.3	13360139	G	C	AT3G33000 (pseudogene, ATP synthase A subunit)
Chr.3	13360160	A	G	AT3G33000 (pseudogene, ATP synthase A subunit)
Chr.3	13360200	A	G	AT3G33000 (pseudogene, ATP synthase A subunit)
Chr.3	13360207	T	G	AT3G33000 (pseudogene, ATP synthase A subunit)
Chr.3	13360242	A	G	AT3G33000 (pseudogene, ATP synthase A subunit)
Chr.3	13360247	T	A	AT3G33000 (pseudogene, ATP synthase A subunit)
Chr.3	13360256	G	C	AT3G33000 (pseudogene, ATP synthase A subunit)

Chr.3	13360357	A	G	AT3G33000 (pseudogene, ATP synthase A subunit)
Chr.3	13360358	A	G	AT3G33000 (pseudogene, ATP synthase A subunit)
Chr.3	13360396	A	G	AT3G33000 (pseudogene, ATP synthase A subunit)
Chr.3	13360476	T	C	AT3G33000 (pseudogene, ATP synthase A subunit)
Chr.3	13360478	T	C	AT3G33000 (pseudogene, ATP synthase A subunit)
Chr.3	13360546	T	C	AT3G33000 (pseudogene, ATP synthase A subunit)
Chr.3	13360563	A	G	AT3G33000 (pseudogene, ATP synthase A subunit)
Chr.3	13360597	T	G	AT3G33000 (pseudogene, ATP synthase A subunit)
Chr.3	13360600	C	A	AT3G33000 (pseudogene, ATP synthase A subunit)
Chr.3	13360621	C	T	AT3G33000 (pseudogene, ATP synthase A subunit)
Chr.3	13360641	G	A	AT3G33000 (pseudogene, ATP synthase A subunit)
Chr.3	13360669	A	G	AT3G33000 (pseudogene, ATP synthase A subunit)
Chr.3	13360802	A	C	Non-coding DNA
Chr.3	13360811	T	C	Non-coding DNA
Chr.3	13360838	T	C	Non-coding DNA
Chr.3	13360888	A	G	Non-coding DNA
Chr.3	13360963	T	A	Non-coding DNA
Chr.3	13361131	C	A	AT3G33002 (pseudogene)
Chr.3	13361194	A	G	AT3G33002 (pseudogene)
Chr.3	13361884	A	G	AT3G33004 (pseudogene)
Chr.3	13362281	G	A	AT3G33004 (pseudogene)
Chr.3	13363544	C	A	AT3G33004 (pseudogene)
Chr.3	13363555	A	G	AT3G33004 (pseudogene)
Chr.3	13363556	G	A	AT3G33004 (pseudogene)
Chr.3	13363574	G	T	AT3G33004 (pseudogene)
Chr.3	13363579	A	C	AT3G33004 (pseudogene)
Chr.3	13363583	C	T	AT3G33004 (pseudogene)
Chr.3	13363601	T	G	AT3G33004 (pseudogene)
Chr.3	13363727	T	C	AT3G33004 (pseudogene)
Chr.3	13363762	C	T	AT3G33004 (pseudogene)
Chr.3	13363796	G	C	AT3G33004 (pseudogene)
Chr.3	13448427	T	A	Non-coding DNA
Chr.3	13895716	C	T	Non-coding DNA
Chr.3	14133416	G	A	Non-coding DNA
Chr.3	14365840	T	C	Non-coding DNA
Chr.3	14502288	G	A	Non-coding DNA
Chr.3	14660358	C	T	Non-coding DNA
Chr.3	14742020	G	A	Non-coding DNA
Chr.3	14806879	G	A	AT3G42993 (Transposable element gene)
Chr.3	14885997	G	A	Non-coding DNA
Chr.3	15354806	G	A	AT3G43726 (transposable element gene)
Chr.3	15469162	A	T	Non-coding DNA
Chr.3	15474733	G	A	Non-coding DNA

Chr.3	15716411	G	A	Non-coding DNA
Chr.3	16210814	G	A	Non-coding DNA
Chr.3	16216759	G	A	AT3G45190
Chr.3	16378522	G	A	Ring U-box protein with C6HC type zinc finger
Chr.3	16389135	T	C	Non-coding DNA
Chr.3	16776757	T	A	AT3G46487 (transposable element gene)
Chr.3	16776831	C	A	AT3G46487 (transposable element gene)
Chr.3	16776927	C	G	AT3G46487 (transposable element gene)
Chr.3	16776928	A	T	AT3G46487 (transposable element gene)
Chr.3	16849723	G	A	Non-coding DNA
Chr.3	16906961	G	A	Non-coding DNA
Chr.3	17038502	G	A	Non-coding DNA
Chr.3	17453575	G	A	Non-coding DNA
Chr.3	17720426	G	A	Cyclin dependent kinase
Chr.3	17940091	G	A	AT3G49350 (Ypt/Rab-GAP domain of gyp1p superfamily)
Chr.3	17962579	G	A	Transducin/WD40 repeat like superfamily protein
Chr.3	18032595	G	A	AT3G49610 (Putative B3 domain containing protein)
Chr.4	2806723	T	C	AT4G05585 (transposable element gene)
Chr.4	2893050	G	T	AT4G05612 (unknown protein)
Chr.4	3139113	G	C	Non-coding DNA
Chr.4	3182555	C	T	Non-coding DNA
Chr.4	3316366	G	A	AT4G06546 (transposable element gene)
Chr.4	3344195	G	A	Non-coding DNA
Chr.4	3353188	T	C	AT4G06550 (transposable element gene)
Chr.4	3579750	G	A	AT4G06599 (Ubiquitin-like domain-containing CTD)
Chr.4	4618097	T	C	AT4G07947 (transposable element gene)
Chr.4	4618099	A	T	AT4G07947 (transposable element gene)
Chr.4	4618101	C	T	AT4G07947 (transposable element gene)
Chr.4	4618105	T	A	AT4G07947 (transposable element gene)
Chr.4	4618106	C	A	AT4G07947 (transposable element gene)
Chr.4	4707449	G	A	Non-coding DNA
Chr.4	4850796	G	A	AT4G08105 (transposable element gene)
Chr.4	5124124	G	A	AT4G08370 (Proline-rich extensin-like family protein)
Chr.4	5124127	T	G	AT4G08370 (Proline-rich extensin-like family protein)
Chr.4	5152252	G	A	Non-coding DNA
Chr.4	5265037	G	A	Non-coding DNA
Chr.4	5712256	T	A	Non-coding DNA
Chr.4	13934685	T	G	AT4G28970 (transposable element gene)
Chr.4	14051734	G	A	AT4G29210 (Gamma-glutamyltranspeptidase 3)
Chr.4	14334724	G	A	Non-coding DNA
Chr.4	14401017	G	A	Non-coding DNA
Chr.4	17893252	T	A	AT4G39180 (Phosphatidylinositol transfer protein SFH2)
Chr.5	53525	C	T	AT5G01150 (Protein of unknown function)

Chr.5	135360	C	T	AT5GO1350
Chr.5	213580	C	T	AT5GO1590 (Protein TIC, 56 Chloroplastic)
Chr.5	765716	G	A	AT5G03270 (lysine decarboxylase family protein)
Chr.5	945490	G	A	Non-coding DNA
Chr.5	1062072	G	A	AT5G04000 (Unknown protein)
Chr.5	1111618	G	A	Non-coding DNA
Chr.5	1238518	G	A	AT5G04440 (Unknown protein)
Chr.5	1446169	G	A	AT5G04970 (Probable pectinesterase/pectinesterase inhibitor 47)
Chr.5	1483088	G	A	Non-coding DNA
Chr.5	1510545	G	A	AT5G05160 (Probable leucine-rich repeat receptor-like protein)
Chr.5	1510553	G	A	AT5G05160 (Probable leucine-rich repeat receptor-like protein)
Chr.5	1748334	C	T	AT5G05880 (UDP-glycosyltransferase 76C4)
Chr.5	1879817	C	T	Non-coding DNA
Chr.5	2148027	C	T	AT5G07000 (Cytosolic sulfotransferase 14)
Chr.5	2258546	C	T	AT5G07270 (E3 ubiquitin-protein ligase XBAT33)
Chr.5	2274437	C	T	AT5G07290 (Protein MEI2-like 4)
Chr.5	2473691	C	T	AT5G07810 (SNF2 domain-containing protein)
Chr.5	2493388	C	T	AT5G07890 (myosin heavy chain-related)
Chr.5	2493952	C	T	AT5G07890 (myosin heavy chain-related)
Chr.5	2529339	C	T	AT5G07980 (dentin sialophosphoprotein-related)
Chr.5	2704036	C	T	AT5G08450 (Histone deacetylation protein Rxt3)
Chr.5	2732642	C	T	AT5G08520 (Duplicated homeodomain-like superfamily protein)
Chr.5	2733564	C	T	AT5G08520 (Duplicated homeodomain-like superfamily protein)
Chr.5	2750181	C	T	Non-coding DNA
Chr.5	2860157	C	T	AT5G09300 (2-oxoisovalerate dehydrogenase subunit alpha 2)
Chr.5	2920834	C	T	AT5G09460
Chr.5	2929931	C	T	AT5G09500 (40S ribosomal protein S15-3)
Chr.5	2934963	C	T	AT5G09530 (hydroxyproline-rich glycoprotein family protein)
Chr.5	2947857	C	T	AT5G09580 (Heat shock protein)
Chr.5	3073868	C	T	AT5G09930 (ABC transporter F family member 2)
Chr.5	3189224	C	T	AT5G10240
Chr.5	3246413	C	T	Non-coding DNA
Chr.5	3286091	C	T	Non-coding DNA
Chr.5	3288806	C	T	Non-coding DNA
Chr.5	3454121	C	T	AT5G11000 (Plant protein of unknown function)
Chr.5	3672903	C	T	AT5G11530 (Protein EMBRYONIC FLOWER)
Chr.5	3679617	C	T	AT5G11540 (L-gulonolactone oxidase 3)
Chr.5	3813196	C	T	Non-coding DNA
Chr.5	3893874	C	T	AT5G12130
Chr.5	3952231	C	T	AT5G12290 (dgd1 suppressor 1)
Chr.5	4057325	C	T	AT5G12930 (unknown protein)
Chr.5	4061832	C	T	Non-coding DNA
Chr.5	4103537	C	T	AT5G13020 (Protein EMSY-LIKE 3)

Chr.5	4317921	C	T	AT5G13530 (E3 ubiquitin-protein ligase KEG)
Chr.5	4373795	C	T	AT5G13670 (WAT1-related protein)
Chr.5	4537496	C	T	AT5G14180 (Triacylglycerol lipase 2)
Chr.5	4580721	C	T	AT5G14310 (Probable carboxylesterase 16)
Chr.5	4658359	C	T	AT5G14550
Chr.5	5236262	C	T	AT5G15140 (Chloroplastic group IIB intron splicing facilitator)
Chr.5	5303979	C	T	AT5G16300 (Vps51/Vps67 family)
Chr.5	6253125	C	T	AT5G18900 (Probable prolyl 4-hydroxylase 4)
Chr.5	6637828	C	T	AT5G19810 (Proline-rich extensin-like family protein)
Chr.5	6649630	C	T	AT5G19840 (2-oxoglutarate (2OG) and Fe(II)-dependent)
Chr.5	7604326	G	A	Non-coding DNA
Chr.5	7632546	G	A	AT5G23000 (Transcription factor RAX1)
Chr.5	7705729	G	A	AT5G23110 (Zinc finger, C3HC4 type)
Chr.5	7768055	G	A	AT5G23260 (Protein TRANSPARENT TESTA 16)
Chr.5	7812152	G	A	AT5G23400 (Leucine-rich repeat (LRR) family protein)
Chr.5	10119953	A	T	AT5G28270 (transposable element gene)
Chr.5	10993705	A	G	AT5G29075 (transposable element gene)
Chr.5	10993826	T	C	AT5G29075 (transposable element gene)
Chr.5	10993847	A	G	AT5G29075 (transposable element gene)
Chr.5	10993850	G	T	AT5G29075 (transposable element gene)
Chr.5	11094005	T	A	Non-coding DNA
Chr.5	11180963	T	C	AT5G30102 (transposable element)
Chr.5	11180964	A	G	AT5G30102 (transposable element)
Chr.5	11577003	G	A	Non-coding DNA
Chr.5	11577080	T	C	Non-coding DNA
Chr.5	11577178	T	C	AT5G31855 (transposable element gene)
Chr.5	11933780	A	C	AT5G32486 (transposable element gene)
Chr.5	12180674	A	G	AT5G32925 (transposable element gene)
Chr.5	12317971	G	A	Non-coding DNA
Chr.5	12500265	A	G	AT5G33422 (transposable element gene)
Chr.5	12762612	T	G	Non-coding DNA
Chr.5	13696172	A	G	AT5G35794 (transposable element gene)
Chr.5	14106542	T	A	AT5G36320 (ECA1 gametogenesis related family protein)
Chr.5	14553679	C	T	Non-coding DNA
Chr.5	15265330	G	A	AT5G38920 (Polynucleotidyl transferase)

Chr. = Chromosome number, SNP position= position of altered base pair in L*er*-0 reference sequence, Ref. = base pair in reference sequence, SNP= single nucleotide polymorphism in *old13*.

Appendix 6. Primer sequences of gene markers used for expression analysis

Gene name	AGI	Forward (5'-3')	Reverse (5'-3')
RBOHD	AT5G47910	CCACTCGTGTGGGACGATATTC	ACGACACCAAGTGGTTCAGAAATG
WRKY53	AT4G23810	CTGTTGCTGAGACTAACGAGAT	CCTCCATCGGCAAACTCTT
SAG13	AT2G29350	CTTGTCACTGGTGGCTCTAA	CAGTTTCCATGAGTTTCACTCG
FSD3	AT5G23310	CCACTCGTGTGGGACGATATTC	ACGACACCAAGTGGTTCAGAAATG
SOD1	AT1G08830	GCAGTGAGGGTGTTACG	CAGTAGACATGCAACCGTTAGT
UPL7	AT3G53090	TTCAAATACTTGCAGCCAACCTT	CCCAAAGAGAGGTATCACAAGAGACT
ACTIN2	AT3G18780	TCCCTCAGCACATTCCAGCACAT	AACGATTCCTGGACCTGCCTCATC
TUB2	AT5G62690	GCCAATCCGGTGCTGGTAACA	CATACCAGATCCAGTTCCTCCTCCC
RPS18	ATCG00650	CTAGACGGGTGAATAGAGTGAC	CTGGTTCTAAGACTAGTAGTTC
GI	AT1G22770	CCACGAGATCCTCAACAAC	CAACGAGCCATCAATAAGAC

Appendix 7.

DRC 16

MASSEY UNIVERSITY
GRADUATE RESEARCH SCHOOL

STATEMENT OF CONTRIBUTION TO DOCTORAL THESIS CONTAINING PUBLICATIONS

(To appear at the end of each thesis chapter/section/appendix submitted as an article/paper or collected as an appendix at the end of the thesis)

We, the candidate and the candidate's Principal Supervisor, certify that all co-authors have consented to their work being included in the thesis and they have accepted the candidate's contribution as indicated below in the *Statement of Originality*.

Name of Candidate: Aakansha Kanojia

Name/Title of Principal Supervisor: Dr Paul Dijkwel

Name of Published Research Output and full reference:

Annual Plant Reviews. Abiotic stress responses are governed by reactive oxygen species and age.

In which Chapter is the Published Work: Chapter 1

Please indicate either:

- The percentage of the Published Work that was contributed by the candidate: 60%

  and / or
- Describe the contribution that the candidate has made to the Published Work:

  Designed concepts, developed ideas, wrote manuscript,

Aakansha Kanojia Digitally signed by Aakansha Kanojia Date: 2018.02.18 00:06:12 +13'00'

Candidate's Signature

18/02/2018

Date

Paul Dijkwel Digitally signed by Paul Dijkwel Date: 2018.02.23 13:17:56 +13'00'

Principal Supervisor's signature

23/2/2018

Date

GRS Version 3– 16 September 2011

MASSEY UNIVERSITY
GRADUATE RESEARCH SCHOOL

STATEMENT OF CONTRIBUTION
TO DOCTORAL THESIS CONTAINING PUBLICATIONS

(To appear at the end of each thesis chapter/section/appendix submitted as an article/paper or collected as an appendix at the end of the thesis)

We, the candidate and the candidate's Principal Supervisor, certify that all co-authors have consented to their work being included in the thesis and they have accepted the candidate's contribution as indicated below in the *Statement of Originality*.

Name of Candidate: Aakansha Kanojia

Name/Title of Principal Supervisor: Dr Paul Dijkwel

Name of Published Research Output and full reference:

Springer protocols.
Identification of Postharvest Senescence Regulators Through Map-Based Cloning Using Detached Arabidopsis Inflorescences as a Model Tissue. In: Guo Y. (eds) Plant Senescence. Methods in Molecular Biology, vol 1744. Humana Press, New York, NY. DOI https://doi.org/10.1007/978-1-4939-7672-0_17

In which Chapter is the Published Work: Chapter 6

Please indicate either:

- The percentage of the Published Work that was contributed by the candidate:

  and / or

- Describe the contribution that the candidate has made to the Published Work:

  A protocol optimized for the isolation of high-quality nuclear enriched genomic DNA from Arabidopsis leaves is added to the published work.

Aakansha Kanojia Digitally signed by Aakansha Kanojia Date: 2018.02.18 00:25:25 +13'00'
Candidate's Signature

18/02/2018
Date

Paul Dijkwel Digitally signed by Paul Dijkwel Date: 2018.02.23 13:13:58 +13'00'
Principal Supervisor's signature

23/2/2018
Date

Bibliography

Aarts, M.G., Keijzer, C.J., Stiekema, W.J and Pereira, A. 1995. Molecular Characterization of the *CER1* Gene of Arabidopsis Involved in Epicuticular Wax Biosynthesis and Pollen Fertility. *The Plant Cell* **7**:2115–27.

Abdel Latef, A.A and Tran, L.S. 2016. Impacts of Priming with Silicon on the Growth and Tolerance of Maize Plants to Alkaline Stress. *Frontiers in Plant Science* **7**:243.

Abogadallah, G.M. 2010. Antioxidative Defense under Salt Stress. *Plant Signaling and Behavior* **5**:369–74.

Abram, N.J. et al., 2016. Early Onset of Industrial-Era Warming across the Oceans and Continents. *Nature* **536**:411–18.

Afzal, I. et al., 2011. Enhancement of Antioxidant Defense System Induced by Hormonal Priming in Wheat. *Cereal Research Communications* **39**:334–42.

Alberts, Bruce et al., 2002. *Molecular Biology of the Cell. Annals of Botany* **91**:401.

Alonso, J.M. and Joseph R.E. 2006. Moving Forward in Reverse: Genetic Technologies to Enable Genome-Wide Phenomic Screens in Arabidopsis. *Nature Reviews. Genetics* **7**:524–36.

Antoniou, C. et al., 2017. Melatonin Systemically Ameliorates Drought Stress-Induced Damage in *Medicago Sativa* Plants by Modulating Nitro-Oxidative Homeostasis and Proline Metabolism. *Journal of Pineal Research* **62**:e12401.

Apel, K and Hirt, H. 2004a. Reactive Oxygen Species: Metabolism, Oxidative Stress, and Signal Transduction. *Annual Review of Plant Biology* **55**:373–99.

Arabidopsis Genome Initiative. 2000. Analysis of the Genome Sequence of the Flowering Plant *Arabidopsis thaliana*. *Nature* **408**:796–815.

Aranega-Bou, P., Leyva, M., Finiti, I., García-Agustín P and González-Bosch C. 2014. Priming of Plant Resistance by Natural Compounds. Hexanoic Acid as a Model. *Frontiers in Plant Science* **5**:488.

Arora, A, Sairam, R.K and Srivastava, G.C. 2002. Oxidative Stress and Antioxidative System in Plants. *Current Science* **82**:1227–38.

Arrom, L and Munné-Bosch, S. 2012. Hormonal Regulation of Leaf Senescence in Lilium. *Journal of Plant Physiology* **169**:1542–50.

Arvidsson, S., Kwasniewski, M., Riano-Pachon, D.M and Mueller-Roeber, B. 2008. QuantPrime - a Flexible Tool for Reliable High-Throughput Primer Design for Quantitative PCR. *BMC Bioinformatics* **9**:465-74.

Assmann, S.M. 2003. Open Stomata1 Opens the Door to ABA Signaling in Arabidopsis Guard Cells. *Trends in Plant Science* **8**:151–53.

Babitha, K. C. et al., 2013. Co-Expression of *AtbHLH17* and *AtWRKY28* Confers Resistance to Abiotic Stress in Arabidopsis. *Transgenic Research* **22**:327–41.

Bajji, M., Jean-marie K., and Stanley L. 2001. The Use of the Electrolyte Leakage Method for Assessing Cell Membrane Stability as a Water Stress Tolerance Test in Durum Wheat. *Plant Growth Regulation* **36**:61–70.

Balasaraswathi, K. et al., 2017. Cr–induced Cellular Injury and Necrosis in Glycine Max L.: Biochemical Mechanism of Oxidative Damage in Chloroplast. *Plant Physiology and Biochemistry* **118**:653-66.

Balazadeh, S., Riaño-Pachón, D.M and Mueller-Roeber, B. 2008. Transcription Factors Regulating Leaf

Senescence in *Arabidopsis thaliana*. *Plant Biology* **10**:63–75.

Balazadeh, S et al., 2011. ORS1, an H2O2-Responsive NAC Transcription Factor, Controls Senescence in *Arabidopsis thaliana*. *Molecular Plant* **4**:346–60.

Barth, C., De Tullio, M and Conklin, P.L. 2006. The Role of Ascorbic Acid in the Control of Flowering Time and the Onset of Senescence. *Journal of Experimental Botany* **57**:1657–65.

Basu, S., Venkategowda, R., Kumar, A and Pereira, A. 2016. Plant Adaptation to Drought Stress. *F1000Research* **5**:1554.

Bernhardt, A., Sutton, M, and Hanjo, H. 2010. Arabidopsis *DDB1a* and *DDB1b* Are Critical for Embryo Development. *Planta* **232**:555–66.

Besseau, S., Jing L., and Palva, E.T. 2012. *WRKY54* and *WRKY70* Co-Operate as Negative Regulators of Leaf Senescence in *Arabidopsis thaliana*. *Journal of Experimental Botany* **63**:2667–79.

Bhattacharjee, S. 2005. Reactive Oxygen Species and Oxidative Burst: Roles in Stress, Senescence and Signal Transduction in Plants. *Current Science* **89**:1113–21.

Bhattacharjee, S. 2012. The Language of Reactive Oxygen Species Signaling in Plants. *Journal of Botany* **12**:1–22.

Biedermann, S., Sutton, M and Hanjo, H. 2011. Recognition and Repair Pathways of Damaged DNA in Higher Plants. *Selected Topics in DNA Repair*, Prof. Clark Chen (Ed.):201–36.

Biesalski, H.K. 2002. Free Radical Theory of Aging. *Current Opinion in Clinical Nutrition and Metabolic Care* **5**:5–10.

Borges, A.A., David J.A., Marino, E.R., Luisa, M.S and Jose A.P. 2014. Priming Crops against Biotic and Abiotic Stresses: MSB as a Tool for Studying Mechanisms. *Frontiers in Plant Science* **5**:1–4.

Boriboonkaset, T et al., 2012. Expression Levels of Some Starch Metabolism Related Genes in Flag Leaf of Two Contrasting Rice Genotypes Exposed to Salt Stress. *Australian Journal of Crop Science* **6**:1579–86.

Boursiac, Y et al., 2013. ABA Transport and Transporters. *Trends in Plant Science* **18**:325–33.

Boyes, D.C. et al., 2001. Growth Stage – Based Phenotypic Analysis of Arabidopsis: A Model for High Throughput Functional Genomics in Plants. *The Plant Cell* **13**:1499–1510.

Braun, N et al., 2008. Conditional Repression of AUXIN BINDING PROTEIN1 Reveals That It Coordinates Cell Division and Cell Expansion during Postembryonic Shoot Development in Arabidopsis and Tobacco. *The Plant Cell* **20**:2746–62.

Breeze, E et al., 2011. High-Resolution Temporal Profiling of Transcripts during Arabidopsis Leaf Senescence Reveals a Distinct Chronology of Processes and Regulation. *The Plant Cell* **23**:873–94.

Britt, A.B. 1996. DNA Damage and Repair in Plants. *Annual Review of Plant Physiology and Plant Molecular Biology* **47**:75–100.

Briviba, K., Klotz, L.O and Sies, H. 1997. Toxic and Signaling Effects of Photochemically or Chemically Generated Singlet Oxygen in Biological Systems. *Biological Chemistry* **378**:1259–65.

Buchanan-Wollaston, V. 1997. The Molecular Biology of Leaf Senescence. *Journal of Experimental Botany* **48**:181–99.

Bundock, P and Hooykaas, P. 2002. Severe Developmental Defects, Hypersensitivity to DNA-Damaging Agents, and Lengthened Telomeres in Arabidopsis *MRE11* Mutants. *The Plant Cell* **14**:2451–62.

Cai, G et al., 2014a. A Maize Mitogen-Activated Protein Kinase Kinase, *ZmMKK1*, Positively Regulated the Salt

and Drought Tolerance in Transgenic Arabidopsis. *Journal of Plant Physiology* **171**:1003–16.

Cai, W et al., 2014b. Increasing Frequency of Extreme El Niño Events due to Greenhouse Warming. *Nature Climate Change* **4**:111–16.

Campos, P.S., Virgínia, Q., José Cochicho, R, and Maria Antonieta, N. 2003. Electrolyte Leakage and Lipid Degradation Account for Cold Sensitivity in Leaves of Coffea Sp. Plants. *Journal of Plant Physiology* **160**:283–92.

Gan, S and Amasino, R.M. 1997. Making Sense of Senescence' Molecular Genetic Regulation and Manipulation of Leaf Senescence. *Plant Physiol*ogy **113**:313–19.

Candela, H., Rubén, C.S, and José, L.M. 2015. Getting Started in Mapping-by-Sequencing. *Journal of Integrative Plant Biology* **57**:606–12.

Caswell, H and Salguero-Gomez, R. 2013. Age, Stage and Senescence in Plants. *Journal of Ecology* **101**:585–95.

Caverzan, A et al., 2012. Plant Responses to Stresses: Role of Ascorbate Peroxidase in the Antioxidant Protection. *Genetics and Molecular Biology* **35**:1011–19.

Cela, J., Caren, C., and Sergi, M.S. 2011. Accumulation of γ-rather than α-Tocopherol Alters Ethylene Signaling Gene Expression in the *vte4* Mutant of *Arabidopsis thaliana*. *Plant and Cell Physiology* **52**:1389–1400.

Chapin, F. S et al., 2000. Consequences of Changing Biodiversity. *Nature* **405**:234–42.

Chardon, F et al., 2014. QTL Meta-Analysis in Arabidopsis Reveals an Interaction between Leaf Senescence and Resource Allocation to Seeds *Journal of Experimental Botany* **65**:3949–62.

Chen, C et al., 2015a. Leaf Senescence Induced by *EGY1* Defection Was Partially Restored by Glucose in *Arabidopsis thaliana*. *Botanical Studies* **57**:5.

Chen, G.H., Chia, P.L., Shu, C.G.C and Long, C.W. 2012. Role of *ARABIDOPSIS A-FIFTEEN* in Regulating Leaf Senescence Involves Response to Reactive Oxygen Species and Is Dependent on *ETHYLENE INSENSITIVE2*. *Journal of Experimental Botany* **63**:275–92.

Chen, G et al., 2011. A Functional Cutin Matrix Is Required for Plant Protection against Water Loss. *Plant Signaling and Behavior* **6**:1297–99.

Chen, J. G., Ullah, H., Young, J.C., Sussman, M.R and Jones, A.M. 2001. ABP1 Is Required for Organized Cell Elongation and Division in Arabidopsis Embryogenesis. *Genes and Development* **15**:902–11.

Chen, J et al., 2017. Arabidopsis WRKY46, WRKY54 and WRKY70 Transcription Factors Are Involved in Brassinosteroid-Regulated Plant Growth and Drought Response. *The Plant Cell* **29**:1425-1439.

Chen, L.Q. 2014. SWEET Sugar Transporters for Phloem Transport and Pathogen Nutrition. *New Phytologist* **201**:1150–55.

Chen, L et al., 2012. The Role of WRKY Transcription Factors in Plant Abiotic Stresses. *Biochimica et Biophysica Acta - Gene Regulatory Mechanisms* **1819**:120–28.

Chen, X et al., 2014. Inhibition of Cell Expansion by Rapid ABP1-Mediated Auxin Effect on Microtubules. *Nature* **516**:90–93.

Chen, Y., Cai, J., Yang, F.X., Zhou, B and Zhou, L.R. 2015b. Ascorbate Peroxidase from Jatropha Curcas Enhances Salt Tolerance in Transgenic Arabidopsis. *Genetics and Molecular Research* **14**:4879–89.

Chen, Y.F et al., 2009a. The WRKY6 Transcription Factor Modulates *PHOSPHATE1* Expression in Response to Low Pi Stress in Arabidopsis. *The Plant Cell* **21**:3554–66.

Chen, Z., Zuyu, Z., Junli, H., Zhibing, L and Baofang, F. 2009b. Biosynthesis of Salicylic Acid in Plants. *Plant*

Signaling and Behavior **4**:493–96.

Cheng, M. C., Liao, P.M., Kuo, W.W and Lin, T.P. 2013. The Arabidopsis *ETHYLENE RESPONSE FACTOR1* Regulates Abiotic Stress-Responsive Gene Expression by Binding to Different Cis-Acting Elements in Response to Different Stress Signals. *Plant Physiology* **162**:1566–82.

Cheng, Y and Yunde, Z. 2007. A Role for Auxin in Flower Development. *Journal of Integrative Plant Biology* **49**:99–104.

Cho, E.J et al., 2016. A Mutation in Plant-Specific *SWI2/SNF2*-Like Chromatin-Remodeling Proteins, *DRD1* and *DDM1*, Delays Leaf Senescence in *Arabidopsis thaliana*. *PLoS ONE* **11**:1–21.

Cho, H. T. and Cosgrove, D.J. 2000. Altered Expression of Expansin Modulates Leaf Growth and Pedicel Abscission in *Arabidopsis thaliana*. *Proceedings of the National Academy of Sciences of the United States of America* **97**:9783–88.

Ciarmiello, LF and Woodrow, P. 2011. Plant Genes for Abiotic Stress, Abiotic Stress in Plants- Mechanisms and Adaptations, *Prof Arun Shanker* (Ed.).

Clauw, P et al., 2015. Leaf Responses to Mild Drought Stress in Natural Variants of Arabidopsis. *Plant Physiology* **167**:800–16.

Colcombet, J and Heribert, H. 2008. *Arabidopsis* MAPKs: A Complex Signalling Network Involved in Multiple Biological Processes. *Biochemical Journal* **413**:217–26.

Conklin, P. L. and Barth, C. 2004. Ascorbic Acid, a Familiar Small Molecule Intertwined in the Response of Plants to Ozone, Pathogens, and the Onset of Senescence. *Plant, Cell and Environment* **27**:959–70.

Conrath, U. 2011. Molecular Aspects of Defence Priming. *Trends in Plant Science* **16**:524–31.

Consiglio, A et al., 2016. A Fuzzy Method for RNA-Seq Differential Expression Analysis in Presence of Multireads. *BMC Bioinformatics* **17**:95-110.

Cordoba, E., Aceves-Zamudio, D.L., Hernandez-Bernal, A.F., Ramos-Vega, M and Leon, P. 2015. Sugar Regulation of SUGAR TRANSPORTER PROTEIN 1 (*STP1*) Expression in *Arabidopsis thaliana*. *Journal of Experimental Botany* **66**:147–59.

Cornish, K. and Zeevaart, J.A.D. 1984. Abscisic Acid Metabolism in Relation to Water Stress and Leaf Age in Xanthium Strumarium. *Plant Physiology* **76**:1029–35.

Couée, I., Sulmon, C., Gouesbet, G and Amrani, E. 2006. Involvement of Soluble Sugars in Reactive Oxygen Species Balance and Responses to Oxidative Stress in Plants. *Journal of Experimental Botany* **57**:449–59.

Dai, F. et al., 2012. *RhNAC2* and *RhEXPA4* Are Involved in the Regulation of Dehydration Tolerance during the Expansion of Rose Petals. *Plant Physiology* **160**:2064–82.

Danquah, A. et al., 2015. Identification and Characterization of an ABA-Activated MAP Kinase Cascade in *Arabidopsis thaliana*. *The Plant Journal* **82**:232–44.

Daudi, A. et al., 2012. The Apoplastic Oxidative Burst Peroxidase in Arabidopsis Is a Major Component of Pattern-Triggered Immunity. *The Plant Cell* **24**:275–87.

Davies, P. J. and Gan, S. 2012. Towards an Integrated View of Monocarpic Plant Senescence. *Russian Journal of Plant Physiology* **59**:467–78.

Dellaporta, S.L., Jonathan, W and James B.H. 1983. A Plant DNA Minipreparation: Version II. *Plant Molecular Biology Reporter* **1**:19–21.

Denekamp, M and Smeekens, S.C. 2003. Integration of Wounding and Osmotic Stress Signals Determines the

Expression of the *AtMYB102* Transcription Factor Gene. *Plant Physiology* **132**:1415–23.

Dennis, E. S. et al., 2000. Molecular Strategies for Improving Waterlogging Tolerance in Plants. *Journal of Experimental Botany* **9**:89–97.

Desikan, R et al., 2004. ABA, Hydrogen Peroxide and Nitric Oxide Signalling in Stomatal Guard Cells. *Journal of Experimental Botany* **55**:205-12.

Desikan, R et al., 2006. Ethylene-Induced Stomatal Closure in Arabidopsis Occurs via *AtrbohF*-Mediated Hydrogen Peroxide Synthesis. *Plant Journal* **47**:907–16.

Dhindsa, R.S., Plumb-dhindsa, P and Thorpe, T.A. 1981. Leaf Senescence: Correlated with Increased Levels of Membrane Permeability and Lipid Peroxidation, and Decreased Levels of Superoxide Dismutase and Catalase. *Journal of Experimental Botany* **32**:93–101.

Diaz, C. et al., 2006. Leaf Yellowing and Anthocyanin Accumulation Are Two Genetically Independent Strategies in Response to Nitrogen Limitation in *Arabidopsis thaliana*. *Plant and Cell Physiology* **47**:74–83.

Dikalov, S. 2011. Cross Talk between Mitochondria and NADPH Oxidases. *Free Radical Biology and Medicine* **51**:1289–1301.

Dong, J., Jiang, Y., Chen, R., Xu, Z and Gao, X. 2011. Isolation of a Novel Xyloglucan Endotransglucosylase (*OsXET9*) Gene from Rice and Analysis of the Response of This Gene to Abiotic Stresses. *African Journal of Biotechnology* **10**:17424–34.

Durand, M. et al., 2017. Carbon Source–sink Relationship in *Arabidopsis thaliana*: The Role of Sucrose Transporters. *Planta* **247**:587–611.

Ebeed, H.T., Nemat, M.H, and Alshafei, M.A. 2017. Exogenous Applications of Polyamines Modulate Drought Responses in Wheat through Osmolytes Accumulation, Increasing Free Polyamine Levels and Regulation of Polyamine Biosynthetic Genes. *Plant Physiology and Biochemistry* **118**:438–48.

Ecker. 1995. The Ethylene Signal Transduction Pathway in Plants. *Science* **268**:667–75.

Ellis, M., Jack, E., Carolyn, J.S, and Antony, B. 2010. Arabinogalactan-Proteins: Key Regulators at the Cell Surface. *Plant Physiology* **153**:403–19.

Elstner, E. F. and Osswald, W. 1994. Mechanisms of Oxygen Activation during Plant Stress. *Proceedingd of the Royal Society of Edinburgh Section B* **102**:131–54.

Enders, T.A., Sookyung, O., Zhenbiao, Y., Beronda, L.M, and Lucia, C.S. 2015. Genome Sequencing of Arabidopsis *abp1-5* Reveals Second-Site Mutations That May Affect Phenotypes. *The Plant Cell* **27**:1820-6.

Endo, A., Masanori, O, and Koshiba, T. 2014. ABA Biosynthetic and Catabolic Pathways. *Abscisic Acid: Metabolism, Transport and Signaling*. Zhang, Da-Peng (Ed.), 191-223.

Eveland, A.L. and David, P.J. 2012. Sugars, Signalling, and Plant Development. *Journal of Experimental Botany* **63**:3367–77.

Fahad, S. et al., 2017. Crop Production under Drought and Heat Stress: Plant Responses and Management Options. *Frontiers in Plant Science* **8**:1147.

Fang, J. et al., 2008. Mutations of Genes in Synthesis of the Carotenoid Precursors of ABA Lead to Pre-Harvest Sprouting and Photo-Oxidation in Rice. *Plant Journal* **54**:177–89.

Feifei, W., Chen, Z.H, and Sergey, S. 2017. Hypoxia Sensing in Plants: On a Quest for Ion Channels as Putative Oxygen Sensors. *Plant Cell Physiology* **58**:1126-42.

Ferris, R., Sabatti, M., Miglietta, F., Mills, R.F and Taylor, G. 2001. Leaf Area Is Stimulated in Populus by Free Air CO_2 Enrichment (POPFACE), through Increased Cell Expansion and Production. *Plant, Cell and Environment* **24**:305–15.

Feys, B.J., Lisa J.M., Newman, M.A and Parker, J.E. 2001. Direct Interaction between the Arabidopsis Disease Resistance Signaling Proteins, EDS1 and PAD4. *EMBO Journal* **20**:5400–11.

Fini, A., Brunetti, C., Di Ferdinando, M., Ferrini, F and Tattini, M. 2011. Stress-Induced Flavonoid Biosynthesis and the Antioxidant Machinery of Plants. *Plant Signaling and Behavior* **6**:709–11.

Finkelstein, R. 2013. Abscisic Acid Synthesis and Response. *The Arabidopsis book / American Society of Plant Biologists* **11**:e0166.

Flowers, T. J. 2004. Improving Crop Salt Tolerance. *Journal of Experimental Botany* **55**:307-19.

Foyer, C. H. and Shigeoka, S. 2011. Understanding Oxidative Stress and Antioxidant Functions to Enhance Photosynthesis. *Plant Physiology* **155**:93–100.

Foyer, C.H. and Graham, N. 2009. Redox Regulation in Photosynthetic Organisms: Signaling, Acclimation, and Practical Implications. *Antioxidants and Redox Signaling* **11**:861–905.

Franklin, D. and Morgan, P.W. 1978. Rapid Production of Auxin-Induced Ethylene. *Plant Physiology* **62**:161–62.

Fujiki, Y., Ito, M., Nishida, I and Watanabe, A. 2000. Multiple Signaling Pathways in Gene Expression during Sugar Starvation. Pharmacological Analysis of Din Gene Expression in Suspension-Cultured Cells of Arabidopsis. *Plant Physiology* **124**:1139–48.

Gall, H. et al., 2015. Cell Wall Metabolism in Response to Abiotic Stress. *Plants* **4**:112–66.

Gamir, J., Sánchez-Bel, P and Flors, V. 2014. Molecular and Physiological Stages of Priming: How Plants Prepare for Environmental Challenges. *Plant Cell Reports* **33**:1935–49.

Gan, S. and Amasino, R.M. 1997. Making Sense of Senescence (Molecular Genetic Regulation and Manipulation of Leaf Senescence). *Plant Physiology* **113**:313–19.

Gao, Y., Zhang, Y., Zhang, D., Dai, X., Estelle, M.and Zhao. 2015. Auxin Binding Protein 1 (*ABP1*) Is Not Required for Either Auxin Signaling or Arabidopsis Development. *Proceedings of the National Academy of Sciences of the United States of America* **112**:2275–80.

Gao, L. et al., 2015. The Tomato *DDI2*, a *PCNA* Ortholog, Associating with *DDB1-CUL*4 Complex Is Required for UV-Damaged DNA Repair and Plant Tolerance to UV Stress. *Plant Science : An International Journal of Experimental Plant Biology* **235**:101–10.

Gao, L., Li, Y and Han, R. 2015. Cell Wall Reconstruction and DNA Damage Repair Play a Key Role in the Improved Salt Tolerance Effects of He-Ne Laser Irradiation in Tall Fescue Seedlings. *Bioscience, Biotechnology and Biochemistry* **80**:682-93.

Gapper, C and Dolan, L. 2006. Control of Plant Development by Reactive Oxygen Species. *Plant Physiology* **141**:341–45.

Gardner, S. D. L. and Shao, B.Y. 2001. Increased Leaf Area Expansion of Hybrid Poplar in Elevated CO_2. From Controlled Environments to Open-Top Chambers and to FACE. *Environmental Pollution* **115**:463–72.

Gaussand, G.M et al., 2011. Programmed Cell Death in the Leaves of the Arabidopsis Spontaneous Necrotic Spots (*Sns-D*) Mutant Correlates with Increased Expression of the Eukaryotic Translation Initiation Factor eIF4B2. *Frontiers in Plant Science* **2**:9.

Gechev, T.S., Van Breusegem, F., Stone, J.M., Denev, I and Laloi, C. 2006. Reactive Oxygen Species as Signals That Modulate Plant Stress Responses and Programmed Cell Death. *BioEssays : News and Reviews in Molecular, Cellular and Developmental Biology* **28**:1091–1101.

Gepstein, S. et al., 2003. Large-Scale Identification of Leaf Senescence-Associated Genes. *Plant Journal* **36**:629–42.

Gill, S.S., Naser A.A., Gill, R., Jha, M and Tuteja, N. 2015. DNA Damage and Repair in Plants under Ultraviolet and Ionizing Radiations. *Scientific World Journal* 2015:250158.

Gill, S.S., Peter Singh, L., Gill, R and Tuteja, N. 2012. Generation and Scavenging of Reactive Oxygen Species in Plants under Stress Improving Crop Resistance to Abiotic Stress, Volume 1 and Volume 2, Tuteja N, Gill S.S, Tiburcio A.F and Tuteja R (Eds.).

Gill, S.S and Tuteja, N. 2010. Reactive Oxygen Species and Antioxidant Machinery in Abiotic Stress Tolerance in Crop Plants. *Plant Physiology and Biochemistry* **48**:909–30.

Giovane, A. et al., 2004. Pectin Methylesterase Inhibitor. *Biochimica et Biophysica Acta - Proteins and Proteomics* **1696**:245–52.

Glazebrook, J. 2001. Genes Controlling Expression of Defense Responses in Arabidopsis--2001 Status. *Current Opinion in Plant Biology* **4**:301–8.

Golubov, A. et al., 2010. Microsatellite Instability in Arabidopsis Increases with Plant Development. *Plant Physiology* **154**:1415–27.

Gou, J. Y., Yu, X.H and Liu, C.J 2009. A Hydroxycinnamoyltransferase Responsible for Synthesizing Suberin Aromatics in Arabidopsis. *Proceedings of the National Academy of Sciences* **106**:18855–60.

Grbic, V and Bleecker, A.B. 1995. Ethylene Regulates the Timing of Leaf Senescence in Arabidopsis. *The Plant Journal* **8**:595–602.

Group, MAPK. 2002. Mitogen-Activated Protein Kinase Cascades in Plants: A New Nomenclature. *Trends Plant Science* **7**:301–8.

Gudesblat, G.E., Norberto D.I, and Morris, P.C. 2007. Guard Cell-Specific Inhibition of Arabidopsis *MPK3* Expression Causes Abnormal Stomatal Responses to Abscisic Acid and Hydrogen Peroxide. *New Phytologist* **173**:713–21.

Guo, Y and Gan, S.S. 2014. Translational Researches on Leaf Senescence for Enhancing Plant Productivity and Quality. *Journal of Experimental Botany* **65**:3901–13.

Guo, Y and Gan, S. 2005. Leaf Senescence: Signals, Execution, and Regulation. *Current Topics in Developmental Biology* **71**:83–112.

Gupta, S., Heinen, J.L., Holaday, S., Burke, J.J and Allen, R.D. 1993. Increased Resistance to Oxidative Stress in Transgenic Plants That Overexpress Chloroplastic Cu/Zn Superoxide Dismutase. *Proceedings of the National Academy of Sciences of the United States of America* **90**:1629–33.

Gupta, D.K., Palma, J.M and Corpas, F.J. 2016. Redox State as a Central Regulator of Plant-Cell Stress Responses. *Springer* 1–386.

Ha, S., Vankova, R., Yamaguchi-Shinozaki, K., Shinozaki, K and Tran, L.S. 2012. Cytokinins: Metabolism and Function in Plant Adaptation to Environmental Stresses. *Trends Plant Sci* **17**:172–79.

Halliwell, B. 1991. Oxygen Radicals - Their Formation in Plant Tissues and Their Role in Herbicide Damage. *Herbicides* **10**:87–129.

Halliwell, B. 2006. Reactive Species and Antioxidants. Redox Biology Is a Fundamental Theme of Aerobic Life. *Plant Physiology* **141**:312–22.

Han, L. et al., 2010. Mitogen-Activated Protein Kinase 3 and 6 Regulate Botrytis Cinerea-Induced Ethylene Production in Arabidopsis. *Plant Journal* **64**:114–27.

Han, Y., Li, A.X., Li, F., Zhao, M.R and Wang, W. 2012. Characterization of a Wheat (*Triticum Aestivum L.*) Expansin Gene, *TaEXPB23*, Involved in the Abiotic Stress Response and Phytohormone Regulation. *Plant Physiology and Biochemistry* **54**:49–58.

Hancock, J. T., Desikan, R and Neill, S.J. 2001. Role of Reactive Oxygen Species in Cell Signalling Pathways. *Biochemical Society Transactions* **29**:345–50.

Hasegawa, P.M., Bressan, R.A., Jian-Kang Z., and Bohnert, H.J. 2000. Plant Cellular and Molecular Responses to High Salinity. *Annual Review of Plant Physiology and Plant Molecular Biology* **51**:463–99.

Hayashi, T and Rumi K. 2011. Functions of Xyloglucan in Plant Cells. *Molecular Plant* **4**:17–24.

He, C. et al., 2017. *DoGMP1* from Dendrobium Officinale Contributes to Mannose Content of Water-Soluble Polysaccharides and Plays a Role in Salt Stress Response. *Scientific Reports* **7**:41010.

Hectors, K. et al., 2010. UV Radiation Reduces Epidermal Cell Expansion in Leaves of *Arabidopsis thaliana*. *Journal of Experimental Botany* **61**:4339–49.

Hekimi, S., Lapointe, J and Wen, Y. 2011. Taking A 'good' look at Free Radicals in the Aging Process. *Trends in Cell Biology* **21**:569–76.

Hensel, L. L., Grbić, V., Baumgarten, D.A and Bleecker, A.B. 1993. Developmental and Age-Related Processes That Influence the Longevity and Senescence of Photosynthetic Tissues in Arabidopsis. *The Plant Cell* **5**:553–64.

Hernandez-Garcia, C.M and John, J.F. 2014. Identification and Validation of Promoters and Cis-Acting Regulatory Elements. *Plant Science* **217**:109–19.

Hernández, J.A., Ferrer, M.A., Jiménez, A., Barceló, A.R and Sevilla, F. 2001. Antioxidant Systems and $O_2^{\cdot-}/H_2O_2$ Production in the Apoplast of Pea Leaves. Its Relation with Salt-Induced Necrotic Lesions in Minor Veins. *Plant Physiology* **127**:817–31.

Hess, M. et al., 1997. Use of the Extended BBCH Scale - General for the Descriptions of the Growth Stages of Mono- and Dicotyledonous Weed Species. *Weed Research* **37**:433–41.

Hetherington, A.M. and Woodward, F.I. 2003. The Role of Stomata in Sensing and Driving Environmental Change. *Nature* **424**:901–8.

Himelblau, E and Amasino, R.M. 2001. Nutrients Mobilized from Leaves of *Arabidopsis thaliana* during Leaf Senescence. *Journal of Plant Physiology* **158**:1317–23.

Hörtensteiner, S. 2006. Chlorophyll Degradation during Senescence. *Annual Review of Plant Biology* **57**:55–77.

Hossain, M.A. et al., 2015. Hydrogen Peroxide Priming Modulates Abiotic Oxidative Stress Tolerance: Insights from ROS Detoxification and Scavenging. *Frontiers in Plant Science* **6**:420.

Hou, K., Wu, W and Su-Sheng, G. 2013. *SAUR36*, a Small Auxin up RNA Gene, Is Involved in the Promotion of Leaf Senescence in Arabidopsis. *Plant Physiology* **161**:1002–9.

Hou, Y. et al., 2015. The Persimmon 9-Lipoxygenase Gene *DkLOX3* Plays Positive Roles in Both Promoting Senescence and Enhancing Tolerance to Abiotic Stress. *Frontiers in Plant Science* **6**:1073.

Hu, X., Tanaka, A and Tanaka, R. 2013. Simple Extraction Methods That Prevent the Artifactual Conversion of

Chlorophyll to Chlorophyllide during Pigment Isolation from Leaf Samples. *Plant Methods* **9**:19.

Huang, C. et al., 2005. Increased Sensitivity to Salt Stress in an Ascorbate-Deficient Arabidopsis Mutant. *Journal of Experimental Botany* **56**:3041–49.

Huang, S., Aken, O.V., Schwarzländer, M., Belt, K and Millar, A.H. 2016. Roles of Mitochondrial Reactive Oxygen Species in Cellular Signalling and Stress Response in Plants. *Plant Physiology* **171**:1551–59.

Hunter D.A. et al., (2018) Identification of Postharvest Senescence Regulators Through Map-Based Cloning Using Detached *Arabidopsis* Inflorescences as a Model Tissue. In: Guo Y. (eds) Plant Senescence. Methods in Molecular Biology, vol 1744. Humana Press, New York, NY

Hussain, S., Khan, F., Hussain, H.A and Nie, L. 2016. Physiological and Biochemical Mechanisms of Seed Priming-Induced Chilling Tolerance in Rice Cultivars. *Frontiers in Plant Science* **7**:116.

Hye, R.W., Kim J.H., Nam, H.G., and Lim, P.O. 2004. The Delayed Leaf Senescence Mutants of Arabidopsis, *ore1*, *ore3*, and *ore9* Are Tolerant to Oxidative Stress. *Plant and Cell Physiology* **45**:923–32.

Islam, F. et al., 2017. 2,4-D Attenuates Salinity-Induced Toxicity by Mediating Anatomical Changes, Antioxidant Capacity and Cation Transporters in the Roots of Rice Cultivars. *Scientific Reports* **7**:10443.

Jajic, I., Sarna, T and Strzalka, K. 2015. Senescence, Stress, and Reactive Oxygen Species. *Plants* **4**:393–411.

Jalil, S,U., Ahmad, I and Ansari, M.I. 2016. Functional Loss of GABA Transaminase (*GABA-T*) Expressed Early Leaf Senescence under Various Stress Conditions in *Arabidopsis thaliana*. *Current Plant Biology* **10**:11-22.

Jalmi, S.K and Sinha, A.K. 2015. ROS Mediated MAPK Signaling in Abiotic and Biotic Stress- Striking Similarities and Differences. *Frontiers in Plant Science* **6**:769.

Jammes, F. et al., 2009. MAP Kinases *MPK9* and *MPK12* Are Preferentially Expressed in Guard Cells and Positively Regulate ROS-Mediated ABA Signaling. *Proceedings of the National Academy of Sciences of the United States of America* **106**:20520–25.

Jander, G. 2002. Arabidopsis Map-Based Cloning in the Post-Genome Era. *Plant Physiology* **129**:440–50.

Jia, H. et al., 2016. A Raf-like MAPKKK Gene, *GhRaf19*, Negatively Regulates Tolerance to Drought and Salt and Positively Regulates Resistance to Cold Stress by Modulating Reactive Oxygen Species in Cotton. *Plant Science* **252**:267–81.

Jiang, Yuanqing and Michael K. Deyholos. 2009. Functional Characterization of Arabidopsis NaCl-Inducible WRKY25 and WRKY33 Transcription Factors in Abiotic Stresses. *Plant Molecular Biology* **69**:91–105.

Jibran, Rubina, Donald A. Hunter, and Paul P. Dijkwel. 2013. Hormonal Regulation of Leaf Senescence through Integration of Developmental and Stress Signals. *Plant Molecular Biology* **82**:547–61.

Jiménez, Ana, José a. Hernández, Gabriela Pastori, Luis a. del Río, and Francisca Sevilla. 1998. Role of the Ascorbate-Glutathione Cycle of Mitochondria and Peroxisomes in the Senescence of Pea Leaves1. *Plant Physiology* **118**:1327–35.

Jing, H. C. et al., 2008. Early Leaf Senescence Is Associated with an Altered Cellular Redox Balance in Arabidopsis cpr5/old1 Mutants. *Plant Biology* **10**:85–98.

Jing, H. C., Hille, J and Dijkwel. P.P. 2003. Ageing in Plants: Conserved Strategies and Novel Pathways. *Plant Biology* **5**:455–64.

Jing, H.C, Schippers, J.H.M., Hille, J and Dijkwel, P.P. 2005. Ethylene-Induced Leaf Senescence Depends on Age-Related Changes and *OLD* Genes in Arabidopsis. *Journal of Experimental Botany* **56**:2915–23.

Jing, H.C., Sturre, M.J., Hille, J and Dijkwel, P.P. 2002. Arabidopsis Onset of Leaf Death Mutants Identify a Regulatory Pathway Controlling Leaf Senescence. *The Plant Journal for Cell and Molecular Biology* **32**:51–63.

Johnson, A and Skotheim, J.M. 2013. Start and the Restriction Point. *Current Opinion in Cell Biology* **25**:717–23.

Jones, A. M. 1994. Auxin-Binding Proteins. *Annual Review of Plant Physiology and Plant Molecular Biology* **45**:393–420.

Jung, J. Y., Shin, R and Schachtman, D.P. 2009. Ethylene Mediates Response and Tolerance to Potassium Deprivation in Arabidopsis. *The Plant Cell Online* **21**:607–21.

Kaku, T., Tabuchi, A., Wakabayashi, K and Hoson, T. 2004. Xyloglucan Oligosaccharides Cause Cell Wall Loosening by Enhancing Xyloglucan Endotransglucosylase/Hydrolase Activity in Azuki Bean Epicotyls. *Plant and Cell Physiology* **45**:77–82.

Kakutani, T., Jeddeloh, J.A., Flowers, S.K., Munakata, K and Richards, E.J. 1996. Developmental Abnormalities and Epimutations Associated with DNA Hypomethylation Mutations. *Proceedings of the National Academy of Sciences of the United States of America* **93**:12406–11.

Kang, S.G., Price, J., Lin, P.C., Hong, J.C and Jang, J.C. 2010. The Arabidopsis bZIP1 Transcription Factor Is Involved in Sugar Signaling, Protein Networking, and DNA Binding. *Molecular Plant* **3**:361–73.

Kang, T.J and Yang, M.S. 2004. Rapid and Reliable Extraction of Genomic DNA from Various Wild-Type and Transgenic Plants. *BMC Biotechnology* **4**:20.

Kanwar, P. et al., 2014. Comprehensive Structural, Interaction and Expression Analysis of *CBL* and *CIPK* Complement during Abiotic Stresses and Development in Rice. *Cell Calcium* **56**:81–95.

Kaplan, F and Guy, C.L. 2004. B -Amylase Induction and the Protective Role of Maltose during Temperature Shock 1. *Plant Physiology* **135**:1674–84.

Kardailsky, I. 1999. Activation Tagging of the Floral Inducer FT. *Science* **286**:1962–65.

Kaushik, D. and Roychoudhury, A. 2014. Reactive Oxygen Species (ROS) and Response of Antioxidants as ROS-Scavengers during Environmental Stress in Plants. *Frontiers in Environmental Science* **2**:1-13.

Kaya, M.D., Okçu, G., Atak, M., Çikili, Y and Kolsarici, O. 2006. Seed Treatments to Overcome Salt and Drought Stress during Germination in Sunflower (*Helianthus Annuus L.*). *European Journal of Agronomy* **24**:291–95.

Kazan, K and Lyons, R. 2016. The Link between Flowering Time and Stress Tolerance. *Journal of Experimental Botany* **67**:47–60.

Kempa, S., Krasensky, J., Santo, S.D., Kopka, J and Jonak, C. 2008. A Central Role of Abscisic Acid in Stress-Regulated Carbohydrate Metabolism. *PLoS ONE* **3**:e3935.

Kerchev, Pavel et al., 2017. Lack of *GLYCOLATE OXIDASE1*, but Not *GLYCOLATE OXIDASE2*, Attenuates the Photorespiratory Phenotype of *CATALASE2*-Deficient Arabidopsis. *Plant Physiology* **171**: 1704–1719.

Khan, M., Rozhon, W and Poppenberger, B. 2013. The Role of Hormones in the Aging of Plants - A Mini-Review. *Gerontology* **60**:49–55.

Khan, N. A., Singh, S.S and Nazar, R. 2007. Activities of Antioxidative Enzymes, Sulphur Assimilation, Photosynthetic Activity and Growth of Wheat (Triticum Aestivum) Cultivars Differing in Yield Potential under Cadmium Stress. *Journal of Agronomy and Crop Science* **193**:435–44.

Kim, H.J. et al., 2014. Gene Regulatory Cascade of Senescence-Associated NAC Transcription Factors Activated by *ETHYLENE-INSENSITIVE2*-Mediated Leaf Senescence Signalling in Arabidopsis. *Journal of Experimental Botany* **65**:4023–36.

Kim, J.H. et al., 2009. Trifurcate Feed-Forward Regulation of Age-Dependent Cell Death Involving *miR164* in Arabidopsis. *Science (New York, N.Y.)* **323**:1053–57.

Kim, M.J., Ciani, S and Schachtman, D.P. 2010. A Peroxidase Contributes to Ros Production during Arabidopsis Root Response to Potassium Deficiency. *Molecular Plant* **3**:420–27.

Kirkman, H. N. and Gaetani, G.F. 1984. Catalase: A Tetrameric Enzyme with Four Tightly Bound Molecules of NADPH. *Proceedings of the National Academy of Sciences of the United States of America* **81**:4343–47.

Knoch, E., Dilokpimol, A and Geshi, N. 2014. Arabinogalactan Proteins: Focus on Carbohydrate Active Enzymes. *Frontiers in Plant Science* **5**:198.

Koffler, B.E., Luschin-Ebengreuth, N., Stabentheiner, E., Müller, M and Zechmann, B. 2014. Compartment Specific Response of Antioxidants to Drought Stress in Arabidopsis. *Plant Science* **227**:133–44.

Koo, J.C. et al., 2017. The Protein Trio RPK1–CaM4–RbohF Mediates Transient Superoxide Production to Trigger Age-Dependent Cell Death in Arabidopsis. *Cell Reports* **21**:3373–80.

Kopka J. et al. (2005). GMD@CSB.DB: the golm metabolome database. *Bioinformatics* **21**:1635–1638.

Kosma, D. K. et al., 2009. The Impact of Water Deficiency on Leaf Cuticle Lipids of Arabidopsis. *Plant Physiology* **151**:1918–29.

Kotchoni, S.O., Larrimore, K.E., Mukherjee, M., Kempinski, C.F and Barth, C. 2008. Alterations in the Endogenous Ascorbic Acid Content Affect Flowering Time in Arabidopsis. *Plant Physiology* **149**:803–15.

Koyama, T. 2014. The Roles of Ethylene and Transcription Factors in the Regulation of Onset of Leaf Senescence. *Frontiers in Plant Science* **5**:650.

Krieger-Liszkay, A. 2005. Singlet Oxygen Production in Photosynthesis. *Journal of Experimental Botany* **56**:337-46.

Krizek, D.T. 2004. Influence of PAR and UV-A in Determining Plant Sensitivity and Photomorphogenic Responses to UV-B Radiation. *Photochemistry and Photobiology* **79**:307–15.

Kushiro, T. et al., 2004. The *Arabidopsis* Cytochrome *P450 CYP707A* Encodes ABA 8'-hydroxylases: Key Enzymes in ABA Catabolism. *The EMBO Journal* **23**:1647–56.

Kwak, J.M. et al., 2003. NADPH Oxidase *AtrbohD* and *AtrbohF* Genes Function in ROS-Dependent ABA Signaling in Arabidopsis. *EMBO Journal* **22**:2623–33.

Lai, A.G., Denton-Giles, M., Mueller-Roeber, B., Schippers, J.H.M and Dijkwel, P.P. 2011. Positional Information Resolves Structural Variations and Uncovers an Evolutionarily Divergent Genetic Locus in Accessions of *Arabidopsis thaliana*. *Genome Biology and Evolution* **3**:627–40.

Lai, X.J. et al., 2015. Glycerol-3-Phosphate Metabolism Plays a Role in Stress Response in the Red Alga Pyropia Haitanensis. *Journal of Phycology* **51**:321–31.

Laloi, C., Apel, K and Danon, A. 2004. Reactive Oxygen Signalling: The Latest News. *Current Opinion in Plant Biology* **7**:323–28.

Lamb, R. S. 2012. Abiotic Stress Responses in Plants: A Focus on the SRO Family. *Advances in Selected Plant Physiology Aspects* 3-22.

Langmead, B and Salzberg, S.L. 2012. Fast Gapped-Read Alignment with Bowtie 2. *Nature methods* **9**:357–59.

Lauter, N., Kampani, A., Carlson, S., Goebel, M and Moose, S.P. 2005. *microRNA172* down-Regulates glossy15 to Promote Vegetative Phase Change in Maize. *Proceedings of the National Academy of Sciences of the United States of America* **102**:9412–17.

Lee, D.H and Lee, C.B. 2000. Chilling Stress-Induced Changes of Antioxidant Enzymes in the Leaves of Cucumber: In Gel Enzyme Activity Assays. *Plant Science* **159**:75–85.

Lee, R. H., Wang, C.H., Huang, L.T and Chen. S.C. 2001. Leaf Senescence in Rice Plants: Cloning and Characterization of Senescence up-Regulated Genes. *Journal of Experimental Botany* **52**:1117–21.

Lee, S.B., Lee, S.J and Kim, S.Y. 2015. AtERF15 Is a Positive Regulator of ABA Response. *Plant Cell Reports* **34**:71–81.

Lee, S.C and Luan, S. 2012. ABA Signal Transduction at the Crossroad of Biotic and Abiotic Stress Responses. *Plant, Cell and Environment* **35**:53–60.

Lee, Y. and Satter, R.L. 1983. Effects of Age, Water Stress, and 1-Aminocyclopropane-1-Carboxylic Acid on Leaflet Movement in Albizzia Julibrissin. *Plant Physiology* **71**:669–72.

Lemoine, R. et al., 2013. Source-to-Sink Transport of Sugar and Regulation by Environmental Factors. *Frontiers in Plant Science* **4**:272.

Leng, P., Yuan, B., Guo, Y and Chen, P. 2014. The Role of Abscisic Acid in Fruit Ripening and Responses to Abiotic Stress. *Journal of Experimental Botany* **65**:4577–88.

Leopold, A.C., Musgrave, M.E and Williams, K.M. 1981. Solute Leakage Resulting from Leaf Desiccation. *Plant Physiology* **68**:1222–25.

Lesk, C., Rowhani, P and Ramankutty, N. 2016. Influence of Extreme Weather Disasters on Global Crop Production. *Nature* **529**:84–87.

Luedemann, A., Strassburg, K., Erban, A., Kopka J. (2008). TagFinder for the quantitative analysis of gas chromatography–mass spectrometry (GC-MS)-based metabolite profiling experiments. *Bioinformatics* **24**:732–737.

Li, C. et al., 2015. Melatonin Mediates the Regulation of ABA Metabolism, Free-Radical Scavenging, and Stomatal Behaviour in Two Malus Species under Drought Stress. *Journal of Experimental Botany* **66**:669–80.

Li, G. et al., 2012. Dual-Level Regulation of ACC Synthase Activity by *MPK3/MPK6* Cascade and Its Downstream WRKY Transcription Factor during Ethylene Induction in Arabidopsis. *PLoS Genetics* **8**:e1002767.

Li, J. et al., 2007. Functional Analysis of Maize *RAD51* in Meiosis and Double-Strand Break Repair. *Genetics* **176**:1469–82.

Li, J., Besseau, S and Petri, T. 2013. Defense-Related Transcription Factors *WRKY70* and *WRKY54* Modulate Osmotic Stress Tolerance by Regulating Stomatal Aperture in Arabidopsis. *The New Phytologist* **200**:457–72.

Li, Jinjie et al., 2017a. *OsASR5* Enhances Drought Tolerance through a Stomatal Closure Pathway Associated with ABA and H_2O_2 Signalling in Rice. *Plant Biotechnology Journal* **15**:183–96.

Li, S., Fu, Q., Huang, W and Yu, D. 2009. Functional Analysis of an Arabidopsis Transcription Factor *WRKY25* in Heat Stress. *Plant Cell Reports* **28**:683–93.

Li, S., Zhou, X., Chen, L., Huang, W and Yu, D. 2010. Functional Characterization of *Arabidopsis thaliana*

WRKY39 in Heat Stress. *Molecules and Cells* **29**:475–83.

Li, Y., Zhao, H., Duan, B., Korpelainen, H and Li, C. 2011. Effect of Drought and ABA on Growth, Photosynthesis and Antioxidant System of Cotinus Coggygria Seedlings under Two Different Light Conditions. *Environmental and Experimental Botany* **71**:107–13.

Li, Y. et al., 2017b. Arabidopsis *MAPKKK18* Positively Regulates Drought Stress Resistance via Downstream MAPKK3. *Biochemical and Biophysical Research Communications* **484**:292–97.

Li, Z., Peng, J., Wen, X and Guo, H. 2012. Gene Network Analysis and Functional Studies of Senescence-Associated Genes Reveal Novel Regulators of Arabidopsis Leaf Senescence. *Journal of Integrative Plant Biology* **54**:526–39.

Li, Z., Peng, J., Wen, X and Guo, H. 2013. *Ethylene-insensitive3* Is a Senescence-Associated Gene That Accelerates Age-Dependent Leaf Senescence by Directly Repressing miR164 Transcription in Arabidopsis. *The Plant Cell* **25**:3311–28.

Liebthal, M and Dietz, K.J. 2017. The fundamental role of reactive oxygen oxygen species in plant stress response. *Methods in Molecular Biology* **1631**:23-39.

Lim, P.O., Kim, H.J and Nam, H.G. 2007. Leaf Senescence. *Annual Review of Plant Biology* **58**:115–36.

Liu, H. et al., 2011. Ectopic Expression of a Grapevine Transcription Factor VvWRKY11 Contributes to Osmotic Stress Tolerance in Arabidopsis. *Molecular Biology Reports* **38**:417–27.

Liu, Y and Zhang, S. 2004. Phosphorylation of 1-Aminocyclopropane-1-Carboxylic Acid Synthase by *MPK6*, a Stress-Responsive Mitogen-Activated Protein Kinase, Induces Ethylene Biosynthesis in Arabidopsis. *The Plant Cell* **16**:3386–99.

Liu, Y., Ye, N., Liu, R., Chen, M and Zhang, J. 2010. H_2O_2 Mediates the Regulation of ABA Catabolism and GA Biosynthesis in Arabidopsis Seed Dormancy and Germination. *Journal of Experimental Botany* **61**:2979–90.

Liu, Y and He, C. 2017. A Review of Redox Signaling and the Control of MAP Kinase Pathway in Plants. *Redox Biology* **11**:192–204.

Ljung, K. et al., 2005. Sites and Regulation of Auxin Biosynthesis in Arabidopsis Roots. *The Plant Cell* **17**:1090–1104.

Lo, H.L. et al., 2005. Differential Biologic Effects of *CPD* and *6-4PP* UV-Induced DNA Damage on the Induction of Apoptosis and Cell-Cycle Arrest. *BMC Cancer* **5**:135.

Loreto, F., Paola, P., Manes, F and Kollist, H. 2004. Impact of Ozone on Monoterpene Emissions and Evidence for an Isoprene-like Antioxidant Action of Monoterpenes Emitted by Quercus Ilex Leaves. *Tree Physiology* **24**:361–67.

Lou, D., Wang, H., Liang, G and Yu, D. 2017. *OsSAPK2* Confers Abscisic Acid Sensitivity and Tolerance to Drought Stress in Rice. *Frontiers in Plant Science* **8**:1–15.

Lu, J and Holmgren, A. 2014. The Thioredoxin Antioxidant System. *Free Radical Biology and Medicine* **66**:75–87.

Lü, P. et al., 2013. *RhEXPA4*, a Rose Expansin Gene, Modulates Leaf Growth and Confers Drought and Salt Tolerance to Arabidopsis. *Planta* **237**:1547–59.

Lu, Z., Liu, D and Liu, S. 2007. Two Rice Cytosolic Ascorbate Peroxidases Differentially Improve Salt Tolerance in Transgenic Arabidopsis. *Plant Cell Reports* **26**:1909–17.

Lutz, K.A., Wang, W., Zdepski, A and Michael, T.P. 2011. Isolation and Analysis of High Quality Nuclear DNA with Reduced Organellar DNA for Plant Genome Sequencing and Resequencing. *BMC Biotechnology* **11**:54.

Maggio, A., Hasegawa, P.M., Bressan, R.A., Consiglio, M.F and Joly, R.J. 2001. Unravelling the Functional Relationship between Root Anatomy and Stress Tolerance. *Australian Journal of Plant Physiology* **28**:999–1004.

Maia, J.M. et al., 2013. Differences in Cowpea Root Growth Triggered by Salinity and Dehydration Are Associated with Oxidative Modulation Involving Types I and III Peroxidases and Apoplastic Ascorbate. *Journal of Plant Growth Regulation* **32**:376–87.

Malinovsky, F.G., Jonatan, U.F, and William, G.T.W. 2014. The Role of the Cell Wall in Plant Immunity. *Frontiers in Plant Science* **5**:178.

Mandadi, K. K., Misra, A., Ren, S and McKnight, T.D. 2009. BT2, a BTB Protein, Mediates Multiple Responses to Nutrients, Stresses, and Hormones in Arabidopsis. *Plant Physiology* **150**:1930–39.

Manickavelu, A., Nadarajan, N., Ganesh, S.K., Gnanamalar, R.P and Chandra B.R. 2006. Drought Tolerance in Rice: Morphological and Molecular Genetic Consideration. *Plant Growth Regulation* **50**:121–38.

Matsuoka, D., Takuto Y., Tomoyuki F, and Takashi N. 2015. An Abscisic Acid Inducible Arabidopsis MAPKKK, *MAPKKK18* Regulates Leaf Senescence via Its Kinase Activity. *Plant Molecular Biology* **87**:565–75.

Mckersie, B.D. et al., 1993. Superoxide Dismutase Enhances Tolerance of Freezing Stress in Transgenic Alfalfa (*Medicago Safiva 1*). *Plant Physiol*ogy **103**:1155–63.

Mehrotra, R. et al., 2014. Abscisic Acid and Abiotic Stress Tolerance - Different Tiers of Regulation. *Journal of Plant Physiology* **171**:486–96.

Meinke, D. W., Cherry, J.M., Dean, C., Rounsley, S.D and Koornneef, M. 1998. *Arabidopsis thaliana*: A Model Plant for Genome Analysis. *Science* **282**:662–82.

Melotto, M. et al., 2009. Protein. *East* **55**:979–88.

Melotto, M., Underwood, W., Koczan, J., Nomura, K and He, S.Y. 2006. Plant Stomata Function in Innate Immunity against Bacterial Invasion. *Cell* **126**:969–80.

Meyer, Y. et al., 2008. Glutaredoxins and Thioredoxins in Plants. *Biochimica et Biophysica Acta - Molecular Cell Research* **1783**:589–600.

Miao, Y., Laun, T., Zimmermann, P and Zentgraf, U. 2004. Targets of the WRKY53 Transcription Factor and Its Role during Leaf Senescence in Arabidopsis. *Plant Molecular Biology* **55**:853–67.

Miao, Y and Zentgraf, U. 2007. The Antagonist Function of Arabidopsis *WRKY53* and *ESR/ESP* in Leaf Senescence Is Modulated by the Jasmonic and Salicylic Acid Equilibrium. *The Plant Cell* **19**:819–30.

Milchunas, D.G. et al., 2004. UV Radiation Effects on Plant Growth and Forage Quality in a Shortgrass Steppe Ecosystems. *Photochemistry and Photobiology* **79**:404–10.

Miles, G.P., Samuel, M.A., Zhang, Y and Ellis, B.E. 2005. RNA Interference-Based (RNAi) Suppression of *AtMPK6*, an Arabidopsis Mitogen-Activated Protein Kinase, Results in Hypersensitivity to Ozone and Misregulation of *AtMPK3*. *Environmental Pollution* **138**:230–37.

Miller-Messmer, M. et al., 2012. RecA-Dependent DNA Repair Results in Increased Heteroplasmy of the Arabidopsis Mitochondrial Genome. *Plant Physiology* **159**:211–26.

Miller, G., Suzuki, N., Ciftci-Yilmaz, S and Mittler, R. 2010. Reactive Oxygen Species Homeostasis and

Signalling during Drought and Salt stresses. *Plant, Cell and Environment* **33**:453–67.

Miller, J. D., Arteca, R. N and Pell, E. J. 1999a. Senescence-Associated Gene Expression during Ozone-Induced Leaf Senescence in Arabidopsis. *Plant Physiology* **120**:1015–24.

Mittler, R. 2002. Oxidative Stress, Antioxidants and Stress Tolerance. *Trends in Plant Science* **7**:405–10.

Mittler, R. et al., 2011. ROS Signaling: The New Wave? *Trends in Plant Science* **16**:300–309.

Mittler, R., Vanderauwera, S., Gollery, M and Breusegem, F.V. 2004. Reactive Oxygen Gene Network of Plants. *Trends in Plant Science* **9**:490–98.

Mitton, F.M., Gonzalez, M., Monserrat, J.M and Miglioranza, K.S.B. 2017. Ecotoxicology and Environmental Safety DDTs-Induced Antioxidant Responses in Plants and Their in Fl Uence on Phytoremediation Process. *Ecotoxicology and Environmental Safety* **147**:151–56.

Mitula, F. et al., 2015. Arabidopsis ABA-Activated Kinase *MAPKKK18* Is Regulated by Protein Phosphatase 2C ABI1 and the Ubiquitin-Proteasome Pathway. *Plant and Cell Physiology* **56**:2351–67.

Møller, I.M., Jensen, P.E and Hansson, A. 2007. Oxidative Modifications to Cellular Components in Plants. *Annual Review of Plant Biology* **58**:459–81.

Moore, B. et al., 2003. Role of the Arabidopsis Glucose Sensor *HXK1* in Nutrient, Light, and Hormonal Signaling. *Science* **300**:332–36.

Morkunas, I., Borek, S., Formela, M and Ratajczak, L. 2012. Plant Responses to Sugar Starvation. *Carbohydrates - Comprehensive Studies on Glycobiology and Glycotechnology*. Prof. Chuan-Fa Chang (Ed.), InTech.

Morkunas, I., Garnczarska, M., Bednarski, W., Ratajczak, W and Waplak, S. 2003. Metabolic and Ultrastructural Responses of Lupine Embryo Axes to Sugar Starvation. *Journal of Plant Physiology* **160**:311–19.

Moustaka, J., Tanou, G., Adamakis, I.D., Eleftheriou, E.P and Moustakas, M. 2015. Leaf Age-Dependent Photoprotective and Antioxidative Response Mechanisms to Paraquat-Induced Oxidative Stress in *Arabidopsis thaliana*. *International Journal of Molecular Sciences* **16**:13989–6.

Mueller-Roeber, B and Balazadeh, S. 2014. Auxin and Its Role in Plant Senescence. *Journal of Plant Growth Regulation* **33**:21–33.

Muhlenbock, P., Plaszczyca, M., Plaszczyca, M., Mellerowicz, E and Karpinski, S. 2007. Lysigenous Aerenchyma Formation in Arabidopsis Is Controlled by *LESION SIMULATING DISEASE1*. *The Plant Cell Online* **19**:3819–30.

Müller, M and Munné-Bosch, S. 2015. Ethylene Response Factors: A Key Regulatory Hub in Hormone and Stress Signaling. *Plant Physiology* **169**:32–41.

Munné-Bosch, S and Alegre, L. 2004. Die and Let Live: Leaf Senescence Contributes to Plant Survival under Drought Stress. *Functional Plant Biology* **31**:203–16.

Munns, R., Schachtman, D and Condon, A. 1995. The Significance of a Two-Phase Growth Response to Salinity in Wheat and Barley. *Australian Journal of Plant Physiology* **22**:561–69.

Munns, R and Termaat, A. 1986. Whole-Plant Responses to Salinity. *Aust. J. Plant Physiology* **13**:143–60.

Murphy, Michael P. 2009. How Mitochondria Produce Reactive Oxygen Species. *Biochemical Journal* **417**:1–13.

Nakabayashi, R. et al., 2014. Enhancement of Oxidative and Drought Tolerance in Arabidopsis by Overaccumulation of Antioxidant Flavonoids. *Plant Journal* **77**:367–79.

Nakano, T. 2006. Genome-Wide Analysis of the ERF Gene Family in Arabidopsis and Rice. *Plant Physiology*

140:411–32.

Nanjo, T. et al., 1999. Biological Functions of Proline in Morphogenesis and Osmotolerance Revealed in Antisense Transgenic *Arabidopsis thaliana*. *Plant Journal* **18**:185–93.

Nawkar, G.M. et al., 2013. UV-Induced Cell Death in Plants. *International Journal of Molecular Sciences* **14**:1608–28.

Neill, S., Desikan, R and Hancock, J. 2002. Hydrogen Peroxide Signalling. *Current Opinion in Plant Biology* **5**:388–95.

Nelson, N. 2011. Photosystems and Global Effects of Oxygenic Photosynthesis. *Biochimica et Biophysica Acta - Bioenergetics* **1807**:856–63.

Nishiyama, R. et al., 2012. Transcriptome Analyses of a Salt-Tolerant Cytokinin-Deficient Mutant Reveal Differential Regulation of Salt Stress Response by Cytokinin Deficiency. *PLoS ONE* **7**:e32124.

Niu, L and Liao, W. 2016. Hydrogen Peroxide Signaling in Plant Development and Abiotic Responses: Crosstalk with Nitric Oxide and Calcium. *Frontiers in Plant Science* **7**:230.

Noctor, G. et al., 2012. Glutathione in Plants: An Integrated Overview. *Plant, Cell and Environment* **35**:454–84.

Noctor, G and Foyer, C.H. 1998. ASCORBATE AND GLUTATHIONE: Keeping Active Oxygen Under Control. *Annual Review of Plant Physiology and Plant Molecular Biology* **49**:249–79.

Noh, Y.S and Amasino, R.M. 1999. Identification of a Promoter Region Responsible for the Senescence-Specific Expression of SAG12. *Plant Molecular Biology* **41**:181–94.

Nordström, K.J.V. et al., 2013. Mutation Identification by Direct Comparison of Whole-Genome Sequencing Data from Mutant and Wild-Type Individuals Using K-Mers. *Nature Biotechnology* **31**:325–30.

O'Brien, J.A., Daudi, A., Butt, V.S and Bolwell, G.P. 2012. Reactive Oxygen Species and Their Role in Plant Defence and Cell Wall Metabolism. *Planta* **236**:765–79.

O'Hara, L.E., Paul, M.J and Wingler, A. 2013. How Do Sugars Regulate Plant Growth and Development? New Insight into the Role of Trehalose-6-Phosphate. *Molecular Plant* **6**:261–74.

Oh, S.A., Lee, S.Y., Chung, I.K., Lee, C.H and Nam, H.G. 1996. A Senescence-Associated Gene of *Arabidopsis thaliana* Is Distinctively Regulated during Natural and Artificially Induced Leaf Senescence. *Plant Molecular Biology* **30**:739–54.

Oliver, C. N., Ahn, B.W., Moerman, E.J., Goldstein, S and Stadtman, E.R. 1987. Age-Related Changes in Oxidized Proteins. *Journal of Biological Chemistry* **262**:5488–91.

Van Oosten, M.J. et al., 2017. A Benzimidazole Proton Pump Inhibitor Increases Growth and Tolerance to Salt Stress in Tomato. *Frontiers in Plant Science* **8**:1220.

Ortiz-Masia, D., Perez-Amador, M.A., Carbonell, J and Marcote, M.J. 2007. Diverse Stress Signals Activate the C1 Subgroup MAP Kinases of Arabidopsis. *FEBS Letters* **581**:1834–40.

Osakabe, Y., Osakabe, K., Shinozaki, K and Tran, L.S.P. 2014. Response of Plants to Water Stress. *Frontiers in Plant Science* **5**:86.

Overmyer, K. et al., 2000. Ozone-Sensitive Arabidopsis rcd1 Mutant Reveals Opposite Roles for Ethylene and Jasmonate Signaling Pathways in Regulating Superoxide-Dependent Cell Death. *The Plant Cell* **12**:1849–62.

Pandey, P., Irulappan, V., Bagavathiannan, M.V and Senthil-Kumar, M. 2017. Impact of Combined Abiotic and Biotic Stresses on Plant Growth and Avenues for Crop Improvement by Exploiting Physio-Morphological

Traits. *Frontiers in Plant Science* **8**:537.

Pandey, P., Ramegowda, V and Senthil-Kumar, M. 2015. Shared and Unique Responses of Plants to Multiple Individual Stresses and Stress Combinations: Physiological and Molecular Mechanisms. *Frontiers in Plant Science* **6**:723.

Pantin, F., Simonneau, T., Rolland, G., Dauzat, M and Muller, B. 2011. Control of Leaf Expansion: A Developmental Switch from Metabolics to Hydraulics. *Plant Physiology* **156**:803–15.

Papp, J.C., Ball, M.C and Terry, N. 1983. A Comparative Study of the Effects of NaCl Salinity on Respiration, Photosynthesis, and Leaf Extension Growth in *Beta Vulgaris L.* (Sugar Beet). *Plant, Cell and Environment* **6**:675–77.

Park, A.K. et al., 2016. Structure and Catalytic Mechanism of Monodehydroascorbate Reductase, MDHAR, from *Oryza Sativa L. Japonica*. *Scientific Reports* **6**:33903.

Parrott, D., Yang, L., Shama, L and Fischer, A.M. 2005. Senescence Is Accelerated, and Several Proteases Are Induced by Carbon 'feast' conditions in Barley (*Hordeum Vulgare L.*) Leaves. *Planta* **222**:989–1000.

Paul, M. J. and Driscoll, S.P. 1997. Sugar Repression of Photosynthesis: The Role of Carbohydrates in Signalling Nitrogen Deficiency through Source:sink Imbalance. *Plant, Cell and Environment* **20**:110–16.

Pech, J.C., Purgatto, E., Bouzayen, M and Latché, A. 2012. Ethylene and Fruit Ripening. *The Plant Hormone Ethylene* **44**:275-304.

Perl, A. et al., 1993. Enhanced Oxidative-Stress Defense in Transgenic Potato Expressing Tomato Cu,Zn Superoxide Dismutases. *Theoretical and Applied Genetics* **85**:568–76.

Perveen, R., Jamil, Y., Ashraf, M., Ali, Q., Iqbal, M., Ahmad, M.R. 2011. He-Ne Laser-Induced Improvement in Biochemical, Physiological, Growth and Yieldcharacteristics in Sunflower (*Helianthus Annuus L.*). *Photochem Photobiol* **87**:1453–63.

Perrot-Rechenmann, C. 2010. Cellular Responses to Auxin: Division versus Expansion. *Cold Spring Harbor Perspectives in Biology* **2**:a001446.

Petronia, C., Annunziata, M.G., Pontecorvo, G., Fuggi, A and Woodrow, P. 2011. Salt stress and Salt Tolerance. *Intech* **6**:111–33.

Petrov, V., Hille, J., Mueller-Roeber, B and Gechev, T.S. 2015. ROS-Mediated Abiotic Stress-Induced Programmed Cell Death in Plants. *Frontiers in Plant Science* **6**:69.

Pitzschke, A. and Hirt, H. 2008. Disentangling the Complexity of Mitogen-Activated Protein Kinases and Reactive Oxygen Species Signaling. *Plant Physiology* **149**:606–15.

Podgórska, A., Burian, M and Szal, B. 2017. Extra-Cellular But Extra-Ordinarily Important for Cells: Apoplastic Reactive Oxygen Species Metabolism. *Frontiers in Plant Science* **8**:1–20.

Poorter, H. 1993. Interspecific Variation in the Growth Response of Plants to an Elevated Ambient CO_2 Concentration. *Vegetatio* **104**:77–97.

Porebski, S., Bailey, L.G and Baum, B.R. 1997. Modification of a CTAB DNA Extraction Protocol for Plants Containing High Polysaccharide and Polyphenol Components. *Plant Molecular Biology Reporter* **15**:8–15.

Qin, Y.M., Hu, C.Y., Zhu, Y.X. 2008. The Ascorbate Peroxidase Regulated by H_2O_2 and Ethylene Is Involved in Cotton Fiber Cell Elongation by Modulating ROS Homeostasis. *Plant Signaling and Behavior* **3**:194–96.

Qiu, Z., Li, J., Zhang, M., Bi, Z and Li, Z. 2013. He-Ne Laser Pretreatment Protects Wheat Seedlings against Cadmium-Induced Oxidative Stress. *Ecotoxicology and Environmental Safety* **88**:135–41.

Qu, J, Kang, S.G., Hah, C and Jang, J.C. 2016. Molecular and Cellular Characterization of GA-Stimulated Transcripts *GASA4* and *GASA6* in *Arabidopsis thaliana*. *Plant Science* **246**:1–10.

Qu, Y., Yan, M and Zhang, Q. 2017. Functional Regulation of Plant NADPH Oxidase and Its Role in Signaling. *Plant Signaling and Behavior* **12**:e1356970.

Raghavendra, A.S., Gonugunta, V.K., Christmann, A and Grill, E. 2010. ABA Perception and Signalling. *Trends in Plant Science* **15**:395–401.

Ramanjulu, S. and Bartels, D. 2002. Drought- and Desiccation-Induced Modulation of Gene Expression in Plants. *Plant, Cell and Environment* **25**:141–51.

Rani, V., Mishra, S., Yadav, T., Yadav, U.C.S and Kohli, S. 2015. Hydrogen Peroxide Sensing and Signaling. *Free Radicals in Human Health and Disease*. Rani V., Yadav U (Eds.),105-16.

Rasmusson, A.G., Geisler, D.A and Møller, I.M. 2008. The Multiplicity of Dehydrogenases in the Electron Transport Chain of Plant Mitochondria. *Mitochondrion* **8**:47–60.

Reidt, W., Wurz, R., Wanieck, K., Chu, H.H and Puchta, H. 2006. A Homologue of the Breast Cancer-Associated Gene *BARD1* Is Involved in DNA Repair in Plants. *The EMBO Journal* **25**:4326–37.

Rejeb, I., Pastor, V and Mauch-Mani, B. 2014. Plant Responses to Simultaneous Biotic and Abiotic Stress: Molecular Mechanisms. *Plants* **3**:458–75.

Ribeiro, C.W. et al., 2017. Rice Peroxisomal Ascorbate Peroxidase Knockdown Affects ROS Signaling and Triggers Early Leaf Senescence. *Plant Science* **263**:55–65.

Riboni, M., Test, A.R., Galbiati, M., Tonelli, C and Conti, L. 2014. Environmental Stress and Flowering Time. *Plant Signaling and Behavior* **9**:e29036.

Del Rio, L. A. et al., 2002. Reactive Oxygen Species, Antioxidant Systems and Nitric Oxide in Peroxisomes. *Journal of Experimental Botany* **53**:1255–72.

Del, R.L.A and López-Huertas, E. 2016. ROS Generation in Peroxisomes and Its Role in Cell Signaling. *Plant and Cell Physiology* **57**:1364–76.

del Río, L.A., Sandalio, L.M., Corpas, F.J., Palma, J.M and Barroso, J.B. 2006. Reactive Oxygen Species and Reactive Nitrogen Species in Peroxisomes. Production, Scavenging, and Role in Cell Signaling. *Plant Physiology* **141**:330–35.

Roden, L.C., Song, H.R., Jackson, S., Morris, K and Carre, I.A. 2002. Floral Responses to Photoperiod Are Correlated with the Timing of Rhythmic Expression Relative to Dawn and Dusk in Arabidopsis. *Proceedings of the National Academy of Sciences of the United States of America* **99**:13313–18.

Roldán-Arjona, T and Ariza, R.R. 2009. Repair and Tolerance of Oxidative DNA Damage in Plants. *Mutation Research - Reviews in Mutation Research* **681**:169–79.

Rolland, F. and Sheen, J. 2005. Sugar Sensing and Signalling Networks in Plants. *Biochemical Society Transactions* **33**:269–71.

Rosa, M. et al., 2009. Soluble Sugars-Metabolism, Sensing and Abiotic Stress a Complex Network in the Life of Plants. *Plant Signaling and Behavior* **4**:388–93.

Rose, J.K.C., Braam, J., Fry, S.C and Nishitani, K. 2002. The XTH Family of Enzymes Involved in Xyloglucan Endotransglucosylation and Endohydrolysis: Current Perspectives and a New Unifying Nomenclature. *Plant and Cell Physiology* **43**:1421–35.

Rouhier, N., Santos, C.V.D., Tarrago, L and Rey, P. 2006. Plant Methionine Sulfoxide Reductase A and B

Multigenic Families. *Photosynthesis Research* **89**:247-62.

Roy, S. 2016. Function of MYB Domain Transcription Factors in Abiotic Stress and Epigenetic Control of Stress Response in Plant Genome. *Plant Signaling and Behavior* **11**:1–7.

Rubinovich, L and Weiss, D. 2010. The Arabidopsis Cysteine-Rich Protein GASA4 Promotes GA Responses and Exhibits Redox Activity in Bacteria and in Planta. *Plant Journal* **64**:1018–27.

Rushton, P.J., Somssich, I.E., Ringler, P and Shen, Q.J. 2010. WRKY Transcription Factors. *Trends in Plant Science* **15**:247–58.

Sah, S.K., Reddy, K.R and Li, J. 2016. Abscisic Acid and Abiotic Stress Tolerance in Crop Plants. *Frontiers in Plant Science* **7**:571.

Sahoo, S., Awasthi, J.P and Sunkar, R. 2017. Plant Stress Tolerance. *Methods in Molecular Biology* **1631**:273–77.

Samota, M.K. et al., 2017. Elicitor-Induced Biochemical and Molecular Manifestations to Improve Drought Tolerance in Rice (*Oryza Sativa L.*) through Seed-Priming. *Frontiers in Plant Science* **8**:934.

Sani, E., Herzyk, P., Perrella, G., Colot, V and Amtmann, A. 2013. Hyperosmotic Priming of Arabidopsis Seedlings Establishes a Long-Term Somatic Memory Accompanied by Specific Changes of the Epigenome. *Genome Biology* **14**:59.

Santino, A. et al., 2013. Jasmonate Signaling in Plant Development and Defense Response to Multiple (A)biotic Stresses. *Plant Cell Reports* **32**:1085–98.

Saradhi, P.P., Alia Arora and Prasad, KV. 1995. Proline Accumulates in Plants Exposed to UV Radiation and Protects Them against UV Induced Peroxidation. *Biochemical and Biophysical Research Communications* **209**:1–5.

Savvides, A., Ali, S., Tester, M., and Fotopoulos, V. 2016. Chemical Priming of Plants Against Multiple Abiotic Stresses: Mission Possible? *Trends in Plant Science* **21**:329–40.

Scandalios, J. G. 2005. Oxidative Stress: Molecular Perception and Transduction of Signals Triggering Antioxidant Gene Defenses. *Brazilian Journal of Medical and Biological Research* **38**:995–1014.

Scarpeci, T.E., Frea, V.S., Zanor, M.I and Valle, E.M. 2017. Overexpression of *AtERF019* Delays Plant Growth and Senescence, and Improves Drought Tolerance in Arabidopsis. *Journal of Experimental Botany* **68**:673–85.

Schaller, G.E. 2012. Ethylene and the Regulation of Plant Development. *BMC Biology* **10**:9.

Schieber, M and Chandel, N.S. 2014. ROS Function in Redox Signaling and Oxidative Stress. *Current Biology* **24**:453-62.

Schippers, J.H.M., Nunes-Nesi, A., Apetrei, R., Hille, J., Fernie, A.R and Dijkwel, P.P. 2008. The Arabidopsis *Onset of Leaf death5* Mutation of Quinolinate Synthase Affects Nicotinamide Adenine Dinucleotide Biosynthesis and Causes Early Ageing. *The Plant Cell Online* **20**:2909–25.

Schippers, J.H.M., Ellens, R., Hille, J and Dijkwel. P.P. 2008. Early Leaf Senescence of *old13* Is Partially Dependent on Salicylic Acid and Associated with Increased Oxidative Stress and Altered Water Balance. University of Groningen, Haren. 67–88.

Schippers, Jos H. M., Hai-chun Jing, Jacques Hille, and Paul P. Dijkwel. 2007. Developmental and Hormonal Control of Leaf Senescence. *Annual Plant Reviews* **26**:9–44.

Sedigheh, H.G. et al., 2011. Oxidative Stress and Leaf Senescence. *BMC research notes* **4**:477.

Sekiya, J., Wilson, L.G and Filner, P. 1982. Resistance to Injury by *Sulfur Dioxide 1*. *Plant Physiology* **70**:437–41.

Sharabi-Schwager, M., Samach, A and Porat, R. 2010. Overexpression of the *CBF2* Transcriptional Activator in Arabidopsis Suppresses the Responsiveness of Leaf Tissue to the Stress Hormone Ethylene. *Plant Biology (Stuttgart, Germany)* **12**:630–38.

Sharabi-Schwager, M., Lers, A., Samach, A., Guy, C.L and Porat, R. 2010. Overexpression of the *CBF2* Transcriptional Activator in Arabidopsis Delays Leaf Senescence and Extends Plant Longevity. *Journal of Experimental Botany* **61**:261–73.

Sharabi-Schwager, M., Lers, A., Samach, A and Porat, R. 2009. Relationship between Plant Stress Tolerance, Senescence and Life Span. *Stewart Postharvest Review* **5**:1–6.

Sharma, I and Ahmad, P. 2014. Catalase: A Versatile Antioxidant in Plants. *Oxidative Damage to Plants: Antioxidant Networks and Signaling* :131-48.

Sharma, P., Jha, A.B., Dubey, R.S and Pessarakli, M. 2012. Reactive Oxygen Species, Oxidative Damage, and Antioxidative Defense Mechanism in Plants under Stressful Conditions. *Journal of Botany* **12**:1–26.

Shavrukov, Y. 2013. Salt Stress or Salt Shock: Which Genes Are We Studying? *Journal of Experimental Botany* **64**:119–27.

Sheard, L.B. et al., 2010. Jasmonate Perception by Inositol-Phosphate-Potentiated COI1-JAZ Co-Receptor. *Nature* **468**:400–05.

Sheldon, C. C. 2000. The Molecular Basis of Vernalization: The Central Role of FLOWERING LOCUS C (*FLC*). *Proceedings of the National Academy of Sciences* **97**:3753–58.

Shen, G., Niu, J and Deng, Z. 2017. Abscisic Acid Treatment Alleviates Cadmium Toxicity in Purple Flowering Stalk (*Brassica Campestris L. Ssp. Chinensis Var. Purpurea Hort.*) Seedlings. *Plant Physiology and Biochemistry* **118**:471–78.

Shendure, J and Ji, H. 2008. Next-Generation DNA Sequencing. *Nat. Biotechnol.* **26**:1135–45.

Shinozaki, K and Yamaguchi-Shinozaki, K. 2007. Gene Networks Involved in Drought Stress Response and Tolerance. *Journal of Experimental Botany* **58**:221-27.

Siaud, N. et al., 2004. *Brca2* Is Involved in Meiosis in *Arabidopsis thaliana* as Suggested by Its Interaction with Dmc1. *The EMBO Journal* **23**:1392–1401.

Simbolo, M. et al., 2013. DNA Qualification Workflow for Next Generation Sequencing of Histopathological Samples. *PLoS ONE* **8**:e62692.

Sinclair, T. R., Tanner, C.B and Bennett, J.M. 1984. Water-Use Efficiency in Crop Production. *BioScience* **34**:36–40.

Singh, R et al., 2017. Reactive Oxygen Species Signaling and Stomatal Movement: Current Updates and Future Perspectives. *Redox Biology* **11**:213–18.

Singh, S.K., Roy, S., Choudhury, S.R and Sengupta, D.N. 2010. DNA Repair and Recombination in Higher Plants: Insights from Comparative Genomics of Arabidopsis and Rice. *BMC Genomics* **11**:443.

Skórzyńska-Polit, E., Drążkiewicz, M and Krupa, Z. 2004. The Activity of the Antioxidative System in Cadmium-Treated *Arabidopsis thaliana*. *Biologia Plantarum* **47**:71–78.

Spangenberg, A., Hobeika, N., Prabhakaran, P., Baldeck, P and Soppera, O. 2015. Recent Advances in Plant DNA Repair. Prof. Clark Chen (Ed.), InTech.

Steffens, B. 2014. The Role of Ethylene and ROS in Salinity, Heavy Metal, and Flooding Responses in Rice. *Frontiers in Plant Science* **5**:685.

Stenzel, I. et al., 2012. ALLENE OXIDE CYCLASE (*AOC*) Gene Family Members of *Arabidopsis thaliana*: Tissue-and Organ-Specific Promoter Activities and in Vivo Heteromerization. *Journal of Experimental Botany* **63**:6125–38.

Suchar, V.A and Robberecht, R. 2015. Integration and Scaling of UV-B Radiation Effects on Plants: From DNA to Leaf. *Ecology and Evolution* **5**:2544–55.

Sukweenadhi, J. et al., 2015. Paenibacillus Yonginensis *DCY84(T)* Induces Changes in *Arabidopsis thaliana* Gene Expression against Aluminum, Drought, and Salt Stress. *Microbiological Research* **172**:7-15.

Sun, S. et al., 2013. *GASA14* Regulates Leaf Expansion and Abiotic Stress Resistance by Modulating Reactive Oxygen Species Accumulation. *Journal of Experimental Botany* **64**:1637–47.

Suzuki, N. et al., 2016. ABA Is Required for Plant Acclimation to a Combination of Salt and Heat Stress. *PLoS ONE* **11**:e0147625.

Suzuki, N., Koussevitzky, S., Mittler, R and Miller, G. 2012. ROS and Redox Signalling in the Response of Plants to Abiotic Stress. *Plant, Cell and Environment* **35**:259–70.

Swartzberg, D., Dai, N., Gan, S., Amasino, R and Granot, D. 2006. Effects of Cytokinin Production under Two SAG Promoters on Senescence and Development of Tomato Plants. *Plant Biology* **8**:579–86.

Szőllősi, R. 2014. Chapter 3 – Superoxide Dismutase (*SOD*) and Abiotic Stress Tolerance in Plants: An Overview. *Oxidative Damage to Plants.* 89-129

Takagi, H. et al., 2013. MutMap-Gap: Whole-Genome Resequencing of Mutant F2 Progeny Bulk Combined with de Novo Assembly of Gap Regions Identifies the Rice Blast Resistance Gene Pii. *New Phytologist* **200**:276–83.

Takashi, Y., Kobayashi, Y., Tanaka, K and Tamura, K. 2009. Arabidopsis Replication Protein a 70a Is Required for DNA Damage Response and Telomere Length Homeostasis. *Plant and Cell Physiology* **50**:1965–76.

Takeno, K. 2012. Stress-Induced Flowering. *Abiotic Stress Responses in Plants: Metabolism, Productivity and Sustainability.* P.Ahmad and M.N.V. Prasad (Eds.), 331-45.

Takeno, K. 2016. Stress-Induced Flowering: The Third Category of Flowering Response. *Journal of Experimental Botany* **67**:4925–34.

Tamaoki, M. et al., 2003. Differential Ozone Sensitivity among Arabidopsis Accessions and Its Relevance to Ethylene Synthesis. *Planta* **216**:552–60.

Tanou, G. et al., 2017. Exploring Priming Responses Involved in Peach Fruit Acclimation to Cold Stress. *Scientific Reports* **7**:11358.

Tanaka, Y., Sano, T., Tamaoki, M., Nakajima, N., Kondo, N. & Hasezawa, S. (2005). Ethylene inhibits abscisic acid-induced stomatal closure in Arabidopsis. Plant physiology, **138**, 2337–2343.

Taylor, N.L. 2005. Differential Impact of Environmental Stresses on the Pea Mitochondrial Proteome. *Molecular and Cellular Proteomics* **4**:1122–33.

Taylor, N.L., Day, D.A and Millar, A.H. 2002. Environmental Stress Causes Oxidative Damage to Plant Mitochondria Leading to Inhibition of Glycine Decarboxylase. *Journal of Biological Chemistry* **277**:42663–68.

Tenhaken, R. 2015. Cell Wall Remodeling under Abiotic Stress. *Frontiers in Plant Science* **5**:771.

Tetley, R.M. and Thimann, K.V. 1974. The Metabolism of Oat Leaves during Senescence: I. Respiration, Carbohydrate Metabolism, and the Action of Cytokinins. *Plant Physiology* **54**:294–303.

Thirugnanasambantham, K. et al., 2015. Role of Ethylene Response Transcription Factor (ERF) and Its Regulation in Response to Stress Encountered by Plants. *Plant Molecular Biology Reporter* **33**:347–57.

Thomas, H. 2002. Ageing in Plants. *Mechanisms of Ageing and Development* **123**:747–53.

Thomas, H. 2013. Senescence, Ageing and Death of the Whole Plant. *New Phytologist* **197**:696–711.

Thomas, S. G., Phillips, A.L and Hedden, P. 1999. Molecular Cloning and Functional Expression of Gibberellin 2- Oxidases, Multifunctional Enzymes Involved in Gibberellin Deactivation. *Proceedings of the National Academy of Sciences of the United States of America* **96**:4698–4703.

Thordal-Christensen, H., Zhang, Z., Wei, Y and Collinge, D.B. 1997. Subcellular Localization of H_2O_2 in Plants. H_2O_2 Accumulation in Papillae and Hypersensitive Response during the Barley-Powdery Mildew Interaction. *Plant Journal* **11**:1187–94.

Thorvaldsdóttir, H., Robinson, J.T and Mesirov, J.P. 2013. Integrative Genomics Viewer (IGV): High-Performance Genomics Data Visualization and Exploration. *Briefings in Bioinformatics* **14**:178–92.

Tripathy, B.C and Oelmüller, R. 2012. Reactive Oxygen Species Generation and Signaling in Plants. *Plant Signaling and Behavior* **7**:1621–33.

Tsai, I.J., Otto, T.D and Berriman, M. 2010. Improving Draft Assemblies by Iterative Mapping and Assembly of Short Reads to Eliminate Gaps. *Genome Biology* **11**:41.

Tuominen, H., Overmyer, K., Keinänen, M., Kollist, H and Kangasjärvi, J. 2004. Mutual Antagonism of Ethylene and Jasmonic Acid Regulates Ozone-Induced Spreading Cell Death in Arabidopsis. *Plant Journal* **39**:59–69.

Tuteja, N and Gill, S.S. 2013. Plant acclimation to environmental stress using priming agents. *Plant Acclimation to Environmental Stress.* Tuteja N., Singh Gill S. (Eds.):1-27.

Tuzhikov, A.I., Vartapetian, B.B., Vartapetian, A.B and Chichkova, N.V. 2008. Abiotic Stress-Induced Programmed Cell Death in Plants: A Phytaspase Connection. *Abiotic Stress Response in Plants - Physiological, Biochemical and Genetic Perspectives.* Prof. Arun Shanker (Eds.):183–96.

Ülker, B and Somssich, I.E. 2004. WRKY Transcription Factors: From DNA Binding towards Biological Function. *Current Opinion in Plant Biology* **7**:491–98.

Valares Masa, C., Sosa, D.T., Alías Gallego, J.C and Chaves Lobón, N. 2016. Quantitative Variation of Flavonoids and Diterpenes in Leaves and Stems of *Cistus Ladanifer L.* at Different Ages. *Molecules (Basel, Switzerland)* **21**:275.

Van Doorn, W.G. 2004. Is Petal Senescence due to Sugar Starvation? *Plant Physiology* **134**:35–42.

Van Doorn, W.G. 2008. Is the Onset of Senescence in Leaf Cells of Intact Plants due to Low or High Sugar Levels? *Journal of Experimental Botany* **59**:1963–72.

Voragen, A.G.J., Coenen, G.J., Verhoef, R.P and Schols, H.A. 2009. Pectin, a Versatile Polysaccharide Present in Plant Cell Walls. *Structural Chemistry* **20**:263–75.

Wada, K.C., Yamada, M and Takeno, K. 2013. Stress-Induced Flowering in Pharbitis—A Review. *American Journal of Plant Sciences* **4**:74.

Wang, C. et al., 2016a. The Cotton Mitogen-Activated Protein Kinase Kinase 3 Functions in Drought Tolerance by Regulating Stomatal Responses and Root Growth. *Plant Cell Physiology* **57**:1629-42.

Wang, C. et al., 2017. *ABP9*, a Maize bZIP Transcription Factor, Enhances Tolerance to Salt and Drought in Transgenic Cotton. *Planta* **246**:453–69.

Wang, H. et al., 2016b. Ethylene-Insensitive Mutants of *Nicotiana Tabacum* Exhibit Drought Stress Resistance. *Plant Growth Regulation* **79**:107–17.

Wang, H., Wu, Z., Han, J., Zheng, W and Yang, C. 2012. Comparison of Ion Balance and Nitrogen Metabolism in Old and Young Leaves of Alkali-Stressed Rice Plants. *PLoS ONE* **7**:1–10.

Wang, J and Bayles, K.W. 2013. Programmed Cell Death in Plants: Lessons from Bacteria? *Trends in Plant Science* **18**:133–39.

Wang, K.L., Li, H and Ecker, J.R. 2002. Ethylene Biosynthesis and Signaling Networks. *Plant Cell* **14**:131–52.

Wang, L. 2002. Gene Cloning and Function Analysis of ABP9 Protein Which Specifically Binds to ABRE2 Motif of Maize *Cat1* Gene. *Chinese Science Bulletin* **47**:1871.

Wang, Y. et al., 2014. The Arabidopsis *RAD51* Paralogs *RAD51B, RAD51D* and *XRCC2* Play Partially Redundant Roles in Somatic DNA Repair and Gene Regulation. *New Phytologist* **201**:292–304.

Wang, Z.S. et al., 2017. Salt Acclimation Induced Salt Tolerance Is Enhancedby Abscisic Acid Priming in Wheat. *Plant, Soil and Environment* **63**:307–14.

Weaver, L. M., Gan, S., Quirino, B and Amasino, R.M. 1998. A Comparison of the Expression Patterns of Several Senescence-Associated Genes in Response to Stress and Hormone Treatment. *Plant Molecular Biology* **37**:455–69.

Weaver, L.M and Amasino, R.M. 2001. Senescence Is Induced in Individually Darkened Arabidopsis Leaves, but Inhibited in Whole Darkened Plants. *Plant Physiology* **127**:876–86.

Weaver, L.M., Gan, S., Quirino, B and Amasino, R.A. 1998. A Comparison of the Expression Patterns of Several Senescence-Associated Genes in Response to Stress and Hormone Treatment. *Plant Molecular Biology* **37**:455–69.

Webb, D.M. and Knapp, S.J. 1990. DNA Extraction from a Previously Recalcitrant Plant Genus. *Plant Molecular Biology Reporter* **8**:180–85.

Wellburn, A.R. 1994. The Spectral Determination of Chlorophylls a and B, as Well as Total Carotenoids, Using Various Solvents with Spectrophotometers of Different Resolution. *Journal of Plant Physiology* **144**:307–13.

Westphal, L., Scheel, D and Rosahl, S. 2008. The *coi1-16* Mutant Harbors a Second Site Mutation Rendering PEN2 Nonfunctional. *The Plant Cell* **20**:824–26.

Wi, S.J., Jang, S.J and Park, K.Y. 2010. Inhibition of Biphasic Ethylene Production Enhances Tolerance to Abiotic Stress by Reducing the Accumulation of Reactive Oxygen Species in Nicotiana Tabacum. *Molecules and Cells* **30**:37–49.

Wienkoop, S., Baginsky, S and Weckwerth, W. 2010. *Arabidopsis thaliana* as a Model Organism for Plant Proteome Research. *Journal of Proteomics* **73**:2239–48.

Wingler, A., Fields, D and Mall, N. 2017. Transitioning to the next Phase : The Role of Sugar Signaling throughout the Plant Life Cycle. *Plant Physiology* **176**:1075-84.

Wu, A. et al., 2012. JUNGBRUNNEN1, a Reactive Oxygen Species-Responsive NAC Transcription Factor, Regulates Longevity in Arabidopsis. *The Plant cell* **24**:482–506.

Wu, G. et al., 2009. The Sequental Actions of miR156 and miR172 Regulates Developmetnal Timing in

Arabidopsis. *Cell* **138**:750–59.

Wu, G and Poethig, R.S. 2006. Temporal Regulation of Shoot Development in *Arabidopsis thaliana* by *miR156* and Its Target *SPL3*. *Development (Cambridge, England)* **133**:3539–47.

Wu, L., Zhang, Z., Zhang, H., Wang, X.C and Huang, R. 2008. Transcriptional Modulation of Ethylene Response Factor Protein JERF3 in the Oxidative Stress Response Enhances Tolerance of Tobacco Seedlings to Salt, Drought, and Freezing. *Plant Physiology* **148**:1953–63.

Xi, J., Chen, Y., Nakashima, J., Wang, S.M and Chen, R. 2013. Medicago Truncatula esn1 Defines a Genetic Locus Involved in Nodule Senescence and Symbiotic Nitrogen Fixation. *Molecular Plant-Microbe Interactions* **26**:893–902.

Xiong, L and Zhu, J.K. 2003. Regulation of Abscisic Acid Biosynthesis. *Plant Physiology* **133**:29–36.

Xu, Juan et al., 2008. Activation of *MAPK Kinase 9* Induces Ethylene and Camalexin Biosynthesis and Enhances Sensitivity to Salt Stress in Arabidopsis. *Journal of Biological Chemistry* **283**:26996–6.

Xu, M.Y. et al., 2014a. Stress-Induced Early Flowering Is Mediated by *miR169* in *Arabidopsis thaliana*. *Journal of Experimental Botany* **65**:89–101.

Xu, T. et al., 2014b. Cell Surface *ABP1-TMK* Auxin-Sensing Complex Activates *ROP* GTPase Signaling. *Science (New York)* **343**:1025–28.

Xu, W., Li, Y., Cheng, Z., Xia, G and Wang, M. 2016. A Wheat Histone Variant Gene *TaH2A.7* Enhances Drought Tolerance and Promotes Stomatal Closure in Arabidopsis. *Plant Cell Reports* **35**:1853–62.

Xu, Z.S. et al., 2007. Isolation and Molecular Characterization of the *Triticum Aestivum L*. Ethylene-Responsive Factor 1 (*TaERF1*) That Increases Multiple Stress Tolerance. *Plant Molecular Biology* **65**:719–32.

Xu, Z., Zhou, G and Shimizu, H. 2010. Plant Responses to Drought and Rewatering. *Plant Signaling and Behavior* **5**:649–54.

Yamasaki, K. et al., 2013. Chloroplast Envelope Localization of *EDS5*, an Essential Factor for Salicylic Acid Biosynthesis in *Arabidopsis thaliana*. *Plant Signaling and Behavior* **8**:e23603.

Yamasaki, S. and Dillenburg, L.C. 1999. Measurements of Leaf Relative Water Content in Araucaria Angustifolia. *Revista Brasilleira de Fisiologia Vegetal* **11**:69–75.

Yang, H.L et al., 2009. Molecular Characterization of a Dehydroascorbate Reductase from Pinus Bungeana. *Journal of Integrative Plant Biology* **51**:993–1001.

Yang, L., Han, R and Sun, Y. 2012. Damage Repair Effect of He-Ne Laser on Wheat Exposed to Enhanced Ultraviolet-B Radiation. *Plant Physiology and Biochemistry* **57**:218–21.

Yang, S. F. and Hoffman, N.E. 1984. Ethylene Biosynthesis and Its Regulation in Higher Plants. *Annual Review of Plant Physiology* **35**:155–89.

Yao, Y., Bilichak, A., Golubov, A and Kovalchuk, I. 2012. *Ddm1* Plants Are Sensitive to Methyl Methane Sulfonate and NaCl Stresses and Are Deficient in DNA Repair. *Plant Cell Reports* **31**:1549–61.

Yao, Y. et al., 2017. ETHYLENE RESPONSE FACTOR 74 (*ERF74*) Plays an Essential Role in Controlling a Respiratory Burst Oxidase Homolog D (*RbohD*)-Dependent Mechanism in Response to Different Stresses in Arabidopsis. *New Phytologist* **213**:1667–81.

Yazdanbakhsh, N., Sulpice, R., Graf, A., Stitt, M and Fisahn, J. 2011. Circadian Control of Root Elongation and C Partitioning in *Arabidopsis thaliana*. *Plant, Cell and Environment* **34**:877–94.

Ye, L. et al., 2015. *MPK3/MPK6* Are Involved in Iron Deficiency-Induced Ethylene Production in Arabidopsis.

Frontiers in Plant Science **6**:953.

Ye, N., Zhu, G., Liu, Y., Li, Y and Zhang, J. 2011. ABA Controls H_2O_2 Accumulation through the Induction of *OsCATB* in Rice Leaves under Water Stress. *Plant and Cell Physiology* **52**:689–98.

Yoo, H.H., Kwon, C., Lee, M.M and Chung, I.K. 2007. Single-Stranded DNA Binding Factor *AtWHY1* Modulates Telomere Length Homeostasis in Arabidopsis. *Plant Journal* **49**:442–51.

You, J. and Chan, Z. 2015. ROS Regulation During Abiotic Stress Responses in Crop Plants. *Frontiers in Plant Science* **6**:1092.

Yousuf, P.Y., Hakeem, K.U.R., Chandna, R and Ahmad, P. 2012. Role of Glutathione Reductase in Plant Abiotic Stress. *Abiotic Stress Responses in Plants* Ahmad P., Prasad M.(Eds.):41-61.

Yu, S. et al., 2013. Sugar Is an Endogenous Cue for Juvenile-to-Adult Phase Transition in Plants. *eLife* **2**:e00269.

Yu, T. S. et al., 2001. The Arabidopsis *sex1* Mutant Is Defective in the R1 Protein, a General Regulator of Starch Degradation in Plants, and Not in the Chloroplast Hexose Transporter. *The Plant Cell* **13**:1907–18.

Yu, T. S., Lue, W.S., Wang, S.M and Chen, J. 2000. Mutation of Arabidopsis Plastid Phosphoglucose Isomerase Affects Leaf Starch Synthesis and Floral Initiation. *Plant Physiology* **123**:319–26.

Yuanyuan, M., Yali, Z., Jiang, L and Hongbo, S. 2010. Roles of Plant Soluble Sugars and Their Responses to Plant Cold Stress. *Journal of Biotechnology* **8**:2004–10.

Zacarias, L and Reid, M.S. 1990. Role of Growth Regulators in the Senescence of *Arabidopsis thaliana* Leaves. *Physiologia Plantarum* **80**:549–54.

Van der Zand, A and Tabak, H.F. 2013. Peroxisomes: Offshoots of the ER. *Current Opinion in Cell Biology* **25**:490–454.

Zandalinas, S.I. et al., 2016. ABA Is Required for the Accumulation of *APX1* and *MBF1c* during a Combination of Water Deficit and Heat Stress. *Journal of Experimental Botany* **67**:5381–90.

Zavala, J. A., Scopel, A.L and Ballaré, C.L. 2001. Effects of Ambient UV-B Radiation on Soybean Crops: Impact on Leaf Herbivory by Anticarsia Gemmatalis. *Plant Ecology* **156**:121–30.

Zechmann, B. 2014. Compartment-Specific Importance of Glutathione during Abiotic and Biotic Stress. *Frontiers in Plant Science* **5**:566.

Zeeman, S. C., Kossmann, J and Smith, A.M. 2010. Starch: Its Metabolism, Evolution, and Biotechnological Modification in Plants. *Annual Review of Plant Biology* **61**:209–34.

De Zelicourt, A., Colcombet, J and Hirt, H. 2016. The Role of MAPK Modules and ABA during Abiotic Stress Signaling. *Trends in Plant Science* **21**:677–85.

Zentgraf, U. 2001. Identification of a Transcription Factor Specifically Expressed at the Onset of Leaf Senescence. *Planta* **213**:469–73.

Zhang, H. et al., 2016a. Ethylene Response Factor *TERF1*, Regulated by ETHYLENE-INSENSITIVE3-like Factors, Functions in Reactive Oxygen Species (ROS) Scavenging in Tobacco (*Nicotiana Tabacum L.*). *Scientific Reports* **6**:29948.

Zhang, M., Smith, J.A.C., Harberd, N.P and Jiang, C. 2016b. The Regulatory Roles of Ethylene and Reactive Oxygen Species (ROS) in Plant Salt Stress Responses. *Plant Molecular Biology* **91**:651–59.

Zhang, X. et al., 2011. Maize *ABP9* Enhances Tolerance to Multiple Stresses in Transgenic Arabidopsis by Modulating ABA Signaling and Cellular Levels of Reactive Oxygen Species. *Plant Molecular Biology* **75**:365–78.

Zhao, Y. et al., 2016. ABA Receptor *PYL9* Promotes Drought Resistance and Leaf Senescence. *Proceedings of the National Academy of Sciences* **113**:1949–54.

Zhong, H. et al., 2012. Two Brassica napus Genes Encoding NAC Transcription Factors Are Involved in Response to High-Salt stress. *Plant Cell Reports* **31**:1991–2003.

Zhou, J. et al., 2013. NBR1-Mediated Selective Autophagy Targets Insoluble Ubiquitinated Protein Aggregates in Plant Stress Responses. *PLoS Genetics* **9**:e1003196.

Zhou, X., Jiang, Y and Yu, D. 2011. *WRKY22* Transcription Factor Mediates Dark-Induced Leaf Senescence in Arabidopsis. *Molecules and Cells* **31**:303–13.

Zhou, Y. et al., 2013. Identification and Functional Characterization of a Rice NAC Gene Involved in the Regulation of Leaf Senescence. *BMC Plant Biology* **13**:132.

Zhu, C., Yang, N., Guo, Z., Qian, M and Gan, L. 2016. An Ethylene and ROS-Dependent Pathway Is Involved in Low Ammonium-Induced Root Hair Elongation in Arabidopsis Seedlings. *Plant Physiology and Biochemistry* **105**:37–44.

Zhu, J.K. 2016. Abiotic Stress Signaling and Responses in Plants. *Cell* **167**:313–24.

Zimmermann, P., Heinlein, C., Orendi, G and Zentgraf, U. 2006. Senescence-Specific Regulation of Catalases in *Arabidopsis thaliana* (L.) Heynh. *Plant, Cell and Environment* **29**:1049–60.

Zou, C., Jiang, W and Yu, D. 2010. Male Gametophyte-Specific *WRKY34* Transcription Factor Mediates Cold Sensitivity of Mature Pollen in Arabidopsis. *Journal of Experimental Botany* **61**:3901–14.

Zuppini, A., Gerotto, C and Baldan, B. 2010. Programmed Cell Death and Adaptation: Two Different Types of Abiotic Stress Response in a Unicellular Chlorophyte. *Plant and Cell Physiology* **51**:884–95.

Zwack, P.J and Rashotte, A.M. 2013. Cytokinin Inhibition of Leaf Senescence. *Plant Signaling and Behavior* **8**:e24737.